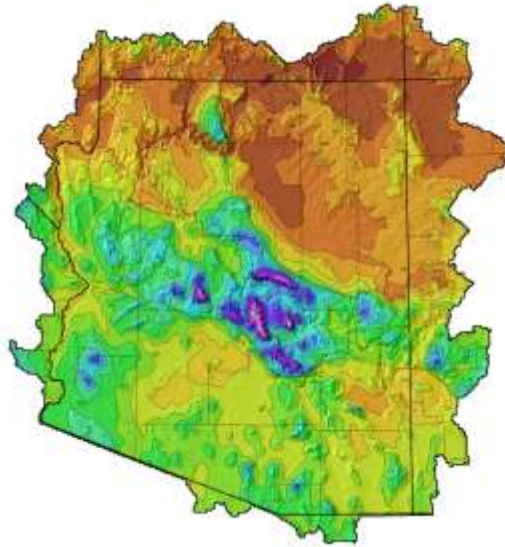# Probable Maximum Precipitation Study for Arizona

Prepared for

Arizona Department of Water Resources

3550 North Central Avenue
Phoenix, AZ 85012
www.azwater.gov

Prepared by

Applied Weather Associates, LLC

PO Box 680
Monument, Co 80132
(719) 488-9117
www.appliedweatherassociates.com

Ed Tomlinson, PhD, Project Manager
Bill Kappel, Senior Meteorologist
Geoff Muhlestein, GIS/Staff Scientist
Douglas Hultstrand, Hydrometeorologist
Tye Parzybok, Senior Meteorologist

July 2013

Notice

This report was prepared by Applied Weather Associates, LLC (AWA). The results and conclusions in this report are based upon best professional judgment using currently available data. Therefore, neither AWA nor any person acting on behalf of AWA can: (a) make any warranty, expressed or implied, regarding future use of any information or method in this report, or (b) assume any future liability regarding use of any information or method contained in this report.

Acknowledgements

Table of Contents

List of Figures

List of Tables

Executive Summary

Applied Weather Associates (AWA) completed a statewide Probable Maximum Precipitation (PMP) study for Arizona. This study produced PMP values for any point within the state of Arizona, using a grid spacing of approximately 2.45 square miles. Variations in topography, climate and storm types across the state were explicitly taken into account. A large set of storm data were analyzed for use in developing the PMP values. These values replace those presented in Hydrometeorological Report (HMR) 49. Temporal patterns of the PMP design storm by storm type (local and tropical/general) were investigated during this study and recommendations for application are provided. Furthermore, results of this analysis reflect the most current practices used for defining PMP, including comprehensive storm analyses procedures, extensive use of geographical information systems (GIS), updated maximum dew point and sea surface temperature climatologies for storm maximization and maximization, and updated understanding of the weather and climate throughout the state.

The approach used in this study follows the same philosophy used in the numerous site-specific and regional PMP studies that AWA has completed in the last ten years. This is the storm-based approach used by the National Weather Service (NWS) in the development of the HMRs. The World Meteorological Organization (WMO) Manual for PMP determination (WMO Operational Hydrology Report 1986, 2009) recommends this same approach. This approach identifies extreme rainfall events that have occurred in a region considered transpositionable to locations in Arizona that have meteorological and topographical characteristics similar to extreme rainfall storms that could occur over similar regions within the state. The largest of these rainfall events are selected for detailed analyses.

The data, assumptions, and analysis techniques used in this study have been reviewed and accepted by the Arizona Department of Water Resources (ADWR) and the Review Committee. Although this study produces deterministic values, it must be recognized that there is some uncertainty associated with the development process. This occurs in areas such as the determination of the storm maximization factors, the determination of the storm transposition limits, and the determination of the PMP design storm temporal distributions. Limitations and uncertainties are recognized and conservative applications are applied when there is uncertainty in the data analysis and quantification. As much as possible, all data and information supporting decisions in the PMP development process have been documented so that results can be reproduced and verified.

Fifty-one extreme rainfall storm events are identified as rainfall centers having similar characteristics to extreme rainfall events that could potentially control PMP values at locations within the state. This includes twelve general winter storms, ten remnant tropical storms, and twenty-nine local convective storms. Each of the fifty-one storms were analyzed using the Storm Precipitation Analysis System (SPAS), which produced Depth-Area-Duration (DAD) values, mass curves, and total storm isohyetals, among other products. National Weather Service Next Generation Weather Radar (NEXRAD) data were incorporated when available. Two of the major storms associated with remnant tropical cyclones (August 1951 and September 1970) had previously been analyzed by the Bureau of Reclamation with results presented in their report titled "Determination of an Upper Limit Design Rainstorm for the Colorado River Basin above Hoover Dam" (Bureau of Reclamation 1990). This project updated those analyses using the latest storm analysis technologies and methods.

Standard procedures for in-place maximization and moisture transposition adjustments were followed. However, new techniques and databases were used in this project to increase accuracy and reliability when justified by advances in technology and meteorological understanding, while adhering to the basic approach used in the HMRs and in the WMO Manual. The NOAA Atlas 14 precipitation frequency data were used to calculate the Orographic Transposition Factor (OTF) for each storm. This process replaces the storm separation method (SSM) used by the NWS in the most recent HMRs. The proportionality constant procedure used to determine the OTFs provides quantifiable and reproducible analyses of the effects of terrain on rainfall. Results of these three factors (maximization, moisture transposition, and orographic transposition) are applied for each storm at each of the grid cells used in this study (64,103 grid cells).

Maximization factors were computed for each of the storms using an updated dew point climatology representing the maximum moisture that could have been associated with the rainfall event. This climatology includes the average 3-, 12-, and 24-hour 100-year return frequency values. The most appropriate duration consistent with the duration of the storm rainfall is used. For storms where the moisture source originated over the ocean, an updated maximum sea surface temperature (SST) climatology based on mean plus 2 sigma values was used. HYSPLIT model trajectories and SST data from the National Center for Atmospheric Research (NCAR) and National Oceanic and Atmospheric Association (NOAA) National Environmental Satellite, Data, & Information Service (NESDIS) were used in the storm adjustment procedures.

To house, analyze, and produce results from the large data set developed in the study, the PMP Evaluation Tool was developed. This tool uses a combination of Excel and GIS to query, calculate, and derive PMP values for each grid cell for each duration for each storm type. For local convective storms, the durations analyzed were 1-, 2-, 3-, 4-, 5-, and 6-hours. For remnant tropical and general winter storms, the durations analyzed were 6-, 12-, 18-, 24-, 48-, and 72-hours. The PMP Evaluation Tool can incorporate new storm rainfall data and analysis updates going forward. It provides a simple interface from which PMP can be computed for any watershed in the state.

The PMP Evaluation Tool is a python scripting language-based tool designed to be run within the ArcGIS environment. The tool produces gridded PMP depths at a spatial resolution of 90 arc-seconds for a user-designated drainage basin. The PMP Evaluation Tool derived the total adjusted DAD value specific to the area sizes of the drainage basin being evaluated for each storm that is transpositionable to a grid cell. These values are temporally distributed based on PMP-design storm guidance provided by ADWR and storm analyses completed during this study. The tool provides output in the form of GIS files (both raster and vector data) and a space delimited text file.

Glossary

Adiabat: Curve of thermodynamic change taking place without addition or subtraction of heat. On an adiabatic chart or pseudo-adiabatic diagram, a line showing pressure and temperature changes undergone by air rising or condensation of its water vapor; a line, thus, of constant potential temperature.

Adiabatic: Referring to the process described by adiabat.

Advection: The process of transfer (of an air mass property) by virtue of motion. In particular cases, advection may be confined to either the horizontal or vertical components of the motion. However, the term is often used to signify horizontal transfer only.

Air mass: Extensive body of air approximating horizontal homogeneity, identified as to source region and subsequent modifications.

Barrier: A mountain range that partially blocks the flow of warm humid air from a source of moisture to the basin under study.

Basin centroid: The point at the exact center of the drainage basin as determined through geographical information systems calculations using the basin outline.

Basin shape: The physical outline of the basin as determined from topographic maps, field survey, or GIS.

Cold front: Front where relatively colder air displaces warmer air.

Convective rain: Rainfall caused by the vertical motion of an ascending mass of air that is warmer than the environment and typically forms a cumulonimbus cloud. The horizontal dimension of such a mass of air is generally of the order of 12 miles or less. Convective rain is typically of greater intensity than either of the other two main classes of rainfall (cyclonic and orographic) and is often accompanied by thunder. The term is more particularly used for those cases in which the precipitation covers a large area as a result of the agglomeration of cumulonimbus masses.

Convergence: Horizontal shrinking and vertical stretching of a volume of air, accompanied by net inflow horizontally and internal upward motion.

Cooperative station: A weather observation site where an unpaid observer maintains a climatological station for the National Weather Service.

Cyclone: A distribution of atmospheric pressure in which there is a low central pressure relative to the surroundings. On large-scale weather charts, cyclones are characterized by a system of closed constant pressure lines (isobars), generally approximately circular or oval in form, enclosing a central low-pressure area. Cyclonic circulation is counterclockwise in the northern hemisphere and clockwise in the southern. (That is, the sense of rotation about the local vertical is the same as that of the earth's rotation).

Depth-Area curve: Curve showing, for a given duration, the relation of maximum average depth to size of area within a storm or storms.

Depth-Area-Duration: The precipitation values derived from Depth-Area and Depth-Duration curves at each time and area size increment analyzed for a PMP evaluation.

Depth-Area-Duration Curve: A curve showing the relation between an averaged areal rainfall depth and the area over which it occurs, for a specified time interval, during a specific rainfall event.

Depth-Area-Duration values: The combination of depth-area and duration-depth relations. Also called depth-duration-area.

Depth-Duration curve: Curve showing, for a given area size, the relation of maximum average depth of precipitation to duration periods within a storm or storms.

Dew point: The temperature to which a given parcel of air must be cooled at constant pressure and constant water vapor content for saturation to occur.

Effective barrier height: The height of a barrier determined from elevation analysis that reflects the effect of the barrier on the precipitation process for a storm event. The actual barrier height may be either higher or lower than the effective barrier height.

Envelopment: A process for selecting the largest value from any set of data. In estimating PMP, the maximum and transposed rainfall data are plotted on graph paper, and a smooth curve is drawn through the largest values.

Explicit transposition: The movement of the rainfall amounts associated with a storm within boundaries of a region throughout which a storm may be transposed with only relatively minor modifications of the observed storm rainfall amounts. The area within the transposition limits has similar, but not identical, climatic and topographic characteristics throughout.

First-order NWS station: A weather station that is either automated, or staffed by employees of the National Weather Service and records observations on a continuous basis.

Front: The interface or transition zone between two air masses of different parameters. The parameters describing the air masses are temperature and dew point.

General storm: A storm event that produces precipitation over areas in excess of 500-square miles, has a duration longer than 6 hours, and is associated with a major synoptic weather feature.

HYSPLIT: Hybrid Single-Particle Lagrangian Integrated Trajectory. A complete system for computing parcel trajectories to complex dispersion and deposition simulations using either puff or particle approaches. Gridded meteorological data, on one of three conformal (Polar, Lambert, or Mercator latitude-longitude grid) map projections, are required at regular time intervals. Calculations may be performed sequentially or concurrently on multiple meteorological grids, usually specified from fine to coarse resolution.

Implicit transpositioning: The process of applying regional, areal, or durational smoothing to eliminate discontinuities resulting from the application of explicit transposition limits for various storms.

Isohyets: Lines of equal value of precipitation for a given time interval.

Isohyetal pattern: The pattern formed by the isohyets of an individual storm.

Isohyetal orientation: The term used to define the orientation of precipitation patterns of major storms when approximated by elliptical patterns of best fit. It is also the orientation (direction from north) of the major axis through the elliptical PMP storm pattern.

Jet Stream: A strong, narrow current concentrated along a quasi-horizontal axis (with respect to the earth's surface) in the upper troposphere or in the lower stratosphere, characterized by strong vertical and lateral wind shears. Along this axis it features at least one velocity maximum (jet streak). Typical jet streams are thousands of kilometers long, hundreds of kilometers wide, and several kilometers deep. Vertical wind shears are on the order of 10 to 20 mph per kilometer of altitude and lateral winds shears are on the order of 10 mph per 100 kilometer of horizontal distance.

Local storm: A storm event that occurs over a small area in a short time period. Precipitation rarely exceeds 6 hours in duration and the area covered by precipitation is less than 500 square miles. Frequently, local storms will last only 1 or 2 hours and precipitation will occur over areas of up to 200 square miles. Precipitation from local storms will be isolated from general-storm rainfall. Often these storms are thunderstorms.

Low Level Jet stream: A band of strong winds at an atmospheric level well below the high troposphere as contrasted with the jet streams of the upper troposphere.

Mass curve: Curve of cumulative values of precipitation through time.

Mesoscale Convective Complex: For the purposes of this study, a heavy rain-producing storm with horizontal scales of 10 to 1000 kilometers (6 to 625 miles) which includes significant, heavy convective precipitation over short periods of time (hours) during some part of its lifetime.

Mesoscale Convective System: A complex of thunderstorms which becomes organized on a scale larger than the individual thunderstorms, and normally persists for several hours or more. MCSs may be round or linear in shape, and include systems such as tropical cyclones, squall lines, and MCCs (among others). MCS often is used to describe a cluster of thunderstorms that does not satisfy the size, shape, or duration criteria of an MCC.

Mid-latitude frontal system: An assemblage of fronts as they appear on a synoptic chart north of the tropics and south of the polar latitudes. This term is used for a continuous front and its characteristics along its entire extent, its variations of intensity, and any frontal cyclones along it.

Moisture maximization: The process of adjusting observed precipitation amounts upward based upon the hypothesis of increased moisture inflow to the storm.

Observational day: The 24-hour time period between daily observation times for two consecutive days at cooperative stations, e.g., 6:00PM to 6:00PM.

One-hundred year rainfall event: The point rainfall amount that has a one-percent probability of occurrence in any year. Also referred to as the rainfall amount that has a 1 percent chance of occurring in any single year.

Polar front: A semi-permanent, semi-continuous front that separates tropical air masses from polar air masses.

Precipitable water: The total atmospheric water vapor contained in a vertical column of unit cross-sectional area extending between any two specified levels in the atmosphere; commonly expressed in terms of the height to which the liquid water would stand if the vapor were completely condensed and collected in a vessel of the same unit cross-section. The total precipitable water in the atmosphere at a location is that contained in a column or unit cross-section extending from the earth's surface all the way to the "top" of the atmosphere. The 30,000 foot level (approximately 300mb) is considered the top of the atmosphere in this study.

Persisting dew point: The dew point value at a station that has been equaled or exceeded throughout a period. Commonly durations of 12 or 24 hours are used, though other durations may be used at times.

Probable Maximum Flood: The flood that may be expected from the most severe combination of critical meteorological and hydrologic conditions that are reasonably possible in a particular drainage area.

Probable Maximum Precipitation: Theoretically, the greatest depth of precipitation for a given duration that is physically possible over a given size storm area at a particular geographic location at a certain time of the year.

Pseudo-adiabat: Line on thermodynamic diagram showing the pressure and temperature changes undergone by saturated air rising in the atmosphere, without ice-crystal formation and without exchange of heat with its environment, other than that involved in removal of any liquid water formed by condensation.

Rainshadow: The region, on the lee side of a mountain or mountain range, where the precipitation is noticeably less than on the windward side.

Saturation: Upper limit of water-vapor content in a given space; solely a function of temperature.

Shortwave: Also referred to as a shortwave trough, is an embedded kink in the trough / ridge pattern. This is the opposite of longwaves, which are responsible for synoptic scale systems, although shortwaves may be contained within or found ahead of longwaves and range from the mesoscale to the synoptic scale.

Spatial distribution: The geographic distribution of precipitation over a drainage according to an idealized storm pattern of the PMP for the storm area.

Storm transposition: The hypothetical transfer, or relocation of storms, from the location where they occurred to other areas where they could occur. The transfer and the mathematical adjustment of storm rainfall amounts from the storm site to another location is termed "explicit transposition." The areal, durational, and regional smoothing done to obtain comprehensive individual drainage estimates and generalized PMP studies is termed "implicit transposition" (WMO, 1986).

Synoptic: Showing the distribution of meteorological elements over an area at a given time, e.g., a synoptic chart. Use in this report also means a weather system that is large enough to be a major feature on large-scale maps (e.g., of the continental U.S.).

Temperature inversion: An increase in temperature with an increase in height.

Temporal distribution: The time order in which incremental PMP amounts are arranged within a PMP storm.

Tropical Storm: A cyclone of tropical origin that derives its energy from the ocean surface.

Total storm area and total storm duration: The largest area size and longest duration for which depth-area-duration data are available in the records of a major storm rainfall.

Transposition limits: The outer boundaries of the region surrounding an actual storm location that has similar, but not identical, climatic and topographic characteristics throughout. The storm can be transpositioned within the transposition limits with only relatively minor modifications to the observed storm rainfall amounts.

Undercutting: The process of placing an envelopment curve somewhat lower than the highest rainfall amounts on depth-area and depth-duration plots.

Warm front: Front where relatively warmer air replaces colder air.

Acronyms and Abbreviations used in the report

ADWR: Arizona Department of Water Resources

ALERT: Automated Local Evaluation in Real Time

AMS: Annual maximum series

AWA: Applied Weather Associates

DA: Depth-Area

DAD: Depth-Area-Duration

.dbf: Database file extension

DD: Depth-Duration

dd: decimal degrees

DEM: Digital elevation model

DND: drop number distribution

DSD: drop size distribution

DWR: Department of Water Resources

ENSO: El Niño/La Nina Southern Oscillation

EPRI: Electric Power Research Institute

F: Fahrenheit

FAFP: Free Atmospheric Forced Precipitation

FPL: Florida Power and Light

GCS: Geographical coordinate system

GEV: Generalized extreme value

GIS: Geographic Information System

GRASS: Geographic Resource Analysis Support System

HMR: Hydrometeorological Report

HYSPLIT: Hybrid Single Particle Lagrangian Integrated Trajectory Model

IPMF: In-place Maximization Factor

mb: millibar

MTF: Moisture Transposition Factor

NCAR: National Center for Atmospheric Research

NCDC: National Climatic Data Center

NCEP: National Centers for Environmental Prediction

NESDIS: National Environmental Satellite, Data, & Information Service

NEXRAD: Next Generation Radar

NOAA: National Oceanic and Atmospheric Administration

NWS: National Weather Service

OTF: Orographic Transposition Factor

PMF: Probable Maximum Flood

PMP: Probable Maximum Precipitation

PW: Precipitable Water

SPAS: Storm Precipitation and Analysis System

SST: Sea Surface Temperature

TAF: Total Adjustment Factor

USACE: US Army Corps of Engineers

USGS: United States Geological Survey

WBD: Watershed Boundary Database

WMO: World Meteorological Organization

1.   Introduction

This study provides Probable Maximum Precipitation (PMP) values for any drainage basin within Arizona. The PMP values are used in the computation of the Probable Maximum Flood (PMF). In addition, the temporal distribution of that PMP rainfall by each storm type is provided. Results of this study supersede Hydrometeorological Report (HMR) 49 (Hansen et al. 1977).

1.1   Background

Definitions of PMP are found in most of the HMRs issued by the National Weather Service (NWS). The definition used in the most recently published HMR is "theoretically, the greatest depth of precipitation for a given duration that is physically possible over a given storm area at a particular geographical location at a certain time of the year" (HMR 59, p. 5). Since the mid-1940s or earlier, several government agencies have been developing methods to calculate PMP in various regions of the United States. The National Weather Service (formerly the U.S. Weather Bureau) and the Bureau of Reclamation have been the primary agencies involved in this activity. PMP estimates presented in their reports are used to calculate the PMF, which, in turn, is often used for the design of significant hydraulic structures. It is important to remember that the methods used to derive PMP and the processes which utilize those values hydrologically adhere to the requirement of being "physically possible". In other words, various levels of conservatism and/or extreme aspects of storms that could not occur in a PMP storm environment should not be compounded to produce combinations of storm characteristics that are not physically consistent in estimating PMP values or for the hydrologic applications of those values.

The generalized PMP studies currently in use in the conterminous United States include HMRs 49 (1977) and 50 (1981) for the Colorado River and Great Basin drainage; HMRs 51 (1978), 52 (1982) and 53 (1980) for the U.S. east of the 105th meridian; HMR 55A (1988) for the area between the Continental Divide and the 103rd meridian; HMR 57 (1994) for the Columbia River Drainage; and HMRs 58 (1998) and 59 (1999) for California. In addition to these HMRs, numerous Technical Papers and Reports deal with specific subjects concerning precipitation (NOAA Tech. Report NWS 25, 1980; NOAA Tech. Memorandum NWS HYDRO 45, 1995). Topics include maximum observed rainfall amounts, return periods for various rainfall amounts, and specific storm studies. Climatological atlases (Technical Paper No. 40, 1961; NOAA Atlas 2, 1973; and NOAA Atlas 14, 2004-2013) are available for use in determining precipitation return periods. A number of site-specific, statewide, and regional studies (e.g. Tomlinson et al, 2002; Tomlinson et al 2003, Tomlinson et al, 2007, Tomlinson et al, 2008, Tomlinson et al, 2009, Tomlinson et al, 2010, Tomlinson et al. 2011, Kappel et al. 2012, Kappel et al. 2013, Tomlinson et al. 2013) augment generalized PMP reports for specific regions included in the large area addressed by HMR 49. The recent site-specific PMP projects completed within the domain covered by HMR 49 have shown serious errors and outdated procedures used to estimate PMP values. PMP results from this study provide values that replace those derived from HMR 49 and other previous PMP studies.

Arizona is fully included within the domain covered by HMR 49 (Figure 1.1). HMR 49 is the oldest of the current HMR series. As Figure 1.1 shows, HMR 49 covers a large area of the Intermountain West and Desert Southwest, where climate and terrain vary greatly. Because of the distinctive climate regions and significant topography, the development of PMP values must account for the complexity of the meteorology and terrain throughout the state. This project incorporated the latest methods, technology, and data to address these topics. Several major issues have been identified with how HMR 49 developed PMP values. Most important among these is the lack of analyzed storm events, the age of the document, and the outdated procedures used to derive PMP.

Previous site-specific, statewide, and regional PMP projects completed by AWA provide examples of PMP studies that explicitly consider the unique topography of the area being studied and the characteristics of historic extreme storms over climatically similar regions surrounding the area. The procedures incorporate the most up-to-date data, techniques, and applications to derive PMP. Each of these PMP studies have received extensive review and the results have been used in computing the PMF for the watersheds. This study follows the same procedures used in those studies to determine the PMP values with updates to the method for quantifying the effect of terrain and application of the data to produce PMP values. This was accomplished through the development of the PMP Evaluation Tool. This tool uses a combination of Excel and GIS to query, calculate, and derive PMP values for each grid cell for each duration for each storm type. For local convective storms, PMP values for 1-, 2-, 3-, 4-, 5-, and 6-hour durations are determined. For remnant tropical and general winter storms, the durations analyzed were 6-, 12-, 18-, 24-, 48-, and 72-hour durations. The PMP Evaluation Tool is able to incorporate new storm rainfall data and analysis updates going forward. It provides a simple interface from which PMP can be computed for any watershed in the state (see Section 9 for more detail).

HMR 49 Boundary
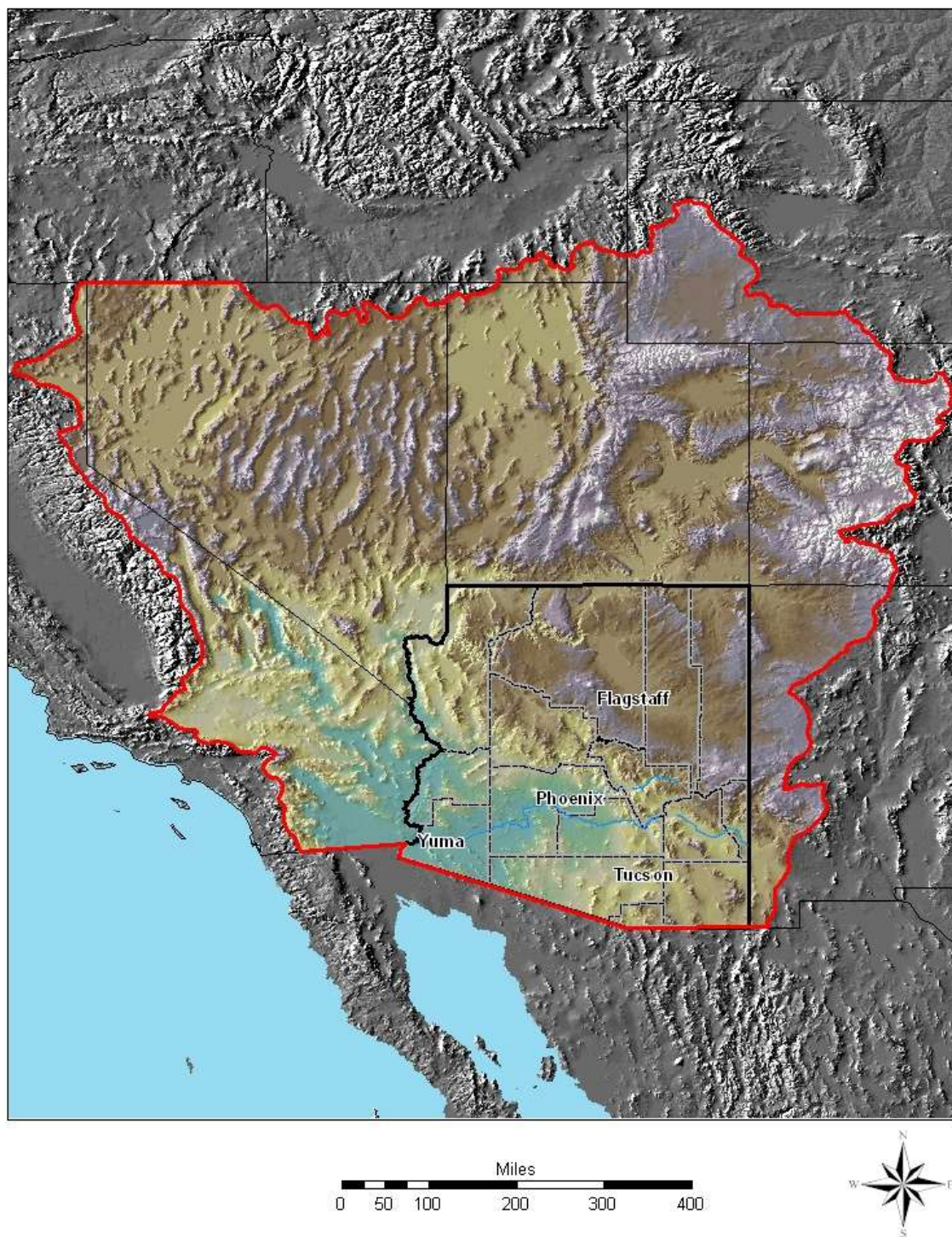
Figure 1.1 Domain covered by HMR 49 (Hansen et al. 1977)

1.2 Objective

The objective of this study was to determine reliable estimates of PMP values for Arizona. The most reliable methods and data currently available have been used and are updates to the methods and data used in HMR 49.

1.3 Approach

The approach used in this study follows the same procedures that were used in the development of the HMRs with updated procedures implemented where appropriate. This includes updates AWA has implemented during several PMP projects recently completed as well as updates developed during this study. These procedures were applied considering meteorology and terrain, and their interactions within Arizona. The weather and climate of the region are discussed in Section 2. The initial step of identifying extreme storms is discussed in Section 3 and the development of the final list of storms used to derive PMP is in Section 4. Procedures used to analyze the storms are presented in Section 5 and 6. Adjustments for storm maximization, storm transposition, and orographics affects are provided in Sections 7, 8, and 9 respectively. The final procedure of developing PMP values from the adjusted rainfall amounts is discussed in Section 10. Results are presented in Section 11. Discussions on sensitivities are provided in Section 12 and recommendations for application are presented in Section 13.

A goal of this study was to maintain as much consistency as possible with the general methods used in recent HMRs, the WMO manual for PMP, and the previous PMP studies completed by AWA.   Deviations were incorporated when justified by developments in meteorological analyses and available data. The basic approach identifies major storms that occurred within the region. Each of the main storm types which produce extreme rainfall were investigated. This includes local convective storms, remnant tropical storms, and general winter storms. The moisture content of each of these storms is maximized to provide worst-case rainfall estimation for each storm at the location where it occurred. Storms are then transpositioned to each grid point with similar topography and meteorological conditions. Adjustments were applied to each storm as it was transpositioned to each grid cell. These adjustments were combined to produce the total adjustment factor for each storm for each grid cell. The total adjustment factor is a function of the in-place maximization factor (IPMF) multiplied by the moisture transposition factor (MTF) multiplied by the orographic transposition factor (OTF).

Total Adjustment Factor = IPMF * MTF * OTF   Equation 1.1

Advanced computer-based technologies, Weather Service Radar WSR-88D NEXt generation RADar (NEXRAD), and HYSPLIT model trajectories were used for storm analyses along with new meteorological data sources. New technology and data were incorporated into the study when they provided improved reliability, while maintaining as much consistency as possible with previous studies. This includes an updated maximum dew point climatology and an updated sea surface temperature (SST) climatology which were used in the IPMF and MTF calculation processes.

For some applications, this study applied standard methods (e.g. WMO Operational Hydrology Reports 1986, 2009), while for other applications, new techniques were developed. Moisture analyses have historically used monthly maximum 12-hour persisting dew points (for Arizona as published in HMR 50, 1980). For this project a new maximum dew point climatology was developed to better represent the storm types and rainfall durations that affect the region. Dew point climatologies representing the 3-hour, 12-hour, and 24-hour average return frequency values at the 100-year recurrence interval were derived and replaced the 12-hour persisting values used in HMR 50. These values better depict the physical processes that are evaluated by determining available atmospheric moisture for each storm. The resulting storm representative dew point (or SST) is representative of the environment that actually led to each storm's rainfall production. The maximum dew point climatologies used the most up to date periods of record, adding over 30 years of data. This approach provides the most complete scientific application compatible with the engineering requirements of consistency and reliability for credible PMP estimates.

In a few cases for remnant tropical and general winter storms, the moisture source originated over the Gulf of California and/or the Eastern Pacific Ocean. In these cases, SSTs were used as a surrogate for surface dew point data. To accomplish this, a SST procedure was used which follows the same approach used in HMRs 57 and 59, and previous studies completed by AWA. An updated SST climatology was developed, replacing the Marine Climate Atlas of the World (U.S. Navy, 1981) used in HMRs 57 and 59. This updated climatology dataset included monthly mean plus 2-sigma SST maps for the eastern Pacific Ocean and Gulf of California from the coastlines of the United States and Mexico to 180°W and from 15°N to 55°N (NOAA, Kent et al. 2007, Reynolds et al. 2007, and Worley et al. 2005). In conjunction with the climatology maps, daily SST maps based on ship and buoy reports, as well as satellite data (after 1979), were produced and used in deriving the storm representative SST values for each analyzed storm event where the moisture source originated over the Pacific Ocean or the Gulf of California.

Environmental Systems Research Institute's ArcGIS Desktop GIS software was extensively used to evaluate topography, terrain, and climatology; analyze spatial relationships; store, organize, and process the large amounts of spatial data; design, implement, and execute the PMP Evaluation Tool; and to provide visualization and cartographic support throughout the process. The Storm Precipitation Analysis System (SPAS) used gridded storm analysis techniques to provide both spatial and temporal analyses for extreme rainfall storm events (see Appendix E for a complete description of SPAS).

1.4   PMP Analysis Domain

An analysis domain was defined to cover the entire State of Arizona as well as watersheds that extended beyond state boundaries. This study allows for gridded PMP values to be determined for each cell within the project domain. The full PMP analysis domain is shown in Figure 1.2.
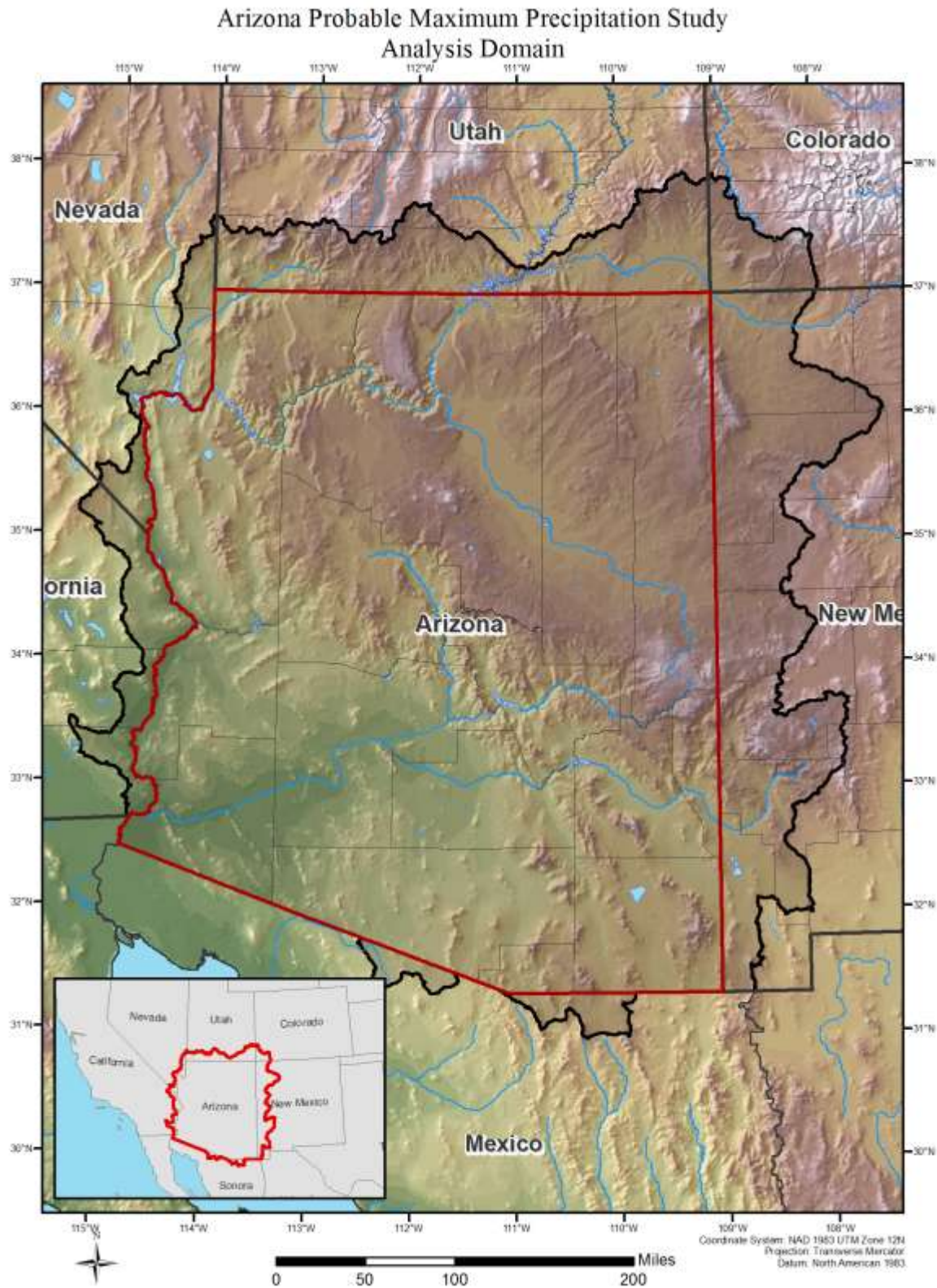
Figure 1.2 Full PMP analysis domain

To account for sites that may potentially include drainage areas that extend beyond the state boundaries, a buffer region was delineated to include watershed regions flowing into the state. The USGS Watershed Boundary Datasets (WBD), at the 2-digit through 8-digit level, were used to delineate the project extent. The USGS uses hydrologic unit codes (HUC) to identify each watershed basin. In general, the study region was constrained to the 2-digit Lower Colorado Region (HUC: 15). Excluded from this region is all area south of the Arizona State border draining away from the state and the upper reach of the 4-digit Lake Mead Basin (HUC: 1501). Several 8-digit sub-basins of the 2-digit Upper Colorado Region (HUC: 14) were added to the domain in the Northwest portion of the state including portions of the Dirty Devil (HUC: 1407) and San Juan (HUC: 1408) sub-basins. Figure 1.3 shows the outline of the 8-digit HUC sub-basin boundaries overlying the 4-digit basins used in the analysis domain.
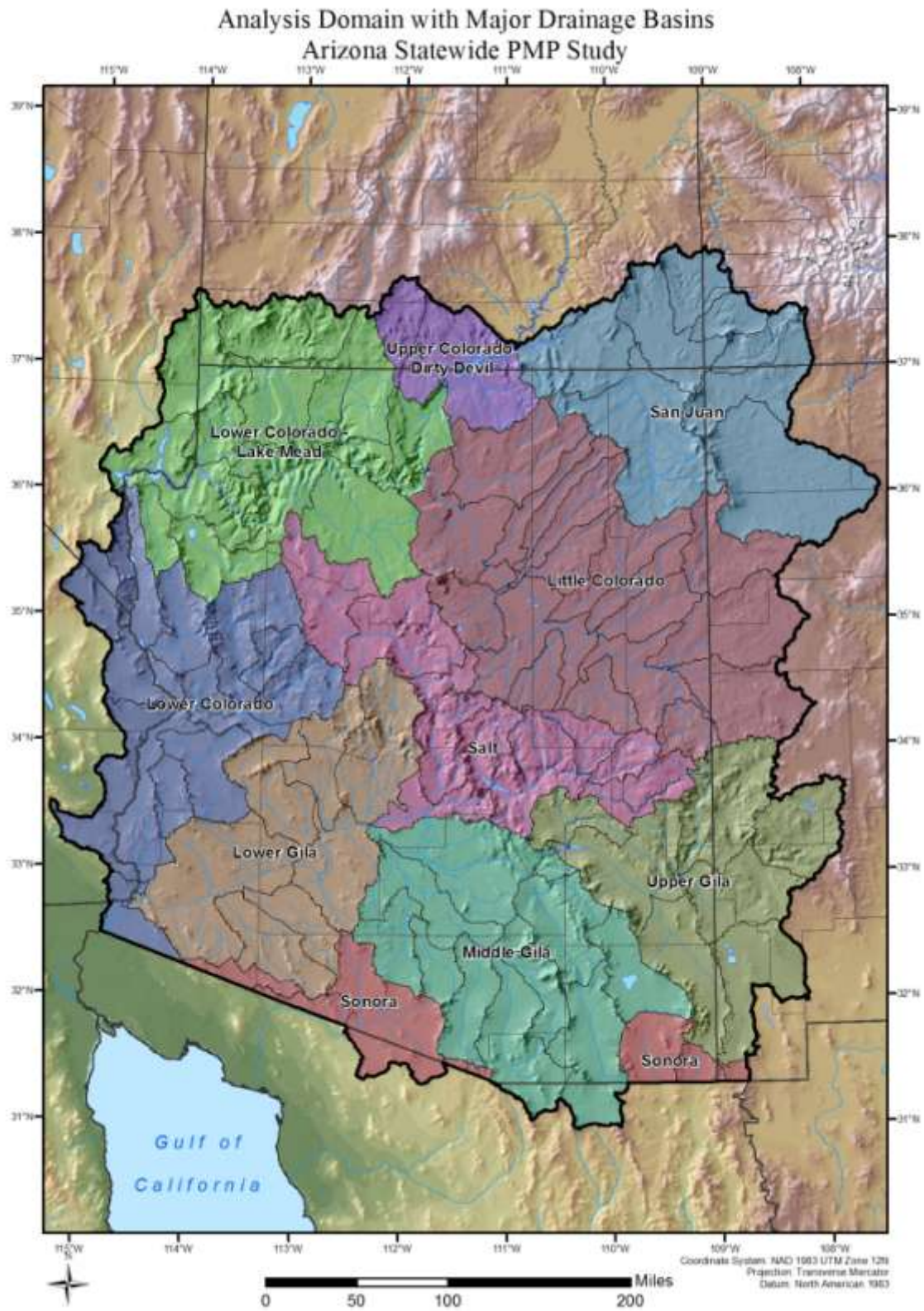
Figure 1.3 Hydrologic watershed boundaries within the analysis domain

1.5   PMP Analysis Grid Setup

A uniform grid network over the PMP analysis domain provides a spatial framework for the analysis. The PMP grid resolution for this study is 0.025 x 0.025 decimal degrees, or 90 arc-seconds, using the geographic coordinate system (GCS) spatial reference with the North American Datum of 1983 (NAD 83). This equates to 64,103 grid cells with centroids within the domain shown in Figure 1.2. The grid cells have an approximate area of 2.45 mi^2 (6.35 km^2). The grid network placement is essentially arbitrary, however, the placement is oriented in such a way that the grid cell centroids are centered over whole number coordinate pairs and then spaced evenly every 0.025 decimal degrees. For example; there is a grid point centered over 32° N and 109° W with the adjacent grid point to the west at 32° N and 109.025° W. An example of the PMP analysis grid over the McMicken Dam basin is shown in Figure 1.4.
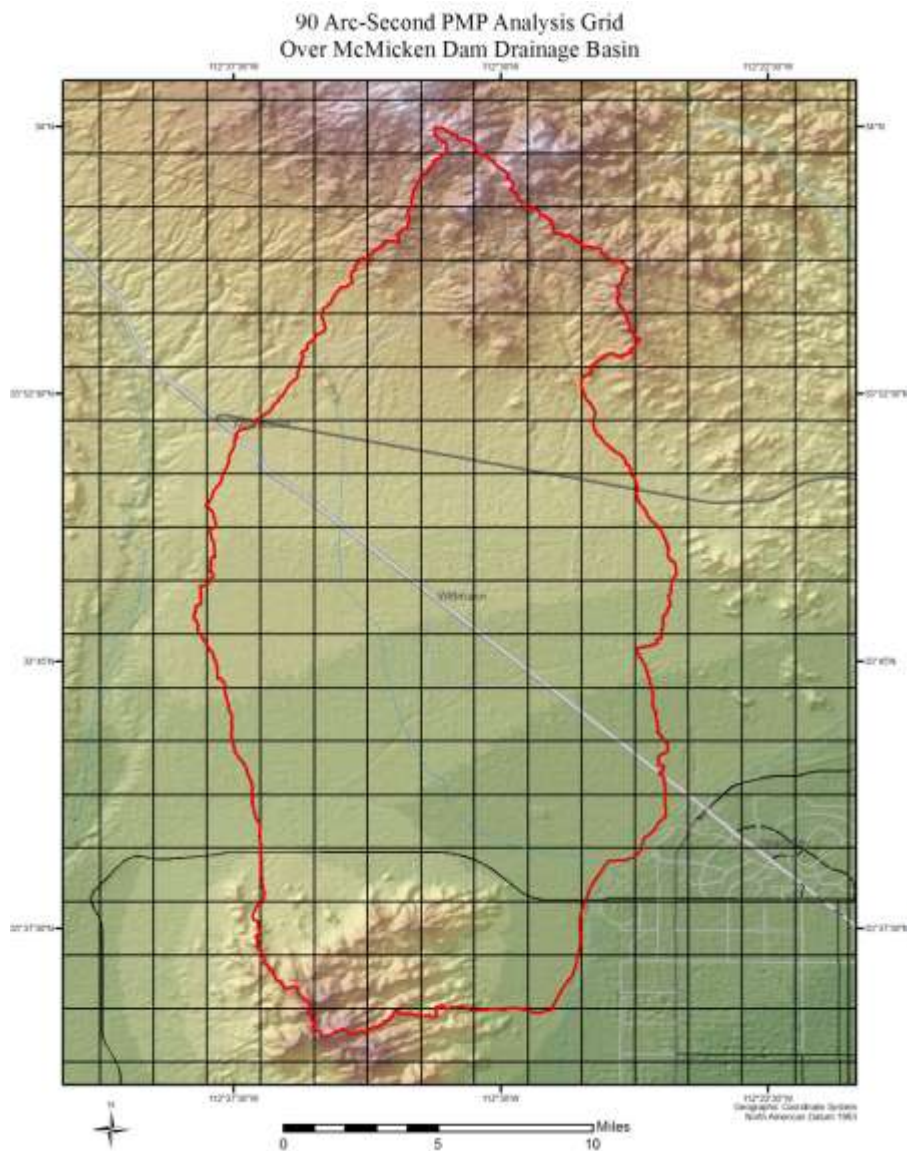
Figure 1.4 PMP analysis grid placement over McMicken Dam basin

2.   Weather and Climate of the Region

This section will describe the general weather and climate of the Arizona and how it relates to the development of PMP. More detailed descriptions of the climate of Arizona and each of the storm types described can be found in numerous references (e.g. Sellers and Hill 1974, Hansen and Schwartz 1980, McCollum et al. 2005, Mesinger et al. 2006). These references provide additional information. Figures 2.1a and 2.1b illustrate the spatial distribution of the PRISM annual maximum and minimum temperatures for the 30-year climatological period of 1981-2010. Figure 2.1c illustrates the PRISM annual precipitation for the same period. Figure 2.2 illustrates the spatial distribution of the NOAA Atlas 14 Volume 1 and Volume 8 100-year 24-hour precipitation frequency values.
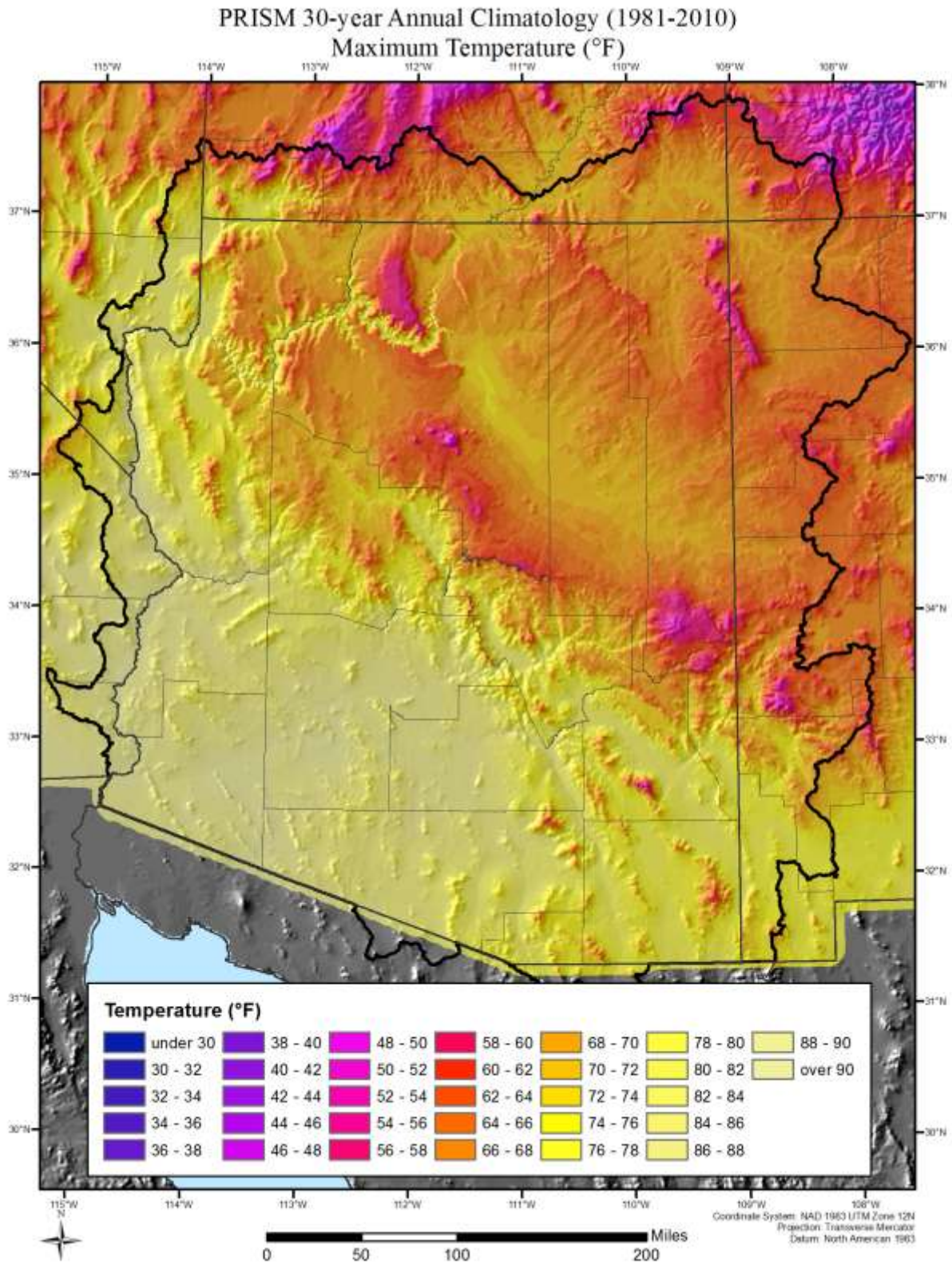
Figure 2.1a PRISM 30-year annual climatology – maximum temperatures

PRISM 30-year Annual Climatology (1981-2010)
Minimum Temperature (°F)
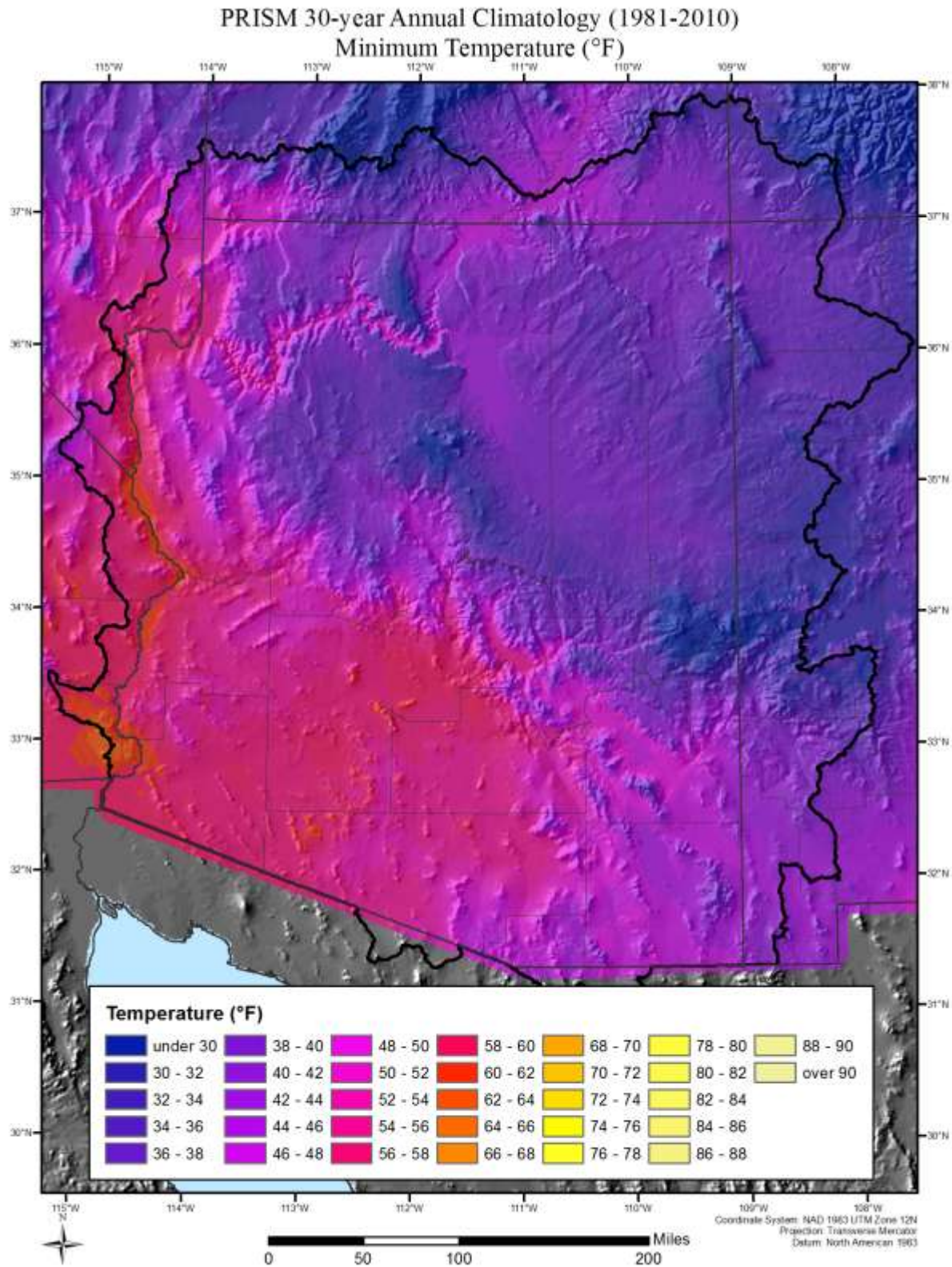
Figure 2.1b PRISM 30-year annual climatology – minimum temperatures

PRISM 30-year Annual Climatology (1981-2010)
Precipitation (inches)

Precipitation (in)

under 2	8 - 10	16 - 18	24 - 26	32 - 34
2 - 4	10 - 12	18 - 20	26 - 28	34 - 36
4 - 6	12 - 14	20 - 22	28 - 30	36 - 38
6 - 8	14 - 16	22 - 24	30 - 32	over 38

Coordinate System: NAD 1983 UTM Zone 12N
Projection: Transverse Mercator
Datum: North American 1983
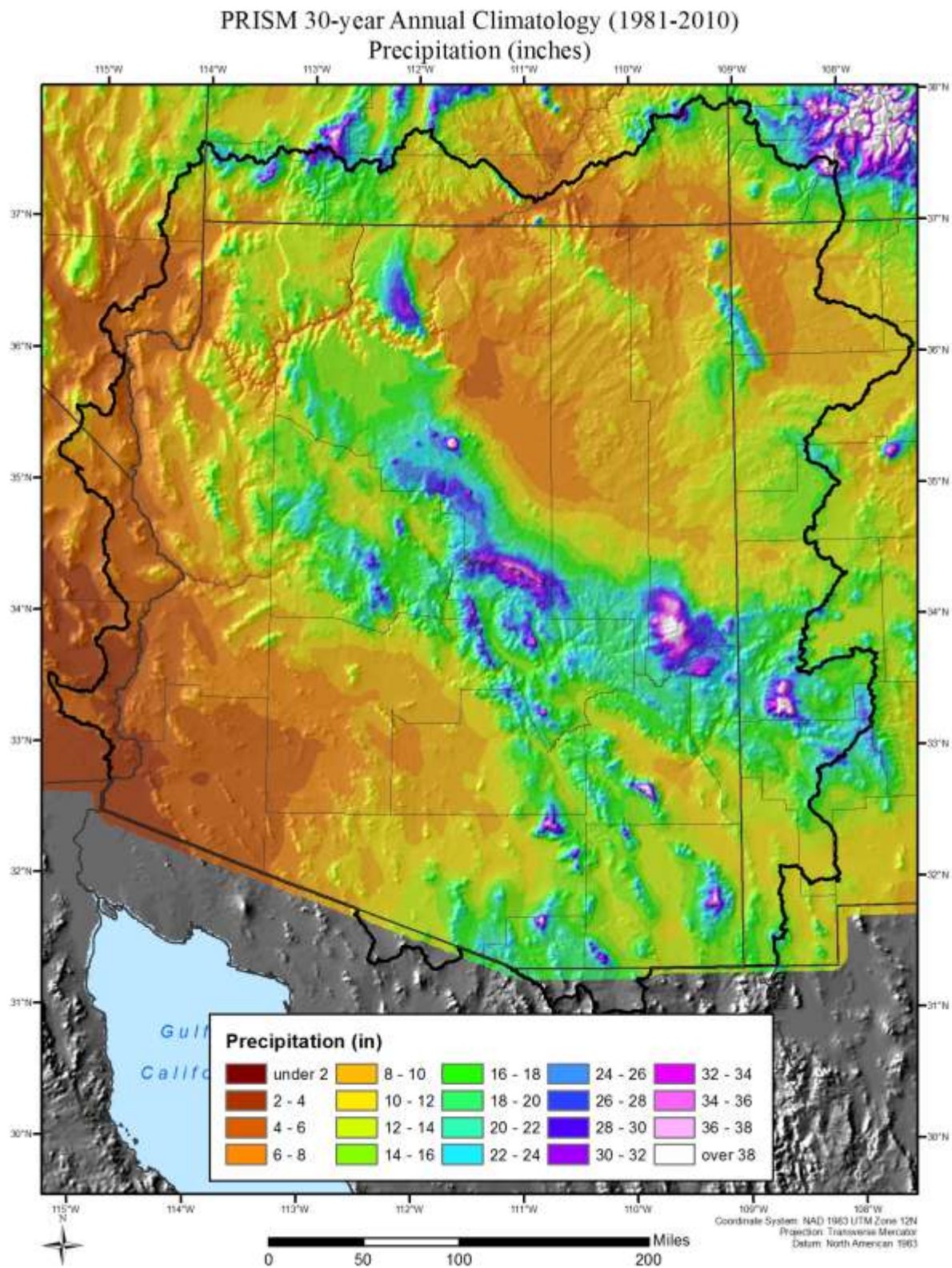
Figure 2.1c PRISM 30-year annual climatology – precipitation totals

13
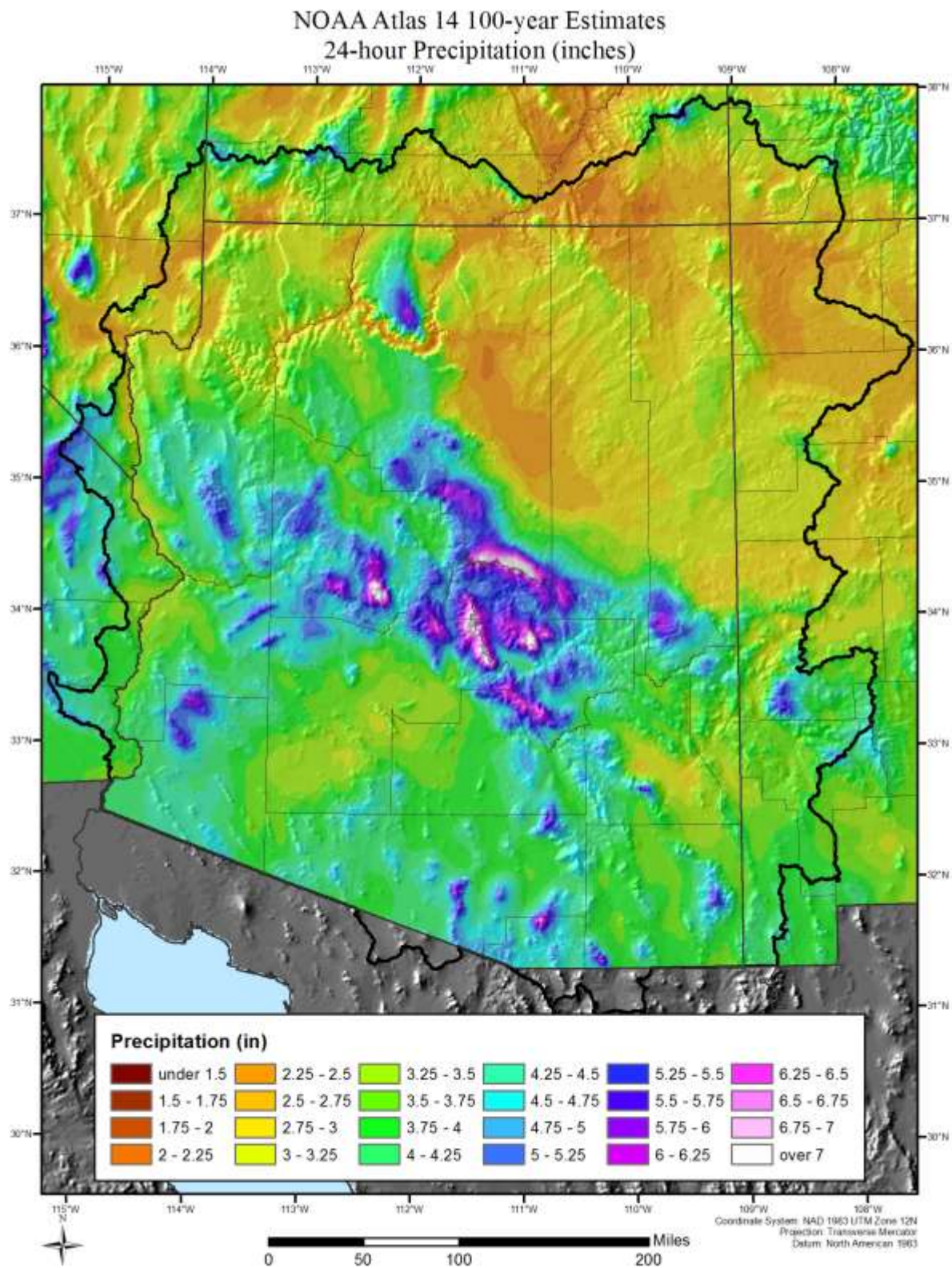
Figure 2.2 NOAA Atlas 14 100-year 24-hour precipitation frequency estimates

2.1   General Climate of Arizona

Exposure to Gulf of California moisture surges, Eastern Pacific tropical systems, and mid latitude winter storms interacting with the transition zone from the southern deserts to the Mogollon Rim create a unique and varying weather pattern across the region. There is a distinct bi-modal seasonal precipitation regime for much of the state, where general frontal winter storms bring precipitation from November through early March while the North American Monsoon (NAM) brings convective rainfall from early July through September. The general frontal winter storms are large-scale storms which often bring rain and snow to much of Arizona over periods of several days. Once the jet stream begins to lift further north during Spring, almost no precipitation occurs from April through late June. This dryness turns quickly to wet conditions beginning in early July when the NAM sets up, an almost daily occurrence of thunderstorms brings locally intense but short duration rainfall to many areas of the state. This pattern shift usually takes place in late June or early July and is signaled by a steady increase in dew point temperatures and thunderstorm activity. The NAM pattern normally lasts through September, sometimes extending into October.

On rare occasions this monsoon pattern can be enhanced by the passage of a decaying tropical system that moves out of the Eastern Pacific and north over the Gulf of California. This type of storm is responsible for the most extreme rainfalls on the synoptic scales (24-hours or longer covering large regions of 500-square miles or more). Some of the most notable of these events occurred in 1906, 1911, 1925, 1939, 1951, 1970, 1983, and 1997. All produced extreme rainfalls throughout the Southwest.

2.2   North American Monsoon Climatology

In June the 500 mb subtropical ridge (approximately 18,000 feet) is located over northwest Mexico (Figure 2.3). As a result, the air flow across Arizona is usually from the southwest. The hot and dry weather conditions experienced across Arizona during the month of June are a direct result of the position of the 500 mb subtropical ridge and dry southwest flow.

June Mean Flow at 18,000 Feet
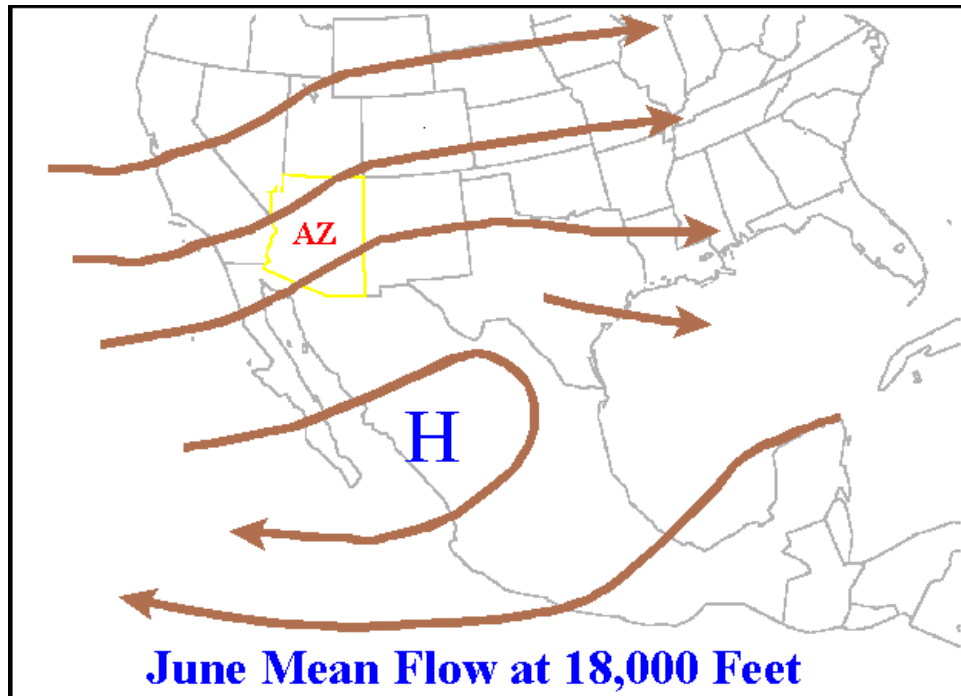
Figure 2.3 June Mean Flow at 500mb (18,000 feet) over the Southwest

Starting in late June and continuing into July, the 500 mb subtropical ridge normally shifts northward and eastward with the center of circulation located over west Texas and New Mexico (Figure 2.4). As a result easterly flow develops over northwest Mexico in the mid-levels, while hot temperatures over the continent result in a general onshore (southerly) flow in the low-levels. The shift in the 500 mb subtropical ridge is followed by a dramatic increase in thunderstorm activity over northwest Mexico. Arizona lies on the northern fringes of this area of enhanced thunderstorm activity. It is during this time that Arizona experiences periodic increases in moisture originating from the Gulf of California (Gulf Surges) and the eastern tropical Pacific. This enhanced moisture often produces thunderstorms (Douglas 1993, Hales 1972).

July Mean Flow at 18,000 Feet
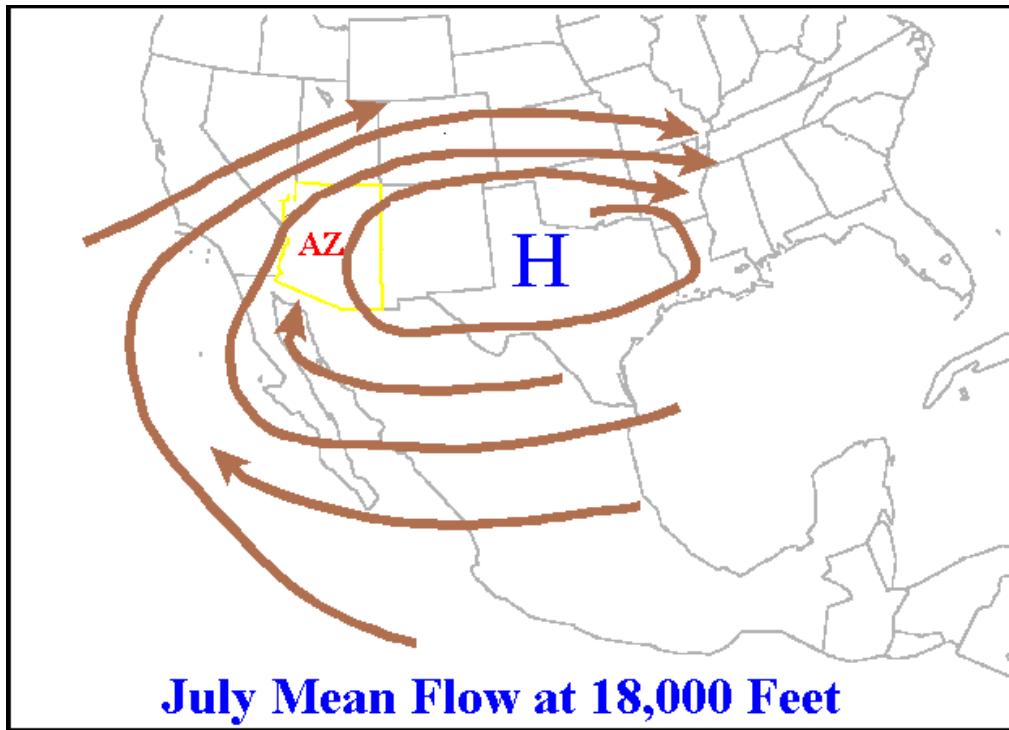
Figure 2.4 July Mean Flow at 500mb (18,000 feet) over the Southwest

Figure 2.5 shows the generalized surface synoptic conditions and moisture source regions that are found during the NAM season. Notice the positioning of the areas of high and low pressure and the attendant circulations around these features. This leads to an average wind inflow from the south/southwest, up the Gulf of California and into Arizona thereby supplying the low level moisture necessary to fuel the intense thunderstorm activity during the NAM season. For more detailed descriptions of the NAM see Grantz et al. 2007, Higgins et al. 2003, Higgins et al. 1999, Adams and Comrie 1997, Higgins et al. 1997, Douglas 1995, Douglas 1993, Smith 1989, and Hales 1972.

Figure 2.5 Generalized surface synoptic patterns associated with the NAM season (from
http://www.wrh.noaa.gov/twc/monsoon/monsoon_info.php, accessed May 2013)

2.2.1   Local Convective Storms

Thunderstorms are an almost daily occurrence once the NAM season sets in, usually
starting in late June or early July (see Section 2.2). Often, the first indicator that severe
convective weather will soon develop is the presence of a "Gulf Surge" of low-level moisture
which often precedes storm development by several hours (Green 2003). Most of the storms
have a life cycle of less than three hours. Storm initiation generally occurs over the elevated
terrain of the Mogollon Rim. Storms then move west and south reaching the lower deserts by
early evening. Additionally, drainage winds and outflow boundaries associated with terrain and
thunderstorm activity converge with hot, moist, and unstable air to initiate thunderstorms over
the lower elevations (Wallace 1999). Environments with exceptionally high atmospheric
moisture levels combine with lift from a short wave trough or area of low pressure moving
through the region to produce storms that can last longer and produce large amounts of rain (1-2
inches per hour for several hours) over the region.

2.2.1.1   Mesoscale Convective Systems

Mesoscale Convective Systems (MCS) are capable of producing extreme amounts of precipitation at short durations and over small area sizes. Although this storm type is not common in the region, they can and do occur. The terrain in the region plays an important role in thunderstorm initiation and propagation during an event (McCollum 1995). Generally, MCSs in Arizona occur with much less frequency, are of shorter duration, and generally produce less rainfall, than their Midwestern counterparts.

The current name of MCS was applied in the late 1970's to these type of "flood producing" strong thunderstorm complexes (Maddox 1980). For Arizona, the term MCS refers to any precipitation system with a spatial scale of 10- to 350-square miles that includes deep convection during part of its life-cycle (Zipser 1982). Mesoscale systems are so named because they are small in areal extent (10s to 100s of square miles), whereas synoptic storm events are 100s to 1000s of square miles. The MCSs also exhibit a distinctive signature on satellite imagery where they show rapidly growing cirrus shields with very high cloud tops. Further, the cirrus shields produced by an MCS usually take on a nearly circular pattern with constantly regenerating thunderstorms fed by moist low-level jet inflow.

Climatologically, MCSs primarily form during the NAM months from late June through September. They are most common from mid-July through mid-August.

2.3   Remnant Tropical Storms

On rare occasions decaying tropical storms have directly affected portions of the state. By the time this type of storm moves this far inland away from its energy source (the Gulf of California and the eastern tropical Pacific), it has lost many of its tropical characteristics. However, high levels of moisture are associated with these storms, enabling them to produce heavy rainfall (HMR 50, Section 2.0). Remnant moisture from these decaying tropical systems has produced some of the largest rainfalls on record throughout Arizona. Classic examples of this storm type are the remnants of Hurricane Norma which brought torrential rains across much of the Four Corners region from September 4-7, 1970. This storm event produced 11.40 inches of rainfall in 24-hours at Workman Creek, AZ which nearly doubled the previous state 24-hour rainfall record (Hansen 1981). A more recent example was the remnants of Hurricane Nora, which produced the new 24-hour state record rainfall for Arizona on September 25-26, 1997 when 11.97 inches fell at Harquahala Mountain. Both of these storms were analyzed as part of this PMP study. Details of these storm analyses are given in Appendix F.

2.4   General Frontal Systems

The polar front and jet stream, which separate cool, dry Canadian air to the north from warm, moist air to the south, sometimes produces heavy rainfall in the region. The frontal systems which develop along this boundary and traverse from west to east with the jet stream contribute large amounts of energy and storm dynamics to weather systems that move through the region. These features are strongest and most active over the region from late fall through early spring.

This type of storm environment (general frontal) will usually not produce high rainfall rates, but produce flooding as moderate rain continues to fall over the same regions for an extended period of time. Often the rainfall can fall on significant snowpack in mountainous locations resulting in large runoff volumes. The series of storm systems that led to record flooding on several rivers during January and February of 1993 are an excellent example of this type of storm environment (House 1997).

2.5   Seasonality of Extreme Storm Events

Once the monsoon pattern sets up in late June or early July, rainfall can be a daily occurrence through the end of summer and early fall. In July and August alone, up to one third of the annual precipitation over and around many locations of central and southern Arizona accumulates. The lull in storm activity between the general frontal storms of winter and the NAM, especially in the spring, shows up well in the seasonality charts for each of the storm types identified in this study (Figures 2.6, 2.7, and 2.8).

Once again the bimodal seasonality of the storm occurrences is evident, with almost all of the NAM local convective storms occurring in July, August, and September and the majority of the general winter storms occurring from December through March. The remnant tropical storms are superimposed upon the NAM rainfall, occurring exclusively from August through October.
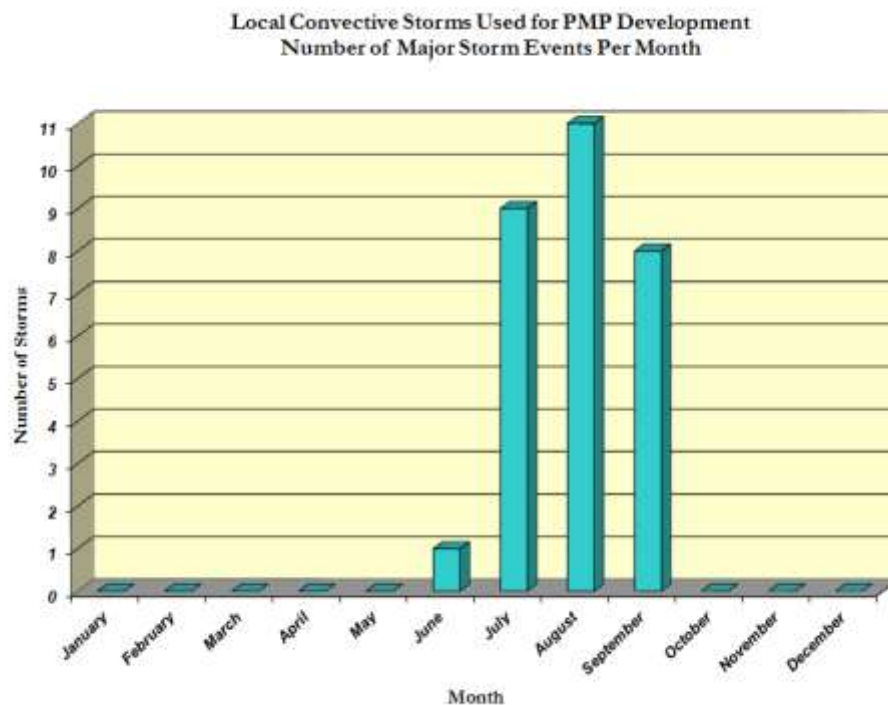
Figure 2.6 Local convective storm seasonality of the storms analyzed during the statewide study
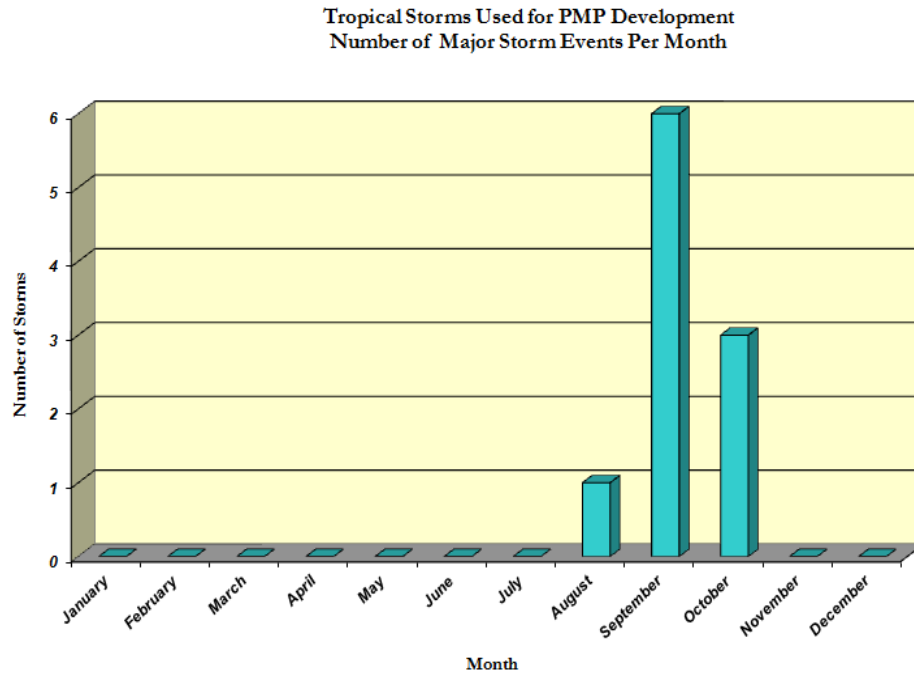
Figure 2.7 Remnant tropical storm seasonality of the storms analyzed during the statewide study
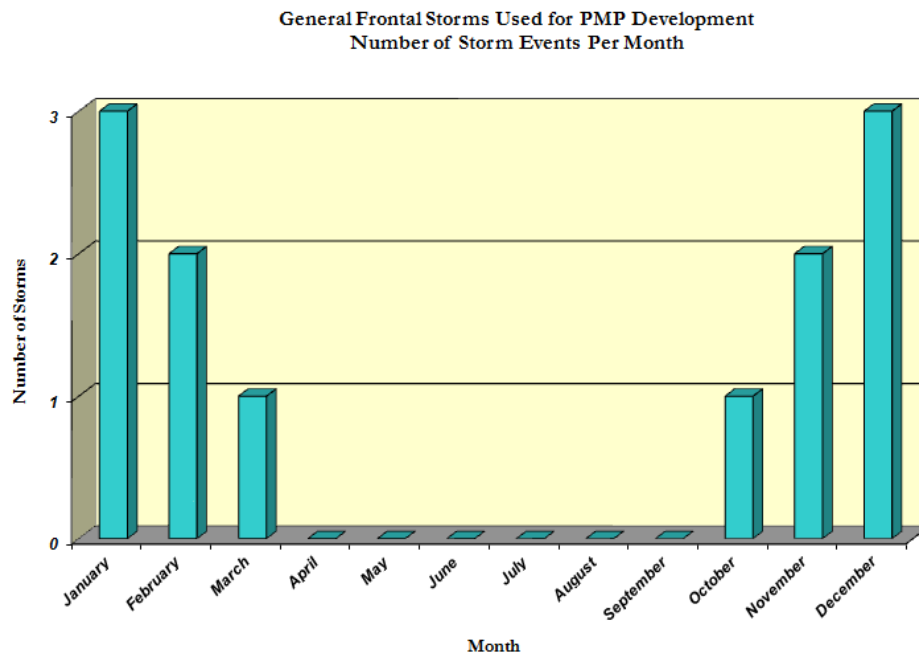
Figure 2.8 General winter storm seasonality of the storms analyzed during the statewide study

21

3. Topographic Effects on PMP Rainfall

The terrain within the state of Arizona varies significantly, often over relatively short distances (Figure 3.1). When a basin has intervening elevated terrain features that deplete some of the atmospheric moisture available to storms before reaching a basin, these must be taken into account during the storm maximization process. Conversely, when a basin includes terrain which enhances the lift in the atmosphere and increases the conversion of moisture to liquid and ice particles, precipitation processes are enhanced. To account for the enhancements and reductions of precipitation by terrain features, called orographic effects, explicit evaluations were performed. This was completed using the NOAA Atlas 14 precipitation amounts to derive the OTF. This approach is similar to what was used in recent HMRs 57 and 59 (Hansen, 1994; Corrigan, 1999) for evaluating barrier heights and orographic effects in topographically significant regions. However, the OTF procedure is significantly more objective and reproducible than the HMR procedure.
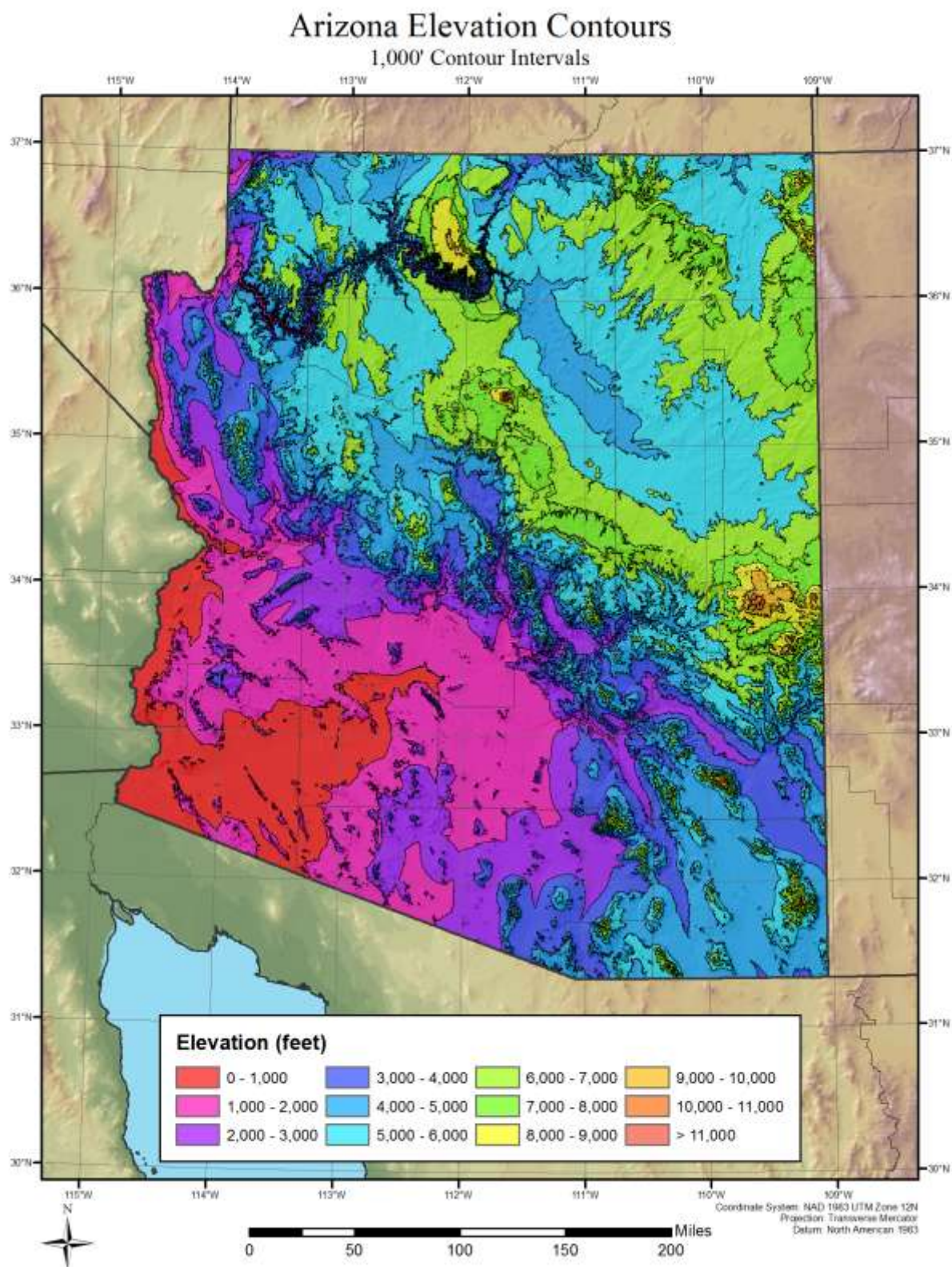
Figure 3.1 1,000-foot elevations contours over Arizona

3.1 Orographic Effects

Orographic effects on rainfall are explicitly captured in climatological analyses. Although the orographic effects at a particular location may vary from storm to storm, the overall effect of the topographic influence is inherent in the climatology of storms that have occurred over various locations, assuming that the climatology is based on storms of the same type being analyzed. For Arizona, extreme storm events (PMP-type storms) include local convective thunderstorms, remnant tropical storms, and general frontal storms. Local convective thunderstorms dominate the precipitation frequency climatology at durations of 6 hours or less, while the remnant tropical systems and general frontal storms are responsible for the precipitation frequency climatology for durations of 12 hours and greater. Hence, climatological analyses of these storms should adequately reflect the differences in topographic influences at different locations when evaluated by storm type and duration.

The procedure used in this study to account for orographic effects determines the differences between the climatological data at the in-place storm location and the individual grid cell. By evaluating the rainfall values for a range of return frequencies at both locations, a relationship between the two locations was established. For this study, precipitation frequency maps developed as part of NOAA Atlas 14, Volume 1 (Bonnin et al. 2004) and NOAA Atlas 14, Volume 8 (Perica et al. 2013) were used to evaluate the orographic effects.

The NOAA Atlas 14 precipitation frequency estimates utilize data from the mean annual maximum grids developed using the Oregon State University Climate Group's PRISM system to help spatially distribute the values between data points (Perica et al. 2011). PRISM is a peer-reviewed modeling system that combines statistical and geospatial concepts to evaluate gridded rainfall with particular effectiveness in orographic areas (Daly et al. 1994, 1997). NOAA Atlas 14 precipitation frequency estimates implicitly express orographic controls through the adoption of the PRISM system. This study assumes the relationship between precipitation frequency dataset values in areas of similar atmospheric characteristics reveal a quantifiable orographic effect and that terrain influence drives the variability in the relationship between NOAA Atlas 14 datasets at two distinct point locations.

The orographically adjusted rainfall for a given storm at a target (grid cell) location may be calculated by applying a coefficient of proportionality, determined by the relationship between a NOAA Atlas 14 data series at the source storm location and the corresponding NOAA Atlas 14 data series at the target location. For the transposition of a single grid cell at a given duration, the orographic relationship is defined as the linear relationship between the NOAA Atlas 14 values, at that duration, over a range of recurrence intervals. This study evaluates the trend of precipitation frequency estimates through the 10-, 25-, 50-, 100-, 200-, 500-, and 1,000-year average recurrence intervals. The relationship between the target and the source can be expressed as a linear function with x as the independent variable and y as the dependent variable as shown in Equation 3.1.

$$P_o = mP_i + b \qquad\qquad \text{Equation 3.1}$$

where,

Po	=	orographically adjusted rainfall (target)
Pi	=	SPAS-analyzed in-place rainfall
m	=	proportionality coefficient (slope)
b	=	transposition offset (y-intercept)

Equation 3.1 provides the orographically transpositioned rainfall depth, as a function of the in-place rainfall depth. The in-place rainfall depth used to calculate the orographically transpositioned rainfall corresponds, in duration, to the NOAA Atlas 14 datasets used (i.e., 3-hour for local storms and 24-hour for general and tropical storms). To express the orographic effect as a ratio, or OTF, the orographically adjusted rainfall (P_o) is divided by the original source in-place rainfall depth (P_i). It is assumed the orographic effect for a given transposition scenario will remain constant over the durations analyzed. Therefore, the 3-hour OTF determined for local storms, or the 24-hour OTF determined for general and tropical storms, is valid for any other analyzed duration for the given storm type.

The orographic relationship can be visualized by plotting the average NOAA Atlas 14 depths for the grid point at the source location on the *x*-axis and the NOAA Atlas 14 depths for the grid point at the target location on the *y*-axis, then drawing a best-fit linear trend line among the seven return frequency data points. The trend line describes the general relationship between the NOAA Atlas 14 values at the grid location and the values at the storm location. As an alternative to producing the best-fit linear trendline graphically, linear regression can be used to apply the function mathematically. An example of the determination of the orographic relationship and development of the OTF is given in Section 8.4.

3.2 Procedure for Determining Precipitation Frequency Estimates for Mexico

A continuous coverage of NOAA Atlas 14 precipitation frequency estimates were needed to produce orographic transposition factors for the entire extent of the study domain. The analysis domain extends beyond the NOAA Atlas 14 Semiarid Southwest and Midwest coverage into a few small areas in Northern Mexico (Figure 3.2).
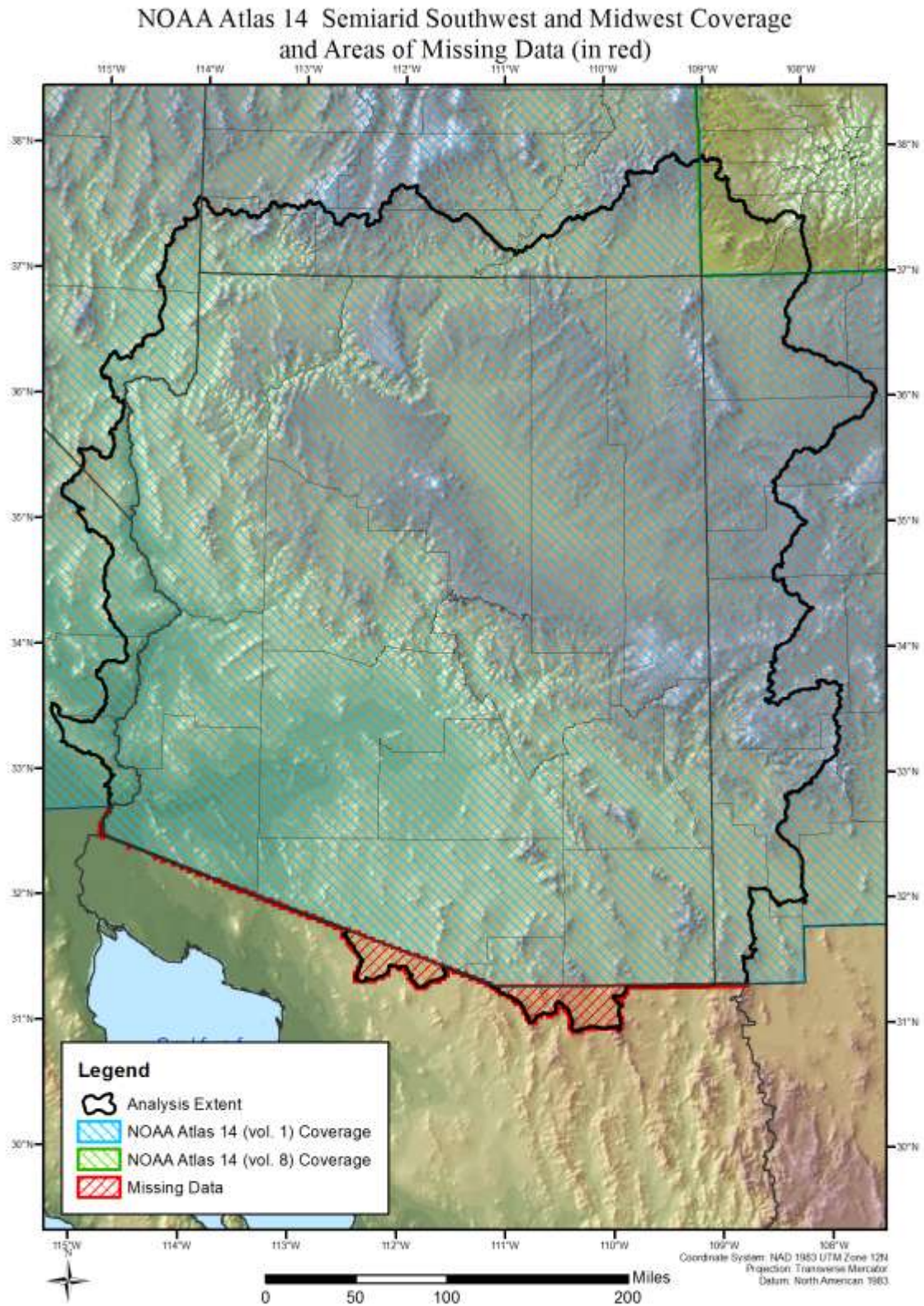
Figure 3.2 NOAA Atlas 14 Midwest and Southwest coverage with areas of missing data

For completeness, it was necessary to estimate the 3-hour and 24-hour precipitation depths at the 10-, 25-, 50-, 100-, 200-, 500-, and 1,000-year recurrence intervals for the areas without NOAA Atlas 14 data. GIS was used to extrapolate the existing NOAA 14 values over the regions without NOAA Atlas 14 values.

The precipitation frequency values in these areas without NOAA Atlas 14 data were estimated using a least squares regression analysis of the relationship between existing NOAA Atlas 14 values and the underlying elevation. The transposition zones (discussed in Section 7.3) were used to classify the terrain underlying these areas in terms of the terrain underlying the known areas. The regions in Northern Mexico are the most topographically similar to transposition zones 1 and 2, southern Arizona. The grid cells in these zones were grouped into 500' elevation classes. Then, for all the cells in each elevation class, the averages of the known NOAA Atlas 14 values were calculated (Table 3.1).

Table 3.1 Average known precipitation frequency estimates for zones 1 & 2 classified by elevation

Zone 1 & 2 Average 3-hour NOAA Atlas 14 Values (in inches) Classified by Elevation								
Elevation Class	COUNT	10-year	25-year	50-year	100-year	200-year	500-year	1000-year
1,000	3031	1.55	2.04	2.45	2.90	3.41	4.18	4.86
1,500	2422	1.61	2.04	2.40	2.78	3.20	3.82	4.34
2,000	1955	1.67	2.10	2.44	2.81	3.20	3.77	4.25
2,500	1600	1.72	2.13	2.45	2.80	3.17	3.69	4.12
3,000	1135	1.79	2.19	2.50	2.84	3.19	3.68	4.09
3,500	987	1.84	2.24	2.55	2.88	3.22	3.71	4.09
4,000	1313	1.87	2.27	2.58	2.91	3.25	3.73	4.11
4,500	2276	1.86	2.25	2.56	2.89	3.23	3.71	4.10
5,000	1866	1.90	2.30	2.62	2.96	3.31	3.80	4.19
5,500	1117	1.94	2.35	2.67	3.01	3.37	3.86	4.26
6,000	575	1.94	2.35	2.67	3.01	3.37	3.86	4.26
6,500	314	1.96	2.37	2.70	3.04	3.39	3.88	4.28
7,000	122	2.09	2.52	2.86	3.22	3.59	4.10	4.52
7,500	63	2.25	2.71	3.08	3.46	3.85	4.39	4.83
8,000	22	2.47	2.97	3.37	3.78	4.20	4.78	5.25
8,500	16	2.45	2.95	3.34	3.74	4.16	4.73	5.19
9,000	8	2.45	2.94	3.33	3.73	4.15	4.71	5.17
9,500	2	2.55	3.06	3.46	3.88	4.30	4.89	5.36
10,000	2	2.41	2.90	3.28	3.67	4.08	4.63	5.07
10,500	2	2.53	3.03	3.42	3.83	4.24	4.80	5.25

The next step was to determine the elevation for each underlying grid cell. The Global Multi-resolution Terrain Elevation Dataset 2010 elevation dataset provided elevations at the grid cell centroids. Linear regression was used to estimate the NOAA Atlas 14 value over each grid cell using the least squares criterion. This was accomplished in an Excel spreadsheet using the Trend function with the elevation classes as the known x values and the corresponding average precipitation frequency values as the y values.

The resulting precipitation frequency values for the grid cells without NOAA Atlas 14 values were merged with the existing values to create a complete continuous dataset over the study area. Figures 3.3 and 3.4 illustrate the estimated precipitation frequency values merged with the known 100-year NOAA Atlas 14 values for the 3-hour and 24-hour durations, respectively.

Reproduction of the rigorous analysis procedures used to determine the NOAA Atlas 14 values for the relatively small areas of missing data was not feasible within the scope of this study. The procedure implemented in this study provides a reasonable estimate of NOAA Atlas 14 values for the areas without data based on the approximate elevation/precipitation relationships.

This estimation method was also applied to the Semiarid Southwest NOAA Atlas 14 (vol. 1) to estimate values for Southwestern Colorado. After the publication of the Midwest NOAA Atlas 14 (vol. 8), the precipitation frequency values were compared to the estimated values over Colorado. Figures 3.5 and 3.6 display the results of these comparisons. The results show good agreement between the two data sets and confirm that the estimation method adequately captures the variations of the precipitation frequency values in the areas without explicit NOAA Atlas 14 climatologies. In the future, if NOAA Atlas 14 values (or similar data) are published for the regions of Mexico, the orographic transposition analysis could be reproduced using the updated datasets for greater certainty.
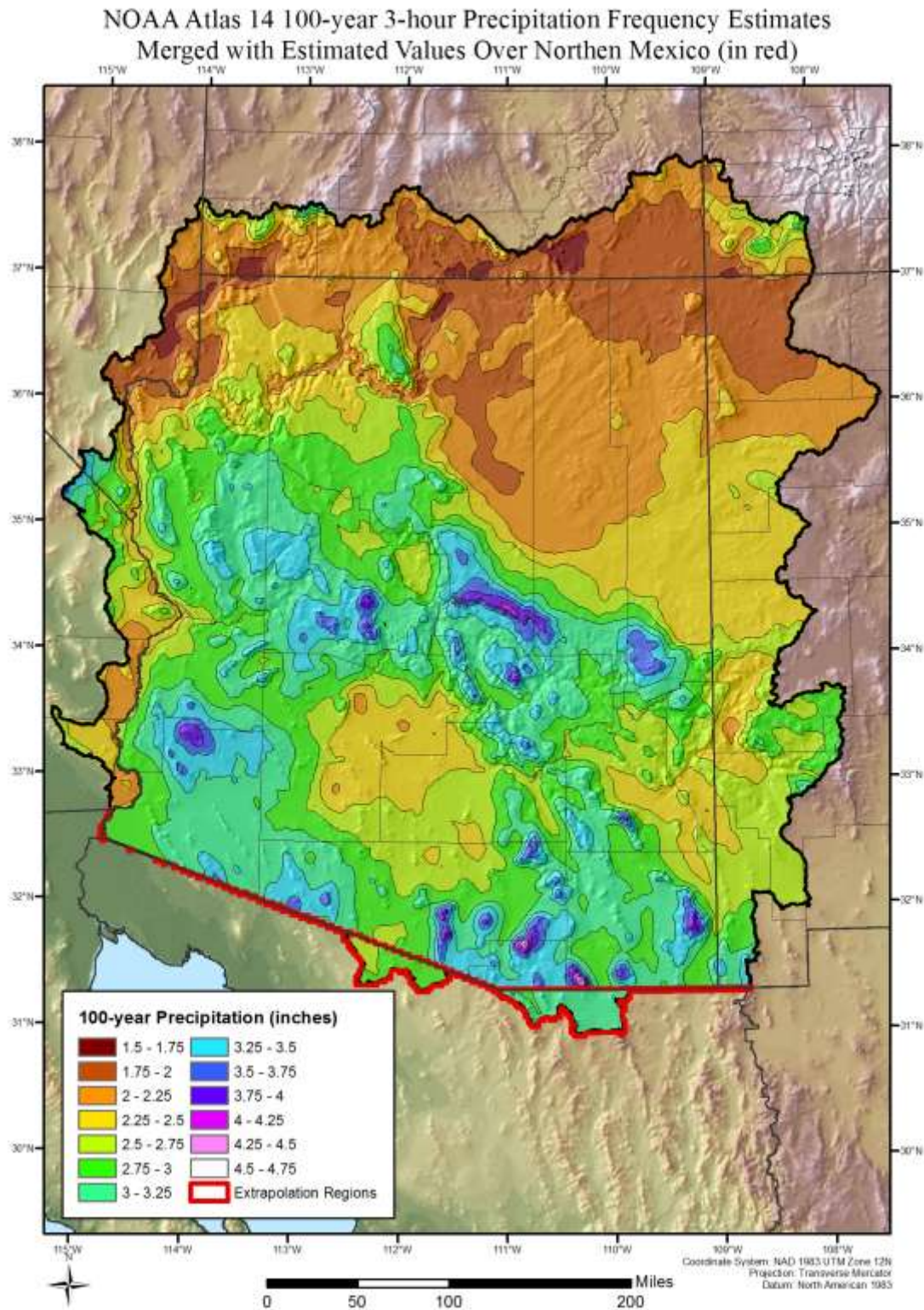
Figure 3.3 NOAA Atlas 14 100-year 3-hour precipitation values merged with estimated 3-hour values over Northern Mexico
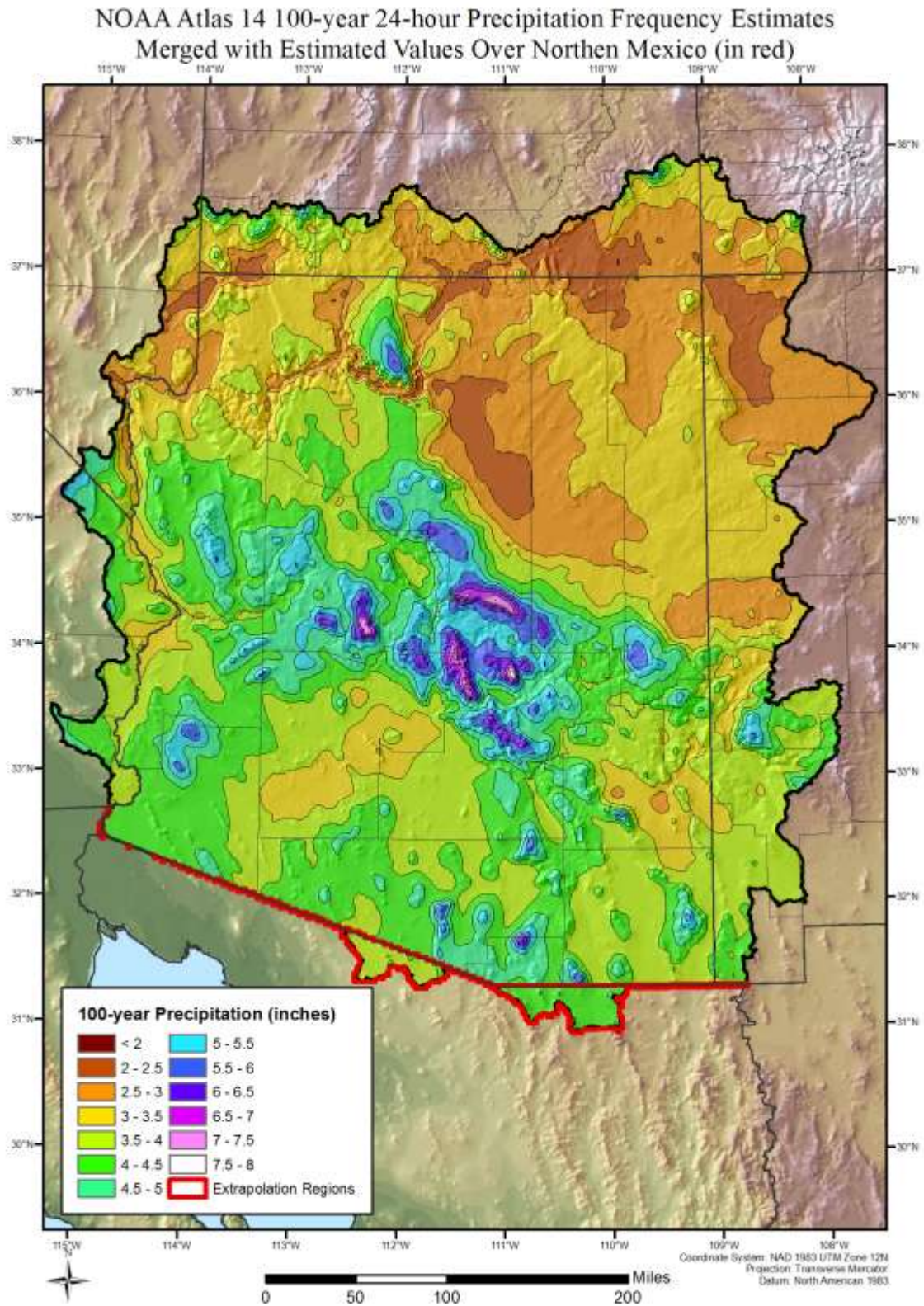
Figure 3.4 NOAA Atlas 14 100-year 24-hour precipitation values merged with estimated 24-hour values over Northern Mexico
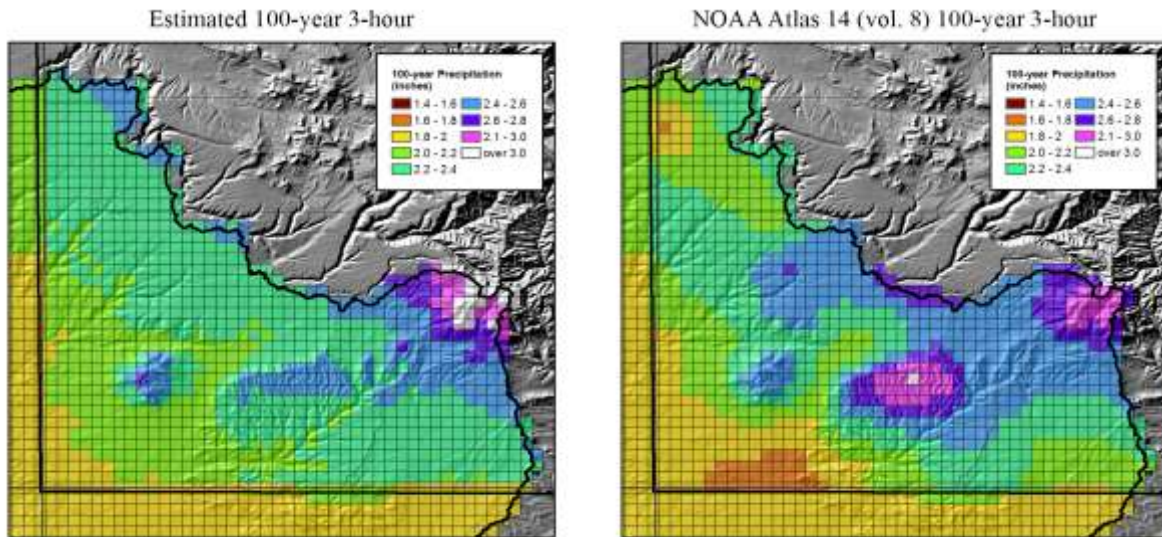
Figure 3.5 100-year 3-hour estimated precipitation depths vs. NOAA Atlas 14 (vol. 8) Midwest
Precipitation Frequency Estimates
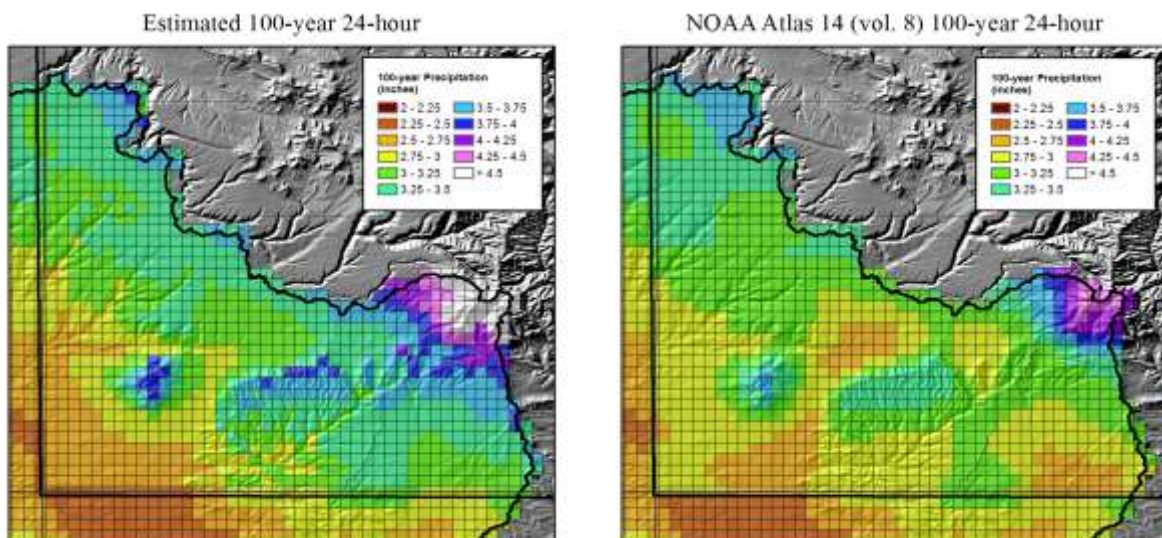
Figure 3.6 100-year 24-hour estimated precipitation depths vs. NOAA Atlas 14 (vol. 8) Midwest
Precipitation Frequency Estimates

4. Hybrid Single Particle Lagrangian Integrated Trajectory (HYSPLIT) Model, Maximum Average Dew Point Climatology, and Sea Surface Temperatures

This study incorporated updated procedures and data analysis methods used in other PMP studies completed by AWA but were not in the development of the HMRs. For this study, there were improvements made through the addition of new data sets and new techniques described below.

4.1 New Data Sets

Several new data sets not used in HMRs 49 and 50 were identified. These data were used for storm maximization and moisture transpositioning in this study. The identification and use of these data sets provide a significant improvement in storm rainfall adjustments, especially relating to the determination of each storm's moisture source and derivation of appropriate maximization factors.

4.1.1 HYSPLIT Trajectory Model

The HYSPLIT trajectory model (Draxler and Rolph, 2003; Draxler and Rolph, 2010) was used to evaluate moisture inflow vectors for all of the short list storms that occurred since 1948. Use of a trajectory model provides increased confidence for determining inflow vectors and storm representative dew points/SSTs. The HYSPLIT model trajectories have been used to analyze the moisture inflow vectors in other PMP studies since 2005. During these analyses, the model trajectory results were verified and the utility explicitly evaluated by several Board of Consultants.

HYSPLIT was used during the analysis of each of the rainfall events that occurred since 1948 and used for determination of maximization factors in this study. The HYSPLIT model was used to determine the trajectory of the moisture inflow for various levels in the atmosphere associated with the storm's rainfall production. This replaces the subjective procedures employed in the HMRs in determining the moisture inflow trajectory using individual surface and upper air maps. The HYSPLIT model was run for trajectories at several levels of the lower atmosphere to capture the moisture source for each storm event. These included 700mb (approximately 10,000 feet) and 850mb (approximately 5,000 feet) as well as the surface elevation at the storm center location. For the majority of the analyses, the surface and 850mb levels were determined to be most appropriate for use in evaluating the upwind moisture source location. Meteorologically, this makes sense as the vast majority of atmospheric moisture available to produce precipitation is contained in the lowest 10,000 feet of the atmosphere.

It is important to note that the resulting HYSPLIT model trajectories are only used as a general guide to identify the moisture source for storms in both space and time. The final determination of the storm representative dew point/SST location is determined following the standard procedures used by AWA in previous PMP studies and as outlined in the HMRs and WMO manuals. Appendix F of this report lists each of the HYSPLIT model trajectories for each storm. As an example, Figure 4.1 shows the HYSPLIT trajectory model results used to analyze the inflow vector from the local convective event that occurred in September 2003 (Roosevelt Lakes, SPAS 1109).
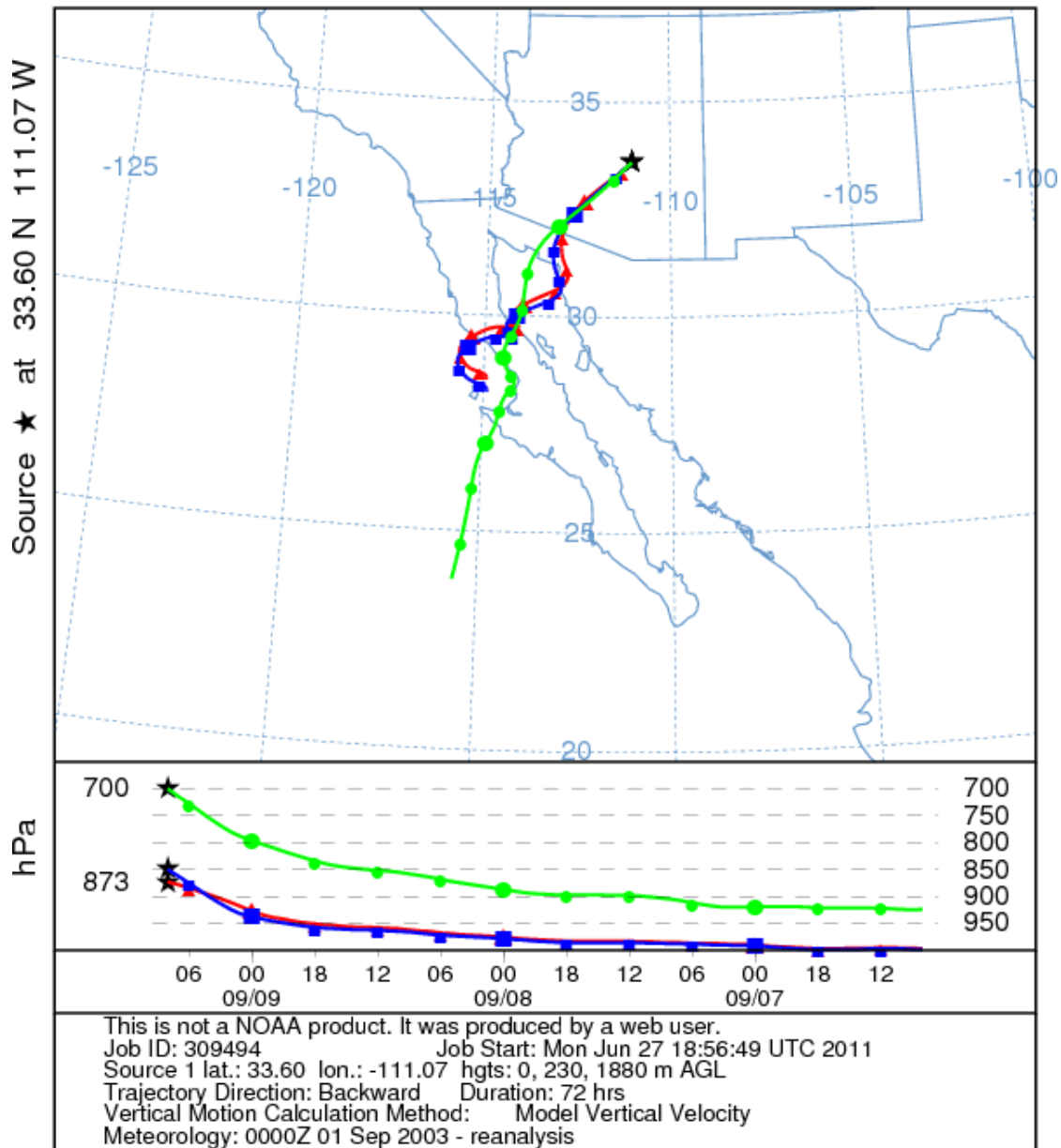
Figure 4.1 HYSPLIT trajectory model results, displaying the surface (red line), 850mb (blue line), and 700mb (green line) trajectories

4.1.2 Maximum Average Dew Point Climatology Methodology

An updated maximum average dew point climatology was developed and used in the storm maximization process. These values replace those provided in HMR 50. The initial task in the development of the updated climatology was a search of the National Climatic Data Center (NCDC) hourly stations that record hourly dew point temperature data within a defined search domain surrounding Arizona (Figure 4.2).
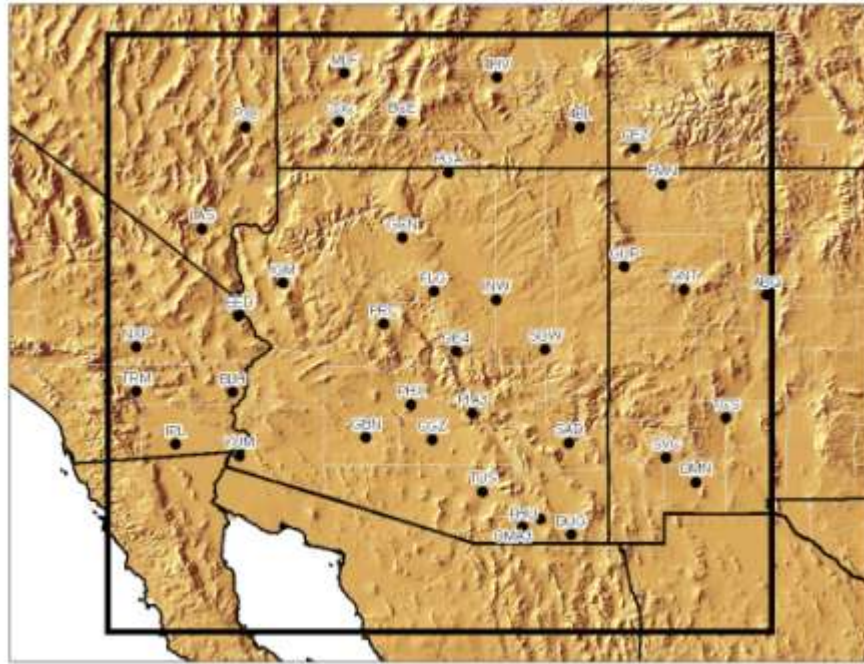
Figure 4.2 Hourly dew point station locations used for the updated maximum dew point climatology

Once these stations were identified, AWA extracted the archived NCDC hourly datasets for the maximum average 3-hr, 12-hr, and 24-hr dew point temperatures for each reporting station. A total of ninety-two hourly stations were within the search domain. These stations are listed in Table 4.1. Initial quality control (QC) limited stations to 30-years or greater period-of-record. However, five stations with less than 30-years were included to help fill in spatial gaps. After this initial QC, thirty-eight hourly stations were selected for the dew point temperature analysis. A script was written to extract each station's monthly maximum dew point temperatures for 3-, 12- and 24-hour durations for each year, providing annual maximum series (AMS) for that station. The AMS for each month for each station served as input to an R-statistical script that calculated L-moment statistics. Using the generalized-extreme-value (GEV) distribution, the 20-year, 50-year, and 100-year return frequency dew point temperature values were calculated for each month for each station. The extracted dew point data were adjusted to the 15th of each month and adjusted to 1,000mb dew point values.

Table 4.1 Stations used to derive the maximum dew point climatology for Arizona

ID	Name	State	Latitude	Longitude	Elevation	POR
4BL	BLANDING	UT	37.6167	-109.4670	6132	31
4HV	HANKSVILLE	UT	38.3667	-110.7170	4311	31
ABQ	ALBUQUERQUE	NM	35.0844	-106.6501	5314	60
BCE	BRYCE CANYON	UT	37.7022	-112.1540	7584	60
BLH	BLYTHE	CA	33.6186	-114.7140	390	31
CDC	CEDAR CITY	UT	37.7000	-113.1000	5618	60
CEZ	CORTEZ	CO	37.3000	-108.6330	5916	31
CGZ	CASA GRANDE	AZ	32.9000	-111.7000	1462	16
DMN	DEMING	NM	32.2597	-107.7200	4300	31
DUG	DOUGLAS	AZ	31.4667	-109.6000	4097	31
EED	NEEDLES	CA	34.7667	-114.6170	887	31
FHU	FT HUACHUCA	AZ	31.5833	-110.3330	4685	31
FLG	FLAGSTAFF	AZ	35.1333	-111.6670	7018	58
FMN	FARMINGTON	NM	36.7500	-108.2330	5502	59
GBN	GILA BEND	AZ	32.9333	-112.7000	866	31
GCN	GRAND CANYON	AZ	35.9500	-112.1500	6972	31
GNT	GRANTS	NM	35.1667	-107.9000	6519	31
GUP	GALLUP	NM	35.5083	-108.7930	6464	35
IGM	KINGMAN	AZ	35.2667	-113.9500	3389	31
INW	WINSLOW	AZ	35.0167	-110.7330	4883	31
IPL	IMPERIAL	CA	32.8344	-115.5750	-58	31
LAS	LAS VEGAS	NV	36.0833	-115.1670	2180	60
MLF	MILFORD	UT	38.4333	-113.0170	5033	60
NXP	29 PALMS	CA	34.2962	-116.1620	2051	21
OE4	PAYSON	AZ	34.2333	-111.3330	4915	22
OMA3	TOMBSTONE	AZ	31.7053	-110.058	4610	31
P38	CALIENTE	NV	37.6167	-114.5170	4380	25
PGA	PAGE	AZ	36.9333	-111.4500	4278	31
PHX	PHOENIX	AZ	33.4333	-112.0170	1107	60
PIA3	SUPERIOR	AZ	33.3008	-111.097	2860	31
PRC	PRESCOTT	AZ	34.6500	-112.4330	5053	60
SAD	SAFFORD	AZ	32.8500	-109.6330	3176	31
SOW	SHOW LOW	AZ	34.2667	-110.0000	6411	31
SVC	SILVER CITY	NM	32.6333	-108.1670	5443	31
TCS	TRTH OR CON	NM	33.2333	-107.2670	4858	58
TRM	THERMAL	CA	33.6319	-116.1640	-112	31
TUS	TUCSON	AZ	32.1167	-110.9330	2555	62
YUM	YUMA	AZ	32.6566	-114.6060	216	29

4.1.2.1   Procedure for Adjusting to the 15th of the Month

The station data were corrected to the 15th of each month using a linear relationship between the previous month, current month, and the next month. The 15th adjustment was performed using a series of Excel macros. The steps are listed below:

1)   Calculated the difference in days between the observed average date of the annual maximum series occurrence and the 15th.
2)   Depending whether the difference in step 1 is positive or negative (direction of adjustment) calculate the ratio/difference between the non-adjusted dew point temperature (for the months of interest) and the number of days between the dates.
3)   Applied the ratio calculated in step 2 to the difference calculated in step 1.
4)   Checked the adjusted dew point value with the previous and next month values, and the other two durations
5)   Calculated the difference between the original dew point value and the adjusted dew point value.
6)   Created station plots of the duration and frequency for additional QC measure.
7)   Created a list of the adjusted dew point values for each station in a GIS format

4.1.2.2   1000mb Adjustment Procedures

A moist lapse rate (2.7°F/1000 feet) was used to adjust the 15th of the month dew point temperature, at the station elevation, to 1,000mb (assumed to be at elevation zero, i.e. sea level). A linear relationship between elevation and lapse rate was created and applied to each station. The June 3-hr maximum average dew point data for Phoenix, AZ are shown in Table 4.2. The table shows the original station data, the data adjusted to the 15th, and the data adjusted to 1,000mb.

Table 4.2 Original dew point data, adjusted dew point data (to the 15th), and the 1000mb dew point data for 20-year, 50-year, and 100-year frequencies at Phoenix, AZ

	20-year	50-year	100-year
Station Data	69.9°F	71.4°F	72.2°F
15th Data	68.8°F	70.3°F	71.0°F
1000mb Data	71.8°F	73.3°F	74.0°F

4.1.2.3   Spatial Interpolation of Data

Maximum and minimum monthly dew point temperature PRISM grids were downloaded for the continental United States for the time period of 1971-2000. PRISM grids were used to calculate the mean monthly dew point temperature $\overline{td}_m$ for this time period:

$$\overline{td}_m = \frac{\sum\limits_{i=1}^{n} x_i}{n}$$

where m is the month of interest, n is the number of months and x_i are the monthly dew temperature values. The PRISM data were converted from degrees Celsius to degrees Fahrenheit. The mean monthly PRISM dew point data were extracted for each of the thirty-eight dew point stations.

The PRISM dew point grids did not cover the entire Arizona domain. In order to address spatial dew point estimates in Mexico, pseudo monthly dew point grids were created based on dew point elevation relationships. These new dew point grids covered the entire domain except for the southwest corner (see Figure 4.3a and b). The terrain and pseudo basemap calculations in the southwest domain were not representative and were not included in the analysis. The steps for derivation of the monthly pseudo basemaps are listed below:

1) Calculated monthly ratio between dew point and elevation, created monthly ratio grids.
2) Grew the monthly ratio grids until entire domain was covered.
3) Estimated monthly dew point grid, multiple grown ratio grid by the elevation.
4) Created a mask (based on PRISM dew point grids).
5) Patched the estimated monthly dew point grids with the PRISM dew point grids. Estimated dew point is only used were PRISM data not available.
6) Smoothed the final dew point grids. These are the grids used for spatial interpolation methods.

a   b
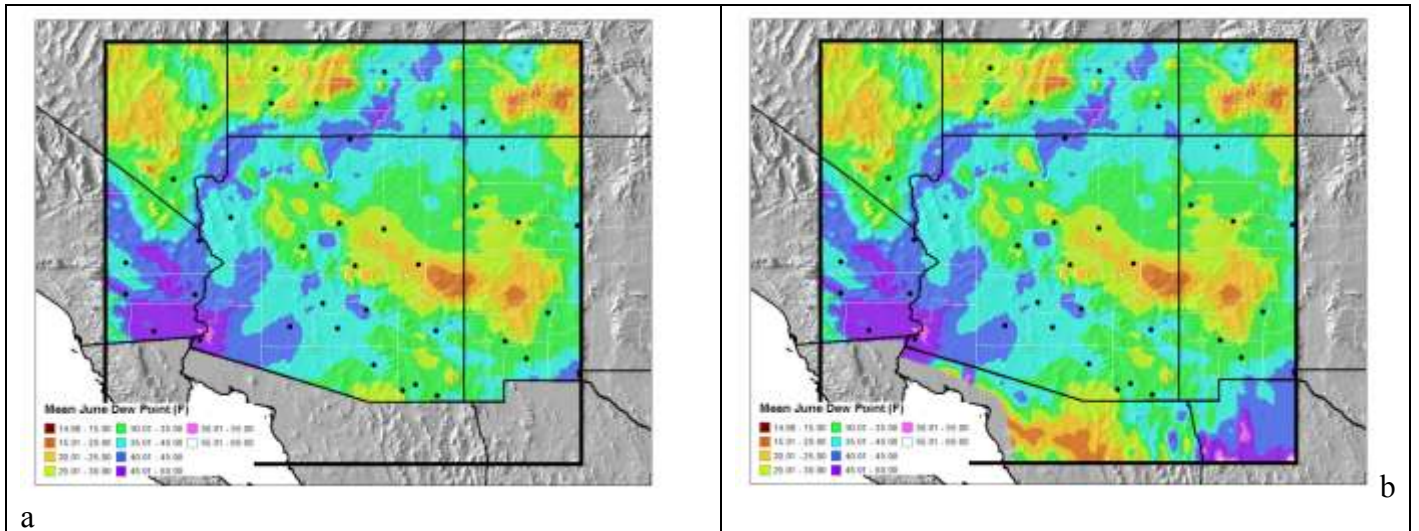
Figure 4.3 Mean June dew point (°F) a) June mean PRISM dew point b) June estimated mean pseudo dew point

Linear relationships between PRISM data (described above) and the station dew point temperature data (1,000mb) for each duration (3-, 12-, and 24-hour) and frequency (20-, 50-, and 100-year) were calculated, where *y* equals the stations dew point temperature (°F) value, and *x* equals the stations mean monthly PRISM dew point temperature (°F) value. An example of the linear relationships between mean monthly PRISM dew point data and the 100-year 24-hour dew point data for June, July, August, and September are shown in Figure 4.4.
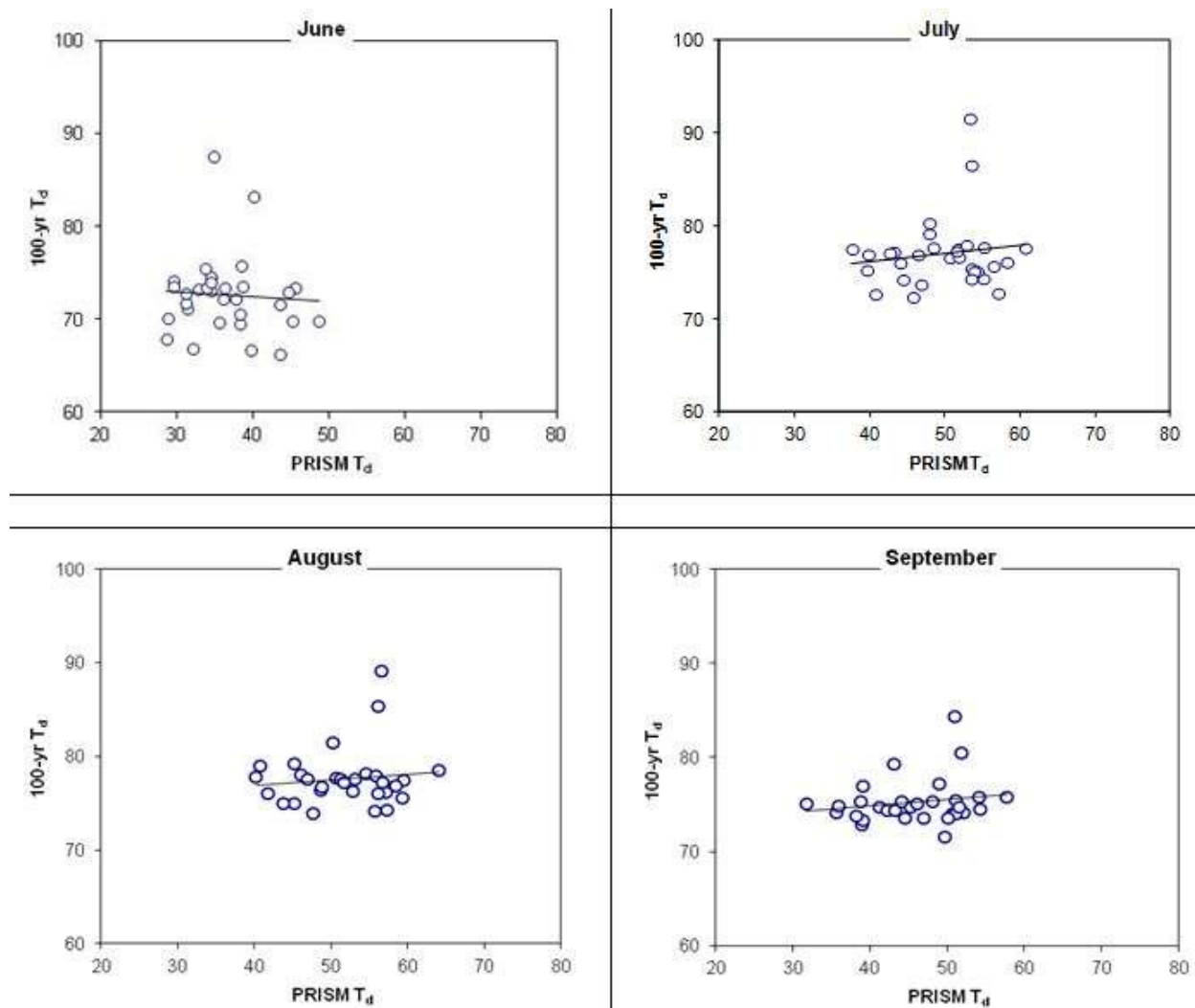
Figure 4.4 Linear relationships between mean monthly PRISM dew point data and the 100-year 24-hour dew point data for June, July, August, and September

The derived linear relationships were applied to the mean monthly dew point PRISM grids, which provided a first estimate of the dew point temperature spatial distribution. Residuals (actual – predicted) between the station and the first estimate were calculated at each station. The 100-year 24-hour dew point residuals for June, July, August, and September are shown in Figure 4.5.

The residuals were spatially distributed across the search domain using an inverse-distance algorithm. The spatially distributed residual grids were smoothed to reduce bulls-eye

38

effects. The smoothed residual grid was added to the first estimate grid to create the second estimate grid. The second estimate grids were smoothed in order to further reduce bulls-eye effects. The smoothed second estimate grids represent the final dew point temperature distribution.

The spatial interpolation method was tested and applied for the Nebraska statewide study (Tomlinson et al. 2008). Perl and R-statistical programs were used to automate the process within GRASS GIS environment. The GRASS GIS script also created 1°F dew point contours from the final interpolated dew point grids. The GRASS GIS dew point analysis and 0.5°F contours for the June, July, August, and September 100-year 24-hour are shown in Figure 4.6 a, b, c and d. The GRASS GIS dew point rasters and contour shapefiles were exported from the GRASS GIS environment to an ArcGIS environment for creation of the final dew point map layouts.

Creation of the final dew point maps used in this project was completed after manual interpretation of the automated contours and meteorological analysis by AWA. During this manual analysis inconsistencies were removed and smoothing was applied where meteorological, climatological, and topographical factors warranted such actions. Further, expertise was used to compensate for the lack of spatial coverage in some sections of Arizona and to ensure continuity between months and durations. Figures 4.7-4.9 display examples of the final dew point maps and Appendix A contains all the maps used as part of this PMP analysis and discusses in detail the need to develop the updated maximum dew point climatology for Arizona.
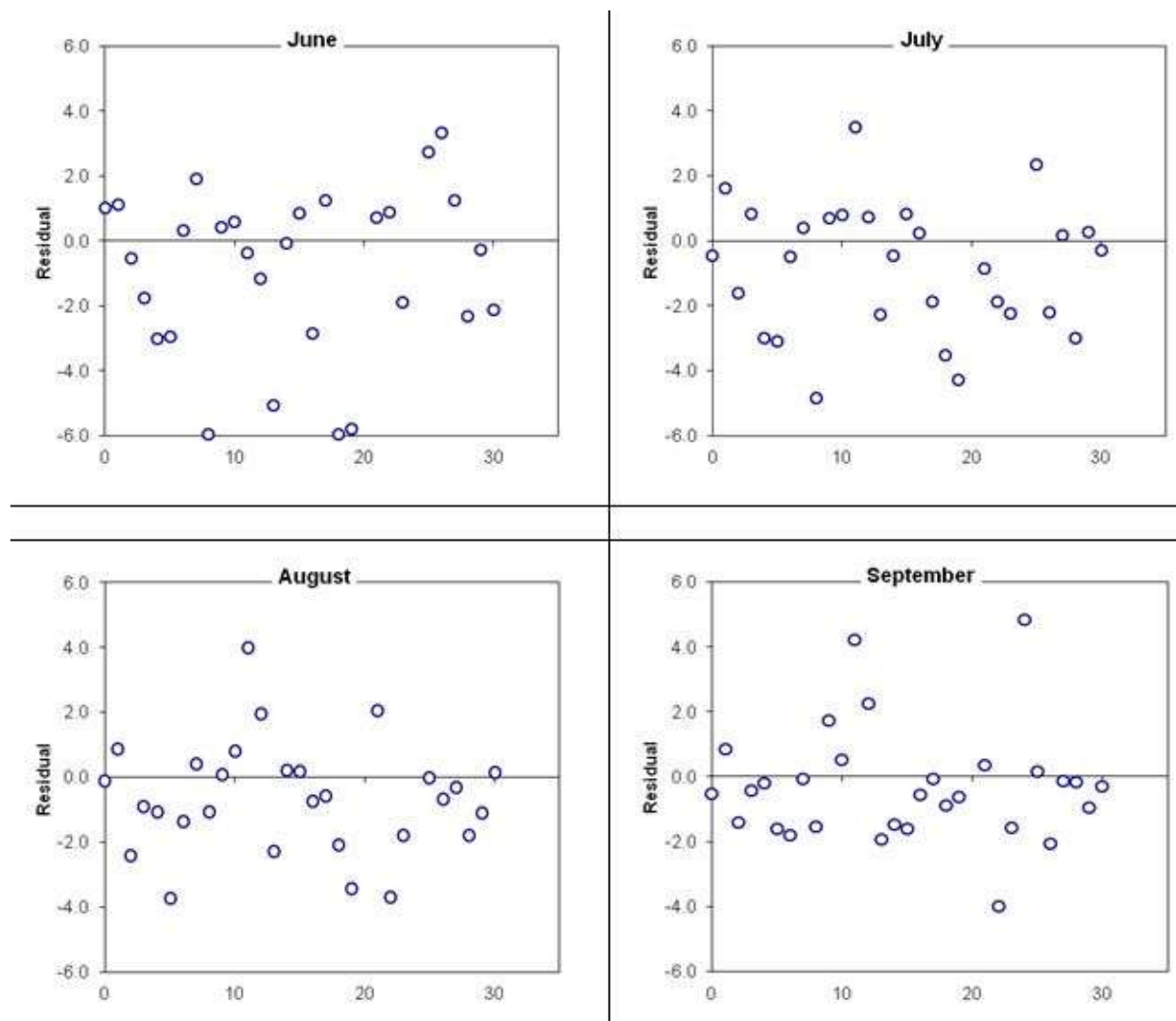
Figure 4.5 Calculated residuals between mean monthly PRISM dew point data and the 100-year 24-hour dew point data for June, July, August, and September
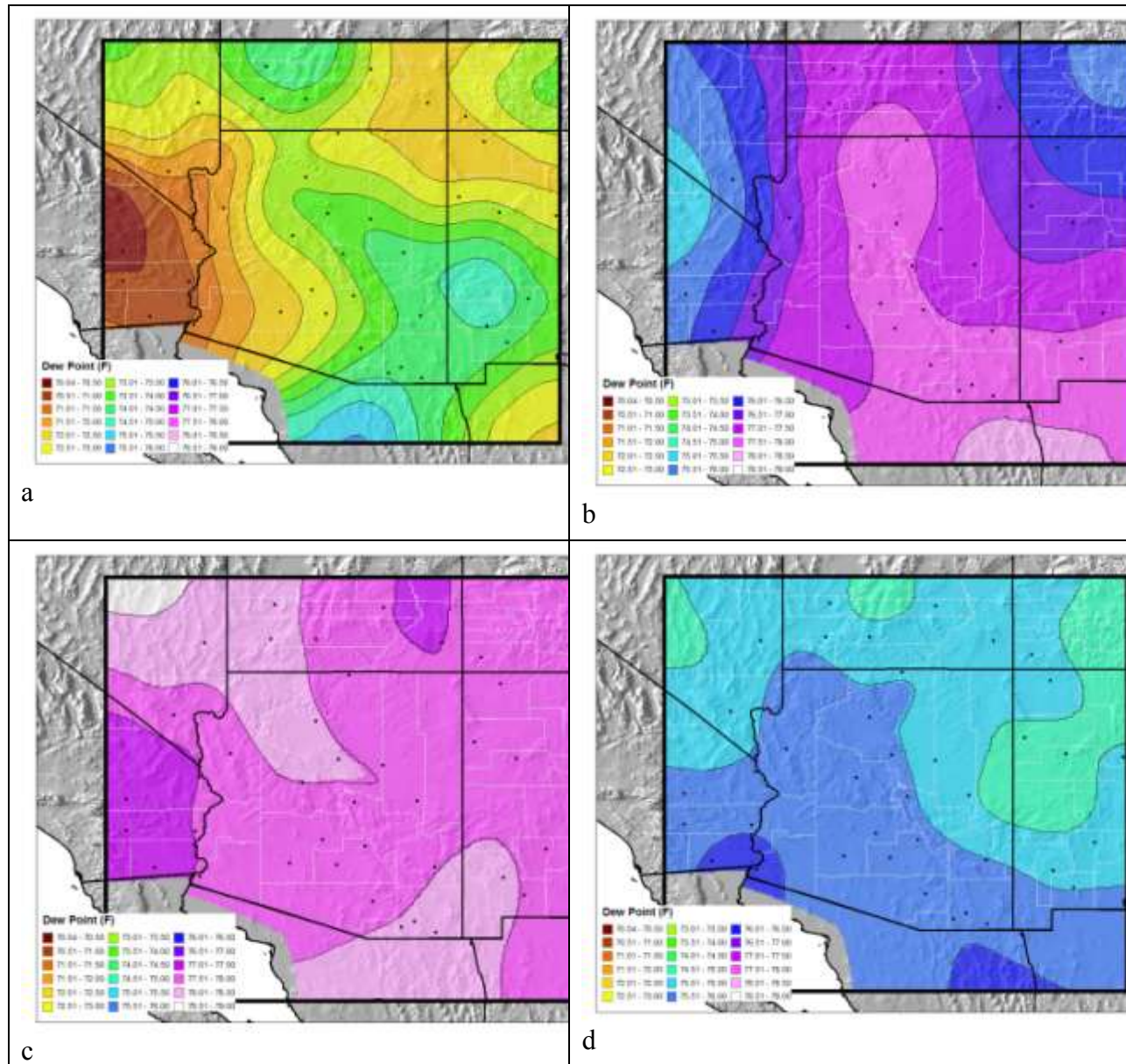
Figure 4.6 Dew point analysis, contours are at 0.5°F intervals a) June 100-year maximum average 24-hour dew point b) July 100-year maximum average 24-hour dew point c) August 100-year maximum average 24-hour dew point d) September 100-year maximum average 24-hour dew point
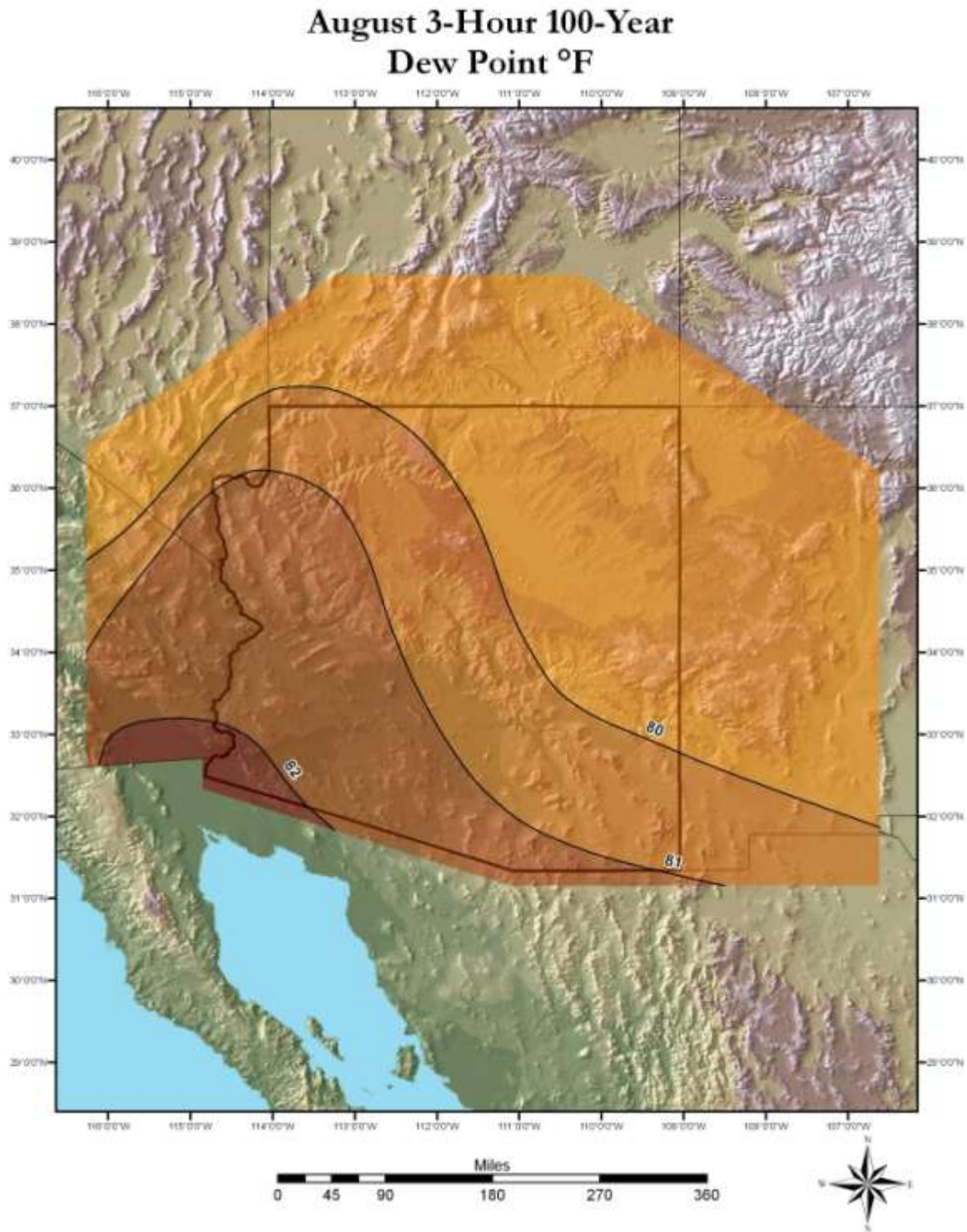
Figure 4.7 August 100-year return frequency maximum average 3-hour dew point map

September 12-Hour 100-Year
Dew Point °F
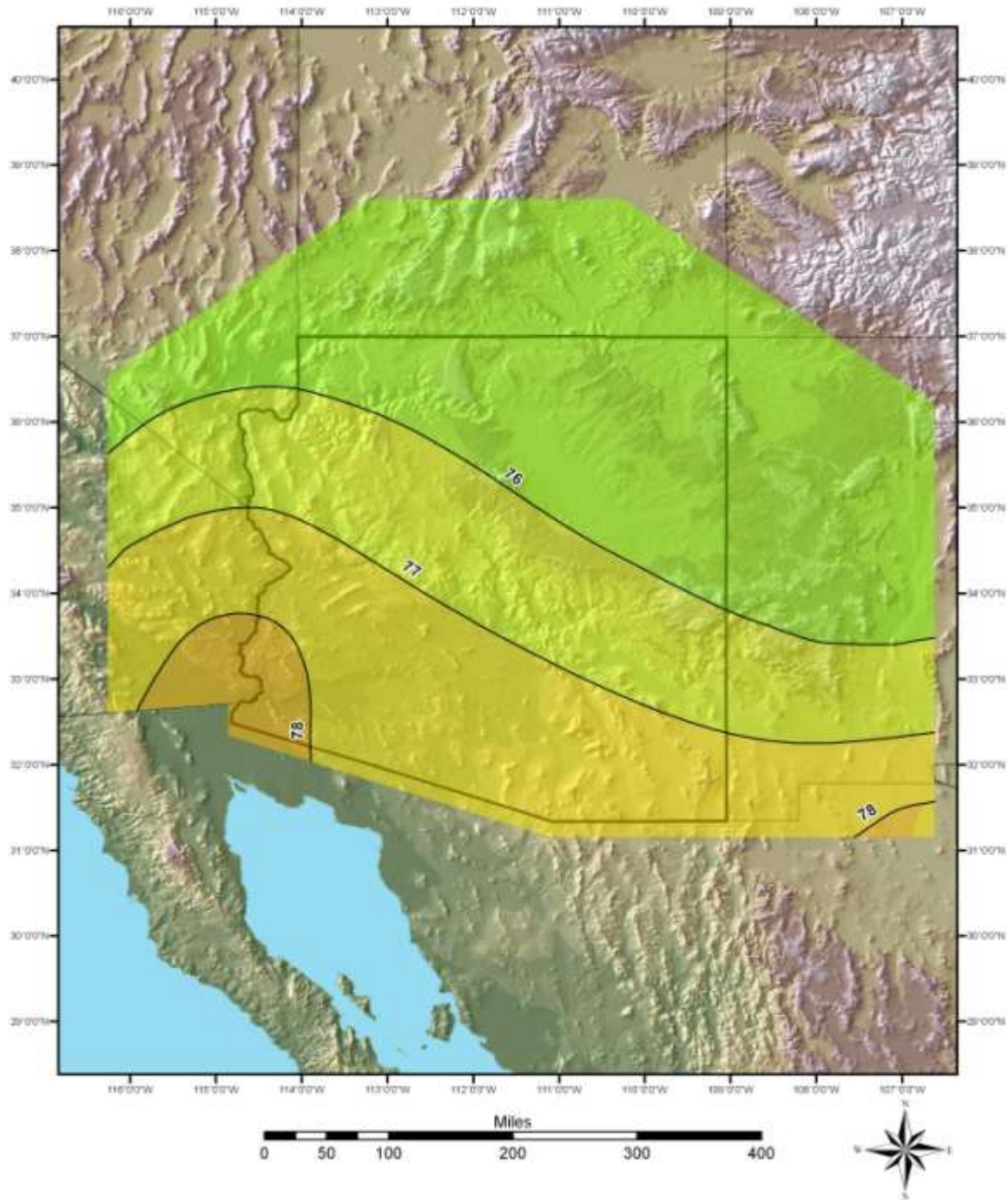
Figure 4.8 September 100-year return frequency maximum average12-hour dew point map
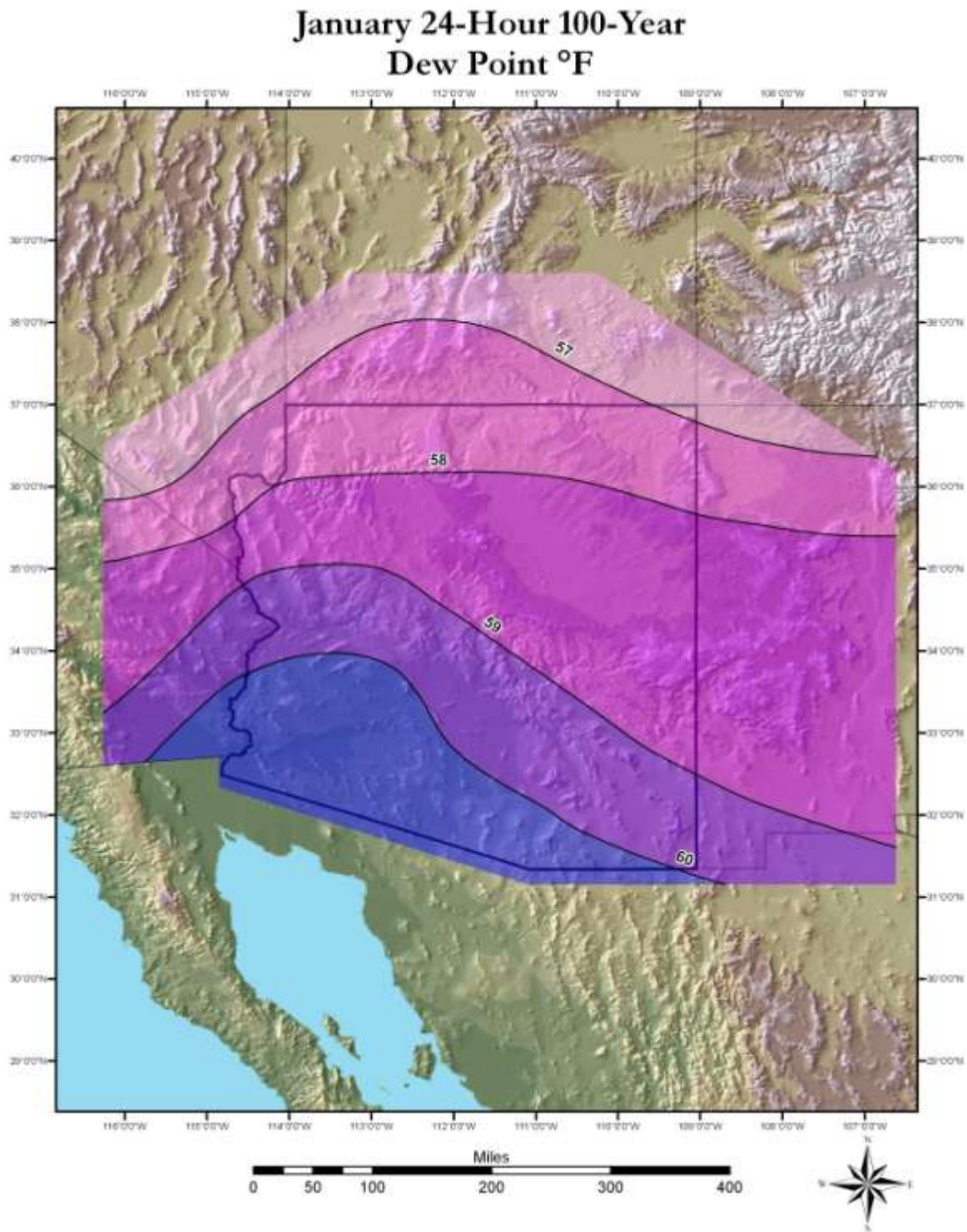
Figure 4.9 January 100-year return frequency maximum average 24-hour dew point map

4.1.3   Sea Surface Temperatures (SSTs)

The second data set used in storm available atmospheric moisture analyses is sea surface temperatures (SSTs). SSTs are derived from various databases available from NOAA. Daily values were obtained from the following sources:

1985 – Present: http://dss.ucar.edu/datasets/ds277.7/
1985 - 1946: http://dss.ucar.edu/datasets/ds195.1/
Prior to 1946: http://dss.ucar.edu/datasets/ds540.0/

SST observations were taken from ships, buoys (moored and drifting), automated coastal fixed platforms and drilling rigs, and satellite observations. Analyses are archived to the nearest 0.02 degrees C, with a spatial resolution of one degree in both latitude and longitude. For storm available atmospheric moisture analyses, daily SSTs were used.

For computing the maximization factors, a climatology of SSTs was computed for every one-degree latitude and longitude, based on twenty-five years of data. The standard deviation for each cell was calculated and two standard deviations were added to mean SST values for each month for each cell. Monthly maps were produced to provide spatial analyses of the mean plus two sigma (two standard deviations warmer than the mean) SST values. Use of the mean plus two sigma SSTs is consistent with the NWS procedure used in the most recent HMRs, HMRs 57 and 59.

The monthly data sets were derived from the following sources:

1981-Present: SST fields:
http://www.emc.ncep.noaa.gov/research/cmb/sst_analysis/
1854-1981:
http://www.ncdc.noaa.gov/oa/climate/research/sst/ersstv3.php

The NWS states in HMR 57 that the two standard deviations warmer values are approximately equal to a 0.02 probability of occurrence. Specifically, Section 4.3, pp 43-44, states that two standard deviations represent about 98 percent of normally distributed values and this "…places the magnitude of this parameter at about the level of other estimates used in this study, e.g. the 100-year frequency values." (HMR 57, Section 4.3). For the 2-sigma probability, there is 0.05 out of 1.00 that is not included under the normal distribution curve. The 0.05 is divided between the extremes on the upper and lower ends of the normal distribution curve. Since only the high end (i.e. SST plus two standard deviations warmer) is used, only half of the 0.05 is excluded from under the normal distribution curve, i.e. 0.025. Hence 0.975 or 97.5% is included under the normal distribution curve. Figure 4.10 shows the normal distribution curve with the +1 sigma and +2-sigma values.
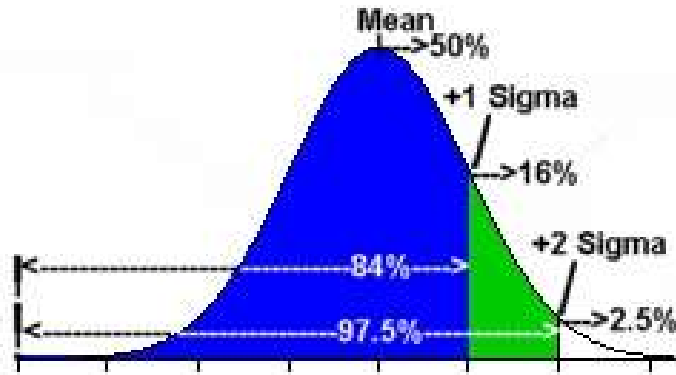
Figure 4.10 Normal distribution curve with +1 sigma and +2-sigma values shown

It appears that the NWS keeps rounding up until they conclude that the value is the 100-year frequency value (0.975 rounded up to 0.98 rounded up to 0.99). Without rounding 0.975 is about a 40-year return frequency value.

4.2   New Procedures

The OTF procedure (see Section 3) was used in this study to quantify the effects of topography on rainfall. This factor was calculated using return frequency values from NOAA Atlas 14 for each grid cell throughout the study domain. The OTF provided a comparison of the effectiveness of the underlying topography at a given location for enhancing or depleting rainfall compared to other locations. The ratio derived during this calculation quantifies the difference in that effect at the source location (i.e. the in-place storm location) versus the target location (i.e. the location to which the in-place storm is transpositioned). The assumption is that the precipitation frequency climatology in NOAA Atlas 14 inherently captures the precipitation behavior at a given location for a given storm type and its interaction with the underlying and upwind topography of that location. If this assumption is valid, then comparing the resulting precipitation frequencies at the source and target locations would result in values which reflect the differences in the effect of topography on moisture availability and rainfall production between the two locations.

Once this factor was calculated for each storm for each grid cell, it was applied linearly in the total adjustment factor calculation the same way the IPMF and MTF factors were applied. The results of the OTF calculation also helped provide guidance as to the transposition limits for given storm events. In cases where the OTF was larger than 1.50 or smaller than 0.50, it was assumed this demonstrated the orographic contribution between the two locations was sufficiently different as to violate the definition of transpositionability in that the topography between the two locations are not "similar". This same limitation in relation to the IPMF is discussed in HMR 51 (Section 3.2.2) and HMR 55A (Section 8.4.1.1). Section 7.3 describes the transposition process and regions used in this study. A description of the process used to define the transposition limits of each storm is also included in that section.

46

5. Extreme Storm Identification

5.1 Storm Search Area

A storm search was conducted based on previous storm search results from several AWA site-specific PMP studies in the state, as well as an expanded domain to capture all storms that could potentially affect PMP values within Arizona. This includes all storms in HMR 49 and those in HMR 59 that occurred in meteorological and topographically homogenous regions similar to Arizona (i.e. the southeastern deserts of California). The search area extended from southern Nevada and Utah to northern Mexico and from southeastern California eastward to the Continental Divide in Colorado and New Mexico (Figure 5.1). This domain insured a large enough area was analyzed to capture all significant storms that could influence final PMP values for the state.

5.2 Data Sources

The storm search was conducted using a database of rainfall data from several sources. The primary data sources are listed below:

1. Cooperative Summary of the Day / TD3200 through 2012. These data are published by the National Climatic Data Center (NCDC).
2. Hourly Weather Observations published by NCDC, U.S. Environmental Protection Agency, and Forecast Systems Laboratory (now National Severe Storms Laboratory).
3. NCDC Recovery Disk
4. Hydrometeorological Reports
5. Corps of Engineers Storm Studies
6. Other data published by state climate offices
7. Previous PMP and storm analysis work in Arizona
8. Concurrent PMP studies (e.g. Wyoming statewide PMP)
9. Reports and discussion from Maricopa County FCD
10. Discussions with various parties involved in the statewide PMP project
11. American Meteorological Society journals
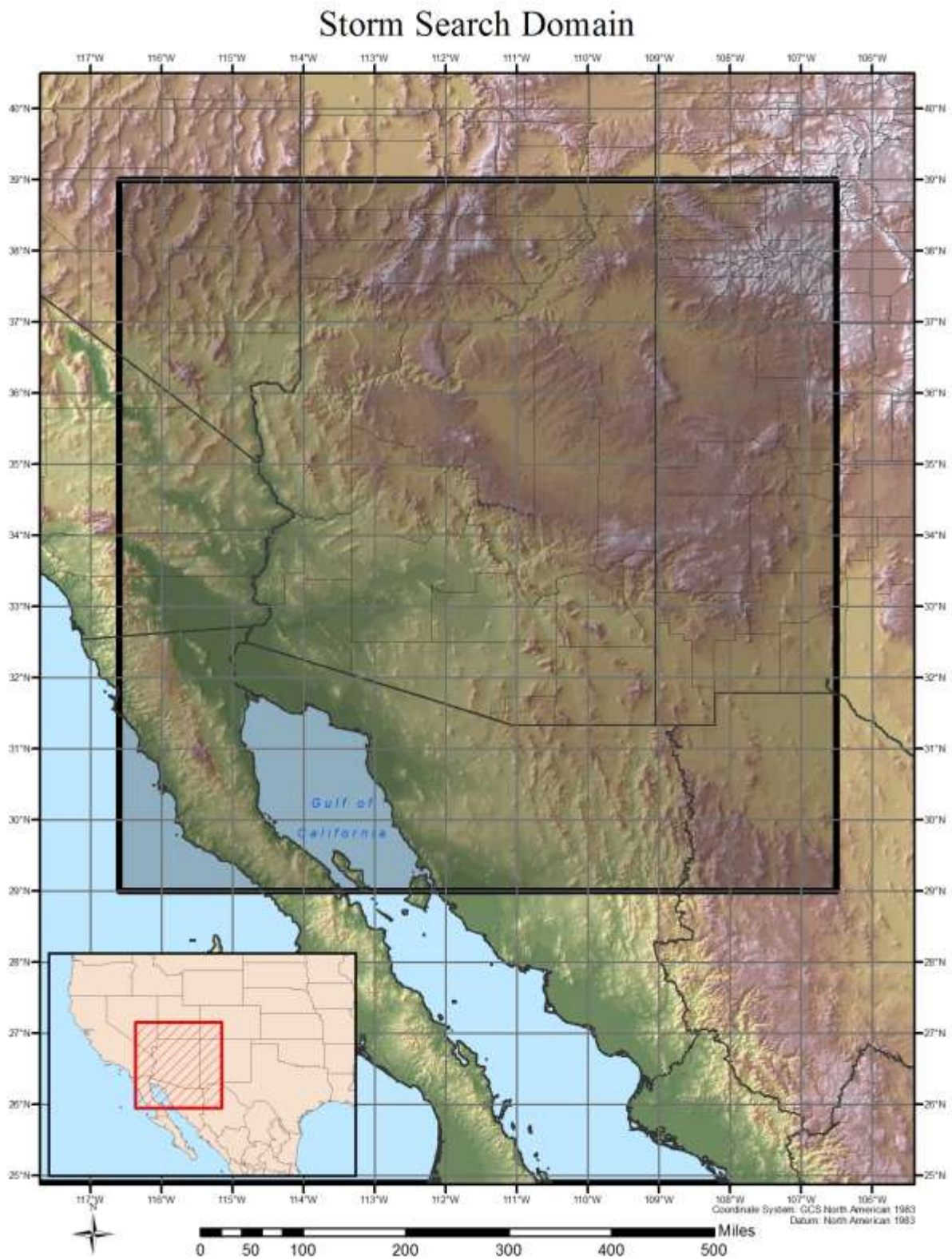
Figure 5.1 Storm search domain

5.3   Storm Search Method

The primary search began with identifying hourly and daily stations that have reliable rainfall data within the storm search domain described previously. These stations were evaluated to identify the largest precipitation totals associated with the three storms types; local convective, remnant tropical, and general frontal. Other reference sources such as HMRs, USGS reports, Flood Control District reports, NWS reports, and climate center reports were reviewed to identify other dates with large rainfall amounts for locations within the storm search domain. The initial cut-off for storms to make the initial list of significant storms (referred to as the long storm list) were events that exceeded the 100-year return frequency value for the specified duration and location.

The resulting long storm list was extensively quality controlled to ensure that only the highest storm rainfall values for each event were selected. Storms were then grouped by storm type and duration for further analysis.

These storms were plotted in GIS to better evaluate the spatial coverage of the events throughout the region. From this initial long storm list, the potential storms to analyze list was derived. This list was developed after communication with the Review Committee, representatives from ADWR and Maricopa County, as well as other stakeholders involved in the project. Each storm was also investigated for references in literature (NWS offices, USGS reports, Maricopa County Flood Reports, HMRs, AMS journals, etc) to determine its significance in the storm and flood history of Arizona.

5.4   Developing the Short List of Extreme Storms

The long storm list was very extensive containing 548 storms. A multiple step process was followed to determine a list of storms that was comprehensive enough to ensure that major events were identified but eliminating smaller events that would not be significant for determining PMP values at any area size or duration after standard adjustments were applied.

The next step was to determine which of these storms would ultimately need to be fully analyzed using the SPAS program. Several steps were taken to compare each of the events on the potential storms to analyze list. Storms were sorted by storm type and location for initial comparison. This helped eliminate several storms which occurred in the same climate region but were of significantly less magnitude compared with others of the same duration in similar locations. The remaining storms were further investigated using various flood reports, discussions with personal familiar with the storm events, and examination of the synoptic environment surrounding the event. The storms which made it through these final evaluations were placed on the short storm list (Table 5.1 and Figure 5.6). Each of these storms was considered to potentially affect PMP values for one or more grid points analyzed in this study. This list contains all the storms analyzed by AWA, a total of 51 storm events. Ultimately, only a small subset of these short list storms control PMP values, with most providing support of those values. The reason more storms were analyzed than was required to derive the PMP values was to ensure no storms were left off which could have affected PMP values after all adjustment

factors were applied. The magnitude of the adjustment factors is unknown at the beginning of the process, as storms with large point values may end up with a relatively small total adjustment factor, while a storm with a relatively smaller but significant rainfall value may end up with a larger total adjustment factor. The combination of these calculations may raise the total adjusted value of the smaller event to a higher level than other storms.

Figures 5.2 through 5.6 show the locations of all the storms contained on the storms to analyze list. Figure 5.2 shows the location of all the storms, Figure 5.3 shows the locations of all the local storms, Figure 5.4 shows the locations of all the remnant tropical storms, and Figure 5.5 shows the locations of all the general winter storms. Finally, Figure 5.6 shows the storm information for all the storms that were analyzed and considered in the derivation of the PMP values.

Table 5.1 Short storm list used to derive PMP values. All storms analyzed with SPAS.

SPAS Storm Number	Storm Name	State	Storm Type	Lat	Lon	Year	Month	Day	Total Storm Rainfall
1107	SAN JUAN MOUNTAINS	CO	tropical	37.663	-106.938	1911	10	4	7.88
1144	MT ORD	AZ	general	33.904	-111.413	1916	1	14	10.63
1077	CROSSMAN PEAK	AZ	tropical	34.546	114.196	1939	9	4	9.65
1061	THATCHER	AZ	local	32.763	-109.829	1939	9	16	4.18
1076	CROWN KING	AZ	tropical	34.204	112.354	1951	8	26	14.99
1096	QUEEN CREEK	AZ	local	33.203	-111.145	1954	8	18	8.06
1064	WELLTON	AZ	local	32.579	-114.338	1955	8	22	6.49
1154	HORSESHOE DAM	AZ	general	33.938	-111.736	1959	10	27	10.86
1083	SONORA DESERT MUSEUM	AZ	tropical	32.179	-111.388	1962	9	25	7.16
1130	PAGE	AZ	local	36.917	-111.450	1963	8	30	2.03
1060	NORTH TUCSON	AZ	local	32.304	-111.004	1964	9	5	5.28
1059	SAHUARITA	AZ	local	32.006	-110.904	1964	9	9	6.77
1137	YOUNG	AZ	general	33.821	-110.921	1965	11	22	11.58
1141	JUNIPINE	AZ	general	36.229	-112.063	1966	12	4	15.86
1133	JAKES CORNER	AZ	general	34.021	-111.379	1967	12	17	10.02
1249	BLANDING	UT	local	37.826	-109.543	1968	8	1	6.67
1118	SELIGMAN	AZ	local	35.317	-112.883	1970	7	21	5.89
1075	WORKMAN CREEK	AZ	tropical	33.820	-110.904	1970	9	4	12.13
1062	PHOENIX	AZ	local	33.517	-112.023	1972	6	21	5.63
1102	JOANNE	AZ	tropical	33.821	-110.921	1972	10	4	11.66
1073	SEDONA	AZ	local	34.882	-111.765	1975	7	13	4.27
1042	YUMA	AZ	local	32.611	-114.631	1977	8	15	6.85
1097	NOGALES	AZ	tropical	31.339	-110.935	1977	10	6	15.97
1150	BEAR SPRING	AZ	general	34.038	-111.488	1978	2	27	15.52
1134	BIG PINE FLAT	AZ	general	33.675	-111.335	1978	12	16	10.37
1138	CROWN KING	AZ	general	34.221	-112.346	1980	2	13	17.63
1135	ALAMO	NV	local	36.554	-114.713	1981	8	10	6.50
1063	PRESCOTT	AZ	local	34.621	-112.554	1983	9	23	17.95
1074	MT GRAHAM	AZ	tropical	33.288	-109.104	1983	9	27	13.99
1122	HARQUAHALA VALLEY	AZ	local	33.488	-113.254	1984	9	2	8.00
1139	KNOLES HOLE SPRING	AZ	general	33.829	-110.913	1993	1	5	13.36
1086	TUCSON	AZ	local	32.390	-110.800	1996	9	3	7.37
1084	HARQUAHALA MOUNTAIN	AZ	tropical	33.815	-113.335	1997	9	25	12.13
1115	JOSEPH CITY	AZ	local	34.945	-110.355	1998	7	31	4.20
1087	SABINO CANYON	AZ	local	32.385	-110.705	1999	7	14	7.87
1043	SOLS WASH	AZ	local	34.130	-113.080	2000	8	29	5.54
1131	BLUFF	UT	local	37.255	-109.575	2001	8	14	6.28
1094	CIRCLE CITY	AZ	local	33.950	-112.340	2003	8	26	10.17
1109	ROOSEVELT LAKE	AZ	local	33.596	-111.065	2003	9	6	11.19
1088	JAVIER	AZ	tropical	34.730	-113.020	2004	9	18	10.10
1147	BIG PINE FLAT	AZ	general	33.685	-111.325	2005	2	10	8.72
1091	CAMP CREEK	AZ	local	34.380	-111.180	2005	9	3	4.93
1120	CEDAR CITY	UT	local	37.375	-113.075	2006	7	31	5.69
1113	PETRIFIED FOREST	AZ	local	34.725	-109.645	2007	7	27	7.18
1149	COOKS MESA	AZ	general	34.460	-111.230	2007	11	30	8.60
1051	MAGMA	AZ	local	33.194	-111.347	2008	7	10	5.34
1128	HAVASUPAI	AZ	local	35.155	-112.575	2008	8	15	4.49
1085	WENDEN & BOUSE	AZ	local	33.915	-113.905	2008	8	26	4.82
1166	WAGON BOW	AZ	local	34.865	-113.455	2009	7	2	7.67
1200	PETERSON RANCH	AZ	general	33.810	-110.910	2010	1	19	14.93
1262	ANTHEM	AZ	local	33.859	-112.141	2012	7	31	6.38
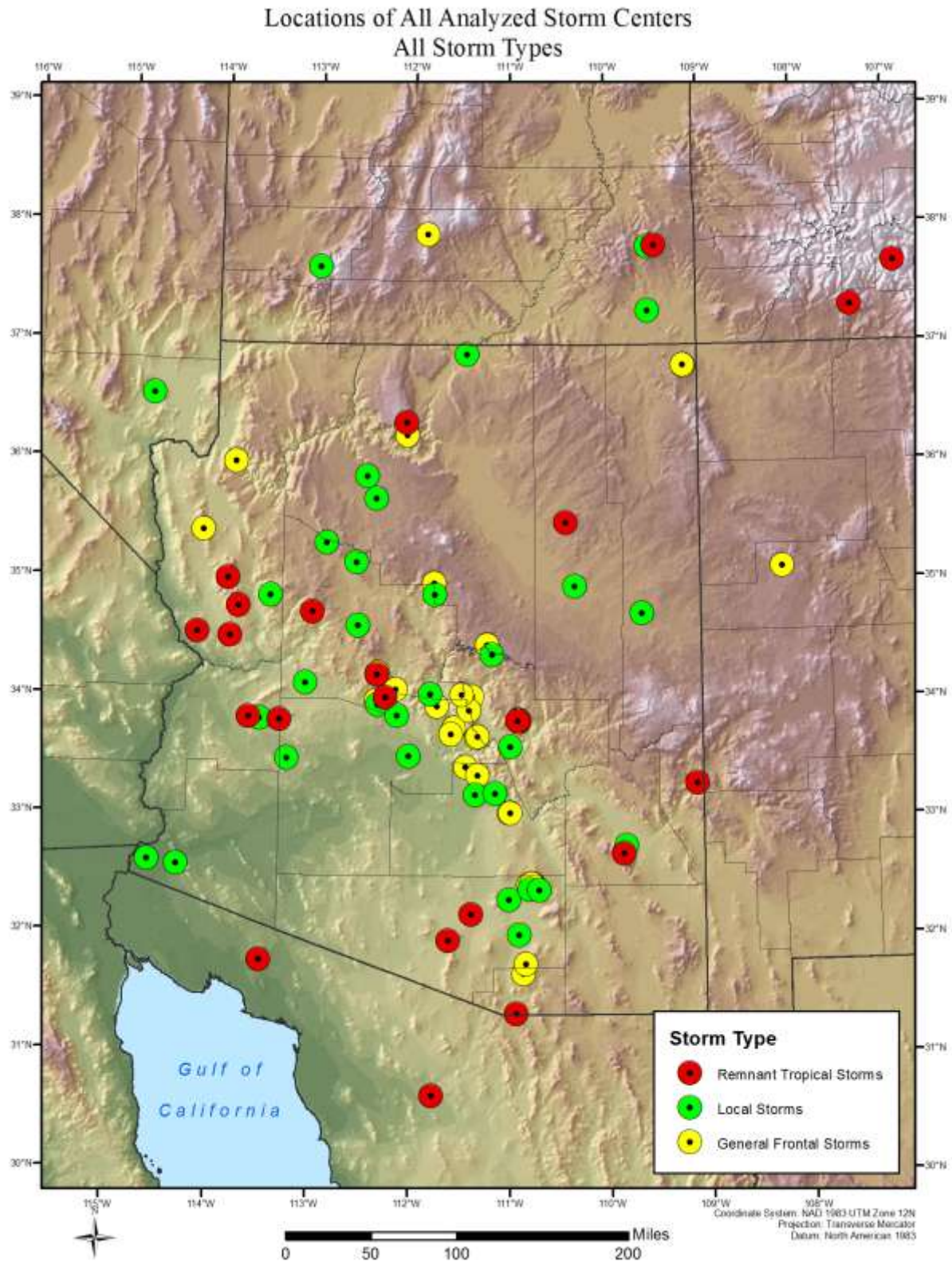
Figure 5.2 Storm locations on the short storm list, all SPAS DAD zones are plotted
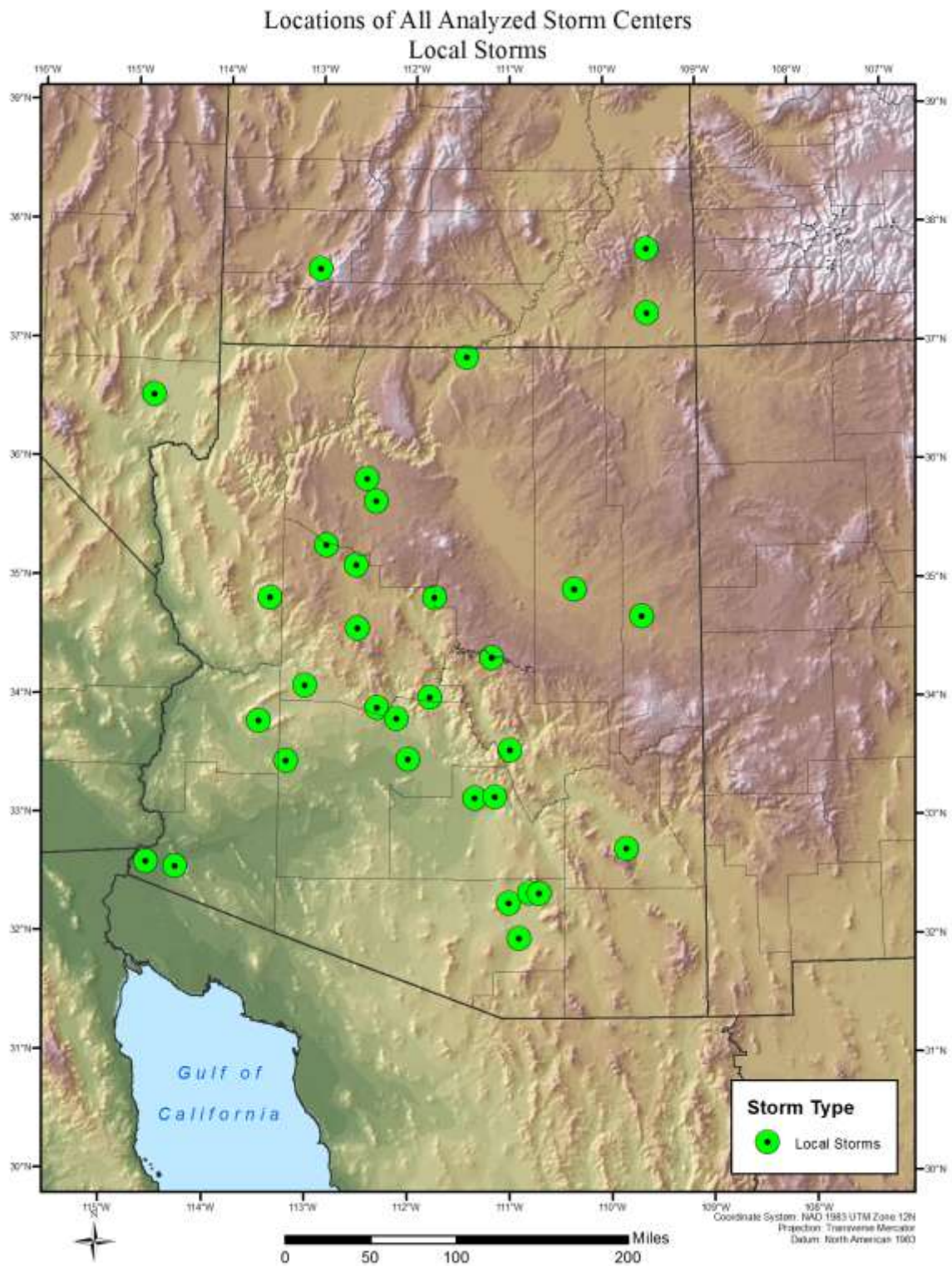
Figure 5.3 Storm locations for local storms on the short storm list, all SPAS DAD zones are
       plotted
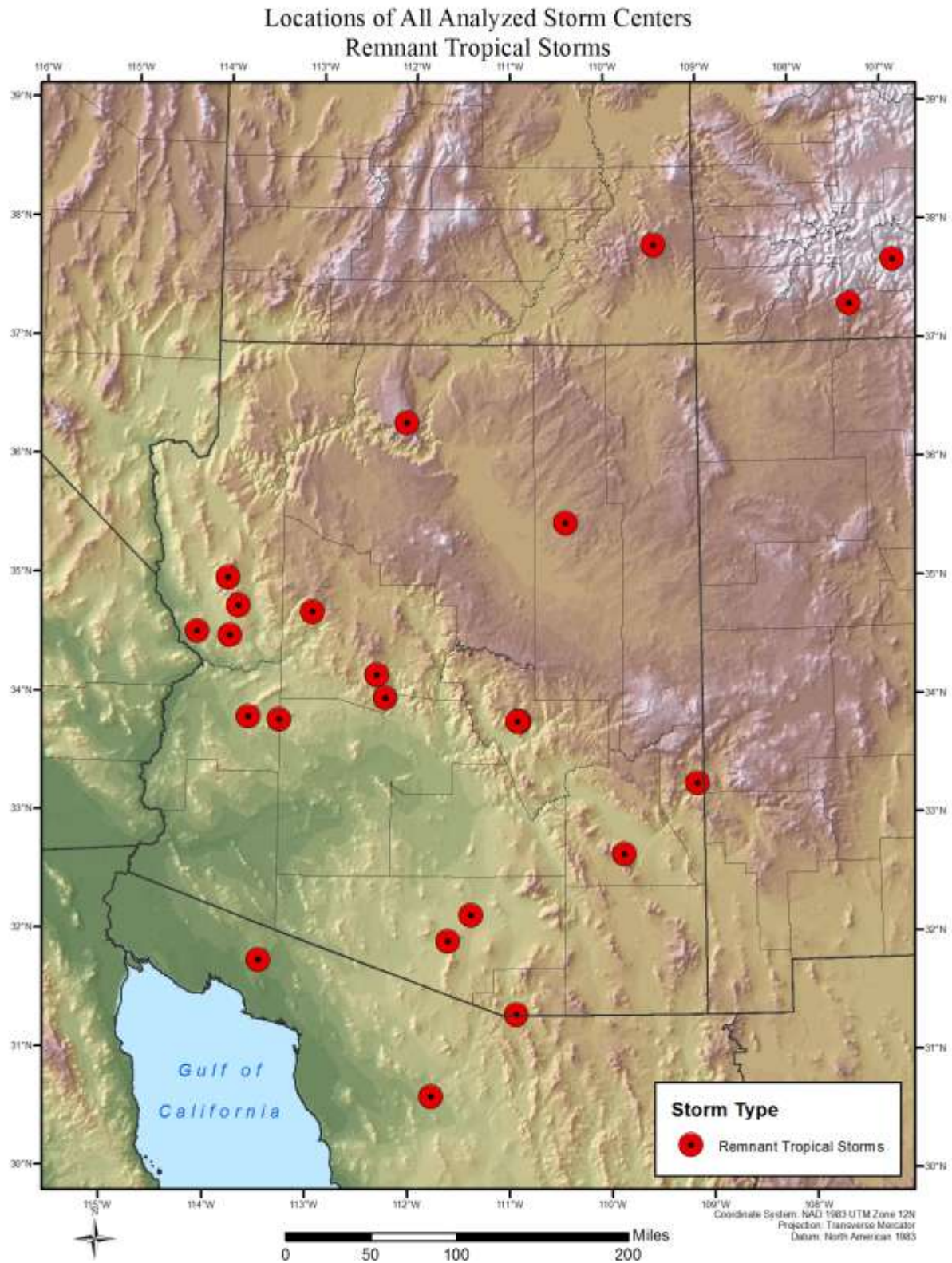
Figure 5.4 Storm locations for remnant tropical storms on the short storm list, all SPAS DAD zones are plotted
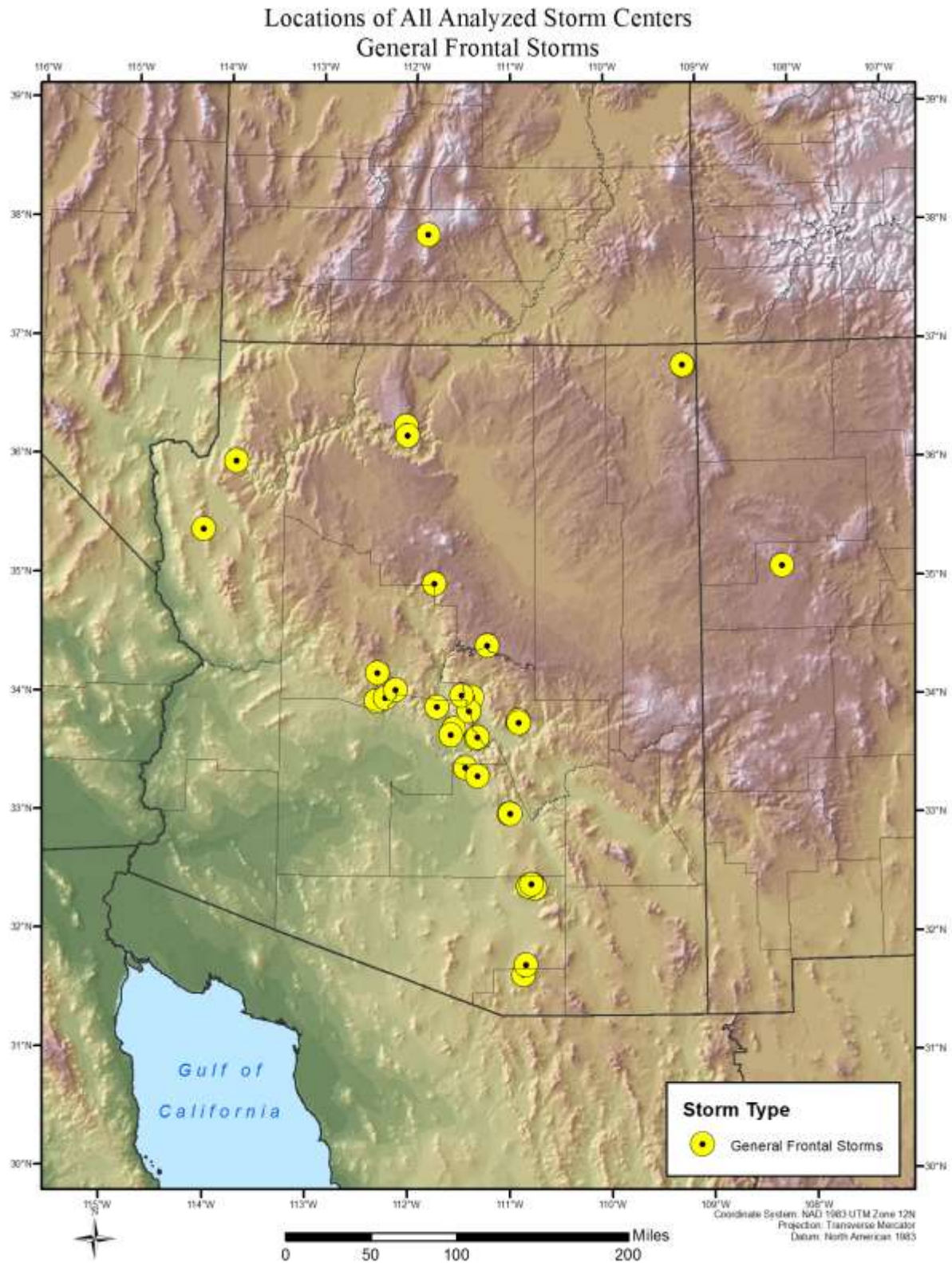
Figure 5.5   Storm locations for general winter storms on the short storm list, all SPAS DAD zones are plotted
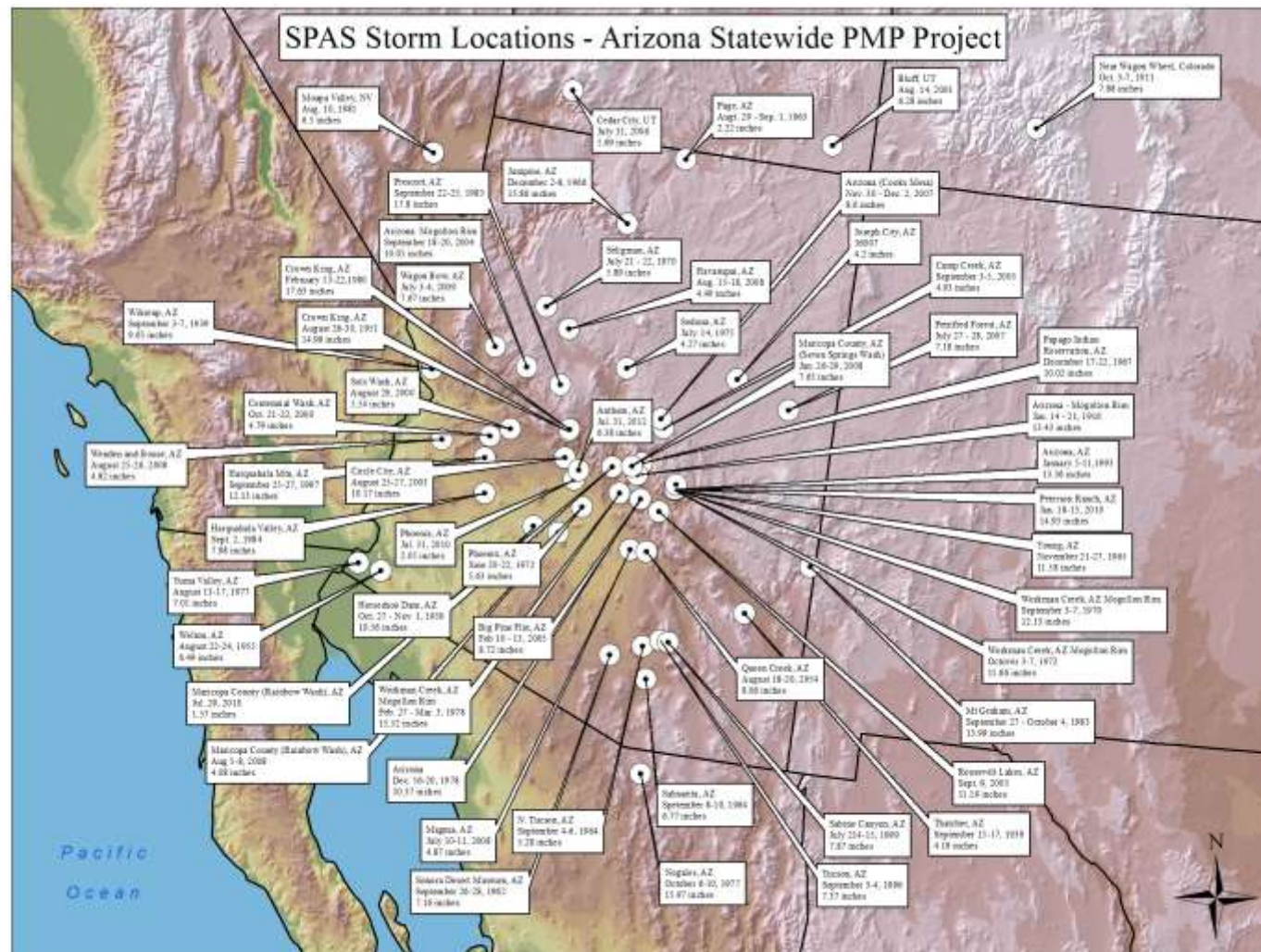
Figure 5.6   Storms analyzed using SPAS to derive the PMP values for Arizona

5.4.1 Re-evaluation of the Harquahala Valley September 1984 Storm

Rainfall information for this storm was taken from the SCS Engineering Report, dated February 1987. This report primarily addresses damage to the Harquahala Valley Watershed Saddleback Diversion from the September 1-2, 1984 storm. This 71-page report includes information on design, flows and damage including pictures of damages that resulted from the flooding. Appendix A from that report contains the following two paragraphs along with two figures associated with the rainfall, a map with plotted reported rainfall values and recorder charts:

Rainfall

Figure 1 shows the rainfall amounts reported at locations near the watershed. The red values were obtained by work unit staff, the green during the study. Reported amounts range from 2 to 11 inches. There are no residences in the drainage area of Saddleback diversion, thus no rainfall information was available there. It appears, however, that the most intense part of the storm traveled from NW to SE and traversed the central and lower portion of the diversion watershed. High water marks at FRS 1 showed that the maximum stage was 4.8 feet over the principal spillway crest. The total capacity at this stage is 1732 acre-feet or .32 inches runoff from the watershed. The sediment pool capacity is 424 acre-feet or .08 inches. Because of the short duration of the storm, and small principal spillway capacity of FRS 1, rainfall above the site was not used in the Saddleback Diversion Study.

The storm distribution was taken from the recorder chart (Figure 2). The tabulated values were used because it was not possible to accurately read shorter time increments from the chart. It is probable that more intensive rainfall occurred during shorter time increments.
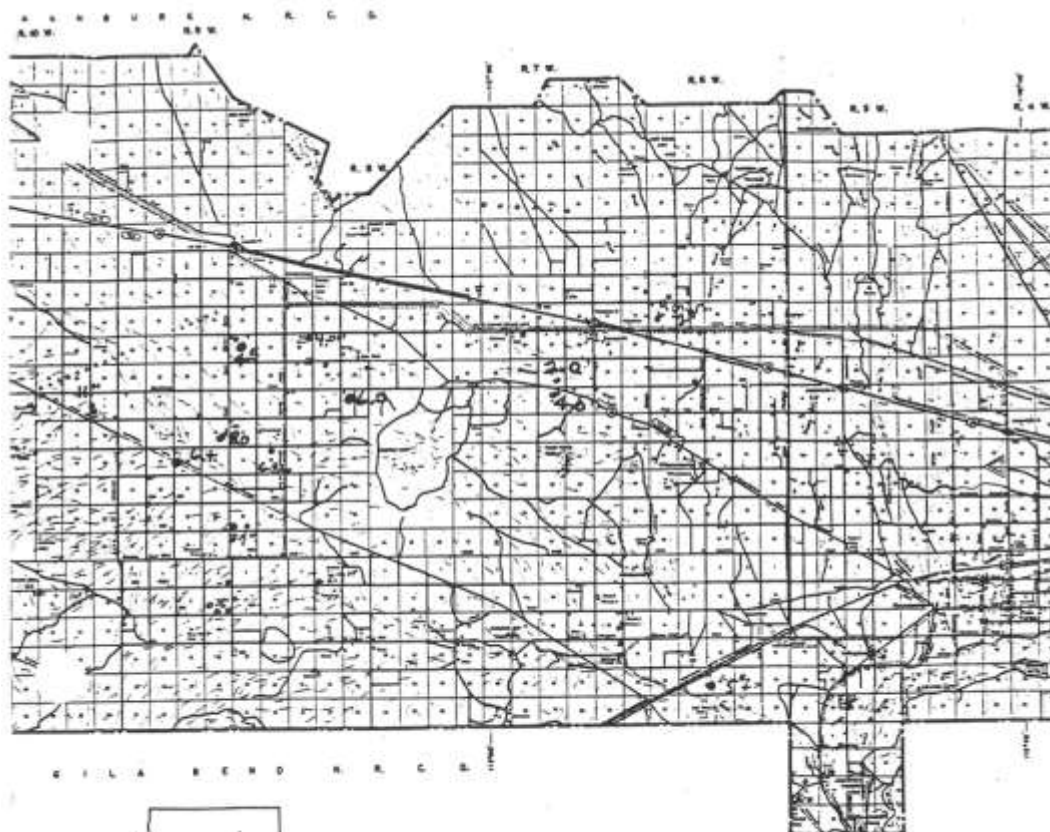
HARQUAHALA VALLEY
RAINFALL AMOUNTS
LABOR DAY STORM 1984
4hr. duration

BUCKEYE-ROOSEVELT
NATURAL RESOURCE CONSERVATION DISTRICT
MARICOPA AND YUMA COUNTIES, ARIZONA

OCTOBER 1976

SCALE 1:310,000

Figure 2
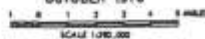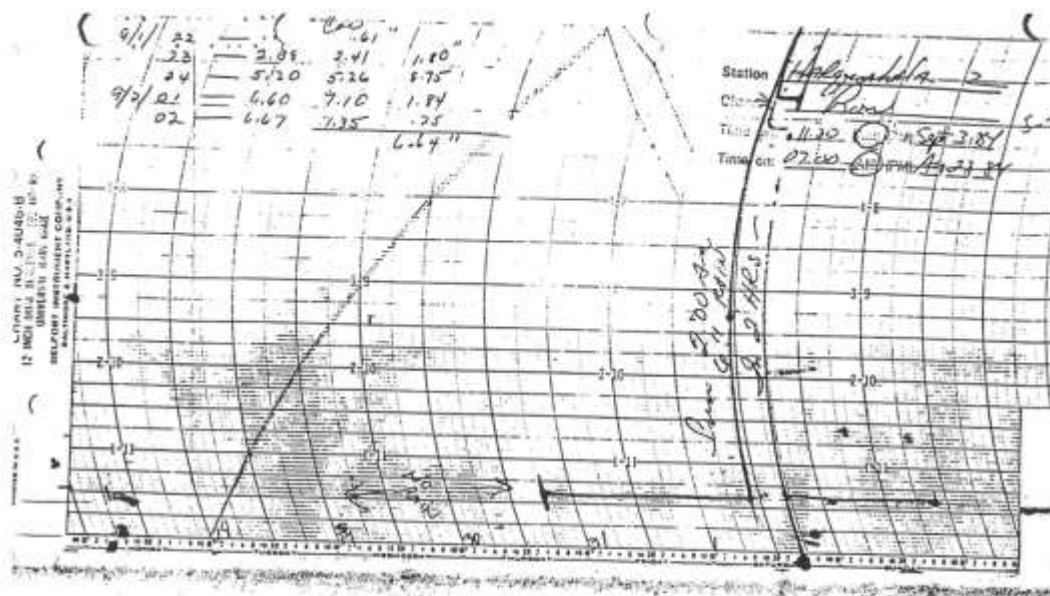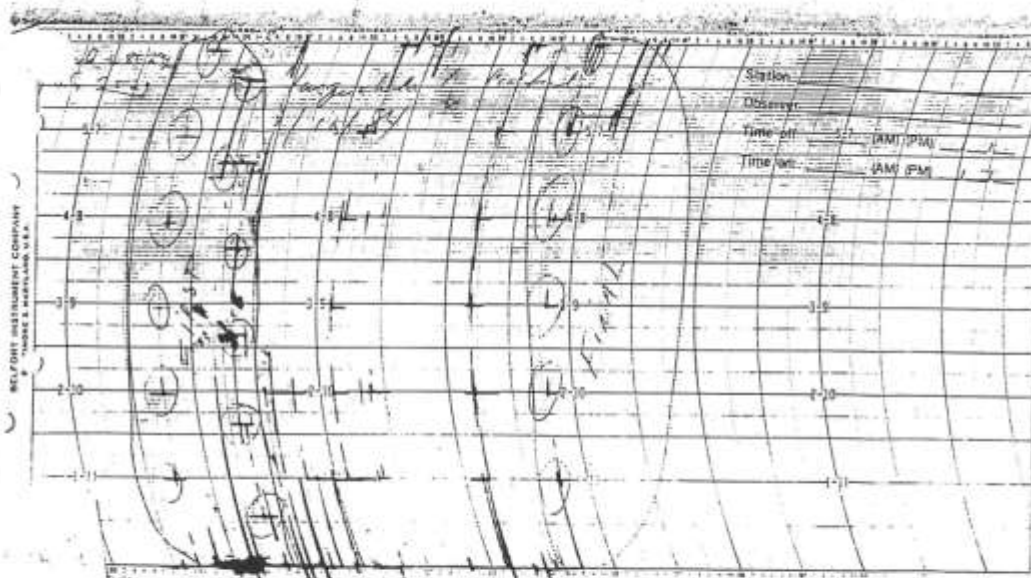
Amir Motamedi from the Flood Control District of Maricopa County completed some investigation on available supporting materials regarding the storm event as a results of discussions during the second Arizona statewide PMP Review Committee meeting (October 22, 2009). He located a file at the Flood Control District with some information collected after the storm. Of particular interest is the notation of 11.00" followed by "Ron Howe, foreman at ranch." A copy of the sheets with the reported rainfall notation is shown below:

① Lady on 481 st said they had gage [illegible crossed out]
; She was in Calif when storm came other
members of family said 6"

② 4" Charlie Nye - Big Horn Ranch
491st Farm Manager - 4" in less than
2 hours - Occurred at midnight
Had rain about week before

③ 4.5" Tom Sykes in less than 2 hrs
511st Dudly Greer Farm

4. [illegible] fingers - Had rain about 10 day [illegible]
3 barrel sat Water [illegible] - Caught 8"
[illegible] rained more in [illegible] on
Mountain.

5. Steve [illegible] Hdg 6"4
Vineyard

The notations above appear to be the source of rainfall information plotted on the map in the SCS report. How the reported rainfall amounts were obtained is not documented. The 11.00" value has what appears to be a telephone number suggesting that possibly the report was obtained via telephone conversation. Another notation indicates a phone conversation with another individual.

These reported rainfall amounts are the sole source of rainfall information for this storm with the exception of the recorder chart traces. Reports such as these are often referred to as "bucket survey" reports. Historically, the Weather Bureau, now renamed the National Weather

Service, has made extensive use of bucket survey rainfall observations obtained from unofficial sources. However, before a bucket survey rainfall report was accepted, the site was visited by someone familiar with rainfall observation criteria and evaluated for reliability. If the evaluation indicated that the reported rainfall was collected in an acceptable container that was sited appropriately and the timing of measurements was well documented, the reported rainfall was used in the storm rainfall analysis.

There is no documentation that the reported rainfall amounts provided in the SCS report or in the District notes were subjected to any quality control evaluations. This does not prove that they are not reliable. Instead, the reports were not evaluated by qualified personnel for reliability, a procedure normally followed by the NWS before the reports are included in official storm rainfall analyses. There are several possibilities that could lead to erroneous reports, including the container not being empty at the beginning of the rainfall, the site of the container too close to a roof or other obstruction (improper siting), or the sides of the container being sloped or not level. Another possibility is that estimates of rainfall amounts have been reported as measured, e.g. a six inch deep container filled and overflowed so maybe twice the amount collected was reported in a well meaning effort to quantify the rainfall.

After further discussions with the Arizona statewide PMP Review Committee, as well as the NRCS (the original agency responsible for the report and storm information), it was agreed that the 11" rainfall value not be considered valid for use and that the initial SPAS run using this 11" value was re-run. The storm was reanalyzed using only the remaining values, as these are considered reasonable based on the amount recorded on an official trace recorder and the number of other similar amounts reported between 4-8 inches. Further validation that the 11" rainfall value was invalid resulted from the initial SPAS storm analysis, which produced a DAD for this storm which was inappropriately higher than all other extreme storm events analyzed and therefore highly questionable. This by itself would not normally invalidate a storm; however, when combined with the evidence discussed and presented to the Review Committee, it became obvious that this observation was not valid. Complete storm analysis details on this storm can be found in Appendix F.

5.4.2 Queen Creek August 1954 storm

The Queen Creek 1954 storm event was a local storm which lasted for a longer than normal duration. This storm controled PMP values for many locations for durations of 2 to 6 hours where it is transpositionable. This storm has also been extensively used for various hydrological purposes in Maricopa and Pinal counties. Unfortunately, none of this storm's rainfall was captured by official NWS rain gauges. This limitation meant that no precipitation values large enough to pass AWA's initial storm search criteria were found. Further, for unknown reasons, the authors of HMR 49 did not include this storm in their report. The current project has benefited greatly from information on historic storm and flood events provided by the Statewide PMP Study Review Committee.

AWA was able to extensively re-evaluate this event for this study based on several reports and additional information. The USACE conducted an analysis of the August 19, 1954 Queen Creek storm and published the results in the USACE Hydrology Part 2, Gila River Basin

New River and Phoenix City Stream Arizona Design Memo No. 2, 1982. The following quote, which provides some important information, is from the memo:

> "Although there was no widespread general precipitation in Arizona during August 1954, one large and very intense thunderstorm occurred over the Queen Creek drainage area, approximately 50 miles east of Phoenix. The storm and flood were the most severe on record in the Queen Creek basin. Precipitation intensities were very high during portions of the storm, especially between 5:00 and 9:00 a.m. on the 19th. The smelter at Ray (about 11 miles southeast of Superior) measured 4.05 inches of rain in less than 2 hours, while the Boyce Thompson Arboretum (about 4 miles west of Superior) measured a total of 5.3 inches for the storm, most of which fell within 3 hours. An estimated 140 square miles of area had over 5 inches of precipitation in the storm, and approximately 850 square miles had over 1 inch."

Given the lack of rain gauge observations for this event (only 26 daily and 4 hourly reporting gauges), a good deal of information was gleamed from the USACE memo. The USACE total storm isohyetal map from that report was georeferenced and digitized into a GIS (Figure 5.7). This provided an ability to add 13 pseudo stations to the SPAS database where stations otherwise did not exist. Rainfall estimates were then derived from the isohyets and latitude/longitude coordinates via the GIS interface. The pseudo stations provided SPAS enough information to produce a similar spatial pattern of rainfall as shown in the original analysis.
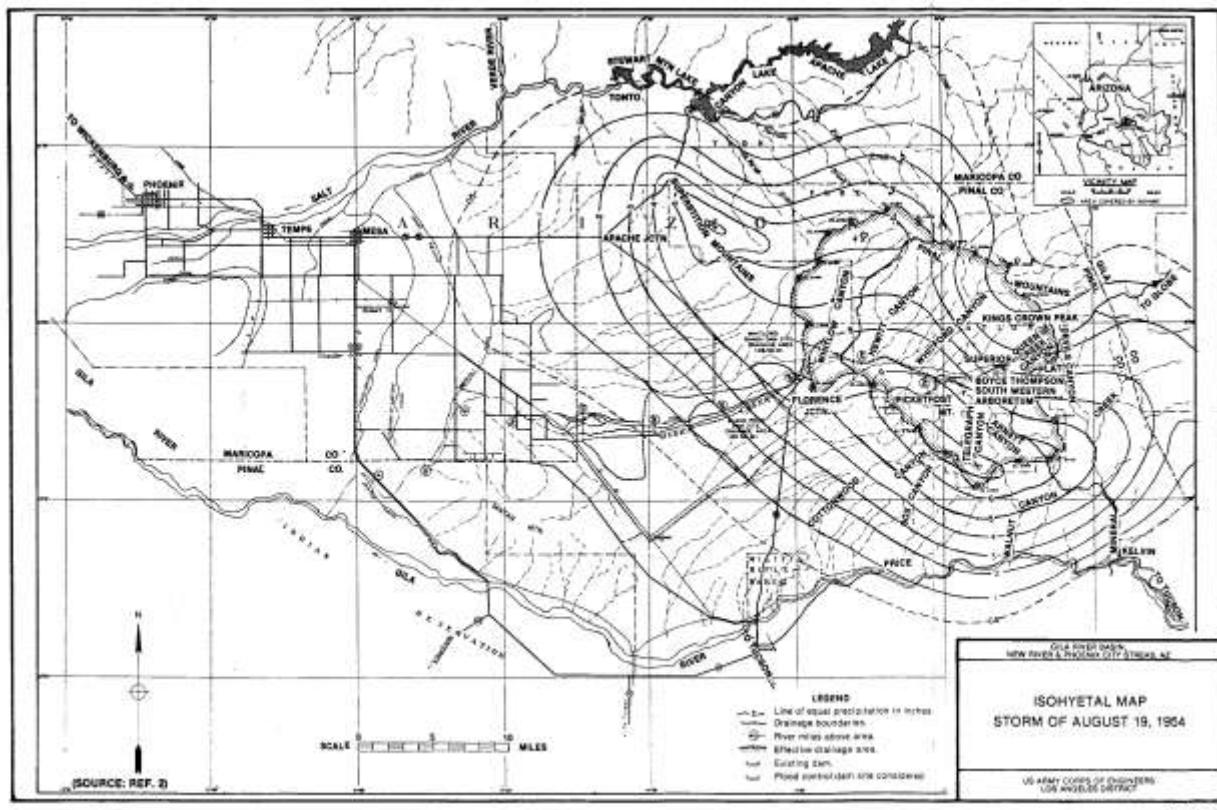
Figure 5.7   Total storm isohyetal for Queen Creek 1954 as analyzed by the USACE

In addition to the existing hourly rainfall data (from recording gauges) and the USACE report, two additional pseudo hourly stations (at Superior and Boyce Thompson Arboretum) were constructed to provide SPAS the temporal information needed to provide consistent DAD results to those published in the USACE report (see Figure 5.8). Two other stations (Martinez Canyon and Randolph Spring) were added per text in the USACE report. Given the weight of USACE memo data into the SPAS analysis, the SPAS results closely match those from the USACE memo. However, SPAS was able to distill all of the information into an objective analysis, which provided better results. Further, because SPAS uses sophisticated spatial interpolation techniques beyond those available at the time of the original analysis, the final SPAS DAD and total storm isohyetal should better represent the actual spatial distribution of the rainfall. Figure 5.9 shows a comparison of the total storm DA results from SPAS vs. the USACE original DA results.
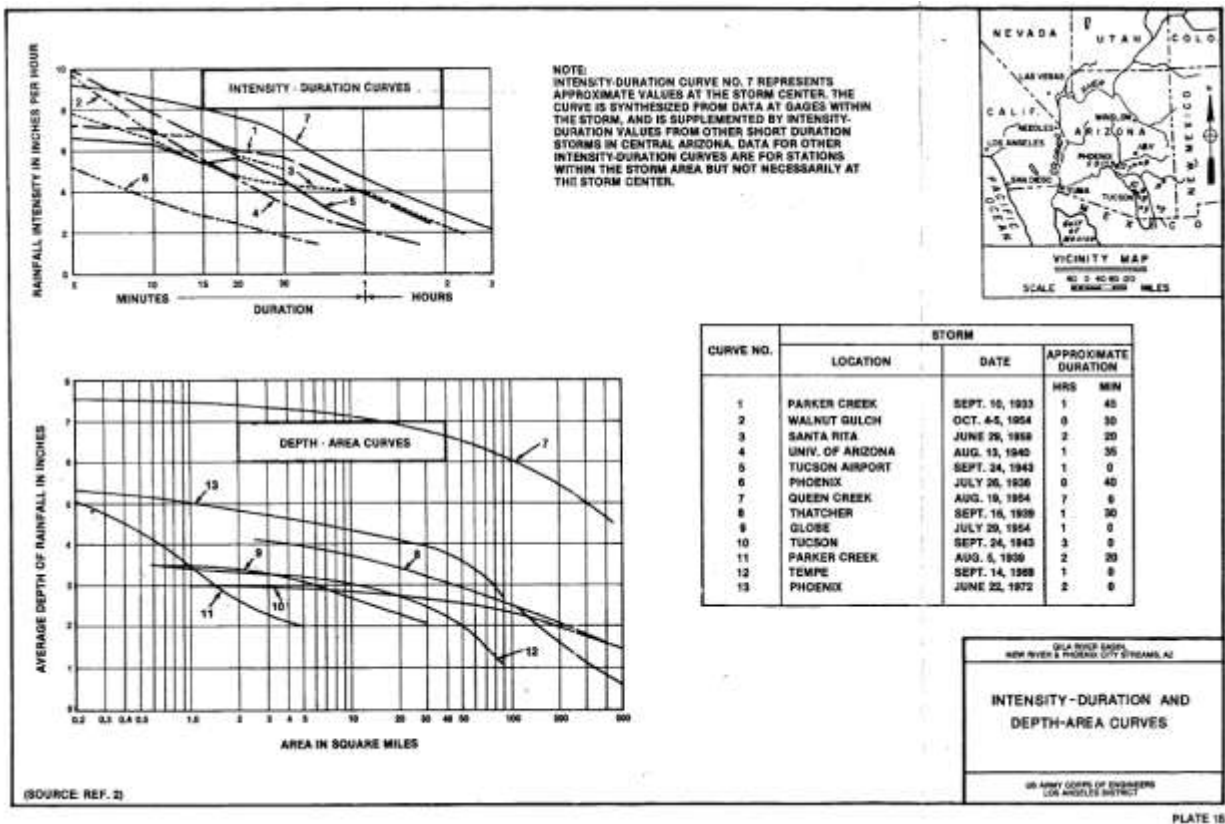
Figure 5.8   USACE-calculated depth-area statistics for several historic Arizona storms, Queen Creek 1954 is storm number 7
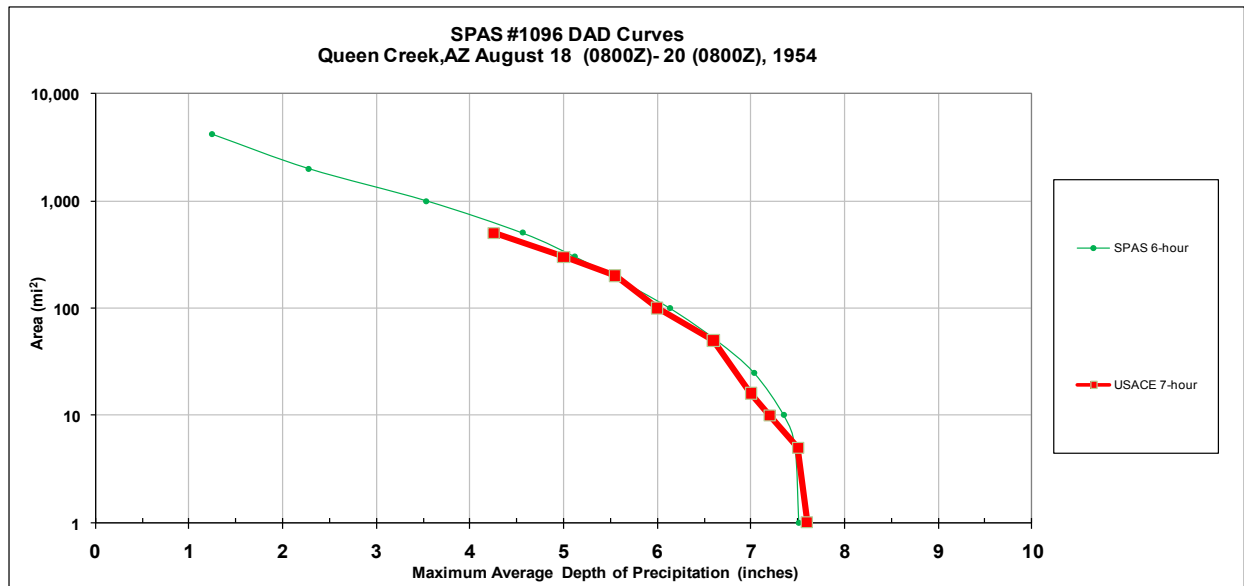
Figure 5.9   Total storm depth-area results for SPAS vs. USACE

6.   Storm Depth-Area-Duration (DAD) Analyses of Storms

For all storms identified as part of this study, DADs needed to be computed. HMR 49 did not analyze DADs for any of the storms used in that study. Therefore, no DADs were available for storms used in HMR 49. Further, gridded rainfall information was required for all storms for the OTF calculations to be completed. Finally, the vast majority of storms used in this study occurred after HMR 49 was published and/or were not included in that document. SPAS was used to compute DADs for all of the storms used in this study.

There are two main steps in the SPAS DAD analysis: 1) The creation of high-resolution hourly rainfall grids and 2) the computation of DA rainfall amounts for various durations, i.e. how the depth of the analyzed rainfall varies with area sizes being analyzed. The reliability of the results from step 2) depends on the accuracy of step 1). Historically the process has been very labor intensive. SPAS utilizes GIS concepts to create spatially-oriented and accurate results in an efficient manner (step 1). Furthermore, the availability of NEXRAD (NEXt generation RADar) data allows SPAS to better account for the spatial and temporal variability of storm precipitation for events occurring since the early 1990s. Prior to NEXRAD, the NWS developed and used a method based on Weather Bureau Technical Paper No. 1 (1946). Because this process has been the standard for many years and holds merit, the DAD analysis process developed for this study attempts to follow the NWS procedure as much as possible. By adopting this approach, some level of consistency between the newly analyzed storms and the hundreds of storms already analyzed by the NWS can be achieved. Comparisons between the NWS DAD results and those computed using the new method for two storms in HMR 51 territory (Westfield, MA 1955 and Ritter, IA 1953) indicated very similar results (see Appendix G for complete discussion, comparisons, and results). For this study and as part of the statewide PMP project, Figures 6.1A-D show comparisons made with 3 SPAS storms where NWS/USACE DA data were available.
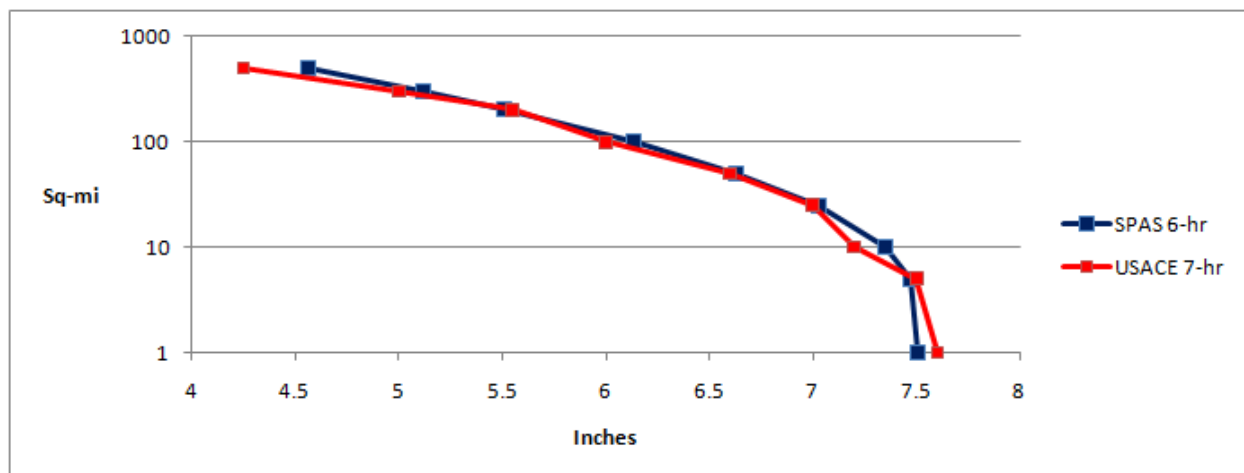
Figure 6.1A   SPAS analyzed 6-hour DA curve vs. USACE analyzed 7-hour DA curve for
              Queen Creek August 1954 SPAS 1096
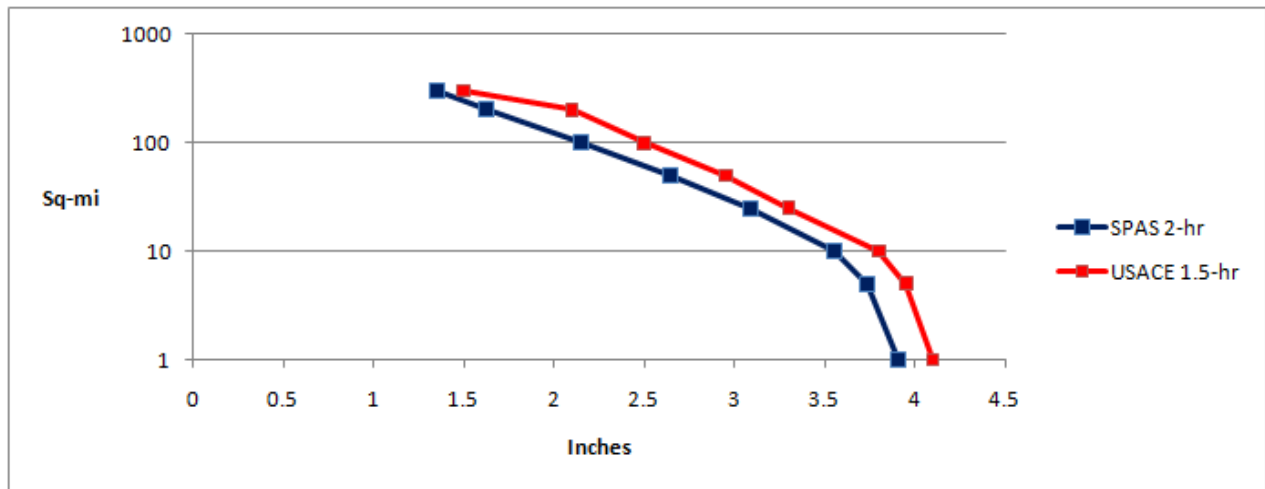
Figure 6.1B   SPAS analyzed 2-hour DA curve vs. USACE analyzed 1.5-hour DA curve for
Thatcher September 1939 SPAS 1061
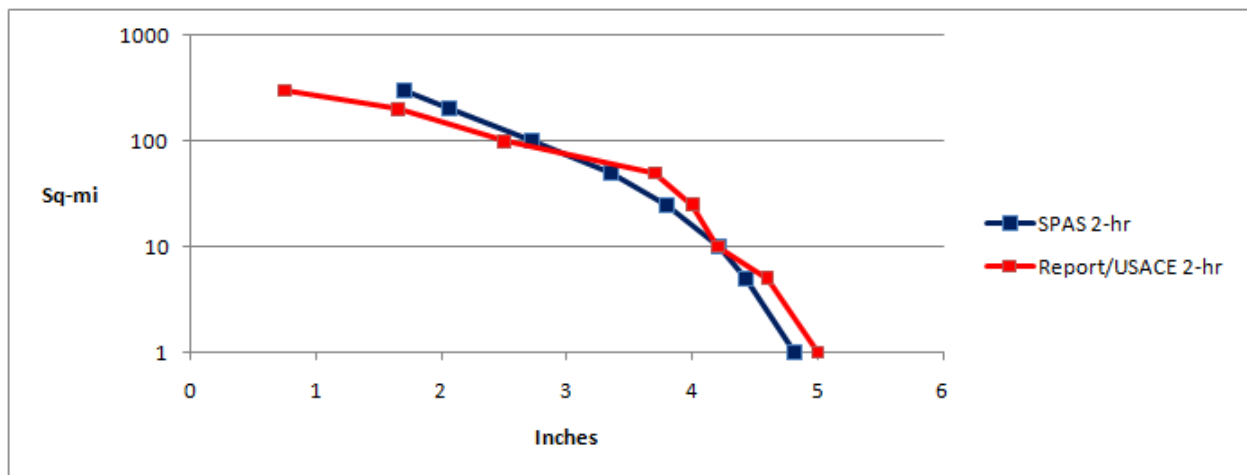
Figure 6.1C   SPAS analyzed 2-hour DA curve vs. USACE analyzed 2-hour DA curve for
Phoenix June 1972 SPAS 1062
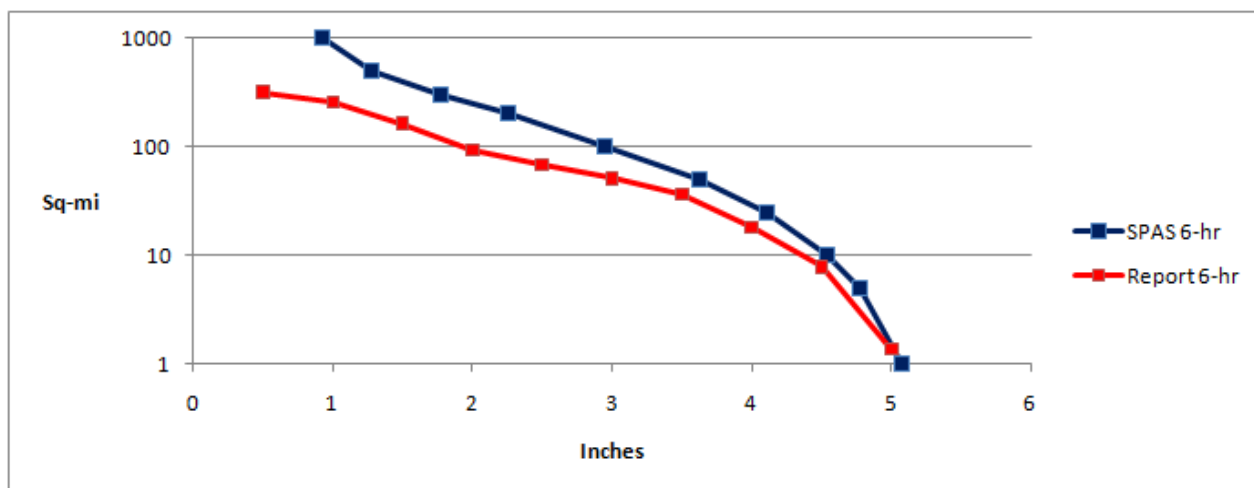
Figure 6.1D   SPAS analyzed 6-hour DA curve vs. USACE analyzed 6-hour DA curve for
Phoenix June 1972 SPAS 1062

6.1   Data Collection

The areal extent of a storm's rainfall is evaluated using existing maps and documents
along with plots of total storm rainfall. Based on the storm's spatial domain (longitude-latitude
box), hourly and daily rain gauge data are extracted from the database for the specified area,
dates, and times. To account for the temporal variability in observation times at daily stations,
the extracted hourly data must capture the entire observational period of all extracted daily
stations. For example, if a station takes daily observations at 8:00 AM local time, then the
hourly data needs to be complete from 8:00 AM local time the day prior. As long as the hourly
data are sufficient to capture all of the daily station observations, the hourly variability in the
daily observations can be properly addressed.

The daily database is comprised of data from NCDC TD-3206 (pre-1948) and TD-3200
(generally 1948 through present). The hourly database is comprised of data from NCDC TD-
3240 and NOAA's Meteorological Assimilation Data Ingest System (MADIS). The daily
supplemental database is largely comprised of data from "bucket surveys," local rain gauge
networks (e.g., ALERT, USGS, COCORAHS, etc.) and daily gauges with accumulated data.

6.2   Mass Curves

The most complete rainfall observational dataset available is compiled for each storm[1].
To obtain temporal resolution to the nearest hour in the final DAD results, it is necessary to
distribute the daily precipitation observations (at daily stations) into hourly bins. In the past, the
NWS had accomplished this process by anchoring each of the daily stations to a single hourly
station for timing. However, this may introduce biases and may not correctly represent hourly
precipitation at locations between hourly observation stations. A preferred approach is to anchor

---

[1] Appendix F contains data showing how many stations were used in each storm analysis, the sources of rainfall
data, whether NEXRAD radar was included, and the SPAS version.

the daily station to some set of nearest hourly stations. This is accomplished using a spatially based approach called the spatially based mass curve (SMC) process (see Appendix G).

6.3 Hourly or Sub-hourly Precipitation Maps

At this point, SPAS can either operate in its standard mode or in NEXRAD-mode to create high resolution hourly or sub-hourly (for NEXRAD storms) grids. In practice both modes are run when NEXRAD data are available so that a comparison can be made between the methods. Regardless of the mode, the resulting grids serve as the basis for the DAD computations.

6.3.1 Standard SPAS mode

The standard SPAS mode requires a full listing of all the observed hourly rainfall values, as well as the newly created estimated hourly data from daily and daily supplemental stations. This is done by creating an hourly file that contains the newly created hourly mass curve precipitation data (from the daily and supplemental stations) and the "true" hourly mass curve precipitation. If not using a base map, the individual hourly precipitation values are simply plotted and interpolated to a raster with an inverse distance weighting (IDW) interpolation routine in a GIS.

6.3.2 NEXRAD mode

Radar has been in use by meteorologists since the 1960s to estimate rainfall depth. In general, most current radar-derived rainfall techniques rely on an assumed relationship between radar reflectivity and rainfall rate. This relationship is described by the equation (1) below:

(1) $Z = a\text{R}^b$

where Z is the radar reflectivity, measured in units of dBZ, R is the rainfall rate, a is the "multiplicative coefficient" and b is the "power coefficient". Both a and b are related to the drop size distribution (DSD) and the drop number distribution (DND) within a cloud (Martner et al 2005).

The NWS uses this relationship to estimate rainfall through the use of their network of Doppler radars (NEXRAD) located across the United States. A standard default Z-R algorithm of $Z = 300\text{R}^{1.4}$ has been the primary algorithm used throughout the country and has proven to produce highly variable results. The variability in the results of Z vs. R is a direct result of differing DSD and DND, and differing air mass characteristics across the United States (Dickens 2003). The DSD and DND are determined by a complex interaction of microphysical processes in a cloud. They fluctuate hourly, daily, seasonally, regionally, and even within the same cloud (see Appendix G for a more detailed description).

Using the technique described above, also discussed in Appendix E, NEXRAD rainfall depth and temporal distribution estimates are determined for the area in question.

6.4   Depth-Area-Duration (DAD) Program

The DAD extension of SPAS runs from within a Geographic Resource Analysis Support System (GRASS) GIS environment[2] and utilizes many of the built-in functions for calculation of area sizes and average rainfall depths. The following is the general outline of the procedure:

1. Given a duration (e.g. x-hours) and cumulative precipitation, sum up the appropriate hourly or sub-hourly precipitation grids to obtain an x-hour total precipitation grid starting with the first x-hour moving window.

2. Determine x-hour precipitation total and its associated areal coverage. Store these values. Repeat for various lower rainfall thresholds. Store the average rainfall depths and area sizes.

3. The result is a table of depth of precipitation and associated area sizes for each x-hour window location. Summarize the results by moving through each of the area sizes and choosing the maximum precipitation amount. A log-linear plot of these values provides the depth-area curve for the x-hour duration.

4. Based on the log-linear plot of the rainfall depth-area curve for the x-hour duration, determine rainfall amounts for the standard area sizes for the final DAD table. Store these values as the rainfall amounts for the standard sizes for the x-duration period. Determine if the x-hour duration period is the longest duration period being analyzed. If it is not, analyze the next longest duration period and return to step 1.

5. Construct the final DAD table with the stored rainfall values for each standard area for each duration period.

---

[2] Geographic Resource Analysis Support System is commonly referred to as GRASS. This is free Geographic Information System (GIS) software used for geospatial data management and analysis, image processing, graphics/maps production, spatial modeling, and visualization. GRASS is currently used in academic and commercial settings around the world, as well as by many governmental agencies and environmental consulting companies. GRASS is an official project of the Open Source Geospatial Foundation.

7.   Storm Maximization

Storm maximization is the process of increasing rainfall associated with an observed extreme storm under the potential condition that additional moisture could have been available to the storm for rainfall production. This is accomplished by increasing the surface dew points (or SSTs) to some climatological maximum and calculating the enhanced rainfall amounts that could potentially have been produced if those enhanced amounts of moisture would have been available. The dew points (or SSTs) are subsequently adjusted to the elevation of the storm location and the elevation of the grid being analyzed. This is done to remove the amount of moisture associated with the analyzed dew point (or SSTs) that would not be available below that elevation, as the moisture associated with those values represents moisture in the atmospheric column above ground level.

An additional consideration is usually applied that selects the climatological maximum dew point or SSTs for a date 15 days towards the warm season from the date that the storm actually occurred. This procedure assumes that the storm could have occurred 15 days earlier or later in the year when maximum dew points or SSTs are higher. This assumption follows HMR guidance and is consistent with procedures used to develop PMP values in all the current HMR documents (e.g. HMR 51 Section 2.3.4 and WMO 1986) as well as all AWA PMP studies. There are rare occasions when this 15-day adjustment is not applied. This occurs when the synoptic weather patterns that produced the rainfall are of such a unique nature that they would not have occurred 15 days further towards the warm season. No storms used in this study fell into that category. A more detailed discussion of this procedure and example calculations are provided in Appendix C.

7.1   Use of Dew Point Temperatures

HMR and WMO procedures for storm maximization use a representative storm dew point (or SST) as the parameter to represent available moisture to a storm. Storm precipitation amounts are maximized using the ratio of precipitable water for the maximum dew point to precipitable water for the observed storm representative dew point.

Maximum dew point (or SST) climatologies are used to determine the maximum atmospheric moisture that could have been available. Prior to the mid-1980s, maps of maximum dew point values from the *Climatic Atlas of the United States* (1968) were the source for maximum dew point values. For the region covered by HMR 49, HMR 50 provided updated dew point climatologies. HMR 55A contained updated maximum dew point values for a portion of United States from the Continental Divide eastward into the Central Plains. The regional PMP study for Michigan and Wisconsin produced return frequency maps using the L-moments method. The Review Committee for that study included representatives from NWS, FERC, Bureau of Reclamation, and others. They agreed that the 50-year return frequency values were appropriate for use in PMP calculations. HMR 57 was published in 1994 and HMR 59 in 1999. These more recent NWS publications also updated the maximum dew point climatology, but used maximum observed dew points instead of return frequency values. For the Nebraska

statewide study, the Review Committee and FERC Board of Consultants agreed that the 100-year return frequency dew point climatology maps were appropriate because this added a layer of conservatism over 50-year return period. This has subsequently been employed in all PMP studies. This study is again using the 100-year return frequency climatology with data updated through 2012 (Figure 7.1).
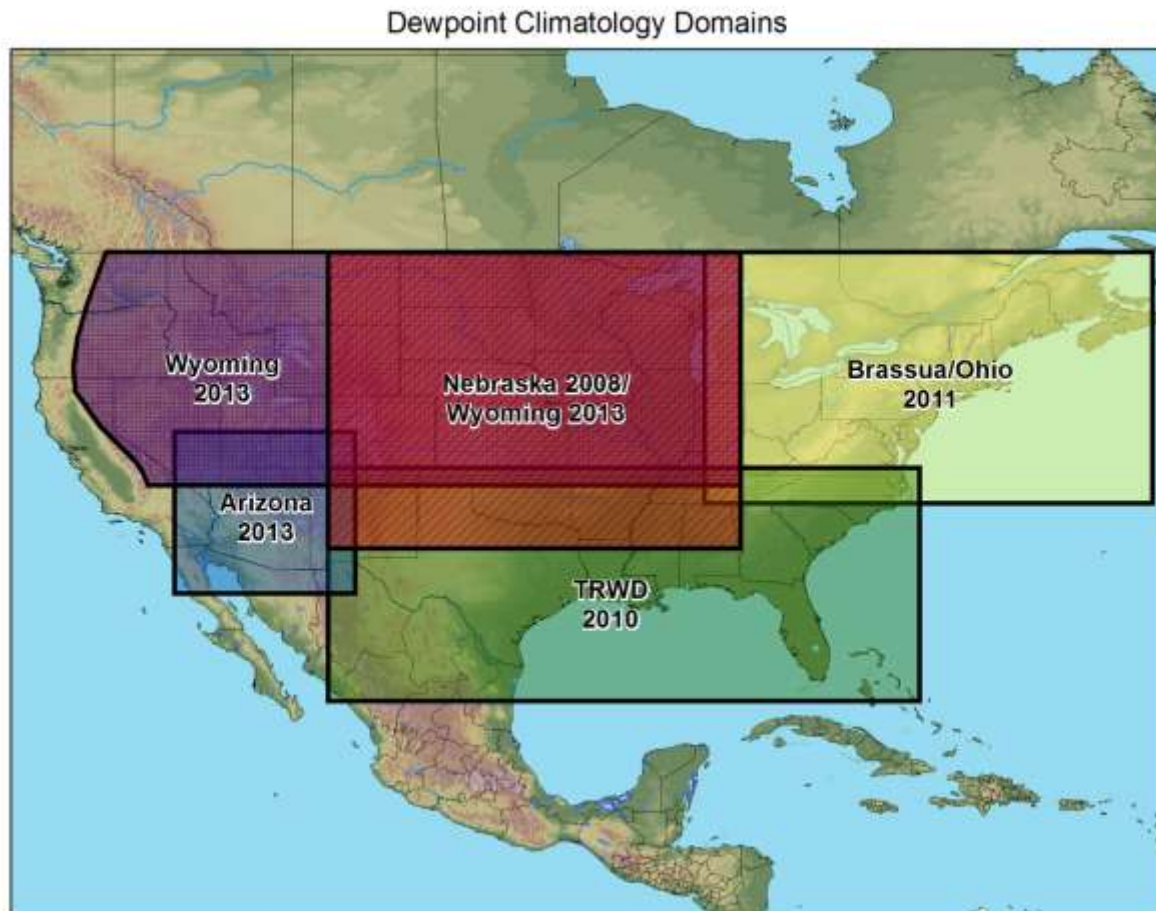
Figure 7.1 Maximum dew point climatology development dates and regions

Observed storm rainfall amounts are maximized using the ratio of precipitable water for the maximum dew point (or SST) to precipitable water for the storm representative dew point (or SST), assuming a vertically saturated atmosphere. The difference between the *maximum* precipitable water and *actual* precipitable water is converted into a percent and the storm rainfall totals as they occurred are enhanced (maximized) by this value, called the IPMF. By definition, maximization factors are always greater than or equal to 1. Following HMR and previous AWA PMP in-place storm maximization guidance (e.g., Tomlinson et al. 2008), the in-place maximization value is capped at 1.50 (HMR 51 Section 3.2.2 and HMR 55A Section 8.4.1.1). This 1.50 limitation is based on the consideration that if the moisture is increased beyond 50% or more, the assumption that the moisture can be increased without altering the storm's dynamics is no longer valid (HMR 55A, Section 8.4.1.1). The assumption is that properly analyzed and

maximized storms should be some percent larger than the actual storm, but increases beyond certain limits (e.g. 50%) would change the characteristics of the storm. The other considerations in these cases when the IPMF is greater than 1.50 reflect a scenario where the storm was a PMP-type but the process to define the storm representative dew point did not adequately find the true moisture source. This is generally because of a lack of data in the region where the moisture originated. In this study, four storms were affected by this 1.50 cap on the IPMF. They were September 1964, SPAS 1060, June 1972, SPAS 1062, August 2008 SPAS 1085, and September 2005 SPAS 1091; all local convective storms. This procedure was followed in this study using the updated maximum dew point climatology described in Section 4. More detailed discussions, along with examples of this procedure, are provided in Appendices C and D.

For storm maximization, average dew point values for the duration most consistent with the actual rainfall accumulation period for an individual storm (i.e. 3-, 12-, or 24-hour) were used to determine the storm representative dew point. To determine which time frame was most appropriate, the total rainfall amount was analyzed. The duration closest to when approximately 90% of the rainfall had accumulated was used to determine the duration used, i.e. 3-hour, 12-hour, or 24-hour.

The storm representative dew point (or SST when appropriate) was derived for each of the 51 storm events analyzed during this study. Once the general upwind location was determined, the hourly surface observations (or daily SSTs) were analyzed for all available stations within the vicinity of the inflow vector. From these data, the appropriate durational dew point value was averaged for each station (3-hour, 12-hour, or 24-hour depending on storm's rainfall accumulation). These values were then taken to 1000mb (approximately sea level) and the appropriate storm representative dew point (or SST) and location derived. The line connecting this point with the storm center location (point of maximum rainfall accumulation) is termed the moisture inflow vector. The information used and values derived for each storm's moisture inflow vector are included in Appendix F.

7.2   Use of Sea Surface Temperatures (SSTs)

Dew point observations are not generally available over ocean regions. When the source region of atmospheric moisture feeding an extreme rainfall event originates from over the ocean, a substitute for dew point observations is required. The NWS has adopted a procedure for using SSTs as surrogates for dew points over the ocean. The value used as the maximum SST in the PMP calculations is determined using the SST that is two standard deviations warmer than the mean SST. This provides a value for the maximum SST that has a probability of occurrence of about 0.025, i.e. about the 40-year return frequency value (see Section 4.1.3 for more detail).

These SST values are then treated the same as dew points and the same process is followed for storm maximization as if the SST values were dew point values from land based stations. A more detailed discussion, along with examples of this procedure, is provided in Appendices C and D.

74

Deriving and using SSTs for in-place maximization and storm transpositioning follows a similar procedure to that used with dew points. The HYSPLIT trajectory model provides a significant improvement in determining the inflow wind vector as compared to older methods. This is particularly significant when extrapolating coastal wind observations over long distances to reach warmer ocean regions. Timing is not as critical for inflow wind vectors extending over the oceans, since SSTs change very slowly compared to dew point values over land. What is important is the changing wind direction for situations where there is curvature in the wind fields as the inflow wind vector is followed upwind for hundreds of miles.

As is the case for the storm representative dew point analysis, timing of the rainfall is determined using the rainfall mass curves from the region of maximum rainfall. The wind speed and direction are determined using NCEP reanalysis wind fields incorporated into the HYSPLIT program to identify source regions for atmospheric moisture originating from the warmer ocean areas. The location of the storm representative SST was determined when SSTs are generally changing less than one degree F in a degree latitude and/or longitude distance following the inflow wind vector upwind. An average of the SST values for that general location were used to determine the storm representative SST.

For storm maximization, the value for the maximum SST is determined using the mean plus two sigma SST for that location for a date 15 days before or after the storm date (which ever represents the climatologically warmer SST). Storm representative SSTs and the mean plus two sigma SSTs are used in the same manner as storm representative dew points and maximum dew points in the maximization and transpositioning procedure.

7.3   Storm Transpositioning

Extreme rain events in a meteorologically homogeneous region surrounding a location are a very important part of the historical evidence on which a PMP estimate for the location is based. Since most locations have a limited period of record for rainfall data collected, the number of extreme storms that have been observed over a given location is limited. Storms that have been observed within similar climate and topographic regions are analyzed and adjusted to provide information describing the storm rainfall as if that storm had occurred over the location being studied. Transfer of a storm from where it occurred to a location that is meteorologically and geographically similar is called storm transpositioning. The underlying assumption is that storms transposed to the location could occur under similar meteorological conditions as the original location. To properly relocate such storms, it is necessary to address issues of similarity as they relate to meteorological conditions, moisture availability, and topography.

The search for extreme rainfall events identified storms that occurred throughout Arizona as well as over much of the southwestern US region west of the Continental Divide and northern Mexico. This region was considered meteorologically and geographically similar to one or more locations within Arizona.

To define general regions across the state where storms could be transpositioned, the state was divided into five transposition zones. Each transposition zone was manually delineated after careful consideration of a combination of criteria including; physiographic provinces (defined by both the Arizona Geological Survey and the USGS), climatological zones defined by the NCDC, variations in topography, and ecological regions. The L-moment statistical station regions

defined in NOAA Atlas 14, Volume 1 (Bonnin et al 2004, pages 22-26) were also evaluated as delineation criteria. These criteria helped identify features of regional precipitation impact such as basin-and-range inflow barriers, low and high desert boundaries (i.e., the Sonoran and Mojave Deserts), the Mogollon Rim, and the Colorado Plateau. Five transposition zones were defined (Figure 7.2): 1) High Desert/Basin and Range, 2) Sonoran Desert, 3) Mojave Desert, 4) Mogollon Rim, and 5) Colorado Plateau. It is recognized that these boundaries are not discrete boundaries in nature but transitional zones. However, for the purpose of modeling, these zones provide a good estimation of acceptable transpositionable extents for each storm.

Each of the 51 storms on the short storm list were individually analyzed to determine their unique transposition limits. Initially AWA placed general transposition limits on all storms and their individual DAD zones based on subjective judgments of the meteorology associated with each and the interacting with topography at the original location versus other areas of the state. Initial results were presented at the 6th Review Board meeting. During the meeting, extensive discussions with all members present took place to explicitly define transposition limits for each of the 91 SPAS analyzed DAD zones. Each storm's meteorological characteristics were evaluated, including the storm type, the seasonality, the storm isohyetal patterns, and the storm's moisture source. Each of these factors were evaluated for each storm to provide reasoning as to where the storm could conservatively be transpositioned. Each storm was assigned to one or more of the five transposition zones across the study domain. In addition, limitations were applied to some storms to account for elevation differences.
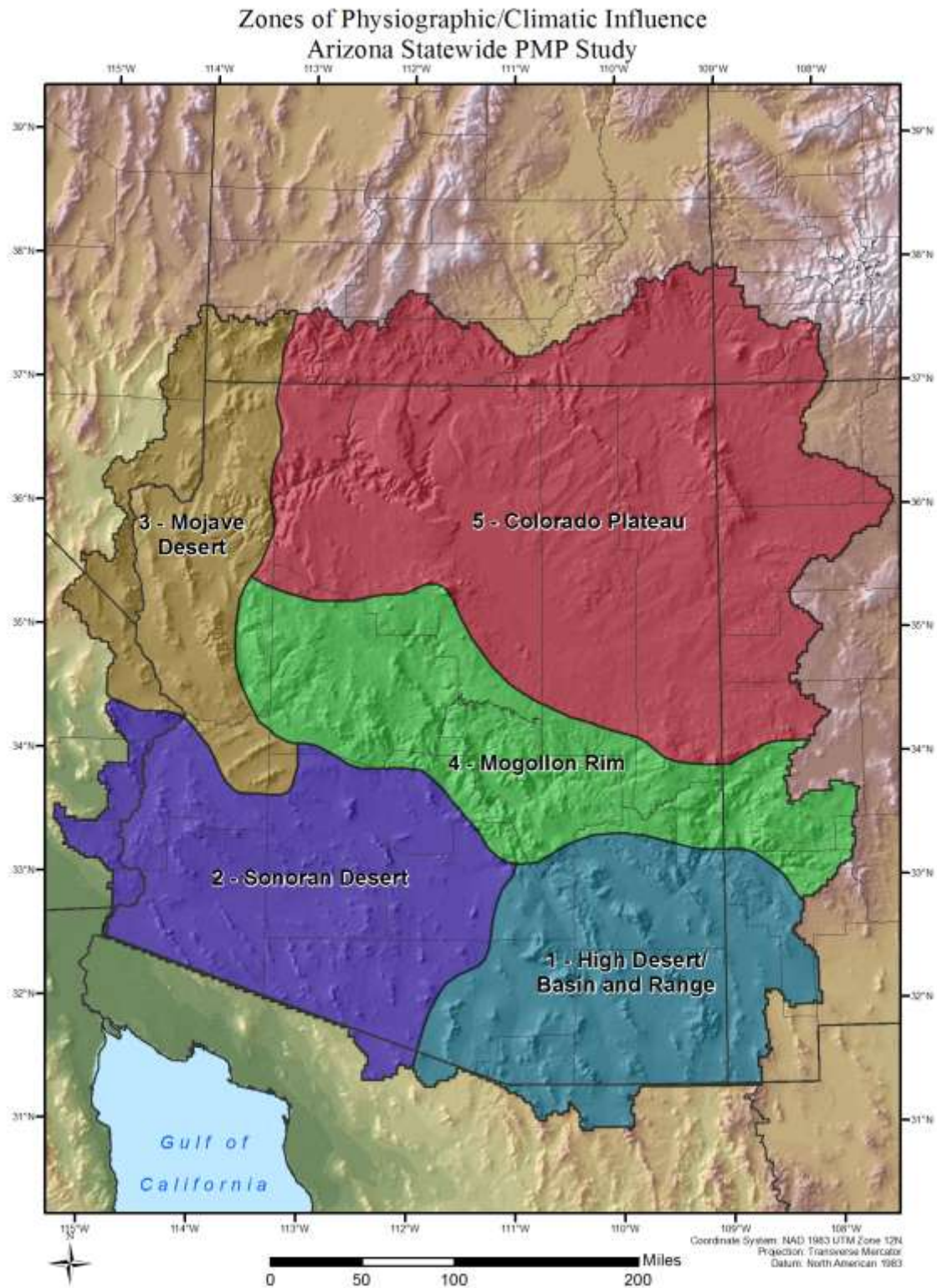
Figure 7.2 Transposition zones used to define transposition limits for individual storms

Using the 5 transposition zones and the analyzed transposition, transposition limits were placed upon each of the 91 SPAS DAD zones with the understanding that additional refinements would take place as the data were run through the PMP Evaluation Tool. Numerous sensitivity runs were performed using the PMP Evaluation Tool to investigate the results based on the initial transposition limits. Several storms were re-evaluated based on the results that showed inconsistencies and/or unreasonable values. Although these decisions were somewhat subjective, as much as possible decisions to adjust the transposition limits for a given storm were based on the resulting maximization factors after the storm was moved to a grid cell. For all storms, the in-place maximization factor does not change during this process. The moisture transposition factor and the OTF change as a storm is moved from its original location to a new location. Further, because the moisture transposition factor is only a function of the difference in available moisture between the original location and the new location, this factor does not vary significantly in space. Generally, most moisture transposition factors result in less than a +/-10% change. Therefore, the most important factor in the transposition process is the OTF. These factors can vary significantly between locations. This is to be expected, as the topography across Arizona varies significantly in elevation, aspect and slope, often over very short distances.

The spatial variations in the OTF were useful in making decisions on transposition limits for a given storm. As described in Section 7, values beyond 1.5 for a storm's maximization factor exceed reasonable limits. In these situations, changing a storm by this amount is likely also changing the storm characteristics. The same concept applies to the OTF. Excess OTF values indicate that transposition limits have most likely been exceeded. Therefore, limitations were placed on the OTF for local storms not allowing an individual storm to be transpositioned to locations that would result in OTF of greater than 1.50. In almost all cases, the OTF for the tropical and general storm types was less than or equal to 1.50, so no limitation was applied to these storm types. The same limitation could be applied to OTF values of 0.50 or less, but in these cases it is not relevant since a storm being affected by an OTF of 0.50 will be reduced to such a level as to not affect PMP values.

From these analyses, refinements such as limiting a particular storm's transposition location by elevation constraint or by OTF amount were applied. Examples include August 1981, SPAS 1135. Originally, this storm was transpositioned to all of transposition zone 2 and 3, and most of zone 4 and 5. However, results of the initial PMP Evaluation Tool runs showed the magnitude of the resulting PMP depth at 1 and 3 hours were significantly higher than other storms both within the transposition zone and at the boundaries of the transposition zones. Because this storm would be a controlling storm at many of the locations, it was very important to determine if the magnitude was appropriate or if other factors were inappropriately increasing the PMP depths at a given location. Investigations into these factors showed that the OTF for this storm was well above 2.00 in many locations (Figure 7.3). As with the IMPF, values above 1.50 are considered inappropriate. These high values were generally the result of the variation in NOAA Atlas 14 values between the in-place storm center locations (southeastern Nevada-see Appendix F) and areas in Arizona (Figure 7.4). In this case, the NOAA Atlas 14 values are very low in magnitude compared to several areas in Arizona. Discussion with the Review Board and internal investigations resulted in the conclusion that some of the NOAA Atlas 14 values in southern and southwestern Arizona seem to be unjustifiably high (especially around the Kofa Mountains). In addition, the values across state lines between Arizona and California do not

match up well. In each instance, the Arizona values are much higher than California. In transposition zones 4 and 5, the elevation limitation was refined for this storm to constrain it within 3,000 feet of the storm center elevation in zone 4 and 2,000 feet in zone 5. This resulted in a better agreement with other storms in each region. Similar analyses were completed for all other controlling storms and storms that were near the controlling storm's PMP depths.
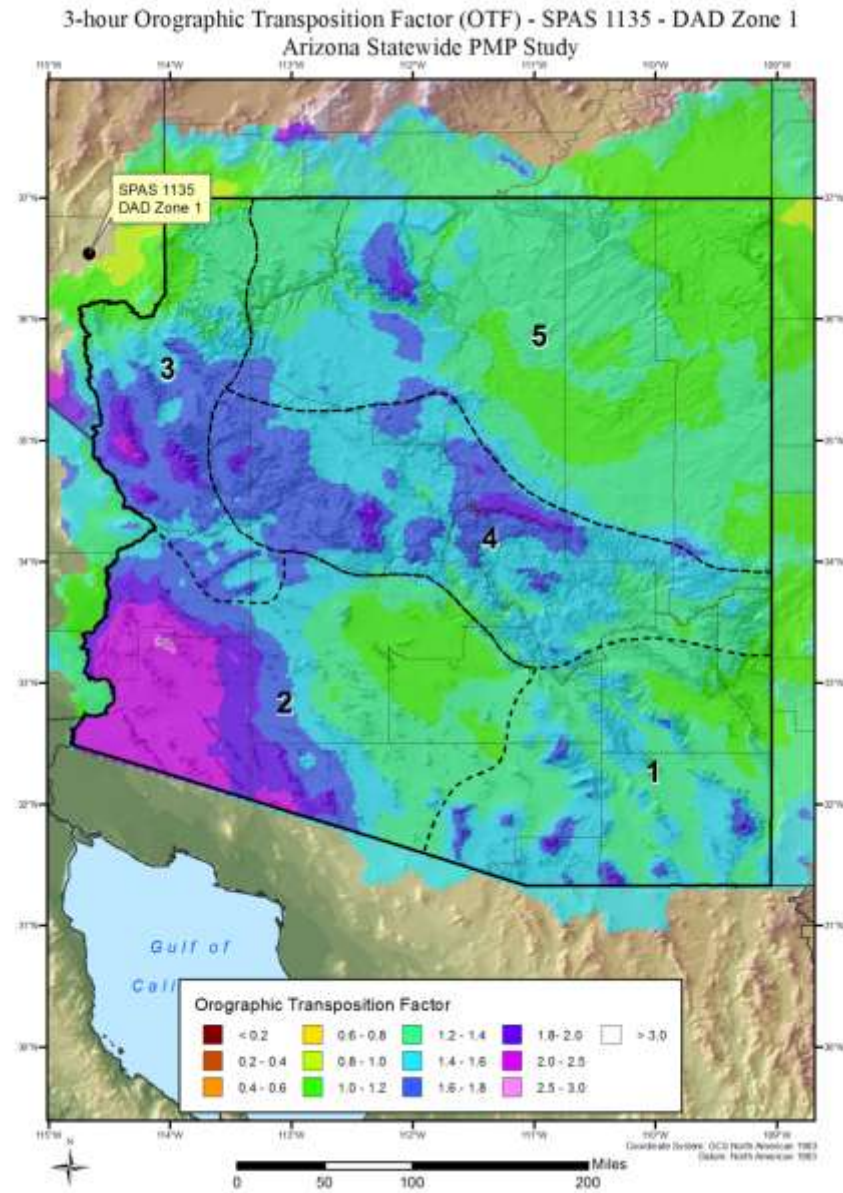
Figure 7.3 Orographic Transposition Factors for August 1981, SPAS 1135
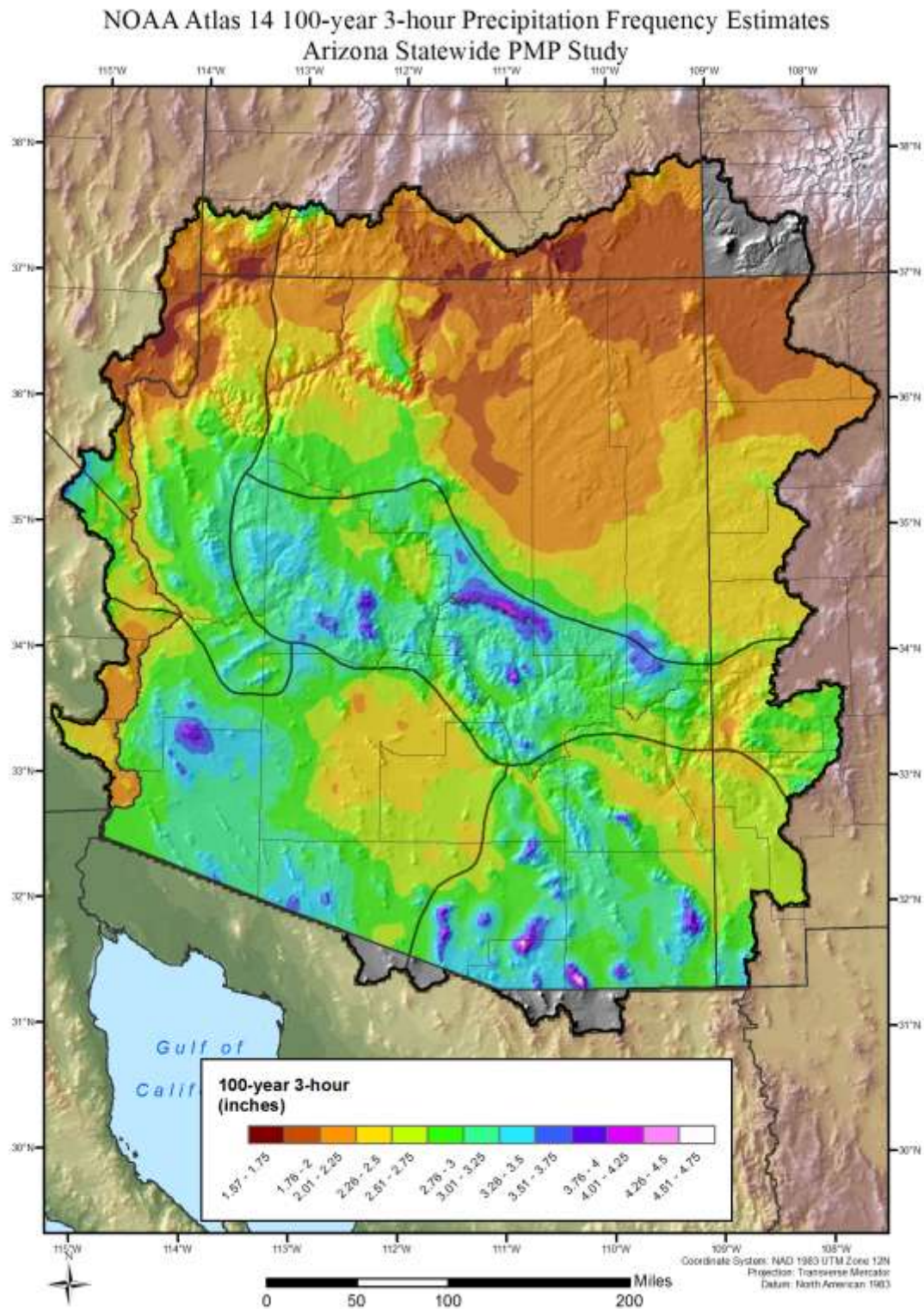
Figure 7.4 NOAA Atlas 14 100-year, 3-hour precipitation frequency climatology

8. Development of PMP Values

PMP depths were calculated by comparing the total adjusted rainfall values for all transpositionable storm events over a given grid point and taking the largest value, a process comparable to the envelopment of all transpositionable events. In this case, envelopment occurs because the largest PMP depth for a given duration is derived after analyzing all the transpositionable storms for each grid point at each location for each duration at the area sizes specific to the basin being analyzed. In addition, several storms can control the PMP depth for a given basin at various grid point and/or durations. This is similar to the adding of an envelopment curve on a DA chart, which encompasses several different storms for each duration.

The adjusted rainfall at a grid point, for a given storm event, was determined by applying a Total Adjustment Factor (TAF) to the SPAS analyzed DAD value corresponding to the target basin area size (in square miles) at the appropriate duration. The TAF is the product of the three separate storm adjustment factors, the IPMF, the MTF, and the OTF. In-place maximization and moisture transposition are described in Section 7. Orographic transposition is described in Section 3. These calculations were completed for all 51 storms and their associated SPAS DAD zones (91 total) for every grid point analyzed over the entire domain.

An Excel storm adjustment spreadsheet was produced for each of the 91 analyzed storm DAD zones. These spreadsheets are designed to perform the initial calculation of each of the three adjustment factors, along with the final TAF. The spreadsheet format allows for the large number of data calculations to be performed correctly and consistently in an efficient template format. In addition to the IPMF, MTF, and OTF calculations, a Boolean transpositionability flag for each grid cell is stored within the spreadsheets, allowing a conditional statement to determine if the given storm is spatially transpositionable to the grid cell based on predetermined criteria (see Section 7.3). Information such as NOAA Atlas 14 data, coordinate pairs, grid point elevation values, equations, and the precipitable water lookup table remain constant from storm to storm and remain static within the spreadsheet template. The spreadsheet contains a final adjusted rainfall tab with the adjustment factors, including the TAF, listed for each grid cell. For each storm, this table was exported to a GIS feature class to be used as input for the PMP Evaluation Tool. This step is designed to provide the PMP Evaluation Tool functionality independent of the storm adjustment spreadsheets. While the spreadsheets were used to calculate the adjustment factors for the storms in this study, they need not be present for the PMP Evaluation Tool to run; only feature classes containing TAFs for each grid cell are required. At any point in the future, new storm feature classes could be added, removed, or edited.

The PMP Evaluation Tool receives the storm TAF feature classes and the corresponding DAD tables for each of the 91 storm events as input, along with a basin outline feature layer as a model parameter. The PMP Evaluation Tool then calculates and compares the total adjusted rainfall, for each transpositionable storm, at the grid points of all grid cells any portion which is within the target basin, and determines the PMP depth for six durations of the PMP event for each of the three storm types (local, general, and tropical). The durations for general frontal and remnant tropical PMP are 6-, 12-, 18-, 24-, 48-, and 72-hours. The durations for local PMP are

1-, 2-, 3-, 4-, 5-, and 6-hours. The grid point PMP values are used to compute an average basin PMP depth for each duration. Furthermore, the PMP Evaluation Tool temporally distributes each of the PMP depths, as well as the basin average value, according to the specified temporal design criteria for each storm type. Finally, GIS files are output to separate folders for each of the storm types.

The following sections describe the procedure for calculating the IPMF, the MTF, the OTF, and the TAF for the creation of the storm adjustment feature classes. Examples of each of these calculations are presented. Then the implementation and application of the PMP Evaluation Tool to calculate basin PMP is discussed.

8.1   Available Moisture at Source and Target Locations

The available atmospheric moisture, in terms of precipitable water depth, must be determined for the storm center location to calculate both the IPMF and MTF. The IPMF is determined by taking the ratio of the maximum precipitable water depth at the storm representative dew point (or SST) location to the storm representative precipitable water depth at the storm representative dew point (or SST) location. The MTF is determined by taking the ratio of the maximum precipitable water depth at the transposition dew point (or SST) location to the maximum precipitable water depth at the storm representative dew point (or SST) location. Use of dew points and SST are described in Sections 7.1 and 7.2, respectively. Note that in the final total adjustment factor calculation, the precipitable water depth at the storm center is used in both the numerator of the IPMF and denominator of the MTF and is ultimately cancelled out of the equation, having no impact on the total adjustment factor. However, it is still important to calculate the storm center precipitable water, and the MTF and IPMF individually, so that the proportion of each component can be quantified for completeness and quality/error control purposes.

The precipitable water depth is calculated from a lookup table stored within the storm adjustment spreadsheets. The lookup table is a digital version of the precipitable water table found in Appendix C of HMR 55A with dew point temperatures every ½ °F for elevations from sea-level to 15,000 feet and through the full atmospheric column height of 30,000 feet. Derivation of precipitable water values associated with dew points or SSTs above 80°F was completed through extending the data series using simple extrapolation of the previous values for a given elevation. This was based on the rate of change for previous values per degree F at that elevation and continuing that trend through the values needed above 80°F.

To determine the temperatures to use in the precipitable water lookup table, GIS was used to extract the values from the appropriate monthly dew point or SST GRID. For each analyzed storm event, the GRIDs were shifted using the Data Management ArcToolbox 'Shift' tool. The raster layer was shifted, in degrees longitude (Δx) and degrees latitude (Δy), according to the moisture inflow vector components for that storm. The Δx could be determined by taking the difference between the storm center longitude and the storm representative dew point (SST) location longitude. The Δy could be determined by taking the difference between the storm center latitude and the storm representative dew point (SST) location latitude. These inflow

82

vectors, analyzed for each storm in this study, are included in Appendix F. An example of a shifted SST GRID layer and resolved moisture inflow vector components is shown in Figure 8.2. In some instances, once the dew point or SST GRID was shifted, the GRID extent did not entirely cover the analysis domain. In this case, the isotherms were manually extrapolated outward for a distance great enough to provide coverage of the analysis domain. The extrapolation was done subjectively by estimating the position based on the isodrosotherm trends over the existing coverage area. Considering the small amount of variability in the final MTF values, the amount of potential error introduced by this extrapolation is negligible.

The shifted GRID temperatures were then extracted to the storm center grid point and stored in a storm adjustment spreadsheet. The shifted GRID temperatures were also extracted to each of the 64,103 domain grid points and stored within the 'MTF' tab of each storm adjustment spreadsheet.
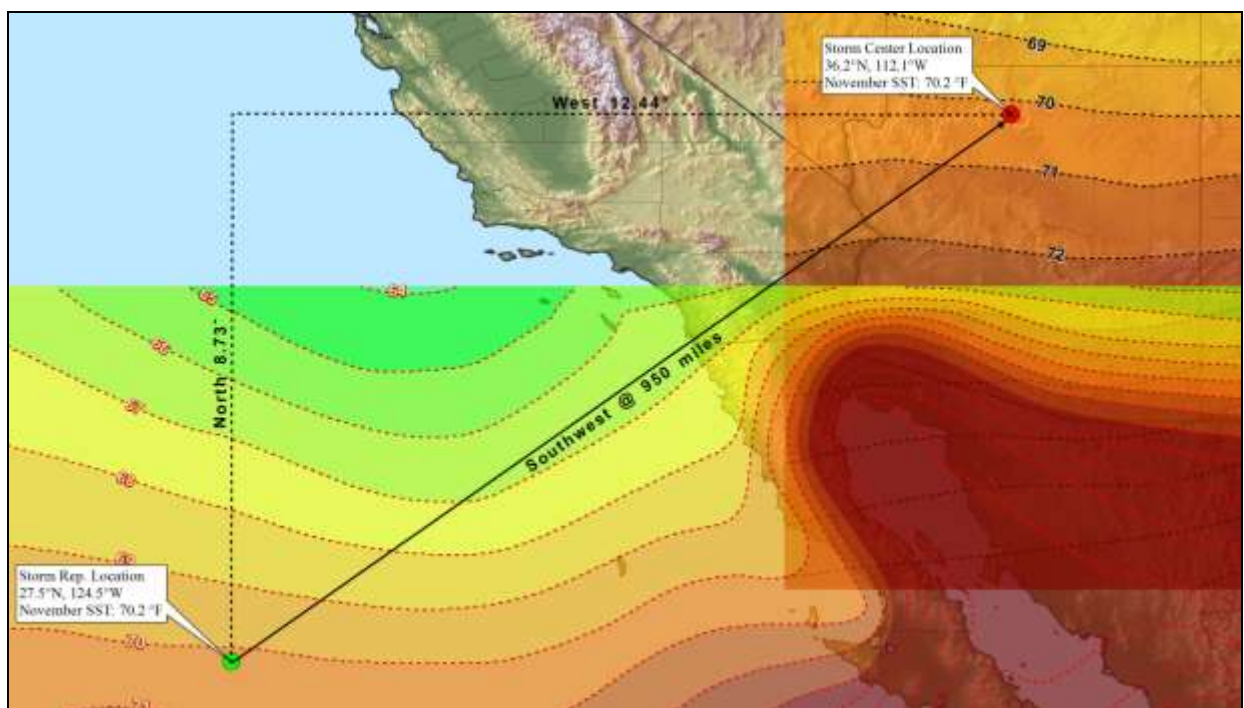
Figure 8.1 Example of shifted SST GRID and moisture inflow vector components.

The precipitable water was calculated for each event, within the storm adjustment spreadsheet, for the storm center grid point and each of the other grid points within the analysis domain using the lookup table with the storm center elevation. Storm center elevations were taken from the NWS Precipitation Frequency Data Server then rounded to the nearest 100', or nearest 500' for elevations above 5,000', to coincide with the values precipitable water lookup table.

As described in Section 7, the precipitable water depths are adjusted for elevation. This is done by determining the precipitable water depth present in the atmospheric column (at

30,000') and subtracting the precipitable water depth that would be present in the atmospheric column between sea-level and the surface at the storm location using Equation 8.1.

$$W_p = W_{p,30,000'} - W_{p,elev}$$ Equation 8.1

8.2 In-Place Maximization Factor

In-place storm maximization is applied to each storm event using the methodology described in Section 7. Storm maximization is quantified by IPMF using Equation 8.2.

$$IPMF = \frac{W_{p,max}}{W_{p,rep}}$$ Equation 8.2

where,
$W_{(p,max)}$ = precipitable water for the maximum dew point
$W_{(p,rep)}$ = precipitable water for the representative dew point

8.3 Moisture Transposition Factor

The change in available atmospheric moisture between the storm center location and the basin target grid cell is quantified as the MTF. This MTF represents the change due to horizontal distance only and is calculated at the storm center elevation. The change due to vertical displacement is quantified in the OTF, described in the next section. The MTF is calculated as the ratio of precipitable water for the maximum dew point (or SST) at the target grid cell location to precipitable water for the storm maximum dew point (or SST) at the storm center location.

$$MTF = \frac{W_{p,trans}}{W_{p,max}}$$ Equation 8.3

where,
$W_{(p,trans)}$ = precipitable water at the target location
$W_{(p,max)}$ = precipitable water at the storm center location

8.4 Orographic Transposition Factor

Section 3.1 provides detail on the methods used in this study to define the orographic effect on rainfall. The OTF is calculated by taking the ratio of orographically adjusted rainfall to non-orographically adjusted rainfall.

84

$$MTF = \frac{P_o}{P_i}$$ Equation 8.4

where,
> P_o = orographically adjusted rainfall (target)
> P_i = SPAS-analyzed in-place rainfall

The orographically adjusted rainfall is determined by applying the function in Equation 3.1 to SPAS-analyzed rainfall depth for the appropriate duration (24-hour for general and tropical events and 3-hour for local events).

$$P_o = mP_i + b$$ Equation 8.5 (from Equation 3.1)

where,
> P_o = orographically adjusted rainfall (target)
> P_i = SPAS-analyzed in-place rainfall
> m = proportionality coefficient (slope)
> b = transpositional offset (y-intercept)

8.5 Total Adjusted Rainfall

The TAF is a product of the linear multiplication of the IPMF, MTF, and OTF. The TAF is a combination of the total moisture and terrain influences on the SPAS analyzed rainfall when maximized and transpositioned to the target grid cell.

$$TAF = IPMF * MTF * OTF$$

from Equation 1.1.

The TAF, along with other data relevant to each grid point, is exported and stored within the storm's adjustment factor feature class. The feature class includes a spatial component, a point feature at each grid cell centroid, and a table component as shown in Figure 8.2. The table stores the grid point ID, the storm ID, the latitude and longitude coordinate pair, the transposition zone ID, the elevation, the storm adjustment factors, and the transpositionability flag, for each of the 64,103 grid points within the analysis domain.

Figure 8.2 Storm adjustment factor feature class table example

8.6 Sample Calculations

The following sections provide sample calculations for the storm adjustment factors for the Bear Spring, AZ, February 28 – March 3, 1978 DAD zone 1 storm event (SPAS 1150_1) and the transposition of that storm to grid point #1 in the McMicken Dam watershed (Figure 8.3 and 8.4).
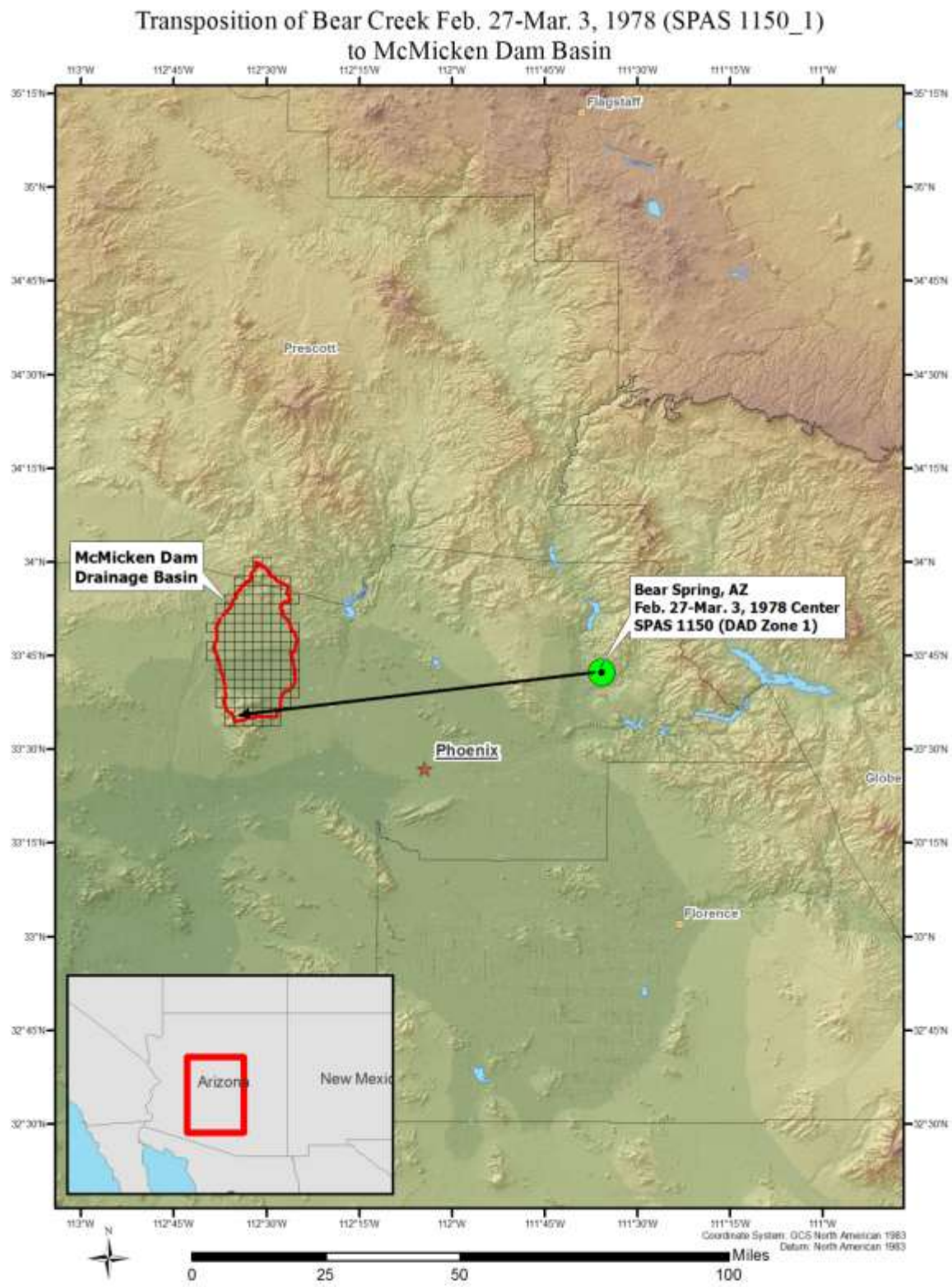
Figure 8.3 Location of Bear Spring1978 (SPAS 1150_1) transposition to McMicken Dam Basin
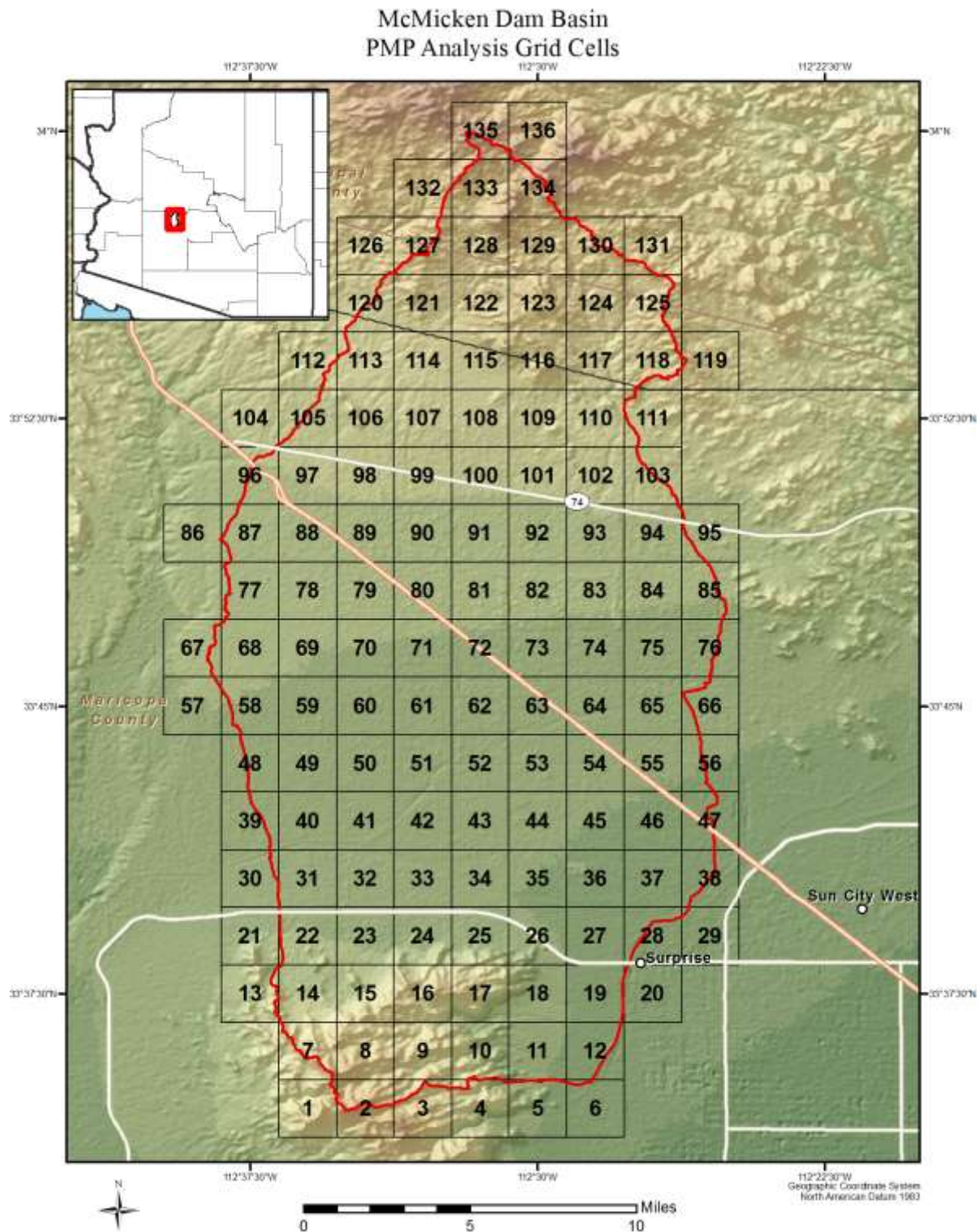
Figure 8.4 McMicken drainage basin with numbered analysis grid network

8.6.1 Example of Precipitable Water Calculations

Using the storm representative dew point temperature and storm center elevation as input, the precipitable water lookup table returns the depth, in inches, to be used in Equation 1.1. The storm representative dew point temperature is 58.5 °F. The storm center elevation is approximated at 2,300 feet at the storm center of 33.70 N, 111.60 W. The storm representative available moisture (Wp, rep) is calculated.

$$W_{p,rep} = W(@58.5°)_{p,30,000'} - W(@58.5°)_{p,2,300'}$$

or,

$$W_{p,rep} = 1.28 - 0.315"$$

$$W_1(p, rep) = 0.965"$$

The temporally transpositioned February maximum dew point temperature at the storm center is 61.0 °F at the in-place elevation of 2,300 feet. The in-place climatological maximum available moisture ($W_{p, max}$) is calculated…

$$W_{p,max} = W(@61.0°)_{p,30,000'} - W(@61.0°)_{p,2,300'}$$

$$W_{p,max} = 1.42 - 0.340$$

$$W_1(p, max) = 1.11"$$

The transpositioned climatological maximum available moisture must be determined for each target grid cell within the McMicken Dam basin domain. There are 136 grid cells within the basin domain. Only the first grid cell #1, at 33.575° N, 112.6° W (in the southwest corner of the basin), will be discussed in this example. The temporally transpositioned February 24-hour climatological maximum dew point temperature, at the location 60 miles south of grid cell #1, is 61.5 °F at the elevation of 2,300 feet[3]. The horizontally transpositioned climatological maximum available moisture ($W_{p, trans}$) is calculated.

$$W_{p,trans} = W(@61.5°)_{p,30,000'} - W(@61.5°)_{p,2,300'}$$

$$W_{p,trans} = 1.49 - 0.350"$$

$$W_1(p, trans) = 1.14"$$

---

[3] Note: Although the elevation at grid point #1 is at 2,600 feet, the elevation of the storm center is used to remove the vertical component of the moisture transposition which will be included in the orographic transposition factor.

8.6.2 In-place Maximization Factor

$$IPMF = \frac{W_{p,max}}{W_{p,rep}}$$

$$IPMF = 1.11/0.965$$

$$\mathbf{IPMF = 1.15}$$

8.6.3 Moisture Transposition Factor

$$MTF = \frac{W_{p,trans}}{W_{p,max}}$$

$$MTF = 1.14/1.11$$

$$\mathbf{MTF = 1.03}$$

8.6.4 Orographic Transposition Factor

Table 8.1 gives an example of NOAA Atlas 14 24-hour values (in inches) at both a storm center location (source) grid point and a basin (target) grid point to be used to determine the orographic relationship.

Table 8.1 10-year through 1,000-year NOAA Atlas 14 depths for SPAS 1150_1 for the storm center grid (SOURCE) and McMicken Dam grid point 1 (TARGET)

	Proportionality Constant - 24-hour						
	10 year	25 year	50 year	100 year	200 year	500 year	1000 year
SOURCE (X-axis)	3.05	3.73	4.27	4.85	5.46	6.32	7.02
TARGET (Y-axis)	2.99	3.65	4.17	4.71	5.28	6.07	6.70

When the NOAA Atlas 14 values are plotted (Figure 8.5), a best fit trendline can be constructed to provide a visualization of the relationship between the NOAA Atlas 14 values at the source and target locations. In this example, the values for the source grid point nearest the Bear Spring (February 1978) storm center are plotted on the x-axis while the target values for the first grid point in the McMicken Dam basin are plotted on the y-axis.
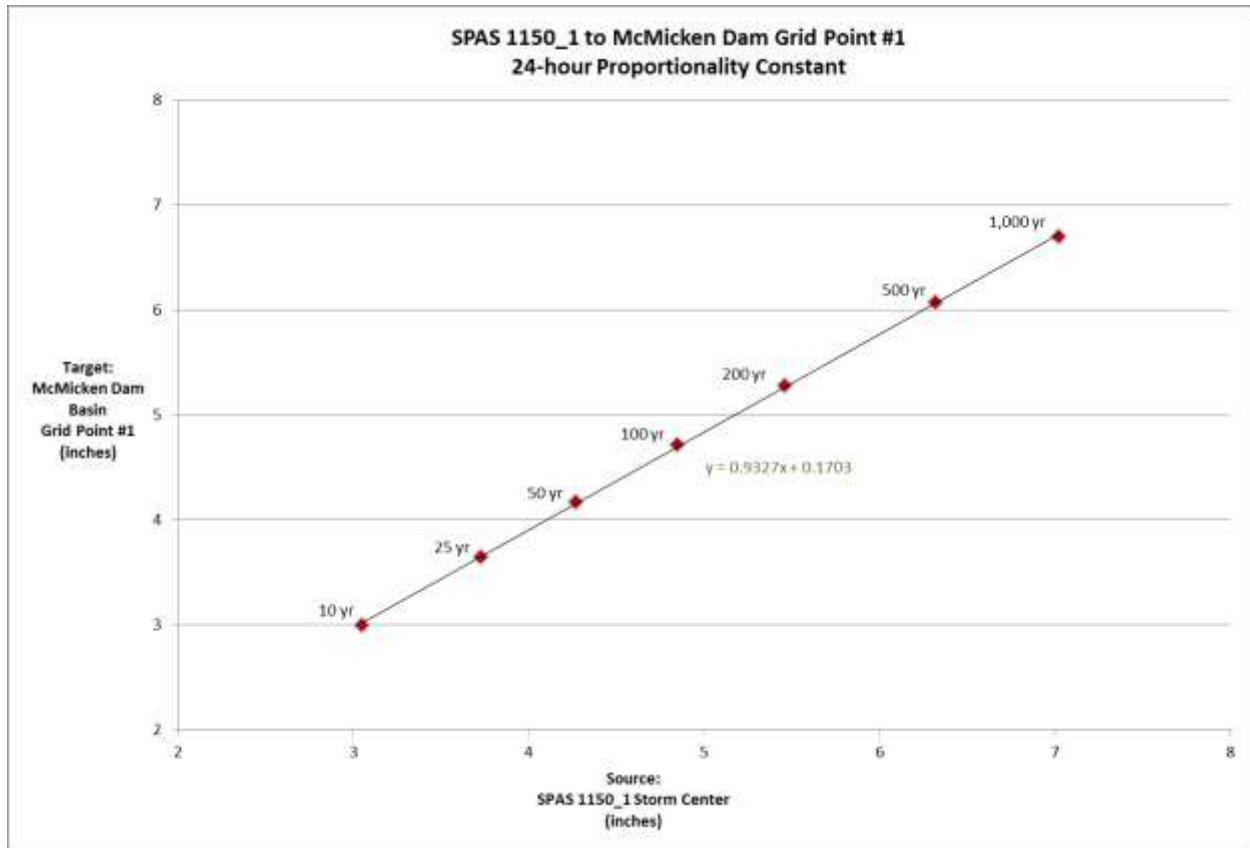
Figure 8.5 Example of orographic proportionality between the SPAS 1150 (Bear Spring, 1978
DAD Zone 1) storm center and the McMicken Dam Basin grid point #1.

The orographically adjusted rainfall at the target location can be estimated using the
equation of the trendline in slope-intercept form.

$$y = mx + b$$ Equation 8.6

The slope, *m* is the proportionality coefficient, representing the direct relationship
between the source and target cells. The *y*-intercept, *b,* is used to correct for spatial variability in
the precipitation frequency estimate recurrence intervals. The equation for the SPAS 1150_1 24-
hour orographically adjusted rainfall transpositioned to McMicken Dam grid point #1, based on
the linear trendline in Figure 8.5 is:

$$y = 0.93x + 0.17$$

The maximum SPAS analyzed 24-hour point rainfall value of 6.13" is entered as the *x*
value to estimate the target *y*-value, or orographically adjusted rainfall (P_o) of 5.87".

91

$$P_o = 0.93(6.13) + 0.17$$

$$P_{\downarrow}o = 5.87"$$

The ratio of the orographically adjusted rainfall (P_o) to the in-place SPAS analyzed 24-hour rainfall (P_i) yields the orographic transposition factor (OTF).

$$OTF = 5.87/6.13$$

$$OTF = 0.96$$

The OTF to grid cell #1 of the McMicken Dam basin is 0.96, or a 4% rainfall decrease from the storm center location due to terrain effects. The OTF is then considered to be a temporal constant for the spatial transposition between that specific source/target grid point pair, for that storm only, and can then be applied to the other durations for the given storm.

8.6.5 Total Adjustment Factor

$$TAF = IPMF * MTF * OTF$$

$$TAF = 1.15 * 1.03 * 0.96$$

$$TAF = 1.14$$

The total adjustment factor for SPAS 1150_1 at McMicken Dam grid point #1, representing storm maximization and transposition, is 1.14, an overall increase of 14% from the original SPAS analyzed in-place rainfall. The TAF can then be applied to the DAD value for the basin size to calculate the total adjusted rainfall. If the total adjusted rainfall is greater than the depth for all other transpositionable storms, it becomes the PMP depth at that grid point.

8.7   PMP Calculation Process

To calculate PMP, the TAF for each storm must be applied to the storm's DAD value for the appropriate basin size to yield a total adjusted rainfall value. The storm's total adjusted rainfall value must then compared with the adjusted rainfall values of every storm in the database transpositionable to the target grid point. This process must be repeated for each grid point within the basin domain and for each duration for the three storm types. The extraordinary numbers of calculations necessary for these comparisons are handled efficiently by a scripted tool. A GIS-based scripted PMP evaluation tool was developed to handle numerous comparisons and calculations in the final steps of the PMP calculation process and is described in Section 9.

Final PMP values are calculated for each grid cell for which any portion is enclosed within the input basin domain. These values, along with the basin average depth, are produced and stored in various GIS files by the GIS-based PMP Evaluation Tool as described in Section 9.

8.8 Temporal Distribution of PMP Values

Once gridded PMP values are determined for each cell within the basin, both they and the basin average value are temporally distributed over the total analysis duration. There are separate distribution guidelines for long duration events (tropical and general storms) and short duration events (local storms).

8.8.1 General Frontal and Tropical Storm Temporal Distribution

The general frontal and tropical storm distribution method is defined as follows for the 72-hour duration:

1st Day: Second Largest Rainfall Day uniformly distributed
2nd day: Largest Rainfall Day sequenced as follows:
      A. Third largest 6-hr period uniformly distributed
      B. Second largest 6-hr period uniformly distributed
      C. Largest 6-hr period uniformly distributed
      D. Fourth largest 6-hr period uniformly distributed
3rd day: Smallest Rainfall Day uniformly distributed [4]

This temporal distribution comes from *PMF Studies for Evaluation of Spillway Adequacy General Guideline* (ADWR, 2004). Analysis of the storm data used in this study showed that those guidelines appropriately capture a reasonable temporal distribution as design criteria for the general and tropical PMP storm patterns.

8.8.2 Local Storm Temporal Distribution

NEXRAD rainfall data from storms analyzed by SPAS was used to develop a recommended temporal distribution for local storm PMP design events in Arizona. The NEXRAD data indicates that for the vast majority of these storms, periods of high intensity rainfall occur in three hours or less. For practical and administrative reasons however, the existing practice of modeling 6-hour local PMP design events is maintained. To decide on an appropriate recommendation, a "hydrologic subcommittee" was formed of various members of the project team, Review Committee, ADWR, and the Flood Control District of Maricopa County, each having experience and expertise in performing hydrologic studies in Arizona. After evaluation of temporal patterns from all of the analyzed storms having NEXRAD data, the hydrologic subcommittee defined and recommended a 6-hour distribution (designated as "LS-6") modified from a storm observed in July 1998 in Navajo County at Joseph City near Holbrook. The LS-6 distribution recommended for local storm PMP design events in Arizona is shown in Figure 8.6.

---

[4] This temporal distribution is from the *PMF Studies for Evaluation of Spillway Adequacy General Guidelines* (ADWR, March 2004). Analysis of the storm data used in this study showed that those guidelines were appropriate in capturing the expected temporal distribution of the general and tropical PMP design storm patterns.
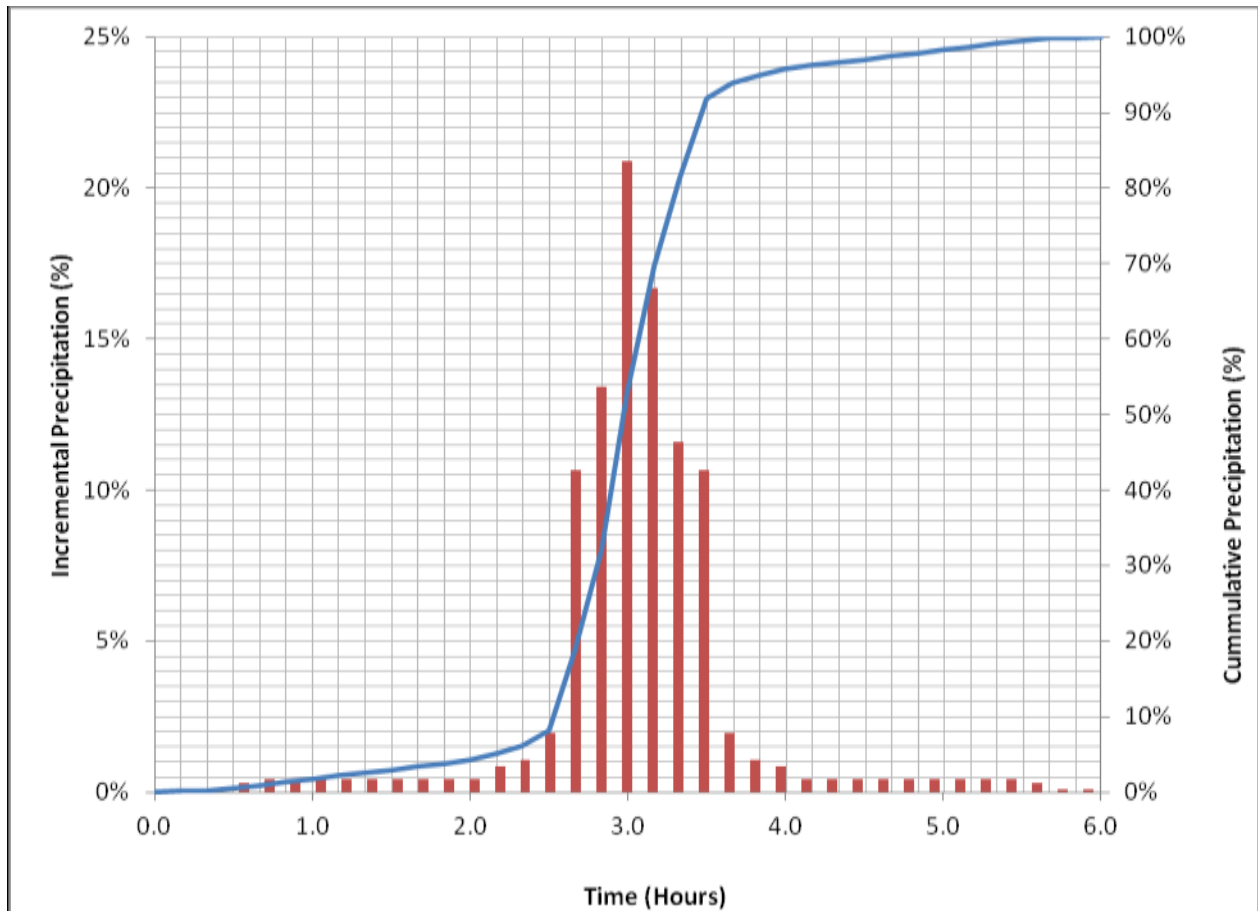
Figure 8.6 LS-6 temporal distribution curve for local storm PMP.

The local storm PMP is temporally distributed within the PMP Evaluation Tool by applying the ratio of incremental rainfall to total 6-hour PMP rainfall at each 10-minute time step to each grid cell. The distribution incremental ratios and the cumulative ratios are listed in Table 8.2.

Table 8.2 LS-6 cumulative and incremental 6-hour PMP ratios at each 10-minute time step

Time (min)	Cumulative	Incremental	Time (min)	Cumulative	Incremental	Time (min)	Cumulative	Incremental
10	0.001	0.001	130	0.051	0.009	250	0.962	0.004
20	0.002	0.001	140	0.061	0.010	260	0.966	0.004
30	0.005	0.003	150	0.081	0.020	270	0.970	0.004
40	0.009	0.004	160	0.187	0.107	280	0.974	0.004
50	0.013	0.004	170	0.322	0.134	290	0.979	0.004
60	0.017	0.004	180	0.530	0.209	300	0.983	0.004
70	0.021	0.004	190	0.697	0.167	310	0.987	0.004
80	0.026	0.004	200	0.813	0.116	320	0.991	0.004
90	0.030	0.004	210	0.919	0.107	330	0.995	0.004
100	0.034	0.004	220	0.939	0.020	340	0.998	0.003
110	0.038	0.004	230	0.949	0.010	350	0.999	0.001
120	0.042	0.004	240	0.958	0.009	360	1.000	0.001

9. PMP Evaluation Tool Description and Usage

The PMP Evaluation Tool was developed under contract for the Arizona Department of Water Resources (ADWR). The tool is a Python-based script designed to run within the ArcGIS environment. The tool provides gridded PMP values at a spatial resolution of 90 arc-seconds for a user-designated drainage basin or area. PMP values are calculated for local storm types at the 1-, 2-, 3-, 4-, 5-, and 6-hour durations and for tropical and general winter storm types at the 6-, 12-, 18-, 24-, 48-, and 72-hour durations. These gridded PMP values are used to compute a basin average PMP depth for each duration. Each of the gridded values and the basin average are then temporally distributed and exported as GIS files.

As an ArcGIS based tool, much of the terminology used to describe and discuss the PMP Evaluation Tool is unique to the ArcGIS environment. The following definitions are applicable in reference to the PMP Evaluation Tool:

1. **Folder** – A container element designed to group files or other folders (also called a directory).
2. **Datasets**– A collection of data often stored as a raster (GRID), vector (Shapefile or Feature Class), or Table.   May or may not have a spatial component.
3. **Geodatabase** – An ArcGIS specific spatial database. The geodatabase is a container used to hold a collection of datasets. Similar to a folder, but specific to the ArcGIS environment. The PMP Evaluation Tool uses File Geodatabases.
4. **GRID** – A raster dataset format (can be either integer or floating point)
5. **Shapefile** – A common vector geospatial dataset format. Contains a collection of shapes, or features.   Can be stored within a folder.
6. **Feature Class** - A single collection of geographic features. Similar to a shapefile but specific to the ArcGIS environment. Feature classes must be stored within a Geodatabase or Feature Dataset.
7. **Feature Dataset** – An ArcGIS specific folder used to store a collection of feature classes with the same spatial reference and extent. Must be stored within a geodatabase.
8. **Metadata** – Information describing a dataset. The databases use the FGDC metadata format. Stored in an .xml file sharing the name of the target dataset.
9. **ArcMap** – A visual GIS mapping application included within the ArcGIS environment.
10. **ArcCatalog** – A GIS file browser included within the ArcGIS environment.
11. **ArcToolbox** – A user interface in ArcGIS used for accessing, organizing, and managing a collection of geoprocessing tools, models, and scripts.
12. **Python** – A high-level scripting language commonly used for geoprocessing automation within the ArcGIS environment.

A fundamental level of experience with the ArcGIS Desktop software suite is recommended for implementation and usage of the PMP Evaluation Tool.

9.1 File Structure

The tool, source script, all input data, and output data locations are all stored within the 'PMP_Evaluation_Tool' project folder. The file and directory structure within the 'PMP_Evaluation_Tool' folder should be maintained as it is provided – as the script will locate various data based on its relative location within the project folder. If the subfolders or geodatabases within are relocated or renamed then the script must be updated to account for these changes.

The file structure consists of only three subfolders: Input, Output, and Script. The 'Input' folder contains all input GIS files (Figure 9.1). There are three ArcGIS file geodatabase containers within the 'Input' folder: DAD_Tables.gdb, Storm_Adj_Factors.gdb, and Non_Storm_Data.gdb. The DAD_Tables.gdb contains the DAD tables (in file geodatabase table format) for each of the 91 SPAS analyzed storm DAD zones. The Storm_Adj_Factors.gdb contains a feature class for each analyzed event and stores the adjustment factors for each grid point as a separate feature. These feature classes are organized into feature datasets, according to storm type (General, Local, and Tropical). The storm adjustment factor feature classes share their name with their DAD Table counterpart. The naming convention is SPAS_XXXX_Y, where XXXX is the SPAS storm ID number and Y is the DAD zone number. Finally, the Non_Storm_Data.gdb contains spatial data not directly relating to the input storms. There is only a single feature dataset within this GDB titled 'Vector_Grid'. Within 'Vector_Grid' are two feature classes: Grid_Points_AZ, a point feature class, and Vector_Grid_AZ, a polygon feature class representing the grid cells for each of 64,103 grid points.

The 'Output' folder is designed to store the model output after it is created and contains a subfolder for each storm type (General_Winter, Local, and Tropical). Within each storm type subfolder, there are two file geodatabases; GRIDs.gdb and PMP.gdb. There are also two sub-folders; Metadata_Templates and Text_Output. The GRID.gdb stores the basin raster output in GRID raster format. The PMP.gdb stores a feature class PMP_Points in vector (point) format. PMP_Points has a separate feature for each basin grid point, located at the grid cell centroids. There is also a PMP_Points_Mean geodatabase table produced in the PMP.gdb which stores the average basin PMP values for each duration. The 'Metadata_Templates' folder contains the .xml metadata templates that are applied to the output GIS files when they are created. The 'Text_Output' folder holds a single space-delimited PMP_Distribution.txt file which stores the basin PMP and temporally distributed PMP values.

The 'Script' folder contains an ArcToolbox called PMP_Tools.tbx and the Python script PMP_Calc.py. The toolbox contains a tool called 'AZ Basin PMP Tool' that is used by ArcGIS to call the script. The ArcToolbox was created with ArcGIS v. 10.1 but has been exported to a version 10.0 toolbox for version compatibility.

ArcCatalog should be used for viewing the GIS tool file structure and interacting with the input and output geospatial data and metadata. A typical operating system's file browser does not allow access to the geodatabase containers and cannot be used to directly run the tool.
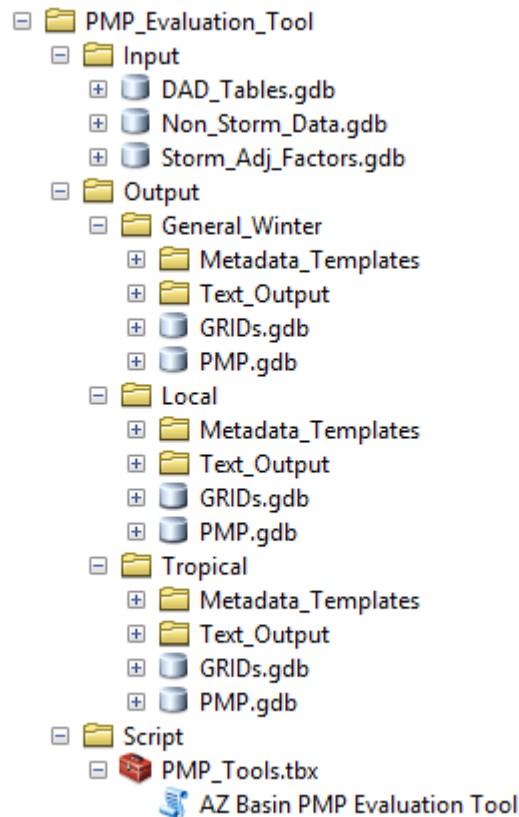
Figure 9.1 GIS file structure for the Arizona PMP Evaluation Tool as viewed from ArcCatalog

9.2 Python Script

Due to the large number of storm datasets and grid points within the project domain, a scripted process is necessary to compare each value efficiently and accurately for a given area of interest and make the necessary calculations. ArcGIS has adopted the Python scripting language as the viable option for compiling powerful geoprocessing operations as clearly and concisely as possible.

The script is stored within the PMP Evaluation Tool project folder at \Script\PMP_Calc.py. A hardcopy version of the code is given in Appendix H. The PMP_Calc.py code can be opened and edited within any text editor. The python script uses the arcpy, arcpy.management, and arcpy.conversion modules. After the input parameters are provided, the script runs the pmpAnalysis() three times, once for each storm type. To shorten and simplify the code, repeatable functions are designed and called within the code when needed. Within the broader pmpAnalysis() function, several smaller functions are called to perform various tasks:

createPMPfc()   Creates the PMP_Points feature class to store vector (point) results

getAOIarea()	Calculates the area of the input basin
dadLookup()	Gets the DAD value for the current storm based on basin area
updatePMP()	Writes the largest adjusted rainfall value (PMP) to the PMP_Points feature class
temporalDistSixHour()	Temporally distributes the 6-hour General and Tropical PMP values
temporalDistTenMin()	Temporally distributes the 10-min Local storm PMP values
outputPMP()	Creates raster PMP output, basin-average table output, text file output, and applies metadata to output GIS files

There is extensive documentation with the code in the form of '#comments'. These comments provide guidance toward its functionality and describe the code.

While the script performs many actions, its primary purpose is to iterate through both the storm list and the grid points within the area of interest (AOI), comparing each, and creating output based on the maximum values. To accomplish this, several layers of nested iterative "for" loops are used.
The following high-level algorithm broadly describes the script process:

- Calculate Basin Area (in mi^2)
- For each Storm Type (general, tropical, and local)
  - For each duration
    - Set all PMP values to 0
    - For each storm in database
      - Lookup storm's depth-area-duration (DAD) value for basin size
      - For each grid point in basin
        - Calculate total adjusted rainfall (TAR) by multiplying DAD value by total adjustment factor for the grid point
        - If TAR > PMP, the TAR becomes the new PMP value for that grid point
  - Create PMP_Point feature class for the storm type
  - Temporally distribute PMP values
  - Create raster GRID files for each duration
  - Create .txt output file for PMP values
  - Create Average PMP geodatabase table
  - Attach metadata to each output file

The 'PMP_Evaluation_Tool' script tool within the PMP_Tools.tbx ArcToolbox opens and runs the script within the ArcGIS environment. The 'PMP_Evaluation_Tool' script tool was set up with two parameters, as described in Section 9.3.1: the basin shapefile with a data type of "Feature Layer"; and the PMP Evaluation Tool folder location, with a data type of "Folder". In addition to running as a standalone tool, the script tool can be incorporated into Model Builder or be called as a sub-function of another script.

9.3 Usage

The 'PMP_Evaluation_Tool' project folder should be stored locally at a location that can be accessed (both read/write) by ArcGIS desktop. The 'AZ Basin PMP Evaluation Tool' is located in the PMP_Tools.tbx toolbox, within the 'Script' folder. The 'AZ Basin PMP Evaluation Tool' ArcToolbox is an ArcGIS Desktop version 10.0 toolbox and can be opened and run from either ArcCatalog or ArcMap. The tool is forward compatible with ArcGIS desktop versions.

9.3.1 Model Input Parameters

The tool requires only two parameters as input. The first parameter is feature layer, such as a basin shapefile or feature class, designed to outline the area of interest for the PMP analysis. The basin shapefile must have a map surface projection spatial reference, with units of either feet or meters (e.g. Universal Transverse Mercator or State Plane). If the feature layer has multiple features (or polygons) the tool will use the combined area as the analysis region. Only the selected polygons will be used if the tool is run from the ArcMap environment with selected features highlighted. If the basin shapefile extends beyond the project analysis domain, only the grid cells within the domain will be analyzed, although the PMP depths will be calculated for the area of the entire basin..

The second input parameter is the file path location of the 'PMP_Evaluation_Tool' project folder. This parameter points the script to the location if the input datasets and tells the script where to place the output.
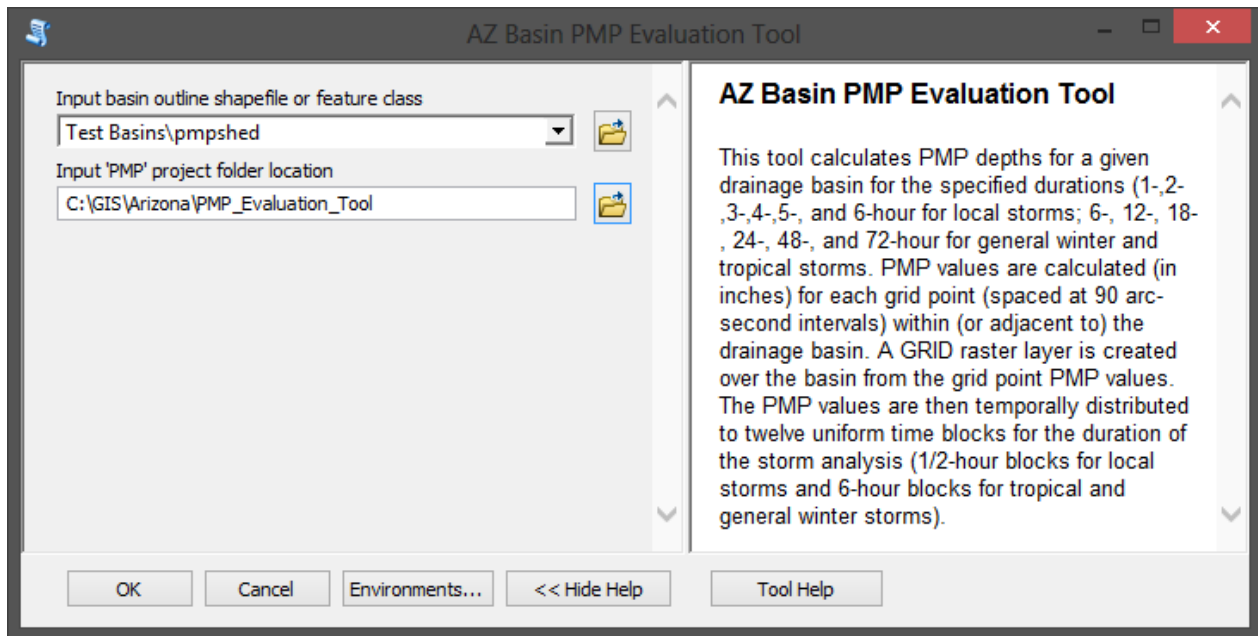
Figure 9.2 Example of PMP Evaluation Tool parameter input dialogue window as run from ArcGIS Desktop

9.3.2 Model Runtime

The tool automatically runs all three storm types at all six analysis durations. On a typical workstation the tool will take 5-15 minutes to run for most drainage basins. Several hours may be needed to complete an analysis of the entire project domain.

The GIS tool continuously outputs text to the ArcGIS geoprocessing message dialogue window while the tool is running. This text is useful for understanding where the tool is in its current iteration while the script is running, identifying errors, and recording run times and dates. After the tool has completed, the geoprocessing dialogue can be referenced and viewed with ArcGIS under the geoprocessing results window.

9.3.3 Model Output

Once the tool has been run, the output folders and geodatabases will be populated with the model results (Figure 9.3). The GIS files can then be brought into an ArcMap, or other compatible GIS environment, for mapping and analysis. The tool is set to have overwrite capabilities. If output data exists, it will be overwritten the next time the tool is run. Output data should be moved to an alternate permanent storage location before the tool is run again, if it is desired that the output data be preserved.

```
⊟ 📁 PMP_Evaluation_Tool
  ⊞ 📁 Input
  ⊟ 📁 Output
    ⊟ 📁 General_Winter
      ⊞ 📁 Metadata_Templates
      ⊟ 📁 Text_Output
          📄 PMP_Distribution.txt
      ⊟ 💿 GRIDs.gdb
        ⊞ ▦ pmp_06
        ⊞ ▦ pmp_12
        ⊞ ▦ pmp_18
        ⊞ ▦ pmp_24
        ⊞ ▦ pmp_48
        ⊞ ▦ pmp_72
      ⊟ 💿 PMP.gdb
          ⦂ PMP_Points
          ▤ PMP_Points_Mean
    ⊟ 📁 Local
      ⊞ 📁 Metadata_Templates
      ⊟ 📁 Text_Output
          📄 PMP_Distribution.txt
      ⊟ 💿 GRIDs.gdb
        ⊞ ▦ pmp_01
        ⊞ ▦ pmp_02
        ⊞ ▦ pmp_03
        ⊞ ▦ pmp_04
        ⊞ ▦ pmp_05
        ⊞ ▦ pmp_06
      ⊟ 💿 PMP.gdb
          ⦂ PMP_Points
          ▤ PMP_Points_Mean
    ⊟ 📁 Tropical
      ⊞ 📁 Metadata_Templates
      ⊟ 📁 Text_Output
          📄 PMP_Distribution.txt
      ⊟ 💿 GRIDs.gdb
        ⊞ ▦ pmp_06
        ⊞ ▦ pmp_12
        ⊞ ▦ pmp_18
        ⊞ ▦ pmp_24
        ⊞ ▦ pmp_48
        ⊞ ▦ pmp_72
      ⊟ 💿 PMP.gdb
          ⦂ PMP_Points
          ▤ PMP_Points_Mean
  ⊞ 📁 Script
```

Figure 9.3 Example of the PMP Evaluation Tool Output folder populated after a run

The output data are organized into two geodatabase containers: GRIDs.gdb, for raster data; and PMP.gdb, for vector and tabular data. The GRIDs.gdb contains a single GRID file for each analyzed duration; six in total. The PMP.gdb contains the PMP_Points feature class which has stores each grid point centroid as a separate feature. Each feature has a field for the grid ID, latitude, longitude, analysis zone, elevation, PMP (for each duration), and temporally adjusted PMP (at each time step). The PMP.gdb also stores a separate table of the basin average PMP values. The 'Text_Output' folder contains a single space-delimited text file with the same PMP values recorded in the PMP_Points feature class. This text file can be opened with ArcGIS, Excel, or other applications capable of reading space-delimited text files.

Many of the field (column header) names are not long enough to provide adequate descriptions of the field data. This is due to the 10-digit limitation on field names. Full descriptions of each field are provided in the metadata for each GIS dataset.

9.3.4   GIS Dataset Metadata

Comprehensive metadata have been included for every data element within the project folder. The metadata were compiled using the Federal Geographic Data Committee (FGDC) .xml format standard and are attached to each file. The metadata can be viewed in ArcCatalog under the description tab (the FGDC metadata style may need to be enabled under ArcCatalog 'options' for proper viewing).

Metadata added primarily consist of a description of the element and a description of each attribute field (when fields are present). Metadata for all existing input data and file structure elements are present with the deliverable project folder. Metadata for each output element is applied with a function within the script during runtime. The output metadata originates from templates stored within each storm type's 'Metadata_Templates' sub-folder within the 'Output' folder.

10.   Basin Testing Results

To test the validity of the PMP Evaluation Tool, test results were produced for several Arizona basins ranging in geographical distribution and overall basin area size. Results of these test runs helped to define storm characteristics and transposition limits as discussed previously. As expected, several different storms controlled PMP values at various duration and area sizes. In some instances a discontinuity of PMP depths between adjacent grid point values occurred. This occurs when a transposition zone bisects a given watershed. In these cases, storms that are transpositionable to one transposition zone may not be transpositionable to the other.   Therefore, different storms are affecting adjacent grid points and often results in a shift in values over a short distance. This occurs because of the requirement to assign specific transposition limits to each storm that result in a storm being either transpositionable to a grid point or not, with no allowance for gradients of transpositionability. In reality, there would be some transition for a given storm, but the process and definition of transpositionability does not allow for this. However, this effect makes little difference in the overall basin average PMP values for most basins and is only seen when analyzing the data at the highest resolution (e.g. individual grid points). This issue could potentially have the most significant effect for small basins where there are a small number of grid points representing the watershed and therefore each grid point value would have an exaggerated effect on the basin average PMP.

Although not a factor in the test results, care should be exercised when using the average PMP depth for small basins covering portions of multiple grid cells. In computing the average depth, the PMP Evaluation Tool counts each cell value equally, regardless of the percentage of its area enclosed within the drainage basin boundary. In rare cases, particularly near transposition zone limits, this approach could lead to anomalous results. In such cases, the user should calculate a weighted average based on cell areas enclosed within the basin boundary.

In addition to the nine test basin values derived using the PMP Evaluation Tool, information was analyzed by looking at the entire domain. To accomplish this, the PMP Evaluation Tool was run against all the grid points to produce values across the entire domain for each of the factors (IPMF, MTF, and OTF). This allowed for an analysis of how the factors vary spatially. This helped to evaluate and quantify the transposition limits applied to individual storms and support the limitations that were placed on some of the maximization factors. In addition, PMP values for each grid point across the entire domain were derived and mapped. This approach allowed for analysis of the values for each duration and area size to be evaluated spatially and in magnitude. This provided another tool used for evaluation of the values to ensure consistency and accuracy. Figures 10.1-10.3 display sample statewide PMP maps used in this evaluation for local storms type at the 10-square mile area size and winter and tropical storms at the 75-square mile area size. Figures 10.4-10.6 display the controlling storms by storm type across the entire domain.
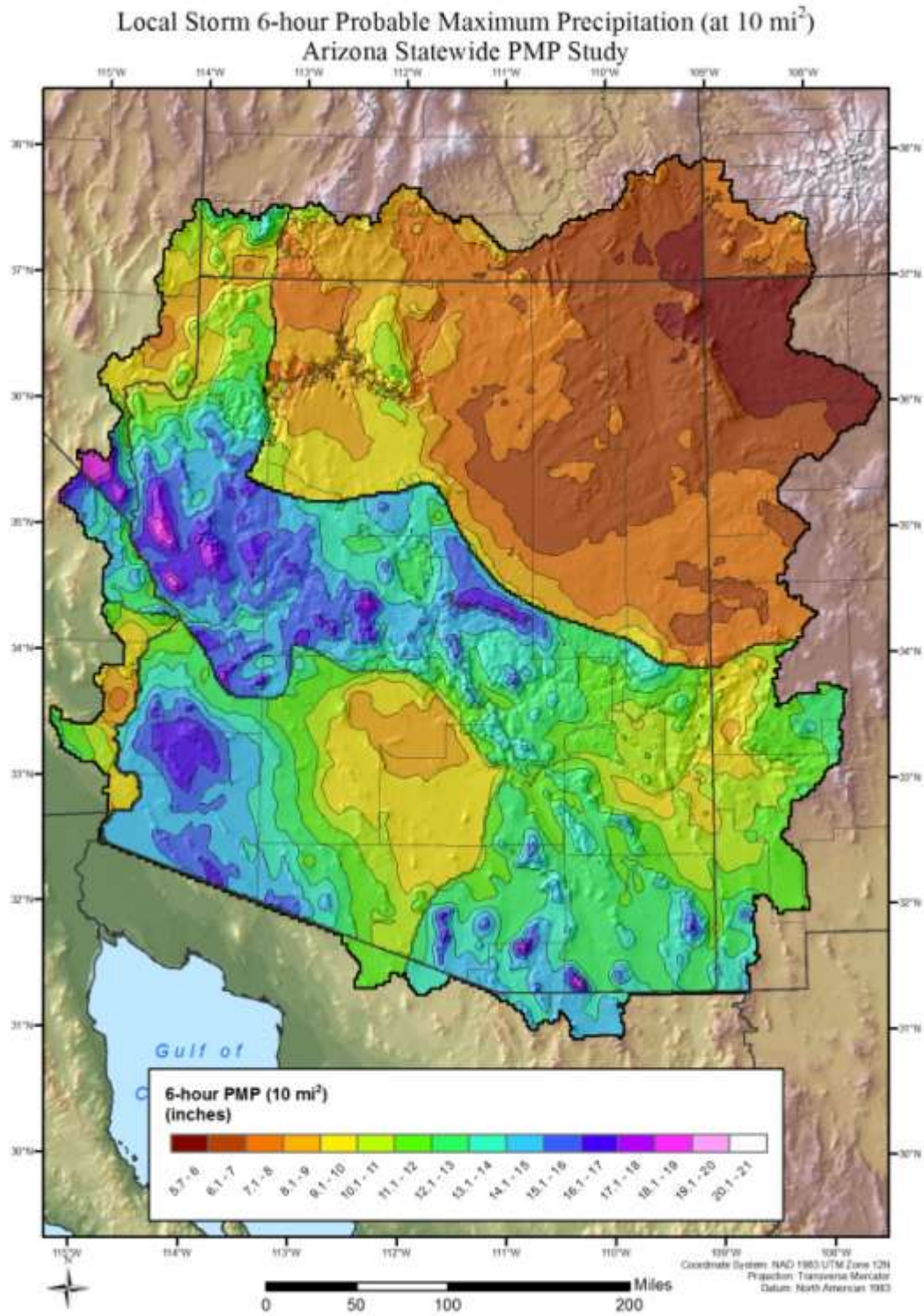
Figure 10.1 Statewide map of the 6-hour, 10-square mile PMP values derived from local convective storms
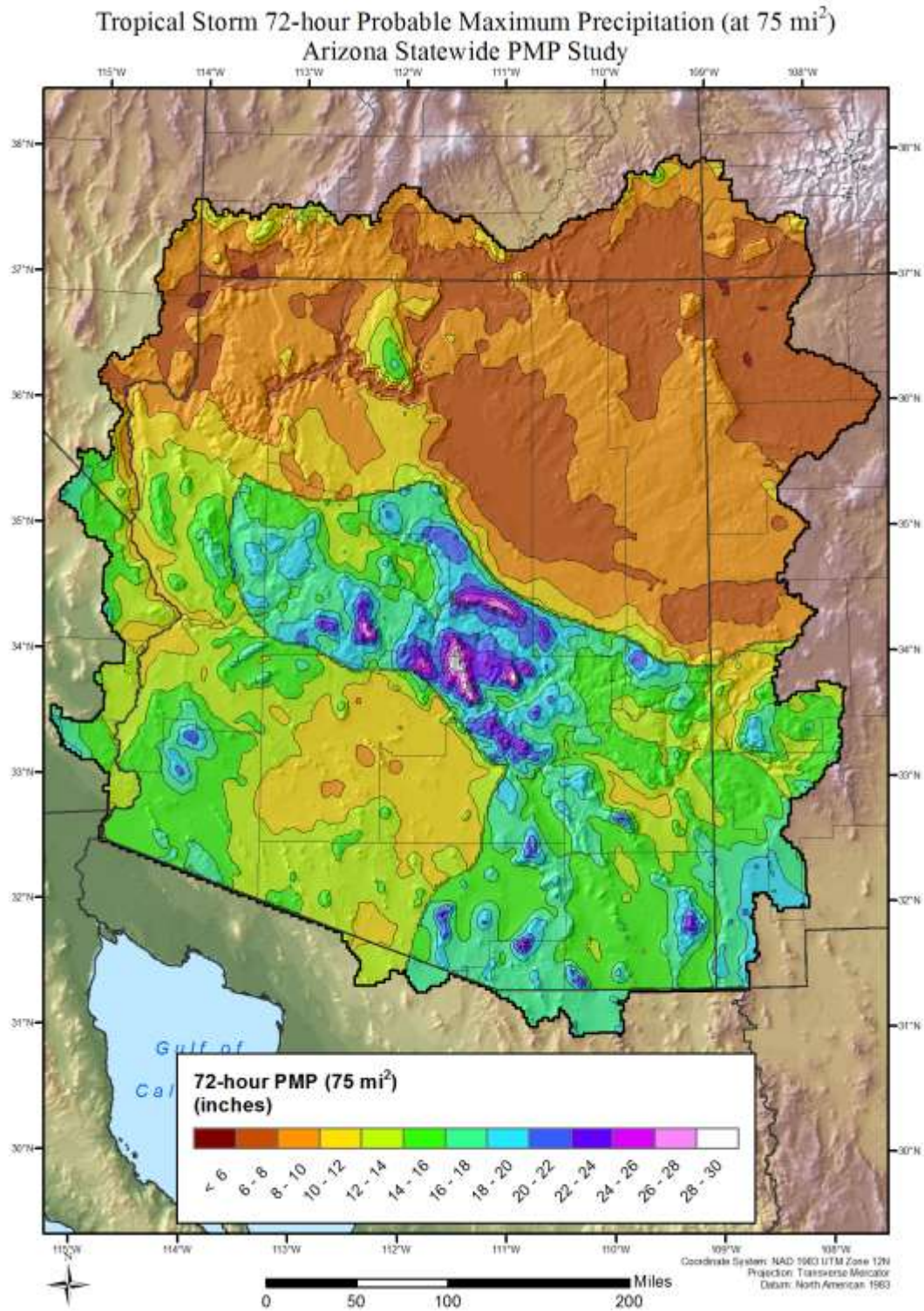
Figure 10.2 Statewide map of the 72-hour, 75-square mile PMP values derived from tropical remnant storms

Figure 10.3 Statewide map of the 72-hour, 75-square mile PMP values derived from general frontal storms
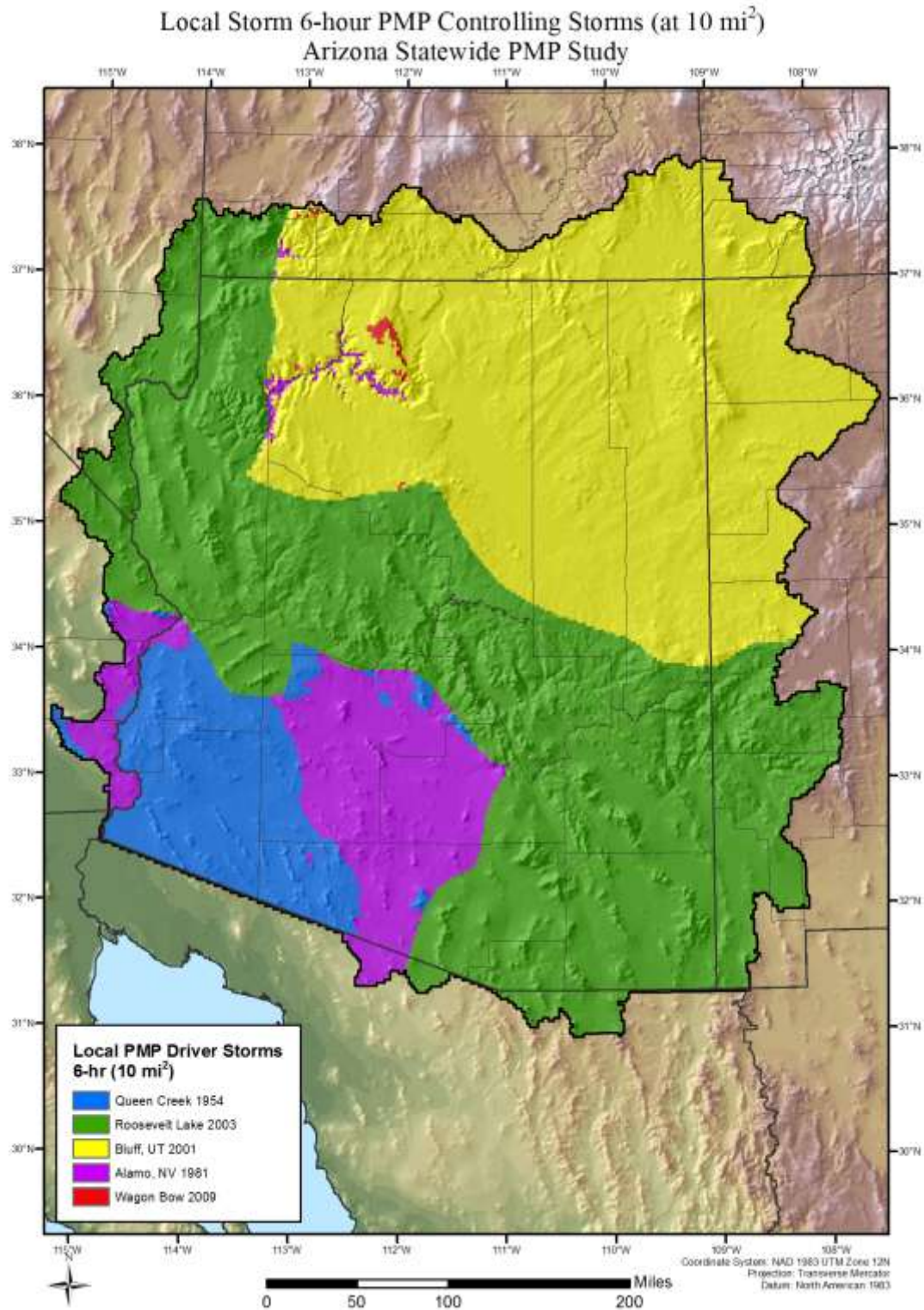
Figure 10.4 Statewide map of the controlling storms at 6-hours 10-square miles
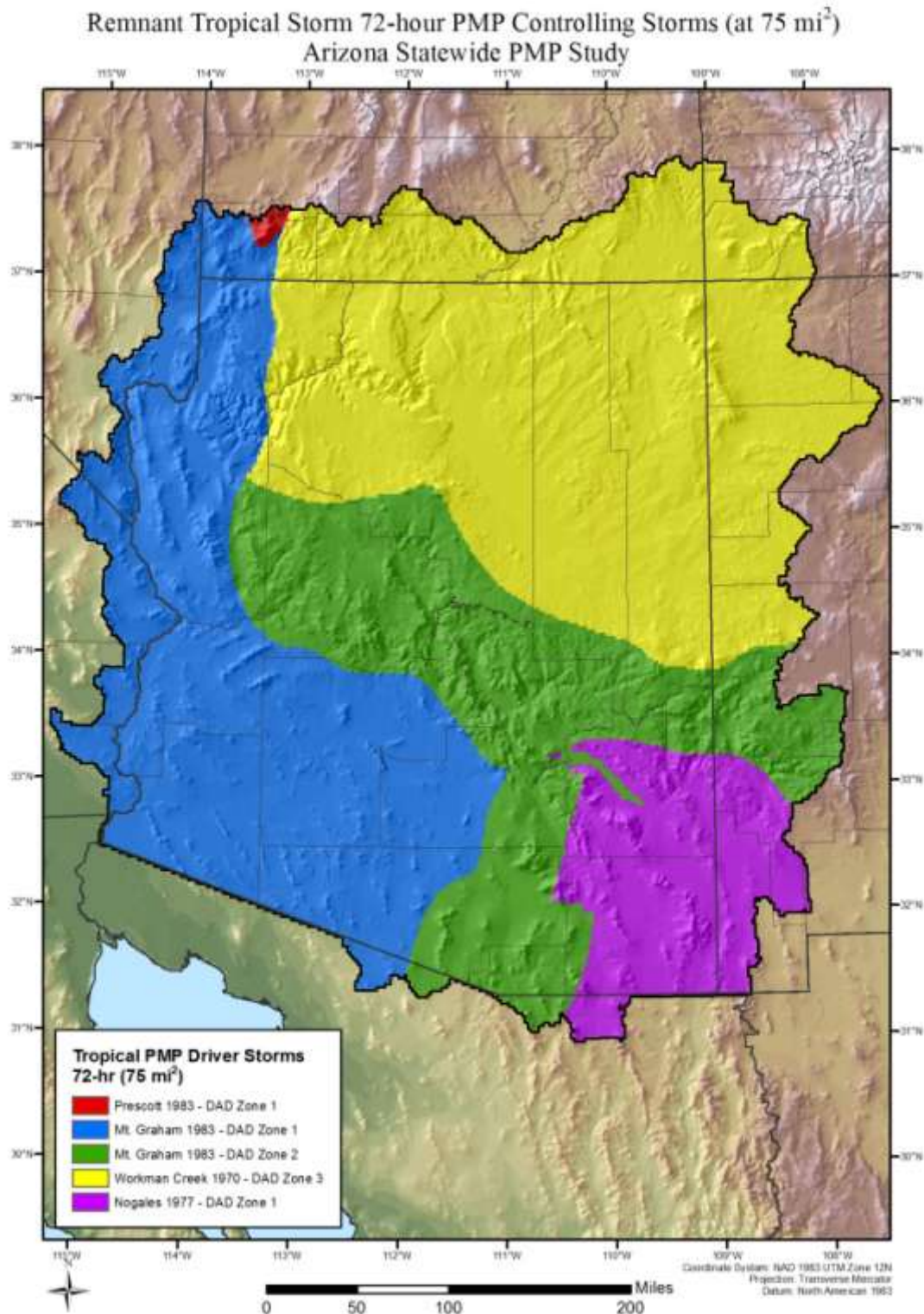
Figure 10.5 Statewide map of the controlling storms at 72-hours 75-square miles for the remnant tropical storms

General Frontal Storm 72-hour PMP Controlling Storms (at 75 mi²)
Arizona Statewide PMP Study

General Frontal PMP Driver Storms 72-hr (75 mi²)

Storm:
- Junipine 1966 - DAD Zone 2
- Mt. Ord 1916 - DAD Zone 3
- Bear Spring 1978 - DAD Zone 1
- Bear Spring 1978 - DAD Zone 2
- Horseshoe Dam 1959 - DAD Zone 2
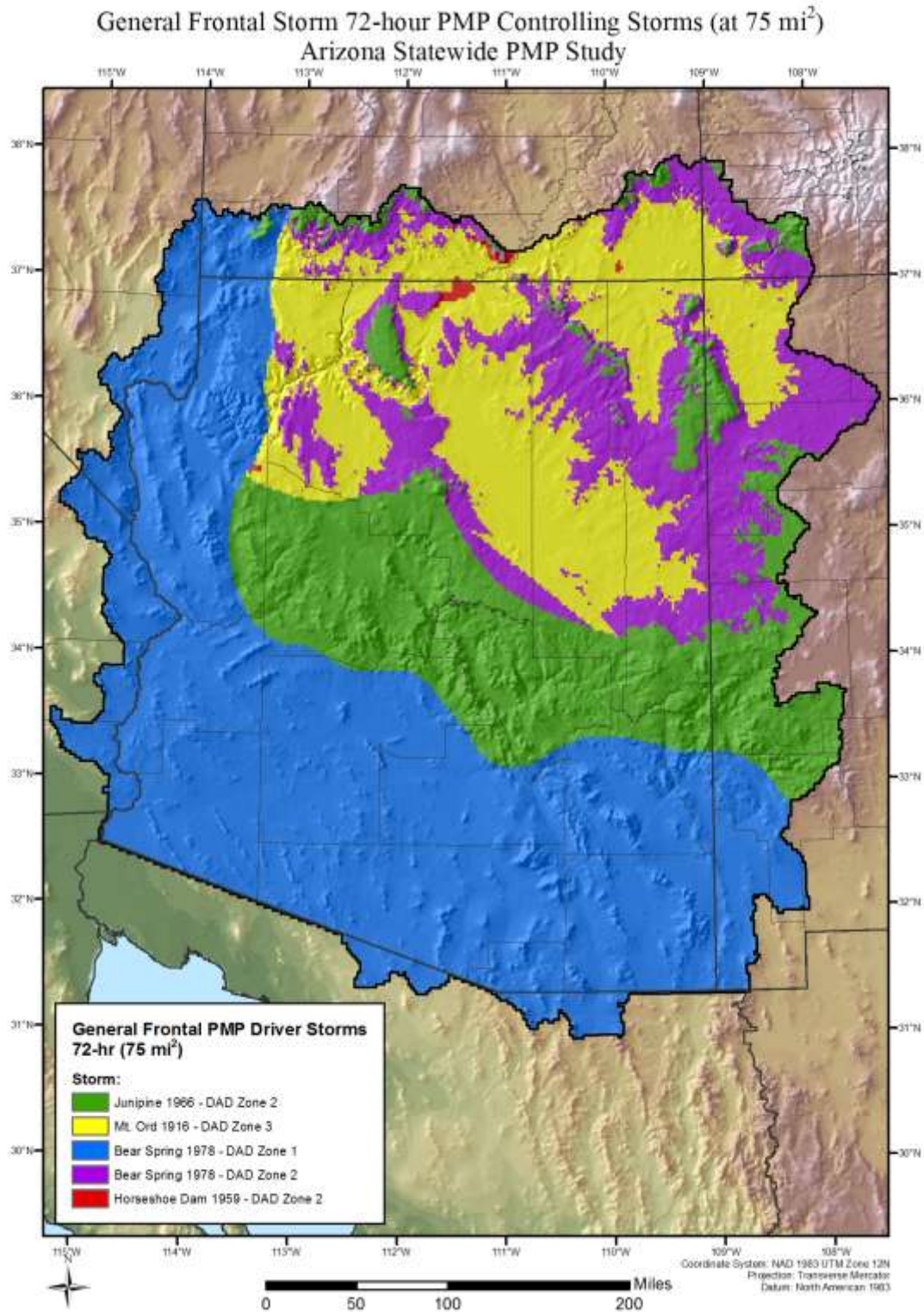
Figure 10.6 Statewide map of the controlling storms at 72-hours 75-square miles for the general frontal storms

10.1 Comparison of the PMP Values with NOAA Atlas 14 100-Year Precipitation Frequency Values

The ratio of the 10-square mile 24-hour PMP to 24-hour 100-year return period rainfall amounts is generally expected to range between two and four, with values as low as 1.7 and as high as 5.5 found in HMRs 57 and 59 (Hansen et al. 1977; Reidel and Schreiner 1980, Hansen et al. 1988, Hansen et al. 1994). Further, as stated in HMR 59 "…*the comparison indicates that larger ratios are in lower elevations where short-duration, convective precipitation dominates, and smaller ratios in higher elevations where general storm, long duration precipitation is prevalent*" (Corrigan 1999**).** It should be noted that comparison of PMP values with rainfall frequencies is made for point locations, i.e., individual locations. Sufficient data are not available to make the comparison at other area sizes. For example, comparison for the 10- or 100-square mile or area size specific to a given basin would be more useful for this study, but return frequency statistics are not available for spatial scales larger than point locations.

PMP values were compared with 100-year rainfall values as a general check that the magnitude of the PMP value is sufficiently larger than the 100-year value. Data from NOAA Atlas 14 found on the NOAA's Hydrometeorological Design Center web interface for Arizona (http://hdsc.nws.noaa.gov/hdsc/pfds/sa/az_pfds.html) were used to determine 100-year return frequency values. The analysis used the 1-square mile PMP amount for 6-, 24-, and 72-hours at six locations across the state (Figure 10.7) for comparison against the NOAA Atlas 14 values at the 6-, 24-, and 72-hour durations and the 100-year return frequency. The 6-hour local storm PMP was chosen to represent short-duration convective events. The 24-hour and 72-hour tropical storm PMP was chosen to represent the longer duration events. The remnant tropical PMP provides a more valid comparison than using general winter event PMP at longer durations since tropical PMP magnitudes exceeds general winter PMP magnitudes over the analysis region. ArcGIS was used to extract and tabulate the PMP and NOAA Atlas 14 values at the six analysis points.
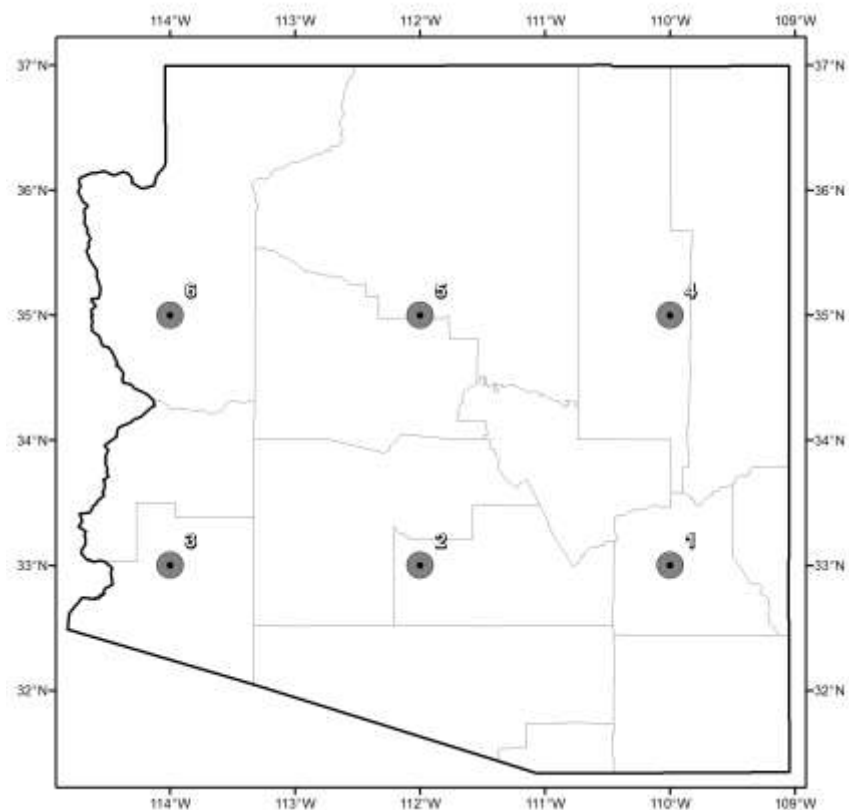
Figure 10.7 Six analysis point locations for comparison of PMP depths to 100-year NOAA Atlas
14 depths

Tables 10.1-10.3 list the 1 mi^2 PMP values at the six analysis points and compare to the
100-year NOAA Atlas 14 values at the same locations for the 6-hour, 24-hour, and 72-hour
durations. Table 10.1 shows the 6-hr NOAA Atlas 14 depths at an average of 24% of the 6-hour
local storm PMP. The 6-hour PMP averages 4.3 times the NOAA Atlas 14 magnitude. These
values show the 6-hour local PMP to be in reasonable proportion to NOAA Atlas 14 at the six
sample points.

Table 10.1 Comparison of 6-hour local storm PMP (1 mi^2) to NOAA Atlas 14 100-year 6-hour
precipitation frequency estimates at six points

Point	Longitude	Latitude	Elevation (ft)	6-hr Local PMP (inches)	6-hr NOAA At. 14 (inches)	NOAA At. 14 Percent of PMP	Ratio of PMP to NOAA At. 14
1	-110	33	2,893	11.04	2.63	24%	4.2
2	-112	33	1,209	10.55	2.65	25%	4.0
3	-114	33	1,526	16.72	3.72	22%	4.5
4	-110	35	5,391	7.82	2.37	30%	3.3
5	-112	35	5,608	14.93	3.17	21%	4.7
6	-114	35	4,739	17.65	3.45	20%	5.1
					Average:	24%	4.3

111

Table 10.2 shows the 24-hr NOAA Atlas 14 depths at an average of 35% of the 24-hour tropical storm PMP. The 24-hour PMP averages 3.0 times the NOAA Atlas 14 magnitude. These values show the 24-hour tropical PMP to be in reasonable proportion to NOAA Atlas 14 at the six sample points.

Table 10.2 Comparison of 24-hour tropical storm PMP (1 mi^2) to NOAA Atlas 14 100-year 24-hour precipitation frequency estimates at six points

Point	Longitude	Latitude	Elevation (ft)	24-hr Tropical PMP (inches)	24-hr NOAA At. 14 (inches)	NOAA At. 14 Percent of PMP	Ratio of PMP to NOAA At. 14
1	-110	33	2,893	11.96	3.31	28%	3.6
2	-112	33	1,209	8.36	3.47	42%	2.4
3	-114	33	1,526	14.89	5.04	34%	3.0
4	-110	35	5,391	7.33	2.90	40%	2.5
5	-112	35	5,608	17.25	4.83	28%	3.6
6	-114	35	4,739	12.59	4.78	38%	2.6
					Average:	35%	3.0

Table 10.3 shows the 72-hr NOAA Atlas 14 depths at an average of 44% of the 72-hour tropical storm PMP. The 72-hour PMP averages 2.3 times the NOAA Atlas 14 magnitude. These values show the 72-hour tropical PMP to be in reasonable proportion to NOAA Atlas 14 at the six sample points.

Table 10.3 Comparison of 72-hour tropical storm PMP (1 mi^2) to NOAA Atlas 14 100-year 72-hour precipitation frequency estimates at six points

Point	Longitude	Latitude	Elevation (ft)	72-hr Tropical PMP (inches)	72-hr NOAA At. 14 (inches)	NOAA At. 14 Percent of PMP	Ratio of PMP to NOAA At. 14
1	-110	33	2,893	8.87	3.89	44%	2.3
2	-112	33	1,209	9.71	4.13	42%	2.4
3	-114	33	1,526	15.74	5.21	33%	3.0
4	-110	35	5,391	6.23	3.26	52%	1.9
5	-112	35	5,608	12.27	6.44	53%	1.9
6	-114	35	4,739	13.54	5.46	40%	2.5
					Average:	44%	2.3

10.2 Comparison of the PMP Values with Individual SPAS Storm Events

PMP values computed for each grid point were compared to six actual SPAS analyzed rainfall amounts at each SPAS DAD center. This was performed as a check ensure the PMP values were sufficiently larger than the unadjusted rainfall and to see what percentage individual SPAS rainfall magnitudes were compared to PMP values at that same location. It should be noted that each grid point used in this study equates to approximately 2.5-square miles in area size, while each SPAS grid equates to approximately 1/3-square mile.

ArcGIS was used to extract and tabulate the 1-hour and 6-hour PMP depths (for local storms) and 24-hour and 72-hour PMP depths (for tropical and general storms) at each of the storm locations shown in Figure 10.8.
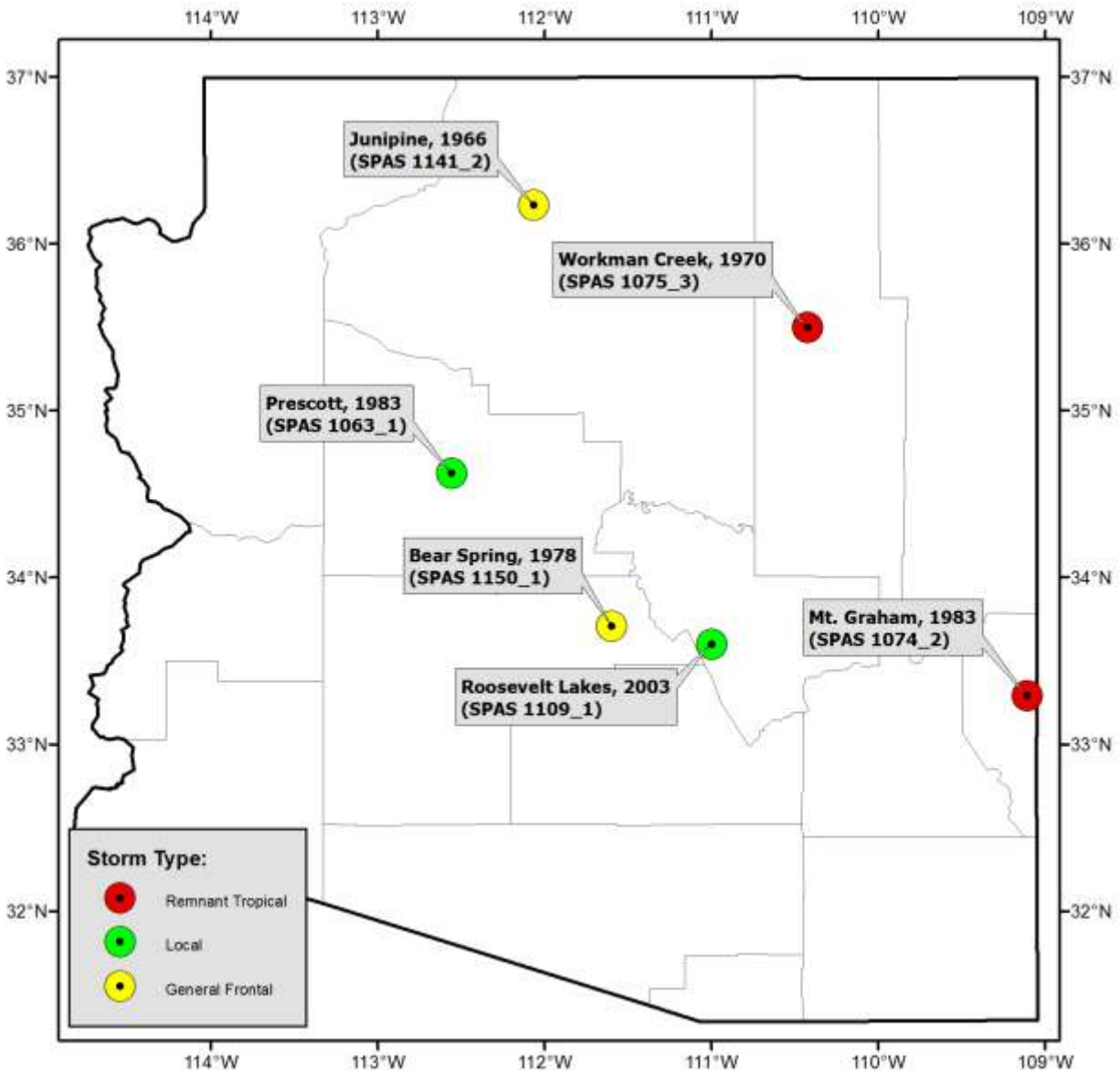
Figure 10.8 Six SPAS storm analysis point locations for comparison of PMP depths to in-place storm rainfall

Tables 10.4 and 10.5 compare the in-place maximized 24-hour and 72-hour SPAS-analyzed 1 mi^2 rainfall at each of the storm center locations to the 24-hour and 72-hour 1 mi^2 PMP depths for the remnant tropical and general winter storm types. Table 10.6 makes a similar comparison for the local storm type at the 1-hour and 6-hour durations.

113

Table 10.4 Comparison of 24-hour and 72-hour SPAS analyzed storm rainfall to tropical PMP at two storm center locations

Storm ID	Storm Place Name	Date	Latitude	Longitude	24-hr Storm Rainfall	72-hr Storm Rainfall	24-hr Tropical PMP	72-hr Tropical PMP	Storm Percent of 24-hour PMP	Storm Percent of 72-hour PMP
1074_2	Mt. Graham, AZ	Sep. 1983	33.288	-109.104	6.45	12.45	12.35	14.19	52%	88%
1075_3	Workman Creek, AZ	Sep. 1970	35.495	-110.421	6.25	6.75	7.38	7.97	85%	85%

Table 10.5 Comparison of 24-hour and 72-hour SPAS analyzed storm rainfall to general winter PMP at two storm center locations

Storm ID	Storm Place Name	Date	Latitude	Longitude	24-hr Storm Rainfall	72-hr Storm Rainfall	24-hr General PMP	72-hr General PMP	Storm Percent of 24-hour PMP	Storm Percent of 72-hour PMP
1141_2	Junipine, AZ	Dec. 1966	36.229	-112.063	7.89	11.30	8.97	12.84	88%	88%
1150_1	Bear Spring, AZ	Feb. 1978	33.704	-111.596	5.87	11.71	9.38	13.44	63%	87%

Table 10.6 Comparison of 1-hour and 6-hour SPAS analyzed storm rainfall to local storm PMP at two storm center locations

Storm ID	Storm Place Name	Date	Latitude	Longitude	1-hr Storm Rainfall	6-hr Storm Rainfall	1-hr Local PMP	6-hr Local PMP	Storm Percent of 1-hour PMP	Storm Percent of 6-hour PMP
1063_1	Prescott, AZ	Sep. 1983	34.621	-112.554	3.70	12.08	9.80	16.16	38%	75%
1109_1	Roosevelt Lakes, AZ	Sep. 2003	33.596	-110.996	5.47	10.91	11.42	12.86	48%	85%

Table 10.4 shows the rainfall for SPAS 1075, DAD zone 3 is 85% of the PMP at both the 24-hour and 72-hour durations; this storm controls the 1 mi^2 PMP at the storm center location. Therefore, in this case there is a 15% envelopment of the SPAS rainfall values by the PMP values. Similar comparisons were made for all of the analyzed DAD events within the study area. The results of these comparisons are listed in Appendix I.

11.   Sensitivity Discussions Related to PMP Derivations

In the process of deriving site-specific PMP values, various assumptions were made and explicit procedures were adopted for use. Additionally, various parameters and derived values are used in the calculations. It is of interest to assess the sensitivity of PMP values to assumptions that were made and to the variability of parameter values.

11.1   Assumptions

11.1.1 Saturated Storm Atmospheres

The atmospheric air masses that provide available moisture to both the historic storm and the PMP storm are assumed to be saturated through the entire depth of the atmosphere and to contain the maximum moisture possible based on the surface dew point. This assumes moist pseudo-adiabatic temperature profiles for both the historic storm and the PMP storm. Limited evaluation of this assumption in the EPRI Michigan/Wisconsin PMP study (Tomlinson 1993) and the Blenheim Gilboa study (Tomlinson et al. 2008) indicated that historic storm atmospheric profiles are generally not entirely saturated and contain somewhat less precipitable water than is assumed in the PMP procedure. It follows that the PMP storm (if it were to occur) would also have somewhat less precipitable water available than the assumed saturated PMP atmosphere would contain. What is used in the PMP procedure is the *ratio* of precipitable water associated with each storm. If the precipitable water values for each storm are both slightly overestimated, the ratio of these values will be essentially unchanged. For example, consider the case where instead of a historic storm with a storm representative dew point of 70° F degrees having 2.25 inches of precipitable water assuming a saturated atmosphere, it actually had 90% of that value or about 2.02 inches. The PMP procedure assumes the same type of storm with similar atmospheric characteristics for the maximized storm but with a higher dew point, say 76° F degrees. The maximized storm, having similar atmospheric conditions, would have about 2.69 inches of precipitable water instead of the 2.99 inches associated with a saturated atmosphere with a dew point of 76° F degrees. The maximization factor computed using the assumed saturated atmospheric values would be 2.99/2.25 = 1.33. If both storms were about 90% saturated instead, the maximization factor would be 2.69/2.02 = 1.33. Therefore potential inaccuracy of assuming saturated atmospheres (whereas the atmospheres may be somewhat less than saturated) should have a minimal impact on storm maximization and subsequent PMP calculations.

11.1.2 Maximum Storm Efficiency

The assumption is made that if a sufficient period of record is available for rainfall observations, at least a few storms would have been observed that attained or came close to attaining the maximum efficiency possible in nature for converting atmospheric moisture to rainfall for regions with similar climates and topography. The further assumption is made that if additional atmospheric moisture had been available, the storm would have maintained the same efficiency for converting atmospheric moisture to rainfall. The ratio of the maximized rainfall

amounts to the actual rainfall amounts would be the same as the ratio of the precipitable water in the atmosphere associated with each storm.

There are two issues to be considered. First is the assumption that a storm has occurred that has a rainfall efficiency close to the maximum possible. Unfortunately, state-of-the-science in meteorology does not support a theoretical evaluation of storm efficiency. However, if the period of record is considered (generally over 100 years), along with the extended geographic region with transpositionable storms, it is accepted that there should have been at least one storm with dynamics that approach the maximum efficiency for rainfall production.

The other issue is the assumption that storm efficiency does not change if additional atmospheric moisture is available. Storm dynamics could potentially become more efficient or possibly less efficient depending on the interaction of cloud microphysical processes with the storm dynamics. Offsetting effects could indeed lead to the storm efficiency remaining essentially unchanged. For the present, the assumption of no change in storm efficiency is accepted.

11.2 Parameters

11.2.1 Storm Representative Dew Point and Maximum Dew Point, and Storm Representative SST and 2-sigma SST

This discussion is applicable to both dew points and SSTs although only dew points will be addressed. SSTs are used as substitutes for dew points for all storms in this study for inflow vectors that originate over ocean regions and have the same sensitivity considerations.

The maximization factor depends on the determination of storm representative dew points, along with maximum historical dew point values. The magnitude of the maximization factor varies depending on the values used for the storm representative dew point and the maximum dew point. Holding all other variables constant, the maximization factor is smaller for higher storm representative dew points as well as for lower maximum dew point values. Likewise, larger maximization factors result from the use of lower storm representative dew points and/or higher maximum dew points. The magnitude of the change in the maximization factor varies depending on the dew point values. For the range of dew point values used in most PMP studies, the maximization factor for a particular storm will change about 5% for every 1° F difference between the storm representative and maximum dew point values. The same sensitivity applies to the transposition factor, with about a 5% change for every 1° F change in either the in-place maximum dew point or the transposition maximum dew point.

For example, consider the following case:

Storm representative dew point: 75°F Precipitable water: 2.85 "
Maximum dew point: 79°F Precipitable water: 3.44"
Maximization factor = 3.44"/2.85" = 1.21

If the storm representative dew point were 74 $^\circ$F with precipitable water of 2.73",
Maximization factor = 3.44"/2.73" = 1.26 (an increase of approximately 5%)

If the maximum dew point were 78 $^\circ$ F with precipitable water of 3.29",
Maximization factor = 3.29"/2.85" = 1.15 (a decrease of approximately 5%)

11.2.2 Sensitivity of the Elevation Adjustment Factor to Changes in Storm Elevation

Elevated topographic features remove atmospheric moisture from an air mass as it moves over the terrain. When storms are transpositioned, the elevation of the original storm is used in this study to compute the amount of atmospheric moisture depleted from or added to the storm atmosphere.   The absolute amount of moisture depletion or addition is somewhat dependent on the dew point values, but is primarily dependent on the elevation at the original storm location and the elevation of the study basin. The elevation adjustment is slightly less than 1% for every 100 feet of elevation change between the original storm location and the study basin elevation.

For example, consider the following case:

Maximum dew point:	79 $^\circ$ F
Study basin elevation:	100 feet
Historic storm location elevation:	500 feet
Precipitable water between 1000-mb and the top of the atmosphere:	3.44 inches
Precipitable water between 1000-mb and 100':	0.03 inches
Precipitable water between 1000-mb and 500':	0.15 inches

Elevation Adjustment Factor = (3.44"-0.03")/(3.44-0.15") = 1.04 (about 1% per 100 feet)

If the historic storm location elevation were 1,000', the precipitable water between 1000mb and 1,000' is 0.28"
Elevation Adjustment Factor = (3.44"-0.03")/(3.44"-0.28") = 1.08 (about 1% per 100 feet)

117

12. Recommendations for Application

12.1 Site-Specific PMP Applications

Site-specific PMP values provide rainfall amounts for use in computing the Probable Maximum Flood (PMF). The study addressed several issues that could potentially affect the magnitude of the PMP storm over any drainage basin within the state of Arizona. It is important to remember that the methods used to derive PMP and the processes which utilize those values hydrologically adhere to the caveat of being "physically possible" as described in the definition of PMP (see Section 1.1). In other words, various levels of conservatism and/or extreme aspects of storms that would not occur/co-occur in a PMP storm environment should not be compounded together to generate unrealistic results in either the PMP values or the hydrologic applications of those values.

The storm search and selection of storms analyzed emphasized storms with the largest rainfall values that occurred over areas that are both meteorologically and topographically similar to locations within the state of Arizona. Each storm type that occurs in the state was analyzed. This included local convective, remnant tropical, and general winter storms. Results of this study should not be used for watersheds where meteorological and/or topographical parameters are different from those found within Arizona without further evaluation.

12.2 Temporal Distribution of PMP for Local, Tropical, and General Storms

Understanding and quantifying how rainfall associated with the PMP design storm accumulates over a given duration (e.g. 6-hours or 72-hours) is essential to the modeling of the PMF. To determine the temporal distribution of the PMP rainfall, design storms which were analyzed to produce the PMP depths as part of this study, were evaluated. Storms were grouped by type; local, tropical, and general. Local storms were analyzed from 1-6 hours. Tropical and general storms were analyzed on a 6-hour basis from 6 through 72 hours, with a final temporal distribution of 6-hour increments used.

These evaluations were performed by the various members of the project team including the Review Committee, ADWR, and the Flood Control District of Maricopa County, each with expertise in flood hydrology within the state of Arizona. The tropical and general PMP design storms are applicable to watersheds of any size, but more likely to be critical for hydrologic design purposes for drainage areas ranging in size from moderate to very large i.e. larger than 50-square miles). The local PMP design storm, however, should generally be limited to smaller watersheds less than 50-square miles in area size.

The recommended temporal distribution for local storms was developed using NEXRAD rainfall data measured at storm centers, i.e. $1/3^{rd}$-square mile areas where the highest rainfall intensities occurred. Storms analyzed for this study indicate these highest intensities can be maintained out to areas at least as large 25-square miles. Although rainfall associated with local

storms often covers much larger areas (as reflected in the DAD tables produced by SPAS) these larger areas reflect the movement of the local storm across an area. Most typical rainfall-runoff modeling applications for PMP design events do not consider storm movement but instead assume simultaneous rainfall across the entire drainage area.

Since it was developed from rainfall intensities measured at storm centers, use of the recommended LS-6 temporal distribution for drainage basins larger than 25-square miles should be performed with care, and its use is generally not recommended for basins greater than 50-square miles in size.

12.3   Climate Change Assumptions

Climate change has occurred in the past, is now occurring, and undoubtedly will continue in the future. This is and has always been a natural part of Earth's cycles. How the climate will change and how this will affect the number and intensity of extreme rainfall events in the state of Arizona is unknown as of the date of this report. Projections can be made using various scenarios, but these are not predictions and only produce possible scenarios for a variety of possible conditions.

With a warming of the atmosphere, there can potentially be an increase in the available atmospheric moisture for storms to convert to rainfall. However, storm dynamics play a significant role in that conversion process and the result of a warming or cooling climate on storm dynamics is not well understood. A warmer or cooler climate may lead to a change in the frequency of storms and/or a change in the intensity of storms, but there is no definitive evidence to indicate the trend or the magnitude of potential changes.

AWA recognizes that the climate is in a constant state of change. However, the current scientific consensus and understanding cannot agree how climate is changing and more importantly what those changes will be for the region. Therefore, one cannot say whether the state will be wetter or drier, warmer or colder and/or experience more or less extreme precipitation events with any quantitative and statistically significant certainty. Further, the values derived in this study have a useful life between 50 to 100 years before they would require re-evaluation. In general, most projected changes that *may* occur within the Earth's climate system would be unlikely to significantly affect the project's PMP related hydrology beyond the bounds of the PMP/PMF values derived using values from this project. Based on these discussions, it is apparent that the current practice of PMP determination should *not* be modified in an attempt to address potential changes associated with climate change. This study has continued the practice of assuming no climate change, as climate trends are not considered when preparing PMP estimates (WMO, Section 1.1.1).

References

Abbs, D.J., 1999:   A Numerical Modeling Study to Investigate the Assumptions Used in the Calculation of Probable Maximum Precipitation, *Water Resources Research*, Vol. 35, No. 3, 785-796.

Adams, D.K., and E.P. Souza, 2009: CAPE and Convective Events in the Southwest during the North American Monsoon. *Mon. Wea. Rev.*, **137**, 83–98.

Adams, D.K., and A.C. Comrie, 1997: The North American Monsoon, *Bulletin of the American Meteorological Society*, Vol. 78, 2197-2212.

Aldridge, B.N., 1968: Floods of September 17 in Southwestern Arizona, in Rostvedt, J.O., and others, Summary of Floods in the United States During 1963: U.S. Geological Survey Water-Supply Paper 1830-B, p98-106.

Aldridge, B.N., and Moosburner, Otto, 1970: Floods of September 9-11 in the Santa Cruz River Basin, Arizona, in Rostvedt, J.O., and others, Summary of Floods in the United States During 1964: U.S. Geological Survey Water-Supply Paper 1840-C, p69-74.

Aldridge, B.N., and Eychaner, J.H., 1984: Floods of October 1977 in Southern Arizona and March 1978 in Central Arizona, U.S. Geological Survey Water-Supply Paper 2223, 143p.

Aldridge, B.N., and Hales, T.A., 1984: Floods of November 1978 to March 1979 in Arizona and west central New Mexico, U.S. Geological Survey Water-Supply Paper 2241, 149p.

American Meteorological Society, 1996: *Glossary of Weather and Climate*, Boston, MA., 272 pp.

Anderson, B.T., and H. Kanamura, 2005: The Diurnal Cycle of the Summertime Atmospheric Hydrologic Cycle over the Southwestern United States. *J. Hydrometeor.*, **9**, 589–600.

Anderson, B.T., J. Wang, S. Gopal, and G. Salvucci, 2009: Influence of Daily Rainfall Characteristics on Regional Summertime Precipitation over the Southwestern United States. *J. Hydrometeor.*, **10**, 1218–1230.

Arkell, R.E. and Richards, F., 1986: *Short Duration Rainfall Frequency Relations for the Western United States*, Office of Hydrology, NOAA, NWS, Silver Spring, MD, 6pp.

Baker, M.B., and G.H. Roe, 2009: The Shape of Things to Come: Why Is Climate Change So Predictable? *J. Climate*, **22**, 4574–4589.

Balling, R.C., and S.W. Brazel, 1987: Diurnal Variations in Arizona Monsoon Precipitation Frequencies. *Mon. Wea. Rev.*, **115**, 342–346.

Barlow, M., S. Nigam, and E.H. Berbery, 1998: Evolution of the North American Monsoon System. *J. Climate*, **11**, 2238–2257.

Becker, E.J., and E.H. Berbery, 2008: The Diurnal Cycle of Precipitation over the North American Monsoon Region during the NAME 2004 Field Campaign. *J. Climate*, **21**, 771–787.

Berbery, E.H., 2001: Mesoscale Moisture Analysis of the North American Monsoon. *J. Climate*, **14**, 121–137.

Bhushan, S., and A.P. Barros, 2007: A Numerical Study to Investigate the Relationship between Moisture Convergence Patterns and Orography in Central Mexico. *J. Hydrometeor.*, **8**, 1264–1284.

Bolsenga, S.J., 1965: The Relationship Between Total Atmospheric Water Vapor and Surface Dewpoint on a Mean Daily and Hourly Basis, *J. Appl. Meteor.*, **4**, 430– 432.

Bonnin, G.M., Todd, D., Lin, B., Parzybok, T., Yekta, M., and D. Riley, 2004: Precipitation-Frequency Atlas of the United States, NOAA Atlas 14, Volumes 1 and 2, NOAA, National Weather Service, Silver Spring, Maryland. http://hdsc.nws.noaa.gov/hdsc/pfds/

Boushaki, F.I., K.L. Hsu, S. Sorooshian, G.H. Park, S. Mahani, and W. Shi, 2009: Bias Adjustment of Satellite Precipitation Estimation Using Ground-Based Measurement: A Case Study Evaluation over the Southwestern United States. *J. Hydrometeor.*, **10**, 1231– 1242.

Brandenburg, F.H., 1911: District No. 9, Colorado Valley. *Mon. Wea. Rev.*, **39**, 1570.

Brandenburg, F.H., 1911: Floods in Southwestern Colorado Northwestern New Mexico. *Mon. Wea. Rev.*, **39**, 1570-1579.

Brazel, A.J., and Evans, K.E., 1984: Major Storms and Floods in Arizona, 1862-1983: Tempe, Arizona, Ariozna State University, Office of the State Climatologistm Climatological Publications, Precipitaiton Series, No. 6, 63p.

Bruintjes, R.T., T.L. Clark, and W.D. Hall, 1994: Interactions between Topographic Airflow and Cloud/Precipitation Development during the Passage of a Winter Storm in Arizona. *J. Atmos. Sci.*, **51**, 48–67.

Bureau of Reclamation, 1990: Determination of an Upper Limit Design Rainstorm for the Colorado River Basin Above Hoover Dam, Denver, CO, 129pp.

Burkham, D.E., 1970: Precipitation, Streamflow, and Major Floods at Selected Sites in the Gila River Drainage Basin Above Coolidge Dam, Arizona: U.S. Geological Survey Professional Paper 655-B, 33p.

Carleton, A.M., D.A. Carpenter, and P.J. Weser, 1990: Mechanisms of Interannual Variability of the Southwest United States Summer Rainfall Maximum. *J. Climate*, **3**, 999–1015.

Carr, J.A., 1951: The Rains Over Arizona, August 26–29, 1951. *Mon. Wea. Rev.*, **79**, 163.

Castro, C.L., T.B. McKee, and R.A. Pielke, 2001: The Relationship of the North American Monsoon to Tropical and North Pacific Sea Surface Temperatures as Revealed by Observational Analyses. *J. Climate*, **14**, 4449–4473.

Cayan, D.R., K.T. Redmond, and L.G. Riddle, 1999: ENSO and Hydrologic Extremes in the Western United States. *J. Climate*, **12**, 2881–2893.

Chin, E.H., Aldridge, B.N., and Longfield, R.J., 1991: Floods of February 1980 in southern California and central Arizona, USGS Professional Paper 1949, 126 pp.

Ciesielski, P.E., and R.H. Johnson, 2008: Diurnal Cycle of Surface Flows during 2004 NAME and Comparison to Model Reanalysis. *J. Climate*, **21**, 3890–3913.

Clark, M.P., and A.G. Slater, 2006: Probabilistic Quantitative Precipitation Estimation in Complex Terrain. *J. Hydrometeor.*, **7**, 3–22.

Clarke, B., and M. Elits, 2007: Real-Time, High Resolution Radar Rainfall Estimation and Short-term Forecasts with Rain Gauge Calibration, *Weather Decisions Technology*, 7pp.

Corbosiero, K.L., M.J. Dickinson, and L.F. Bosart, 2009: The Contribution of Eastern North Pacific Tropical Cyclones to the Rainfall Climatology of the Southwest United States. *Mon. Wea. Rev.*, **137**, 2415–2435.

Corps of Engineers, U.S. Army, 1945-1973: Storm Rainfall in the United States, Depth-Area-Duration Data. Office of Chief of Engineers, Washington, D.C.

Corrigan, P., D.D. Fenn, D.R. Kluck, and J.L. Vogel, 1999: Probable Maximum Precipitation for California, *Hydrometeorological Report Number 59*, National Weather Service, National Oceanic and Atmospheric Administration, U. S. Department of Commerce, Silver Spring, Md, 392 pp.

Costa, J.E., and R.D. Jarrett, 2008: An Evaluation of Selected Extraordinary Floods in the United States Reported by the U.S. Geological Survey and Implications for Future Advancement of Flood Science, http://pubs.er.usgs.gov/usgspubs/sir/sir20085164/.

Daly, C., R.P. Neilson, and D.L. Phillips, 1994: A Statistical-Topographic Model for Mapping Climatological Precipitation over Mountainous Terrain. *J. Appl. Meteor.*, **33**, 140–158.

Daly, C., G. Taylor, and W. Gibson, 1997: The PRISM Approach to Mapping Precipitation and Temperature, 10th Conf. on Applied Climatology, Reno, NV, Amer. Meteor. Soc., 10-12.

Das, T., H.G. Hidalgo, M.D. Dettinger, D.R. Cayan, D.W. Pierce, C. Bonfils, T.P. Barnett, G. Bala, and A. Mirin, 2009: Structure and Detectability of Trends in Hydrological Measures over the Western United States. *J. Hydrometeor.*, **10**, 871–892.

Demko, J. Cory, Bart Geerts, 2010: A Numerical Study of the Evolving Convective Boundary Layer and Orographic Circulation around the Santa Catalina Mountains in Arizona. Part II: Interaction with Deep Convection. *Mon. Wea. Rev.*, **138**, 3603–3622.

Dickens, J., 2003: On the Retrieval of Drop Size Distribution by Vertically Pointing Radar. American Meteorological Society 32nd Radar Meteorology Conference, Albuquerque, NM, October 2005.

Dominguez, F., P. Kumar, and E.R. Vivoni, 2008: Precipitation Recycling Variability and Ecoclimatological Stability—A Study Using NARR Data. Part II: North American Monsoon Region. *J. Climate*, **21**, 5187–5203.

Doswell, C. A., H. E. Brooks, and R. A. Maddox: 1996: Flash Flood Forecasting: An Ingredients-Based Methodology, *Wea. Forecasting*, **11**, 560–581.

Douglas, A.V., and P.J. Englehart, 2007: A Climatological Perspective of Transient Synoptic Features during NAME 2004. *J. Climate*, **20**, 1947–1954.

Douglas, E.M., and A.P. Barros, 2003: Probable Maximum Precipitation Estimation Using Multifractals: Application in the Eastern United States. *J. Hydrometeor.*, **4**, 1012–1024.

Douglas, M.W., and J.C. Leal, 2003: Summertime Surges over the Gulf of California: Aspects of Their Climatology, Mean Structure, and Evolution from Radiosonde, NCEP Reanalysis, and Rainfall Data. *Wea. Forecasting*, **18**, 55–74.

Douglas, M.W., A. Valdez-Manzanilla, and R. Garcia Cueto, 1998: Diurnal Variation and Horizontal Extent of the Low-Level Jet over the Northern Gulf of California. *Mon. Wea. Rev.*, **126**, 2017–2025.

Douglas, M.W., and S. Li, 1996: Diurnal Variation of the Lower-Tropospheric Flow over the Arizona Low Desert from SWAMP-1993 Observations. *Mon. Wea. Rev.*, **124**, 1211–1224.

Douglas, M.W., 1995: The Summertime Low-Level Jet over the Gulf of California, *Monthly Weather Review*, Vol. 123, 2334-2346.

Douglas, M.W., Maddox, R.A., K. Howard, 1993: The Mexican Monsoon, *Journal of Climate*, Vol. 6, 1665-1667.

Draxler, R.R. and Rolph, G.D., 2003: HYSPLIT (HYbrid Single-Particle Lagrangian Integrated Trajectory) Model access via NOAA ARL READY Website (http://www.arl.noaa.gov/ready/hysplit4.html), NOAA Air Resources Laboratory, Silver Spring, MD.

Draxler, R.R. and Rolph, G.D., 2010: HYSPLIT (HYbrid Single-Particle Lagrangian Integrated Trajectory) Model access via NOAA ARL READY Website (http://ready.arl.noaa.gov/HYSPLIT.php), NOAA Air Resources Laboratory, Silver Spring, MD.

Eidemiller, D.I., 1978: The Frequency of Tropical Cyclones in the Southwestern United States and Northwestern New Mexico: Tempe, Arizona, Arizona State University, Office of State Climatologist, Climatological Publications, Scientific Paper No. 1, 41p.

Ely, L.L., Enzel, Y., and Cayan, D.R., 1994: Anomalous North Pacific Atmospheric Circulation and Large Winter Floods in the Southwestern United States, *Journal of Climate*, Vol. 7, p. 977-987.

Englehart, P.J., and A.V. Douglas, 2006: Defining Intraseasonal Rainfall Variability within the North American Monsoon. *J. Climate*, **19**, 4243–4253.

Environmental Data Service, 1968: Maximum Persisting 12-Hour, 1000mb Dew Points (°F) Monthly and of Record. *Climate Atlas of the United States*, Env. Sci. Srv. Adm., U.S. Dept of Commerce, Washington, D.C., pp 59-60.

Farfán, L.M., and J.A. Zehnder, 1994: Moving and Stationary Mesoscale Convective Systems over Northwest Mexico during the Southwest Area Monsoon Project. *Wea. Forecasting*, **9**, 630–639.

Fuller, R.D., and D.J. Stensrud, 2000: The Relationship between Tropical Easterly Waves and Surges over the Gulf of California during the North American Monsoon. *Mon. Wea. Rev.*, **128**, 2983–2989.

Fulton, R.A., J.P. Breidenbach, D.J. Seo, D.A. Miller, and T. O'Bannon, 1998: The WSR-88D Rainfall Algorithm. *Wea. Forecasting*, **13**, 377-395.

Gatewood, J.S., 1945: Notable Local Floods of 1939, Part 1, Floods of September 1939 in Colorado River Basin Below Boulder Dam, in Gatewood, J.S., Schrader, F.F., and Stackpole, M.R., Notable Local Floods of 1939: U.S. Geological Survey Water-Supply Paper 967, 37p.

Gochis, D.J., J.C. Leal, W.J. Shuttleworth, C.J. Watts, and J. Garatuza-Payan, 2003: Preliminary Diagnostics from a New Event-Based Precipitation Monitoring System in Support of the North American Monsoon Experiment. *J. Hydrometeor.*, **4**, 974–981.

Gochis, D.J., W.J. Shuttleworth, and Z.L. Yang, 2003: Hydrometeorological Response of the Modeled North American Monsoon to Convective Parameterization. *J. Hydrometeor.*, **4**, 235–250.

Gochis, D.J., A. Jimenez, C.J. Watts, J. Garatuza-Payan, and W.J. Shuttleworth, 2004: Analysis of 2002 and 2003 Warm-Season Precipitation from the North American Monsoon Experiment Event Rain Gauge Network. *Mon. Wea. Rev.*, **132**, 2938–2953.

Gochis, D.J., C.J. Watts, J. Garatuza-Payan, and J. Cesar-Rodriguez, 2007: Spatial and Temporal Patterns of Precipitation Intensity as Observed by the NAME Event Rain Gauge Network from 2002 to 2004. *J. Climate,* **20**, 1734–1750.

Goodrich, G.B., 2006: Influence of the Pacific Decadal Oscillation on Winter Precipitation and Drought during years of Neutral ENSO in the Western United States, *Weather and Forecasting*, Vol. 22, 116-124.

Goodrich, G.B., and A.W. Ellis, 2008: Climatic Controls and Hydrologic Impacts of a Recent Extreme Seasonal Precipitation Reversal in Arizona. *J. Appl. Meteor. Climatol.*, **47**, 498–508.

GRASS (Geographic Resources Analysis Support System) GIS is an open source, free software GIS with raster, topological vector, image processing, and graphics production functionality that operates on various platforms. http://grass.itc.it/.

Green, G.D., and E.S. Pytlak, 2003: Severe Weather Outbreak over Phoenix Arizona on July 14, 2002, Tucson National Weather Service Office, 7pp.

Guirguis, K.J., and R. Avissar, 2008: A Precipitation Climatology and Dataset Intercomparison for the Western United States. *J. Hydrometeor.*, **9**, 825–841.

Guirguis, K.J., and R. Avissar, 2008: An Analysis of Precipitation Variability, Persistence, and Observational Data Uncertainty in the Western United States. *J. Hydrometeor.*, **9**, 843–865.

Gunther, E., and R. Cross, 1984: Eastern North Pacific Tropical Cyclones of 1983. *Mon. Wea. Rev.*, **112**, 1419–1440.

Hales, J.E., Jr., 1972: Surges of Maritime Tropical Air Northward over the Gulf of California, *Monthly Weather Review*, Vol. 100, 298-306.

Hansen, E.M., L.C. Schreiner and J.F. Miller, 1982: Application of Probable Maximum Precipitation Estimates – United States East of the 105th Meridian. *Hydrometeorological Report No. 52*, U.S. Department of Commerce, Washington, D.C., 168 pp.

_____, F.K. Schwarz, and J.T Reidel, 1977: Probable Maximum Precipitation Estimates. Colorado River and Great Basin Drainages. *Hydrometeorological Report No. 49*, NWS, NOAA, U.S. Department of Commerce, Silver Spring, Md, 161 pp.

_____, and F.K. Schwartz, 1981: Meteorology of Important Rainstorms in the Colorado River and Great Basin Drainages. *Hydrometeorological Report No. 50*, National Weather Service, National Oceanic and Atmospheric Administration, U.S. Department of Commerce, Silver Spring, MD, 167 pp.

_____, Schwarz, F.K., and J.T. Riedel, 1994: Probable Maximum Precipitation- Pacific Northwest States, Columbia River (Including portion of Canada), Snake River, and Pacific Drainages. *Hydrometeorological Report No. 57*, National Weather Service, National Oceanic and Atmospheric Administration, U.S. Department of Commerce, Silver Spring, MD, 353 pp.

_____, Fenn, D.D., Schreiner, L.C., Stodt, R.W., and J.F., Miller, 1988: Probable Maximum Precipitation Estimates, United States between the Continental Divide and the 103rd Meridian, *Hydrometeorological Report Number 55A*, National weather Service, National Oceanic and Atmospheric Association, U.S. Dept of Commerce, Silver Spring, MD, 242 pp.

Hidalgo, H.G., and J.A. Dracup, 2002: ENSO and PDO Effects on Hydroclimatic Variations of the Upper Colorado River Basin, *Journal of Hydrometeorology*, Vol. 4, 5-22.

Higgins, R.W., Y. Yao, and X.L. Wang, 1997: Influence of the North American Monsoon System on the U.S. Summer Precipitation Regime. *J. Climate*, **10**, 2600–2622.

Higgins, R.W., K.C. Mo, and Y. Yao, 1998: Interannual Variability of the U.S. Summer Precipitation Regime with Emphasis on the Southwestern Monsoon. *J. Climate*, **11**, 2582–2606.

Higgins, R.W., Y. Chen, and A.V. Douglas, 1999: Interannual Variability of the North American Warm Season Precipitation Regime. *J. Climate*, **12**, 653–680.

Higgins, R.W., and W. Shi, 2000: Dominant Factors Responsible for Interannual Variability of the Summer Monsoon in the Southwestern United States. *J. Climate*, **13**, 759–776.

Higgins, R.W., J.K.E. Schemm, W. Shi, and A. Leetmaa, 2000: Extreme Precipitation Events in the Western United States Related to Tropical Forcing. *J. Climate*, **13**, 793–820.

Higgins, R.W., and W. Shi, 2001: Intercomparison of the Principal Modes of Interannual and Intraseasonal Variability of the North American Monsoon System. *J. Climate*, **14**, 403–417.

Higgins, R.W., W. Shi, and C. Hain, 2004: Relationships between Gulf of California Moisture Surges and Precipitation in the Southwestern United States. *J. Climate*, **17**, 2983–2997.

Higgins, R.W., and W. Shi, 2005: Relationships between Gulf of California Moisture Surges and Tropical Cyclones in the Eastern Pacific Basin. *J. Climate*, **18**, 4601–4620.

House, P.K., and K.K. Hirschboeck, 1997: Hydroclimatological and Paleohydrological context of Extreme Winter Flooding in Arizona, 1993, *in* Larson, R.A., and Slosson, J.E., eds., Storm-Induced Geologic Hazards: Case Histories from the 1992-1993 Winter in Southern California and Arizona: Boulder, Colorado, Geological Society of America Reviews in Engineering Geology, Vol. XI, 27pp.

Hu, Q., and S. Feng, 2002: Interannual Rainfall Variations in the North American Summer Monsoon Region: 1900–98. *J. Climate*, **15**, 1189–1202.

Hurd, W.E., 1939: North Pacific Ocean, September 1939. *Mon. Wea. Rev.*, **67**, 356–358

Information about Climate Change and the Myths of Human Caused Global Warming, Icecap, www.icecap.us

Jennings, A.H., 1952: Maximum 24-hour Precipitation in the United States, *Technical Paper Number 16*, U.S. Weather Bureau, U.S. Department of Commerce, Washington, DC, 284 pp.

Johnson, G.L., and C.L. Hanson, 1995: Topographic and Atmospheric Influences on Precipitation Variability over a Mountainous Watershed. *J. Appl. Meteor.*, **34**, 68–87. Johnson, R.H., P.E. Ciesielski, B.D. McNoldy, P.J. Rogers, and R.K. Taft, 2007: Multiscale Variability of the Flow during the North American Monsoon Experiment. *J. Climate*, **20**, 1628–1648.

Johnson, R.H., P.E. Ciesielski, B.D. McNoldy, P.J. Rogers, and R.K. Taft, 2007: Multiscale Variability of the Flow during the North American Monsoon Experiment. *J. Climate*, **20**, 1628–1648.

Kahya, E., and J.A. Dracup, 1994: The Influences of Type 1 El Niño and La Niña Events on Streamflows in the Pacific Southwest of the United States. *J. Climate*, **7**, 965–976.

Kalnay, E., M. Kanamitsu, R. Kistler, W. Collins, D. Deaven, L. Gandin, M. Iredell, S. Saha, G. White, J. Woollen, Y. Zhu, A. Leetmaa, R. Reynolds, M. Chelliah, W. Ebisuzaki, W.

Higgins, J. Janowiak, K. Mo, C. Ropelewski, J. Wang, R. Jenne, and D. Joseph, 1996: The NCEP/NCAR 40-Year Reanalysis Project. *Bull. Amer. Meteor. Soc.*, **77**, 437–471.

Kandgieser, P.C., 1972: Weather Note: Unusually Heavy 24-Hour Rainfall at Workman Creek 1, Arizona. *Mon. Wea. Rev.*, **100**, 206–207.

Kappel, W.D., Hultstrand, D.M., Tomlinson, E.M., and G.A., Muhlestein, August 2012: Site-Specific Probable Maximum Precipitation (PMP) Study for the Tarrant Regional Water District-Benbrook and Floodway Basins, Ft Worth, TX.

_____, W.D., Hultstrand, D.M., Tomlinson, E.M., Muhlestein, G.A., and T.P. Parzybok, September 2012: Site-Specific Probable Maximum Precipitation (PMP) Study for the Quad Cities Nuclear Generating Station, Quad Cities, IA.

_____, W.D., Hultstrand, D.M., Tomlinson, E.M., Muhlestein, G.A., and T.P. Parzybok, March 2013: Site-Specific Probable Maximum Precipitation (PMP) Study for the Indian Point Energy Center, Peekskill, NY.

_____, W.D., Hultstrand, D.M., Tomlinson, E.M., Muhlestein, G.A., and T.P. Parzybok, March 2013: Site-Specific Probable Maximum Precipitation (PMP) Study for the Vermont Yankee Nuclear Power Plant, Vernon, VT.

Kent E.C, S. D. Woodruff, and D. I. Berry, 2007: Metadata from WMO Publication No. 47 and an Assessment of Voluntary Observing Ship Observation Heights in ICOADS. *J. Atmos and Ocean Tech.*, **24(2)**, 214-234.

Kirshbaum, D.J., R. Rotunno, and G.H. Bryan, 2007: The Spacing of Orographic Rainbands Triggered by Small-Scale Topography. *J. Atmos. Sci.*, **64**, 4222–4245.

Koutsoyiannis, D., 1999: A Probabilistic view of Hershfield's Method for Estimating Probable Maximum Precipitation, *Water Resources Research*, Vol. 35, No. 4, 1313-1322.

Koutsoyiannis, D., A. Efstratiadis, N. Mamassis, and A. Christofides, 2008: On the Credibility of Climate Predictions, *Hydrological Sciences Journal*, 53 (4), 671-684.

Lang, T.J., D.A. Ahijevych, S.W. Nesbitt, R.E. Carbone, S.A. Rutledge, and R. Cifelli, 2007: Radar-Observed Characteristics of Precipitating Systems during NAME 2004. *J. Climate*, **20**, 1713–1733.

Lang, T. J., S. A. Rutledge, and R. Cifelli, 2010: Polarimetric Radar Observations of Convection in Northwestern Mexico during the North American Monsoon Experiment. *J. Hydrometeor*, **11**, 1345–1357.

Lewis, D.D., 1968: Floods of September 26-28 near Marana, Arizona, in Rostvedt, J.O., and others, Summary of Floods in the United States During 1962: U.S. Geological Survey Water-Supply Paper 1820, p105-106.

Leverson, V.H., 1986: Rainfall Characteristics of the Prescott, Arizona, Storm of 23–24 September 1983. *Mon. Wea. Rev.*, **114**, 2344–2351.

Liebmann, B., I. Bladé, N.A. Bond, D. Gochis, D. Allured, and G.T. Bates, 2008: Characteristics of North American Summertime Rainfall with Emphasis on the Monsoon. *J. Climate*, **21**, 1277–1294.

MacNish, R.D., Smith, C.F., and Goddard, K.E., 1993:   Floods in Arizona, January 1993, USGS Open-File Report 93-54, 2 pp.

Maddox, R. A., Canova, F., and L. R. Hoxit, 1980: Meteorological Characteristics of Flash Flood Events over the Western United States, *Monthly Weather Review*, Vol. 108, 1866-1877.

Martner, B.E, and V. Dubovskiy, 2005: Z-R Relations from Raindrop Disdrometers: Sensitivity to Regression Methods And DSD Data Refinements. 32nd Radar Meteorology Conference, Albuquerque, NM, October, 2005

Martner, B.E., S.E. Yuter, A.B. White, S.Y. Matrosov, D.E. Kingsmill, and F.M. Ralph, 2008: Raindrop Size Distributions and Rain Characteristics in California Coastal Rainfall for Periods with and without a Radar Bright Band. *J. Hydrometeor.*, **9**, 408–425.

McCollum, D.M., Maddox, R.A., and K.W. Howard, 1995: Case Study of a Severe Mesoscale Convective System in Central Arizona, *Weather and Forecasting*, September 1995, Vol. 10 643-665.

McGeehin, J.P., Barron, J.A., Anderson, D.M., and D.J. Verardo, 2009: Abrupt Climate Change, Synthesis and Assessment Product 3.4, http://downloads.climatescience.gov/sap/sap3-4/sap3-4-final-report-all.pdf, USGS, 477p.

Mejia, J.F., M.W. Douglas, and P.J. Lamb, 2010: Aircraft Observations of the 12–15 July 2004 Moisture Surge Event during the North American Monsoon Experiment. *Mon. Wea. Rev.*, **138**, 3498–3513.

Mesinger, F., G. DiMego, E. Kalnay, K. Mitchell, P.C. Shafran, W. Ebisuzaki, D. Jović, J. Woollen, E. Rogers, E.H. Berbery, M.B. Ek, Y. Fan, R. Grumbine, W. Higgins, H. Li, Y. Lin, G. Manikin, D. Parrish, and W. Shi, 2006: North American Regional Reanalysis. *Bull. Amer. Meteor. Soc.*, **87**, 343–360.

Michaels, P.J., 2004: Meltdown, The Predictable Distortion of Global Warming by Scientists, Politicians, and the Media, the Cato Institute, Washington D.C., 255pp.

Michele, C.D., Kottegoda, N.T., and R. Rosso, 2001: The Derivation of Areal Reduction Factor of Storm Rainfall from its Scaling Properties, *Water Resources Research,* Vol. 37, N. 12, 3247-3252.

Miller, J.F., R.H. Fredrick, and R.J. Tracey, 1973: *NOAA Atlas 2, Precipitation-Frequency Atlas of the Western United States.* U.S. Department of Commerce, National Oceanic and Atmospheric Administration, National Weather Service, Silver Spring, Md.

Miller, W.P., and T.C. Piechota, 2008: Regional Analysis of Trend and Step Changes Observed in Hydroclimatic Variables around the Colorado River Basin. *J. Hydrometeor.*, **9**, 1020–1034.

Mitchell, D.L., D. Ivanova, R. Rabin, T.J. Brown, and K. Redmond, 2002: Gulf of California Sea Surface Temperatures and the North American Monsoon: Mechanistic Implications from Observations. *J. Climate*, **15**, 2261–2281.

Mo, K.C., and R.W. Higgins, 1998: Tropical Influences on California Precipitation. *J. Climate*, **11**, 412–430.

Mo, K.C., and R.W. Higgins, 1998: Tropical Convection and Precipitation Regimes in the Western United States. *J. Climate*, **11**, 2404–2423.

Mo, K., and R.W. Higgins, 2008: Relationships between Sea Surface Temperatures in the Gulf of California and Surge Events. *J. Climate*, **21**, 4312–4325.

Mock, C.J., 1996: Climatic Controls and Spatial Variations of Precipitation in the Western United States. *J. Climate*, **9**, 1111–1125.

Myers V.A., and R.M Zehr. and 1980: NOAA Technical Report NWS 24, *A Methodology for Point-to-Area Rainfall Frequency Ratios*, Silver Spring, MD 176pp.

National Climatic Data Center (NCDC). NCDC TD-3200 and TD-3206 datasets - Cooperative Summary of the Day

National Climatic Data Center (NCDC) Heavy Precipitation Page http://www.ncdc.noaa.gov/oa/climate/severeweather/rainfall.html#maps

National Oceanic and Atmospheric Association, Forecast Systems Laboratory FSL Hourly/Daily Rain Data, http://precip.fsl.noaa.gov/hourly_precip.html

National Weather Service Forecast Office, Phoenix, AZ, 2009: http://www.wrh.noaa.gov/psr/

National Weather Service Forecast Office, Tucson, AZ, 2009:

http://www.wrh.noaa.gov/twc/

NCEP_Reanalysis data provided by the NOAA/OAR/ESRL PSD, Boulder, Colorado, USA, from their Web site at http://www.esrl.noaa.gov/psd/data/reanalysis/reanalysis.shtml

NCEP_Reanalysis 2 data provided by the NOAA/OAR/ESRL PSD, Boulder, Colorado, USA, from their Web site at http://www.esrl.noaa.gov/psd/

Negri, A.J., R.F. Adler, R.A. Maddox, K.W. Howard, and P.R. Keehn, 1993: A Regional Rainfall Climatology over Mexico and the Southwest United States Derived from Passive Microwave and Geosynchronous Infrared Data. *J. Climate*, **6**, 2144–2161.

Neiman, P.J., F.M. Ralph, B.J. Moore, M. Hughes, K.M. Mahoney, J.M. Cordeira, and M.D. Dettinger, 2012: The Landfall and Inland Penetration of a Flood-Producing Atmospheric River in Arizona. Part I: Observed Synoptic-Scale, Orographic, and Hydrometeorological Characteristics. *J. Hydrometeor.*, **14**, 460–484.

Nesbitt, S.W., D.J. Gochis, and T.J. Lang, 2008: The Diurnal Cycle of Clouds and Precipitation along the Sierra Madre Occidental Observed during NAME-2004: Implications for Warm Season Precipitation Estimation in Complex Terrain. *J. Hydrometeor.*, **9**, 728–743.

O'Connor, J.E, and J.E. Costa, 2003: Large Floods in the United States: Where They Happen and Why, U.S. Geological Survey Circular 1245, 18p.

Oliver, V.J., 1951: The Weather and Circulation of August 1951. *Mon. Wea. Rev.*, **79**, 160–162.

Perica, S., Dietz, S., Heim, S., Hiner, L., Maitaria, K., Martin, D., Pavlovic, S., Roy, I., Trypaluk, C., Unruh, D., Yan, F., Yekta, M., Zhao, T., Bonnin, G., Brewer, D., Chen, L., and J. Yarchoan (2013). NOAA Atlas 14 Volume 8 in press, *Precipitation-Frequency Atlas of the United States, Midwestern States.* NOAA, National Weather Service, Silver Spring, MD.

Parzybok, T. W., and E. M. Tomlinson, 2006: A New System for Analyzing Precipitation from Storms, *Hydro Review*, Vol. XXV, No. 3, 58-65.

Physical Sciences Division of NOAA/ESRL http://www.cdc.noaa.gov/

PRISM Mapping Methodology
http://www.ocs.oregonstate.edu/prism/index.phtml

Pyke C.B., 1975: The Indio, California thunderstorms of 24 September 1939, US. Corps of Engineers Los Angeles District, *presented at American Geophysical Union National Symposium on Precipitation Analysis for Hydrologic Modeling*, June 26-28, 1975.

Randerson, D., 1976: Meteorological Analysis for the Las Vegas, Nevada Flood of 3 July, 1975, *Monthly Weather Review*, Vol. 104, 719-727.

Remote Automated Weather Stations RAWS, http://www.raws.dri.edu/index.html

Reynolds, R.W., T.M. Smith, C. Liu, D.B. Chelton, K.S. Casey, and M.G. Schlax, 2007: Daily High-resolution Blended Analysis for Sea Surface Temperature. *J. Climate.*, **20**, 5473-5496.

Riedel, J.T., and L.C. Schreiner, 1980: Comparison of Generalized Estimates of Probable Maximum Precipitation with Greatest Observed Rainfalls, *NOAA Technical Report NWS 25*, US Department of Commerce, NOAA, Silver Spring, Md, 46 pp.

Roeske, R., Garrett, J., and Eychaner, J., 1989: Floods of October 1983 in southeastern Arizona, USGS Water-Resources Investigations Report 85-4225-C, 77 pp.

Roeske, R., Cooley, M. E., and Aldrige B. N., 1978: Floods of September 1970 in Arizona, Utah.

Rogers, P.J., and R.H. Johnson, 2007: Analysis of the 13−14 July Gulf Surge Event during the 2004 North American Monsoon Experiment. *Mon. Wea. Rev.*, **135**, 3098–3117.

Rolph, G.D., 2003: Real-time Environmental Applications and Display sYstem (READY) Website (http://www.arl.noaa.gov/ready/hysplit4.html). NOAA Air Resources Laboratory, Silver Spring, MD.

Rolph, G.D., 2010. Real-time Environmental Applications and Display sYstem (READY) Website (http://ready.arl.noaa.gov). NOAA Air Resources Laboratory, Silver Spring, MD.

Rostvedt, J.O., and Others, 1971: Summary of Floods in the United States During 1966, U.S. Geological Survey Water-Supply Paper 1870-D, 108pp.

Rowe, A.K., S.A. Rutledge, T.J. Lang, P.E. Ciesielski, and S.M. Saleeby, 2008: Elevation-Dependent Trends in Precipitation Observed during NAME. *Mon. Wea. Rev.*, **136**, 4962–4979.

Saleeby, S.M., and W.R. Cotton, 2004: Simulations of the North American Monsoon System. Part I: Model Analysis of the 1993 Monsoon Season. *J. Climate*, **17**, 1997–2018

Schmitz, J.T., and S.L. Mullen, 1996: Water Vapor Transport Associated with the Summertime North American Monsoon as Depicted by ECMWF Analyses. *J. Climate*, **9**, 1621–1634.

Schreiner, L.C., and J.T. Riedel, ,1978: Probable Maximum Precipitation Estimates, United States East of the 105th Meridian. *Hydrometeorological Report No. 51*, U.S. Department of Commerce, Silver Spring, Md, 242 pp.

Sellers, W.D., and Hill, R.H., 1974: Arizona Climate, 1931-1972, Tucson, University of Arizona Press, 616 pp.

Sellers, W.D., Hill, R.H., and Sanderson-Rae, Margaret, editors, 1985: Arizona Climate-the First Hundred Years: Tucson, Arizona, University of Arizona Press, 80pp.

Shands, A.L. and G.N. Brancato, March 1946: Applied Meteorology: Mass Curves of Rainfall. Hydrometeorological Section, Office of Hydrologic Director.

Smith, R.B., and I. Barstad, 2004: A Linear Theory of Orographic Precipitation. *J. Atmos. Sci.*, **61**, 1377–1391.

Smith, W, 1986: The Effects of Eastern North Pacific Tropical Cyclones on the Southern United States, NOAA Technical Memorandum, NWS WR-197.

Smith, W.P., and R.L. Gall, 1989: Tropical Squall Lines of the Arizona Monsoon, *Monthly Weather Review*, Vol. 117, 1553-1569.

Spencer, R., 2008: Climate Confusion: How Global Warming Hysteria Leads to Bad Science, Pandering Politicians and Misguided Policies that Hurt the Poor, Encounter Books, New York, NY, 184 pp.

Stahle, D.W., M.K. Cleaveland, H.D. Grissino-Mayer, R.D. Griffin, F.K. Fye, M.D. Therrell, D.J. Burnette, D.M. Meko, and J. Villanueva Diaz, 2009: Cool- and Warm-Season Precipitation Reconstructions over Western New Mexico. *J. Climate*, **22**, 3729–3750.

Stensrud, D.J., R.L. Gall, and M.K. Nordquist, 1997: Surges over the Gulf of California during the Mexican Monsoon. *Mon. Wea. Rev.*, **125**, 417–437.

Stensrud, D.J., R.L. Gall, S.L. Mullen, and K.W. Howard, 1995: Model Climatology of the Mexican Monsoon. *J. Climate*, **8**, 1775–1794.

Storm Studies – Pertinent Data Sheets, and Isohyetal Map, U.S. Department of Interior, Bureau of Reclamation, Denver, CO.

Svoma, B. M., 2010: The Influence of Monsoonal Gulf Surges on Precipitation and Diurnal Precipitation Patterns in Central Arizona, *Wea. Forecasting*, **25**, 281–289.

Tang, M., and E.R. Reiter, 1984: Plateau Monsoons of the Northern Hemisphere: A Comparison between North America and Tibet. *Mon. Wea. Rev.*, **112**, 617–637.

Taubensee, R.E., 1973: Weather and Circulation of October 1972. *Mon. Wea. Rev.*, **101**, 85–90

Thomas, B.E., Hjalmarson, H.W., and S.D. Waltemeyer, 1994: Methods for Estimating Magnitude and Frequency of Floods in the Southwestern United States, U.S. Geological Survey Water Supply Paper 2433, 205pp.

Tomlinson, E.M., 1993: Probable Maximum Precipitation Study for Michigan and Wisconsin, Electric Power Research Institute, Palo Alto, CA, TR-101554, V1.

_____, Ross A. Williams, and Tye W. Parzybok, September 2002: Site-Specific Probable Maximum Precipitation (PMP) Study for the Upper and Middle Dams Drainage Basin, Prepared for FPLE, Lewiston, ME.

_____,Ross A. Williams, and Tye W. Parzybok, September 2003: Site-Specific Probable Maximum Precipitation (PMP) Study for the Great Sacandaga Lake / Stewarts Bridge Drainage Basin, Prepared for Reliant Energy Corporation, Liverpool, New York.

_____, Ross A. Williams, and Tye W. Parzybok, September 2003: Site-Specific Probable Maximum Precipitation (PMP) Study for the Cherry Creek Drainage Basin, Prepared for the Colorado Water Conservation Board, Denver, CO.

_____, Kappel W.D., Parzybok, T.W., Hultstrand, D., Muhlestein, G., and B. Rappolt, May 2008: Site-Specific Probable Maximum Precipitation (PMP) Study for the Wanahoo Drainage Basin, Prepared for Olsson Associates, Omaha, Nebraska.

_____, Kappel W.D., Parzybok, T.W., Hultstrand, D., Muhlestein, G., and B. Rappolt, June 2008: Site-Specific Probable Maximum Precipitation (PMP) Study for the Blenheim Gilboa Drainage Basin, Prepared for New York Power Authority, White Plains, NY.

_____, Kappel W.D., and T.W. Parzybok, February 2008: Site-Specific Probable Maximum Precipitation (PMP) Study for the Magma FRS Drainage Basin, Prepared for AMEC, Tucson, Arizona.

_____, Kappel W.D., Parzybok, T.W., Hultstrand, D., Muhlestein, G., and P. Sutter, December 2008: Statewide Probable Maximum Precipitation (PMP) Study for the state of Nebraska, Prepared for Nebraska Dam Safety, Omaha, Nebraska.

_____, Kappel, W.D., and Tye W. Parzybok, July 2009: Site-Specific Probable Maximum Precipitation (PMP) Study for the Scoggins Dam Drainage Basin, Oregon.

_____, Kappel, W.D., and Tye W. Parzybok, February 2009: Site-Specific Probable Maximum Precipitation (PMP) Study for the Tuxedo Lake Drainage Basin, New York.

_____, Kappel, W.D., and Tye W. Parzybok, February 2011: Site-Specific Probable Maximum Precipitation (PMP) Study for the Magma FRS Drainage Basin, Arizona.

_____, Kappel, W.D., and Tye W. Parzybok, March 2011: Site-Specific Probable Maximum Precipitation (PMP) Study for the Tarrant Regional Water District, Texas.

_____, Kappel, W.D., Hultstrand, D.M., Muhlestein, G.A., and T. W. Parzybok, November 2011: Site-Specific Probable Maximum Precipitation (PMP) Study for the Lewis River basin, Washington State.

_____, Kappel, W.D., Hultstrand, D.M., Muhlestein, G.A., and T. W. Parzybok, December 2011: Site-Specific Probable Maximum Precipitation (PMP) Study for the Brassua Dam basin, Maine.

_____, Kappel, W.D., Hultstrand, D.M., Muhlestein, G.A., S. Lovisone, and T. W. Parzybok, March 2013: Statewide Probable Maximum Precipitation (PMP) Study for Ohio.

_____, and W. D. Kappel, October 2009: Revisiting PMPs, _Hydro Review_, Vol. 28, No. 7, 10-17.

Tucson National Weather Service Monsoon Page, http://www.wrh.noaa.gov/twc/monsoon/mexmonsoon.php

U.S. Army Corps of Engineers, 1954: Report on Flood of 19 August 1954 Queen Creek and Vicinity, Arizona: U.S. Army Corps of engineers, Los Angeles District, 17pp.

U.S. Army Corps of Engineers, 1963: Flood damage report on storm and flood of 26-30 September 1962, Santa Cruz River and Santa Rosa Wash, southern Arizona: U.S. Army Corps of Engineers, Los Angeles District, 32pp.

U.S. Army Corps of Engineers, 1982: Gila River Basin New River and Phoenix City Streams, Arizona, _Design Memorandum No. 2 Hydrology Part 2_, U.S. Army Corps of Engineers, Los Angeles District, 113pp.

U.S. Dept of Agriculture, Soil Conservation Service, 1987: Engineering Report, Storm of Sept 2, 1984, Saddleback Diversion, Harquahala Valley Watershed, Maricopa County, AZ, 71pp.

U.S. Dept of Commerce, Weather Bureau, 1954: Climatological Data, Arizona, August 1954, No. 8, 16pp.

U.S. Dept of Commerce, Weather Bureau, 1954: Hourly Precipitation Data, Arizona, August 1954, Vol. 4 No. 8, 4pp.

U.S. National Climatic Data Center, updated monthly: NOAA Optimum Interpolation 1/4 Degree Daily Sea Surface Temperature Analysis, Version 2. _Dataset ds277.7 published by the CISL Data Support Section at the National Center for Atmospheric Research, Boulder, CO, available online at_ http://dss.ucar.edu/datasets/ds277.7/.

U.S. Weather Bureau, 1946: Manual for Depth-Area-Duration analysis of storm precipitation. *Cooperative Studies Technical Paper No. 1*, U.S. Department of Commerce, Weather Bureau, Washington, D.C., 73pp.

U.S. Weather Bureau, 1951: Tables of Precipitable Water and Other Factors for a Saturated Pseudo-Adiabatic Atmosphere. *Technical Paper No. 14*, U.S. Department of Commerce, Weather Bureau, Washington, D.C., 27 pp.

Velasco, I., and J.M. Fritsch, 1987: Mesoscale convective complexes in the Americas. *J. Geophys. Res*., **92**, 9591-9613.

Vivoni, E.R., K. Tai, and D.J. Gochis, 2009: Effects of Initial Soil Moisture on Rainfall Generation and Subsequent Hydrologic Response during the North American Monsoon. *J. Hydrometeor.*, **10**, 644–664.

Waananen, A.O, D.D. Harris, and R.C. Williams, 1971: Floods of December 1964 and January 1965 in the Far Western United States, U.S. Geological Survey Water-Supply Paper 1866-A, 276pp.

Wallace, C.E, Maddox, R.A., and K.W. Howard, 1999: Summertime Convective Storm Environments in Central Arizona: Local Observations, *Weather and Forecasting*, Vol. 14, 994-1001.

Weather Underground, http://www.wunderground.com/stationmaps/

Webb, R. H, and J. L., Betancourt, 1992: Climatic Variability and Flood Frequency of the Santa Cruz River, Pima County, Arizona, USGS Water-Supply Paper 2379, 40 pp.

World Meteorological Organization, 1986: Manual for Estimation of Probable Maximum Precipitation*, Operational Hydrology Report No 1*, 2nd Edition, WMO, Geneva, 269 pp.

World Meteorological Organization, 2009: Manual for Estimation of Probable Maximum Precipitation*, Operational Hydrology Report No 1045*, WMO, Geneva, 259 pp.

Worley, S.J., S.D. Woodruff, R.W. Reynolds, S.J. Lubker, and N. Lott, 2005: ICOADS Release 2.1 data and products. *Int. J. Climatol. (CLIMAR-II Special Issue)*, **25**, 823-842.

Wu, M.L.C., S.D. Schubert, M.J. Suarez, and N.E. Huang, 2009: An Analysis of Moisture Fluxes into the Gulf of California. *J. Climate*, **22**, 2216–2239.

Xu, J., X. Gao, J. Shuttleworth, S. Sorooshian, and E. Small, 2004: Model Climatology of the North American Monsoon Onset Period during 1980–2001. *J. Climate*, **17**, 3892–3906.

Zehr, R.M. and V.A. Myers, 1984: NOAA Technical Memorandum NWS Hydro 40, *Depth-Area Ratios in the Semi-Arid Southwest United States*, Silver Spring, MD 55pp.

Appendix A

Average Dew Point Maps for 3-hour, 12-hour, 24-hour 100-year Return Frequencies

And

Plus 2 sigma Sea Surface Temperatures Maps

January 3-Hour 100-Year
Dew Point °F
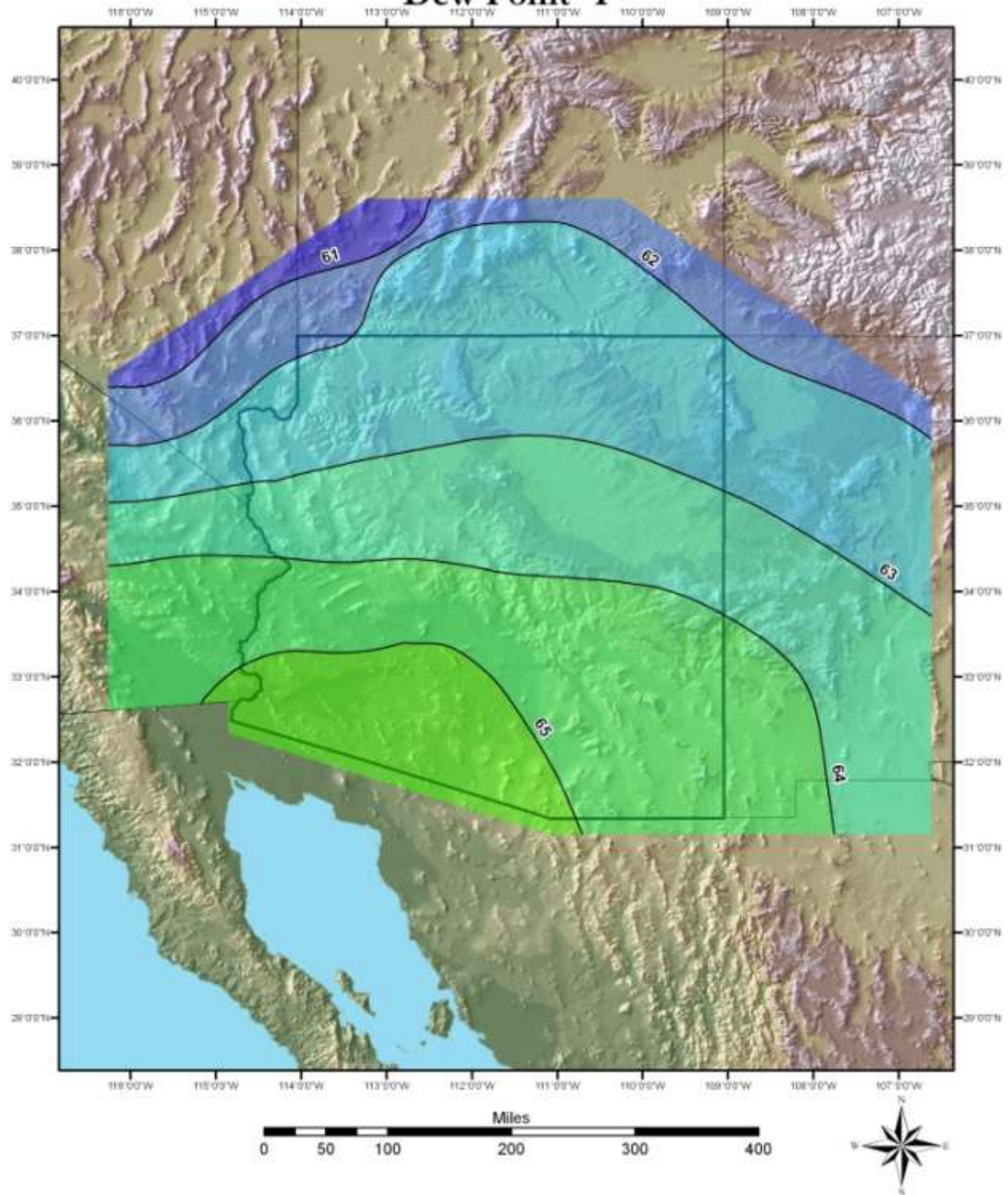
February 3-Hour 100-Year
Dew Point °F
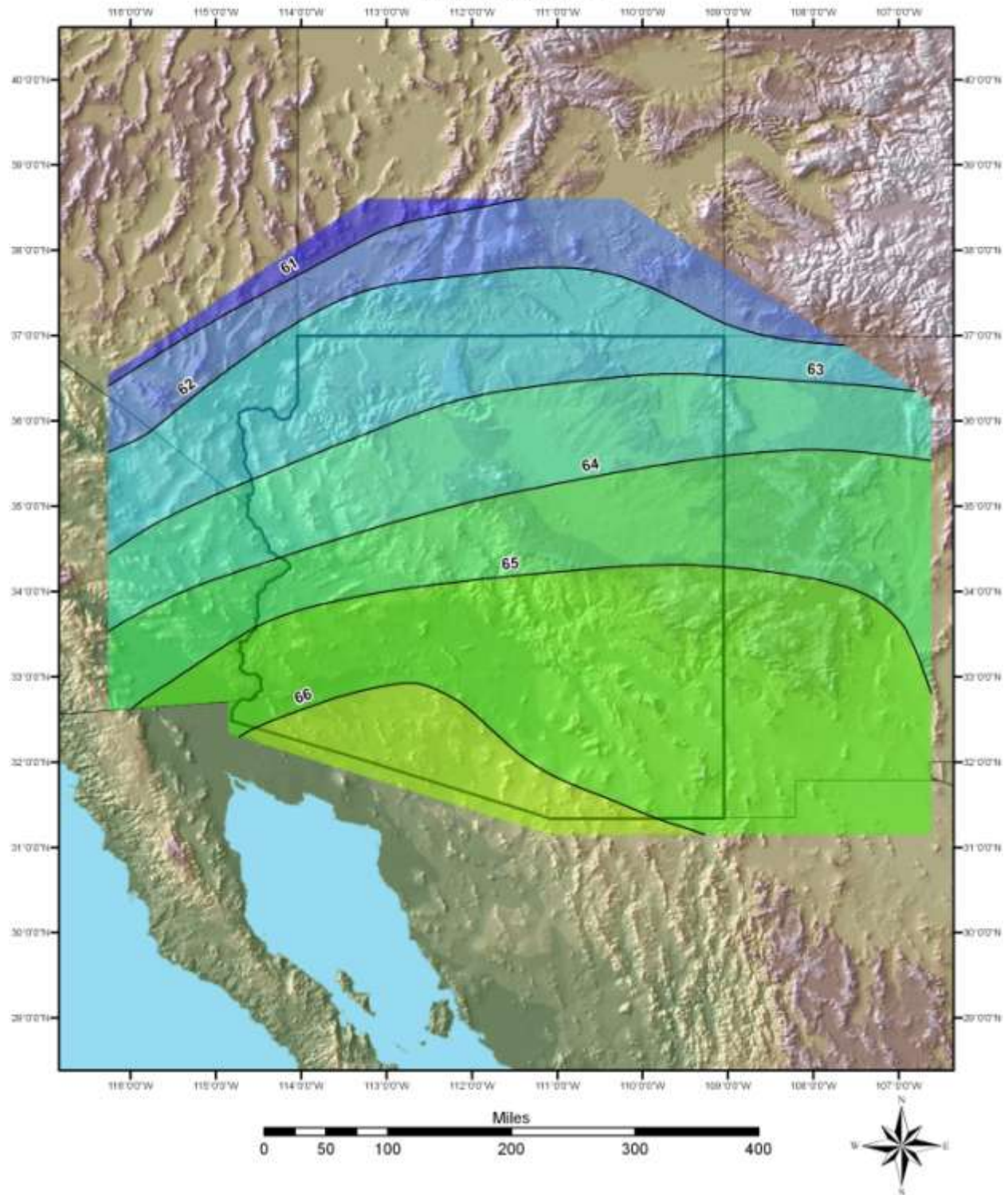
March 3-Hour 100-Year
Dew Point °F

A-4
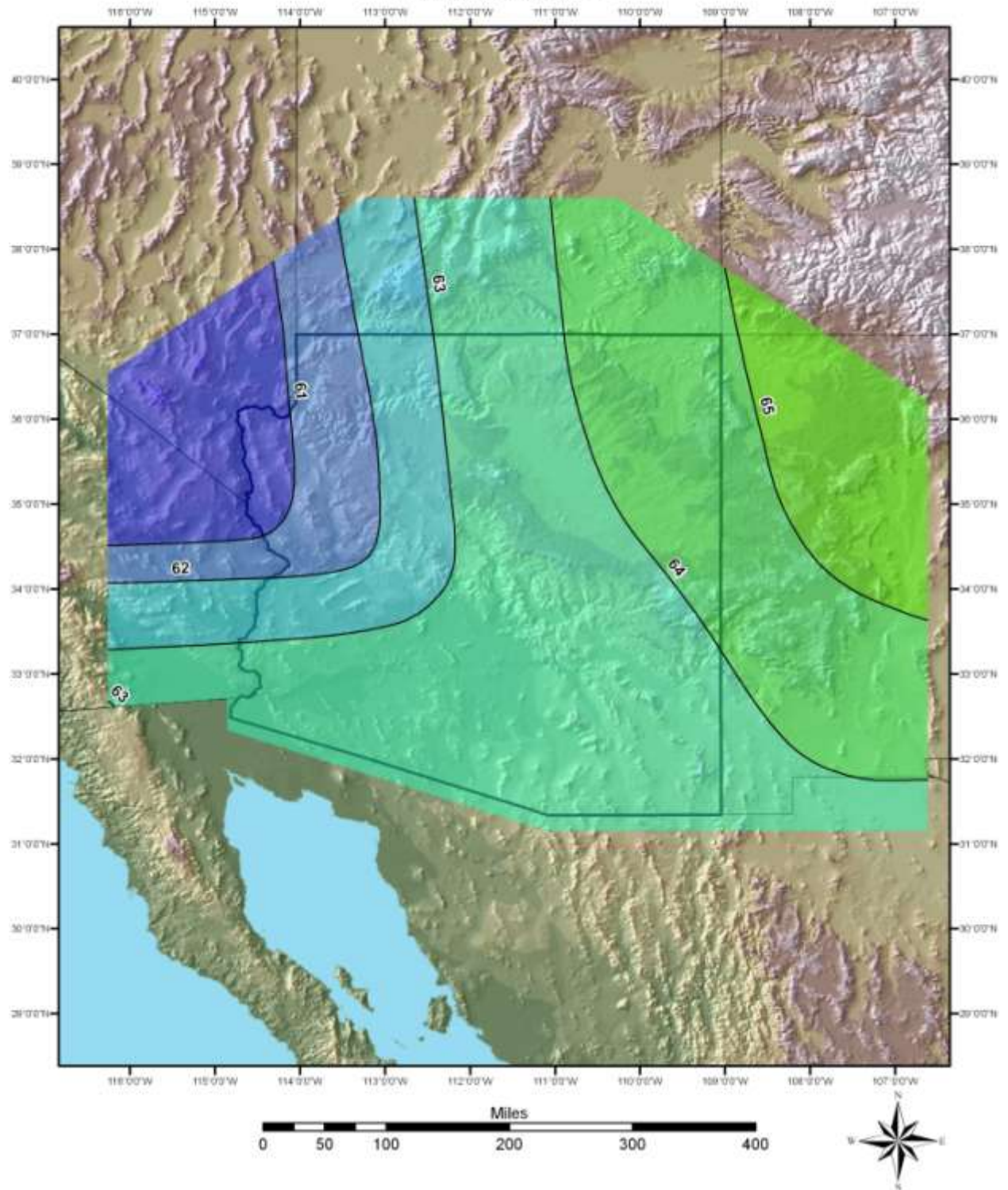
April 3-Hour 100-Year
Dew Point °F

A-5
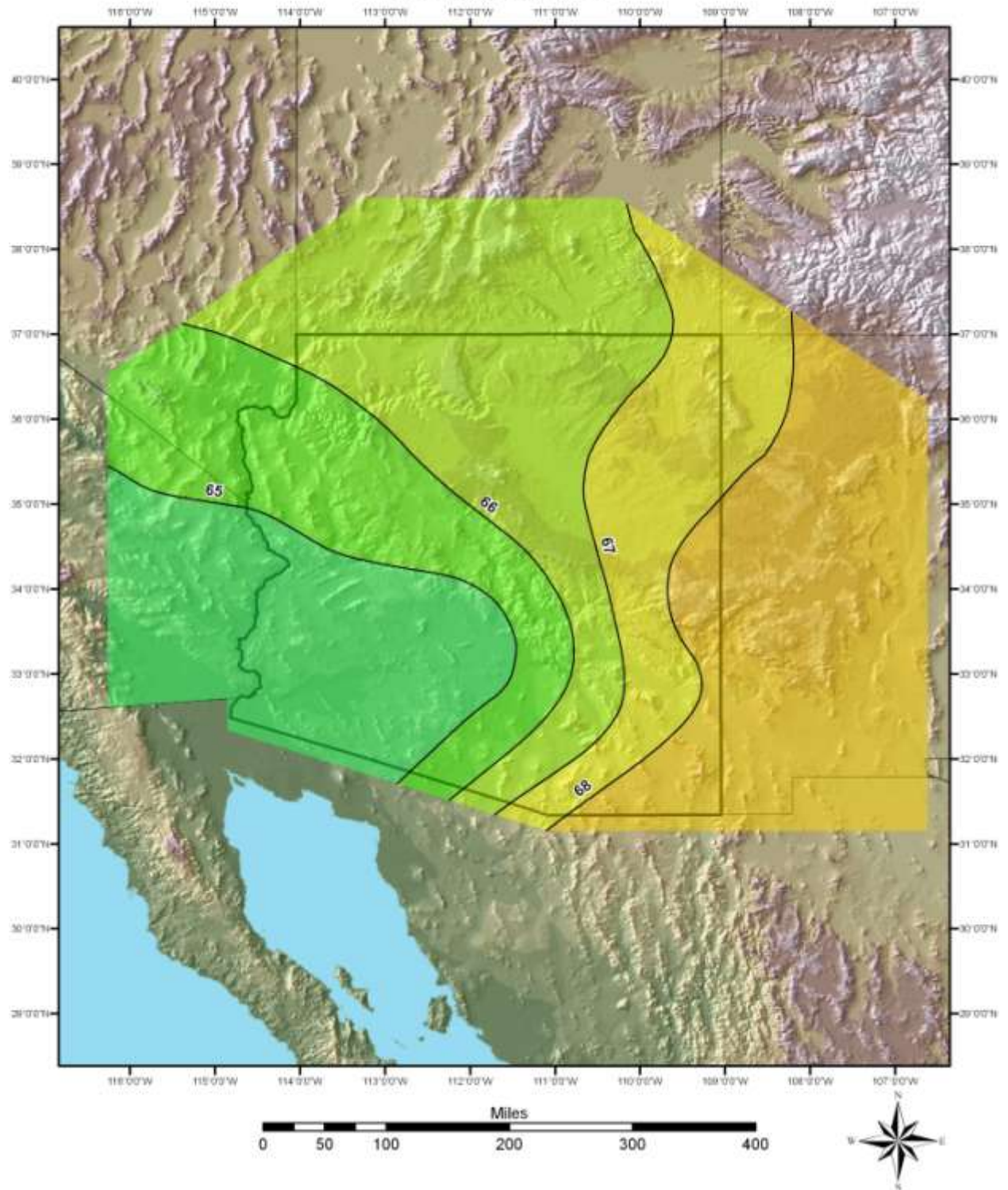
May 3-Hour 100-Year
Dew Point °F

A-6
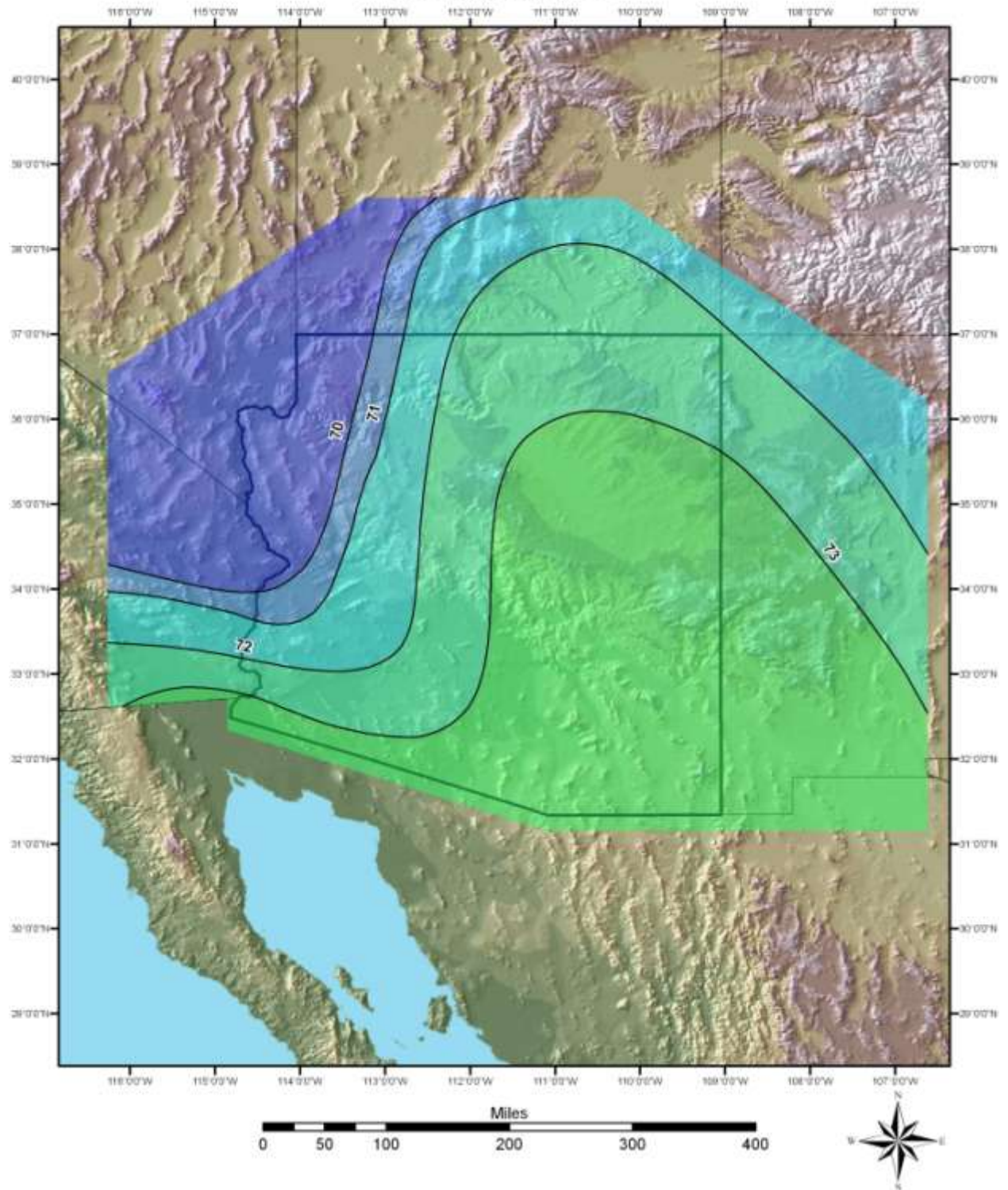
June 3-Hour 100-Year
Dew Point °F
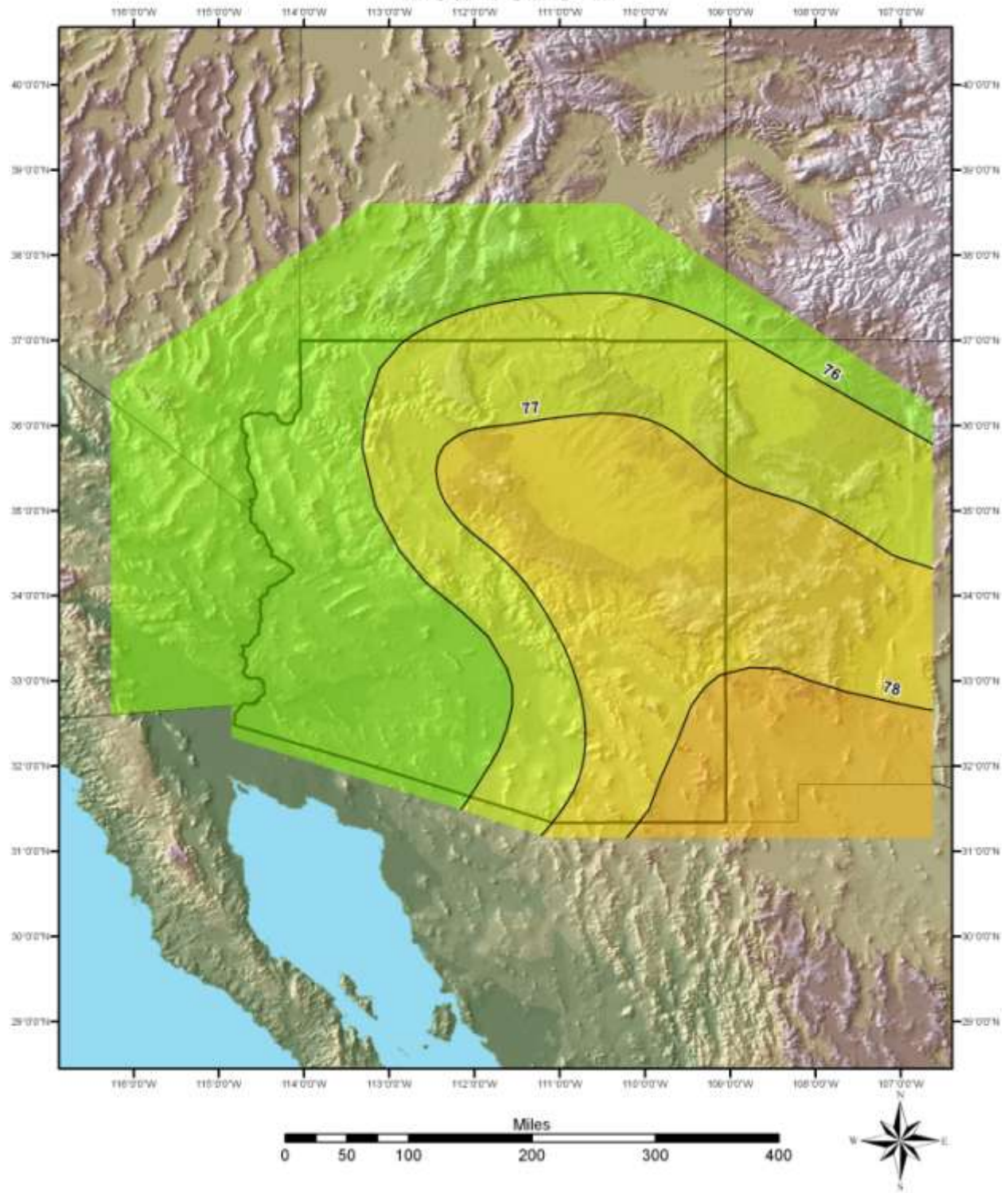
July 3-Hour 100-Year
Dew Point °F

A-8
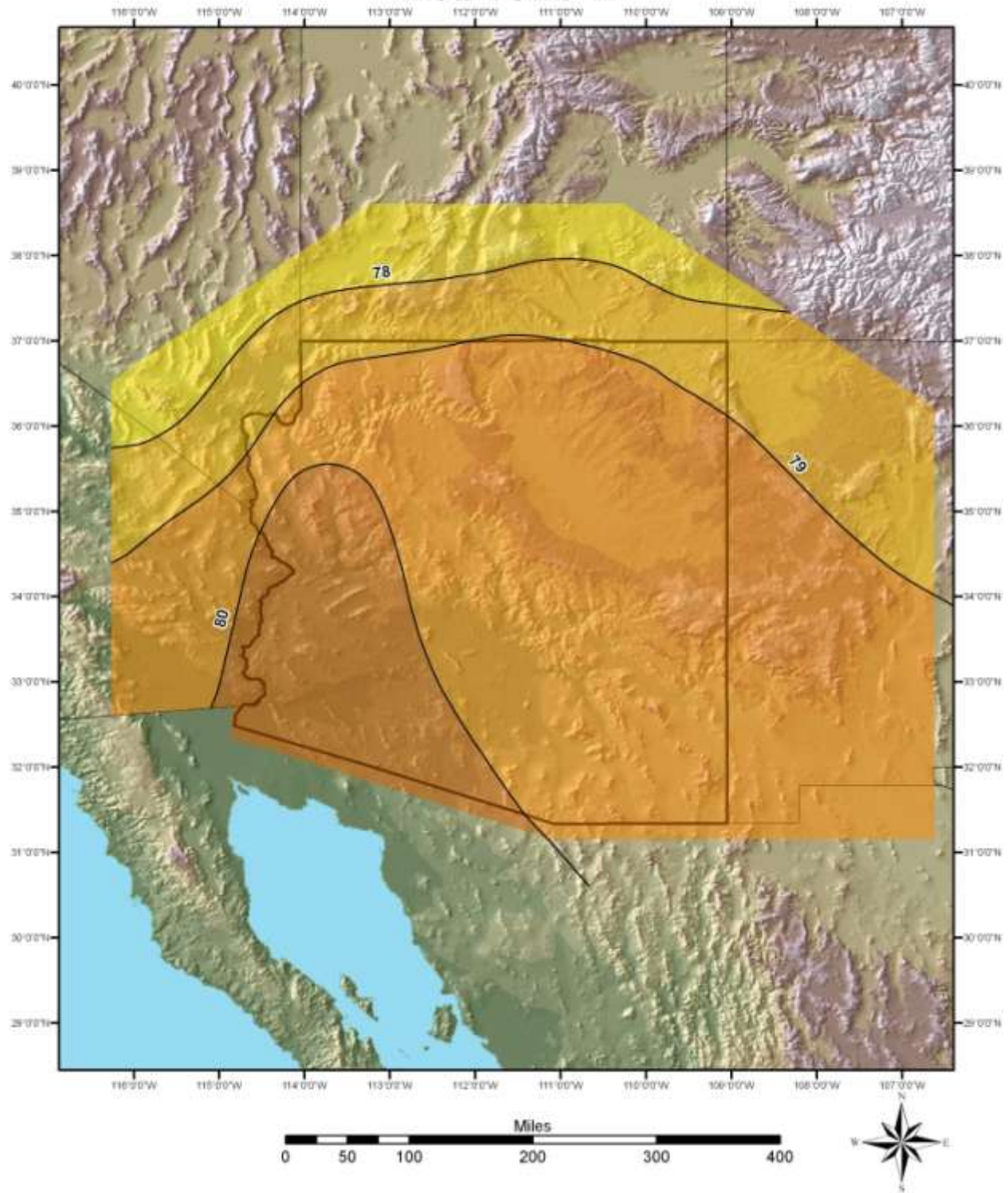
August 3-Hour 100-Year
Dew Point °F
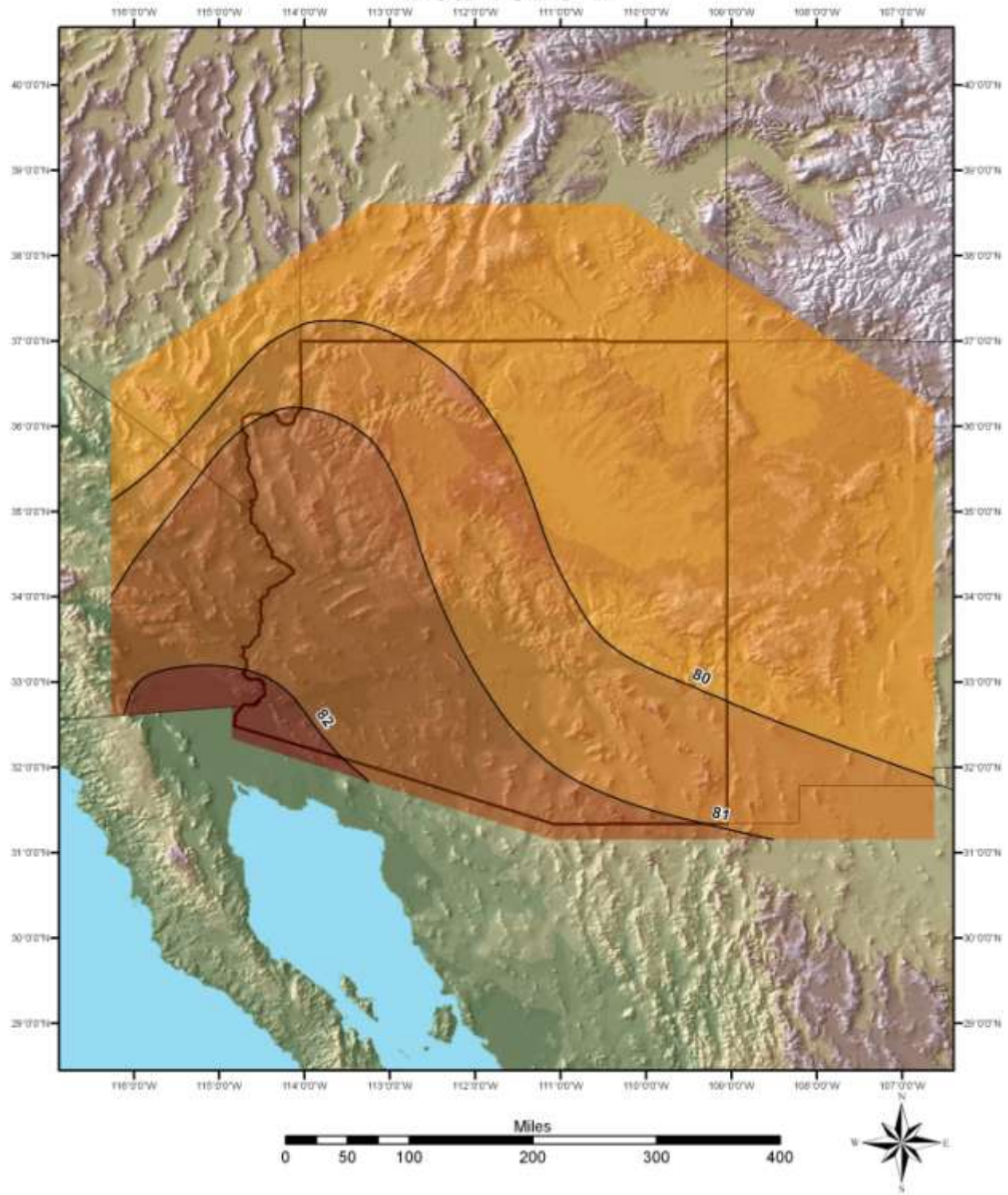
September 3-Hour 100-Year
Dew Point °F
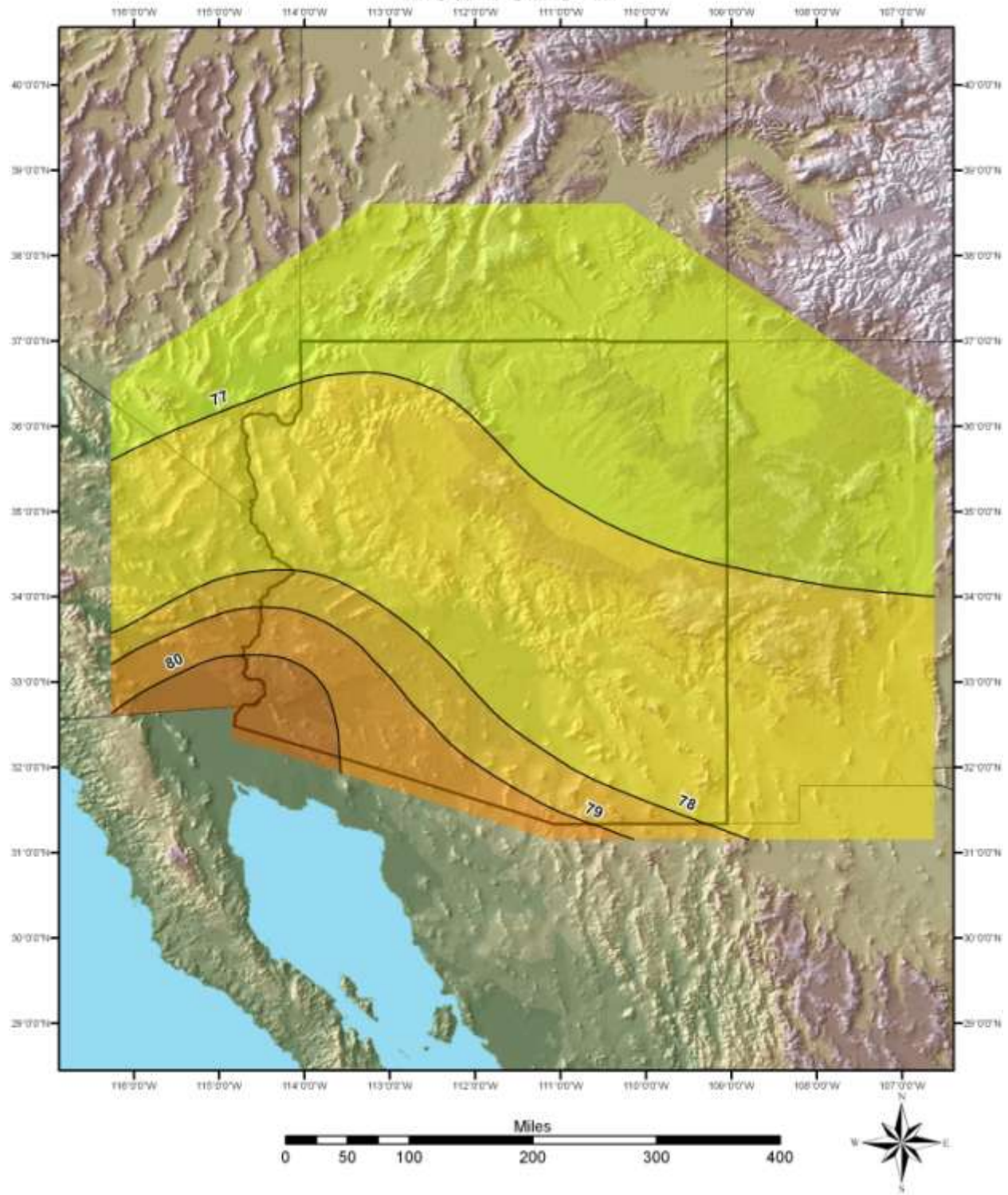
October 3-Hour 100-Year
Dew Point °F

A-11
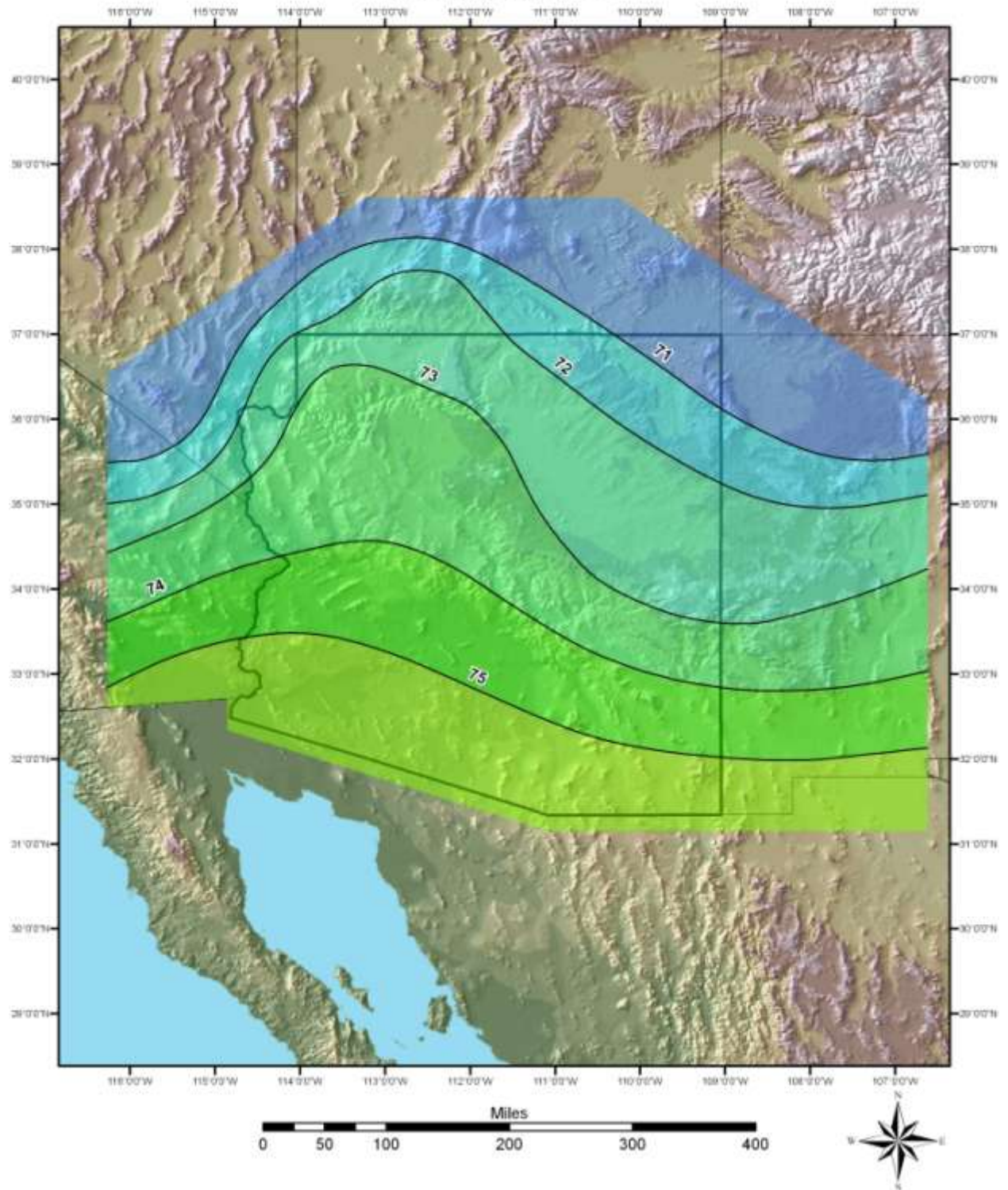
November 3-Hour 100-Year
Dew Point °F
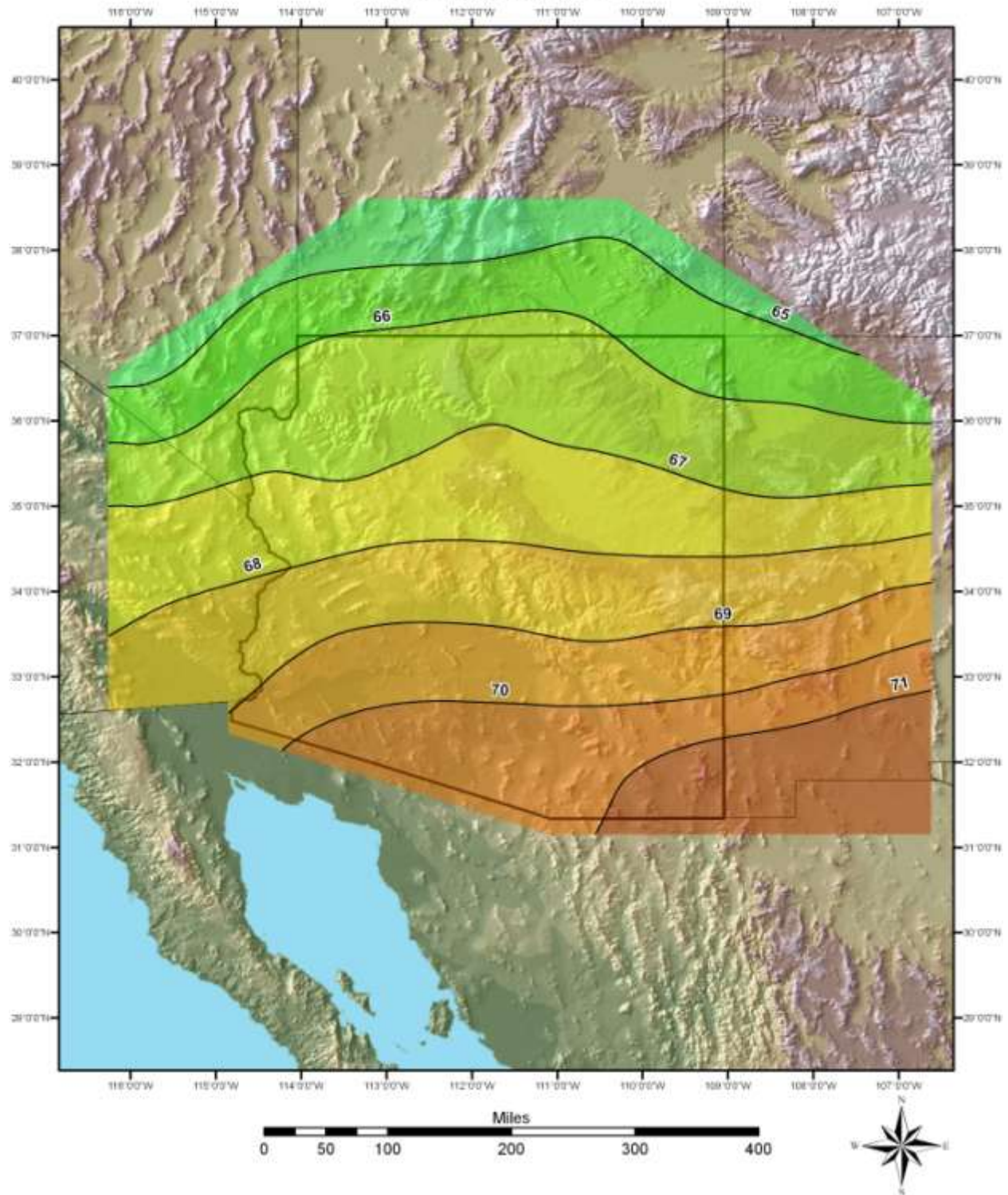
December 3-Hour 100-Year
Dew Point °F

A-13
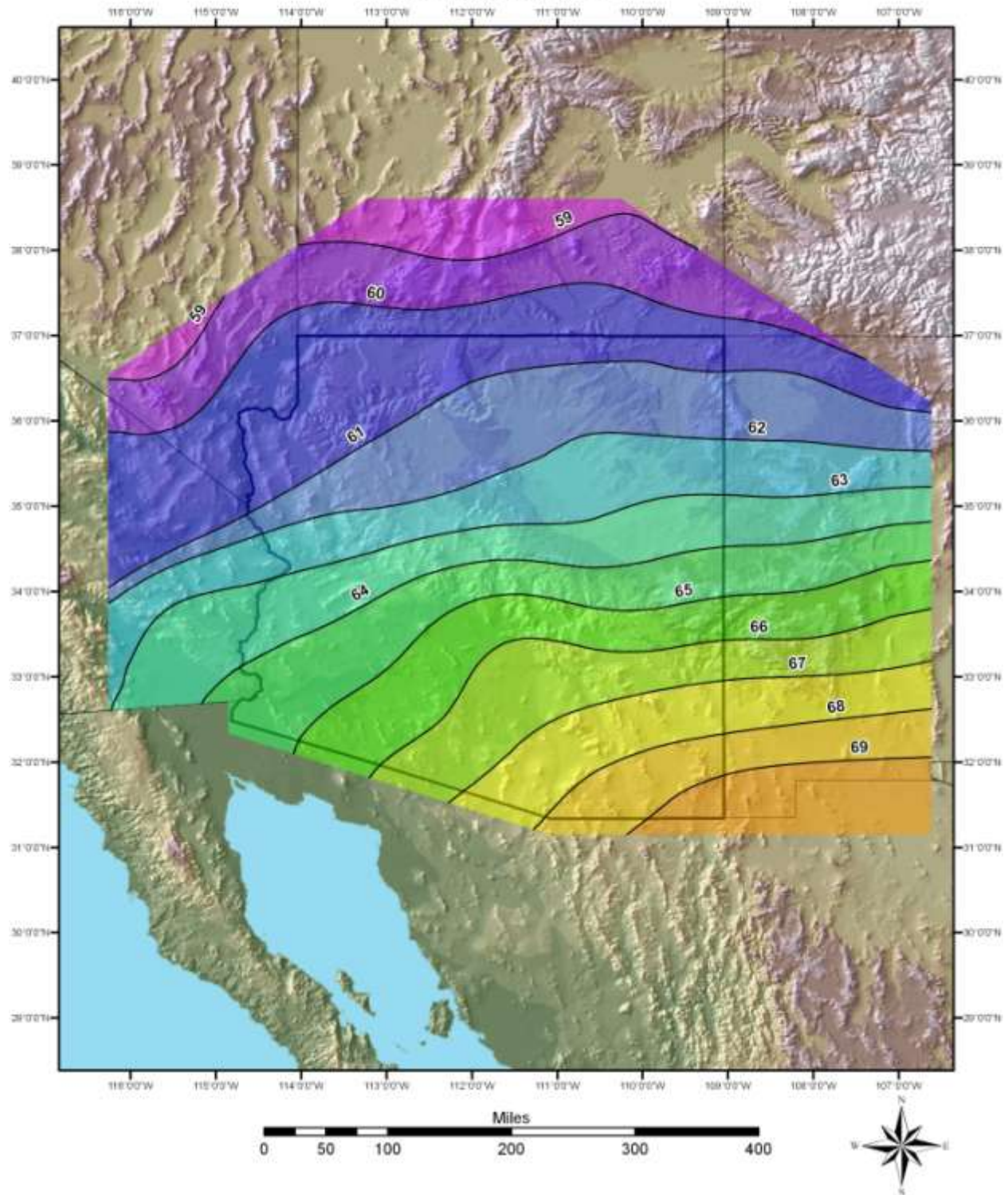
January 12-Hour 100-Year
Dew Point °F
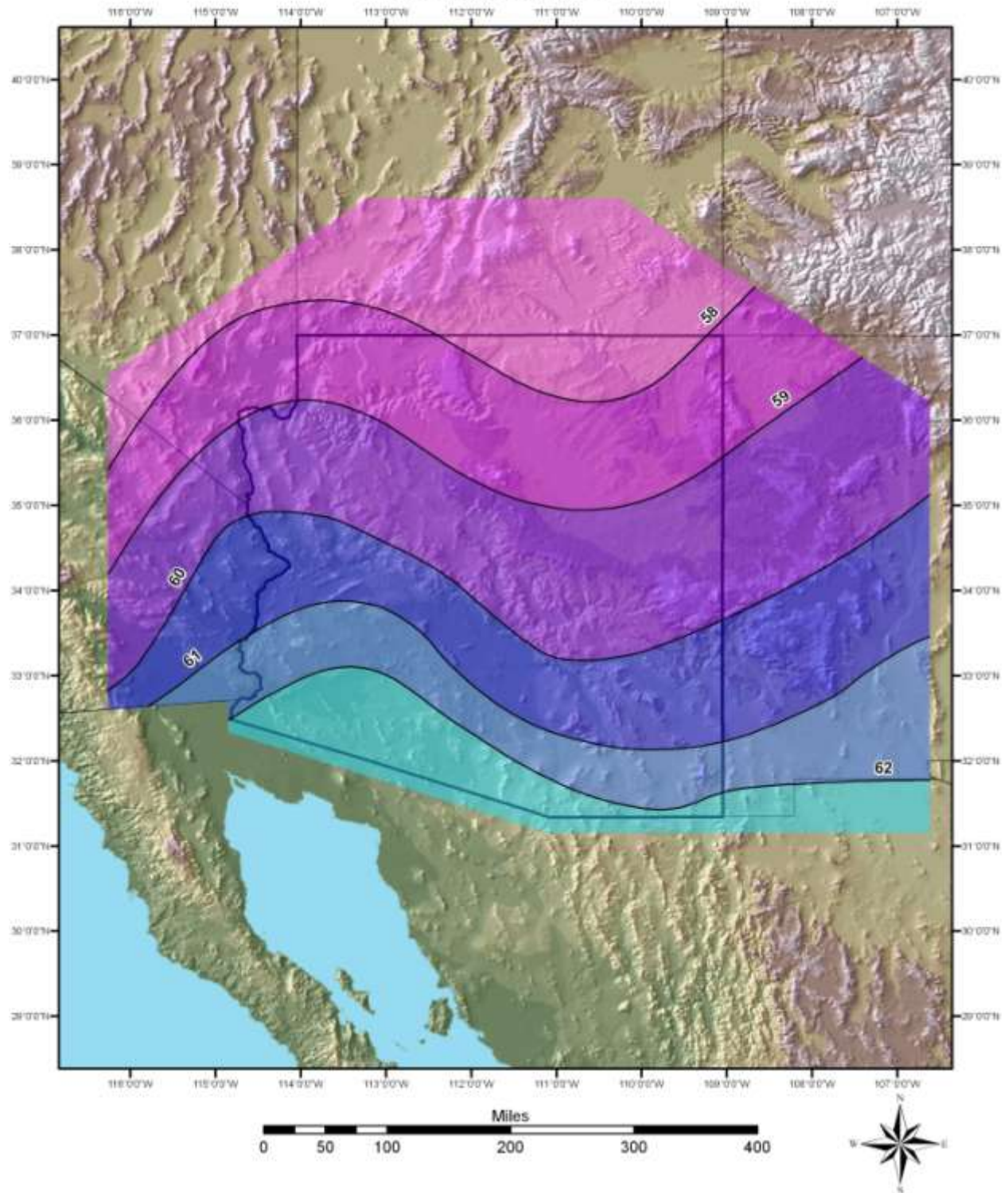
February 12-Hour 100-Year
Dew Point °F

A-15
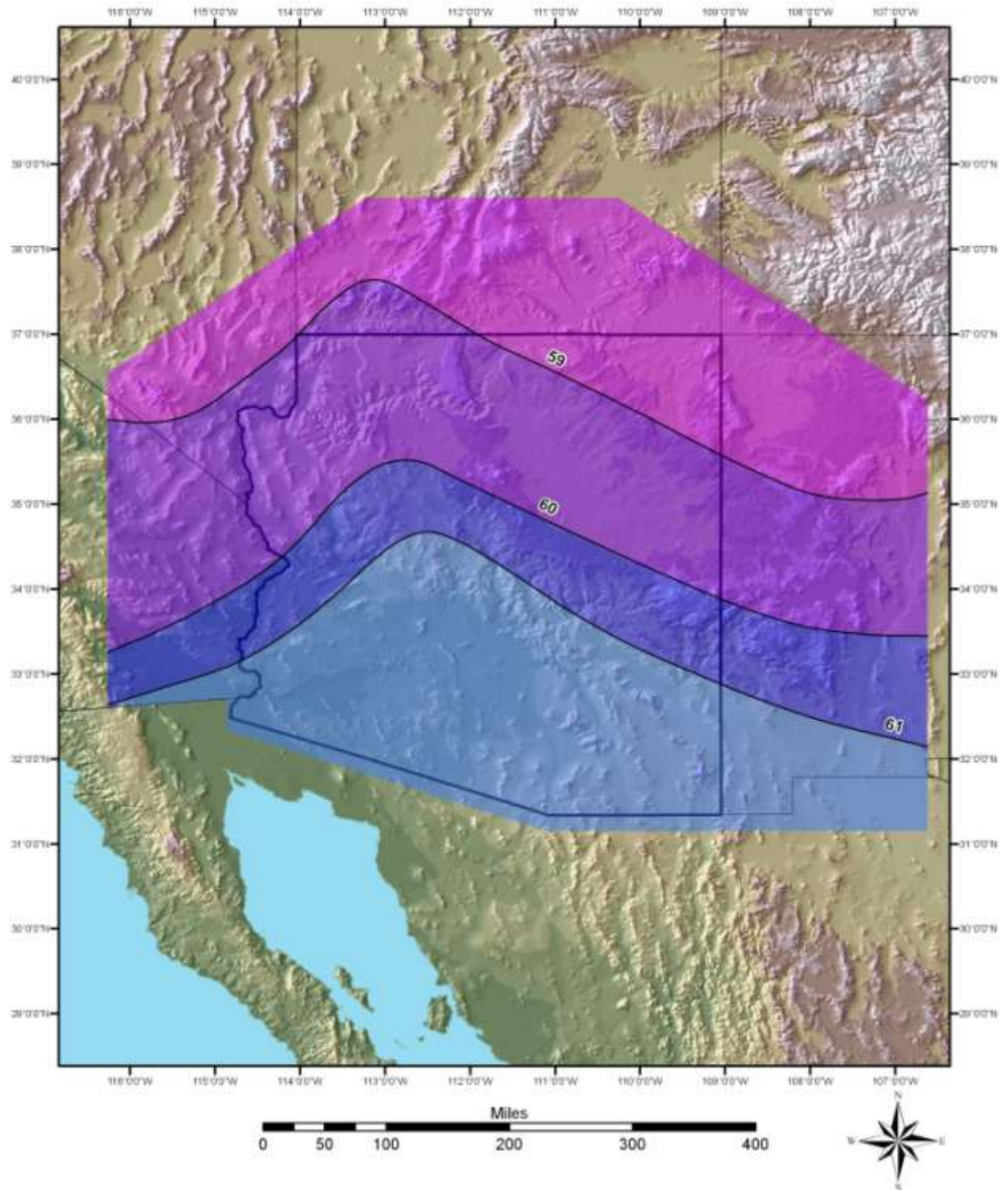
March 12-Hour 100-Year
Dew Point °F
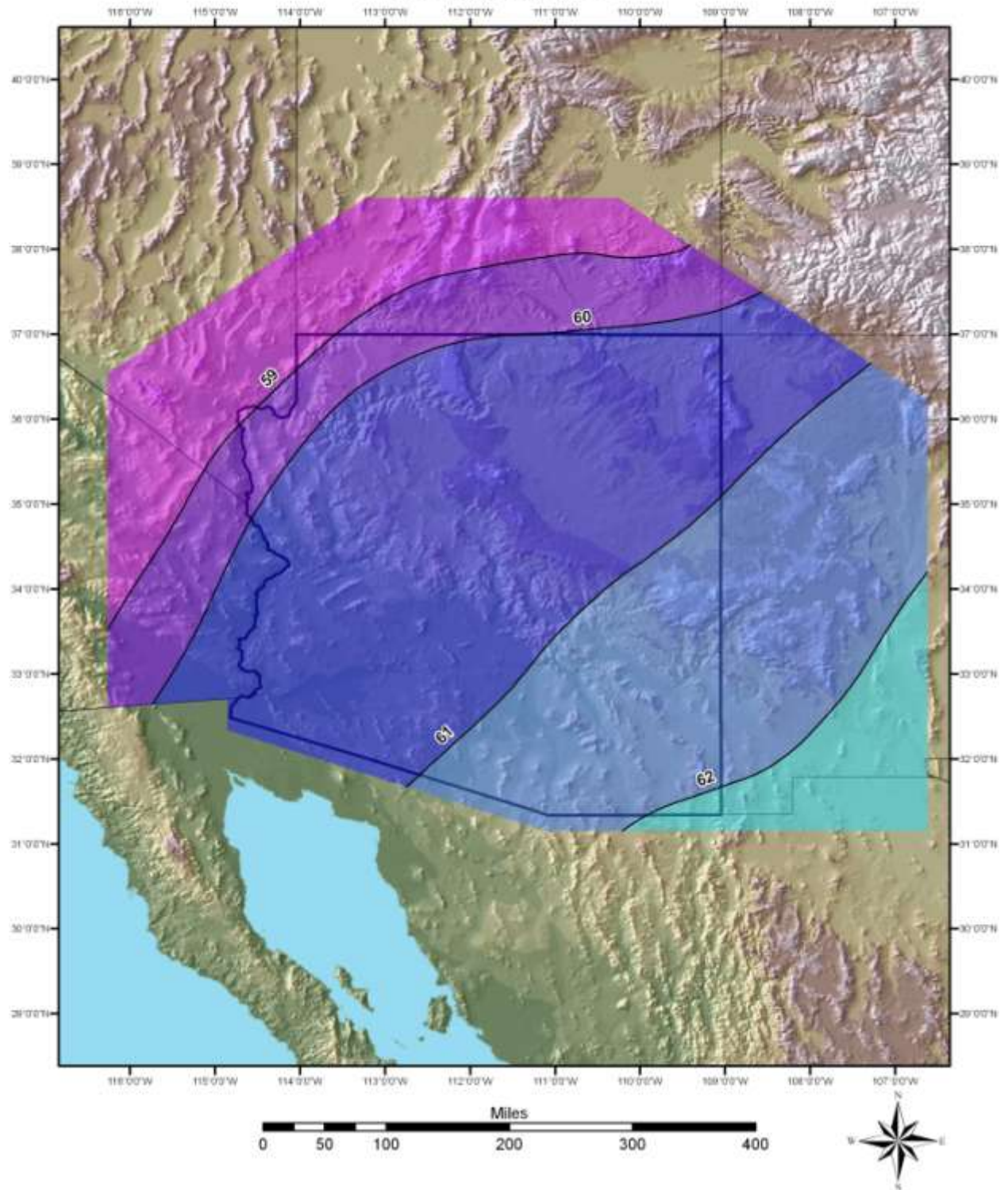
April 12-Hour 100-Year
Dew Point °F

A-17
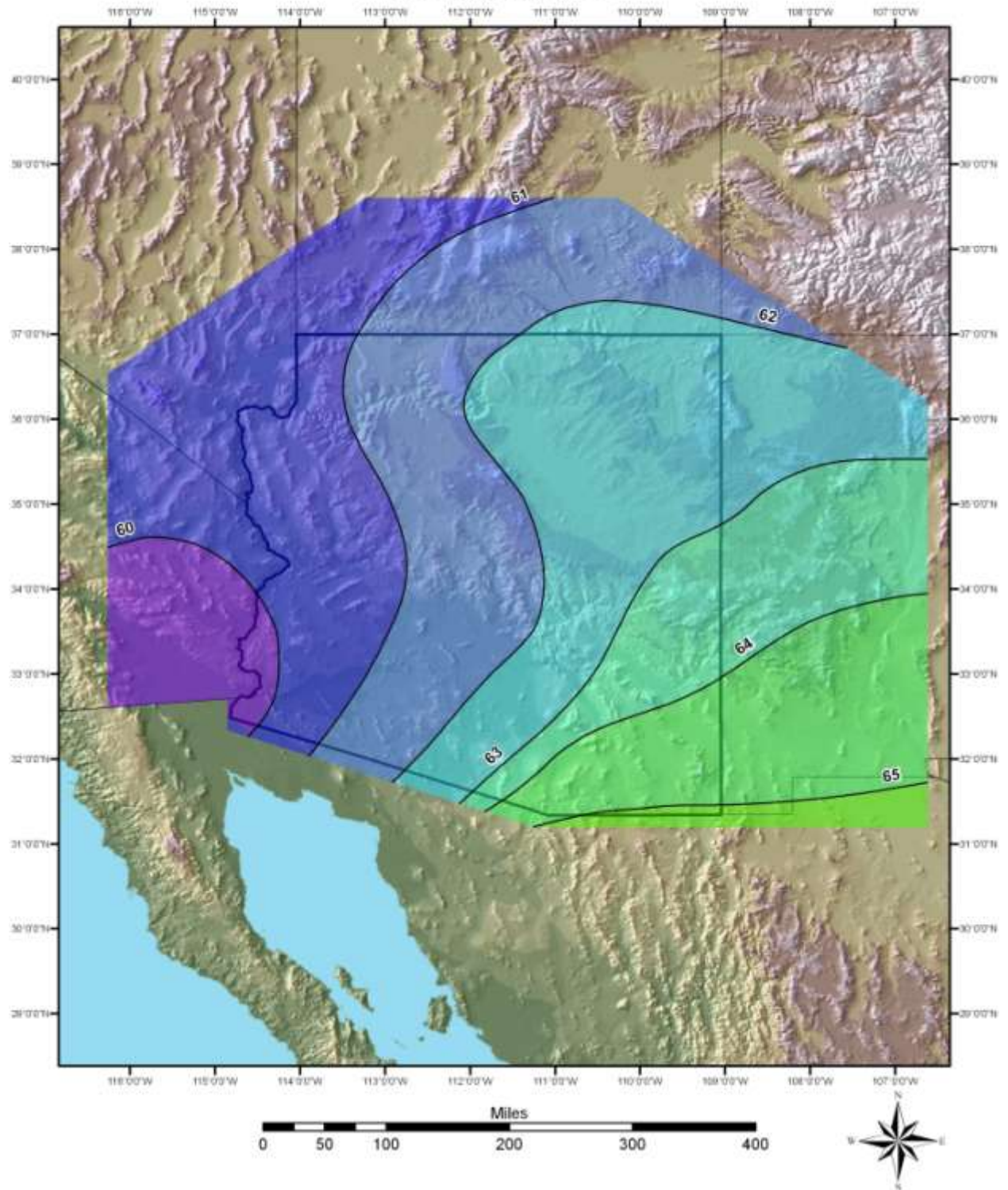
May 12-Hour 100-Year
Dew Point °F

A-18
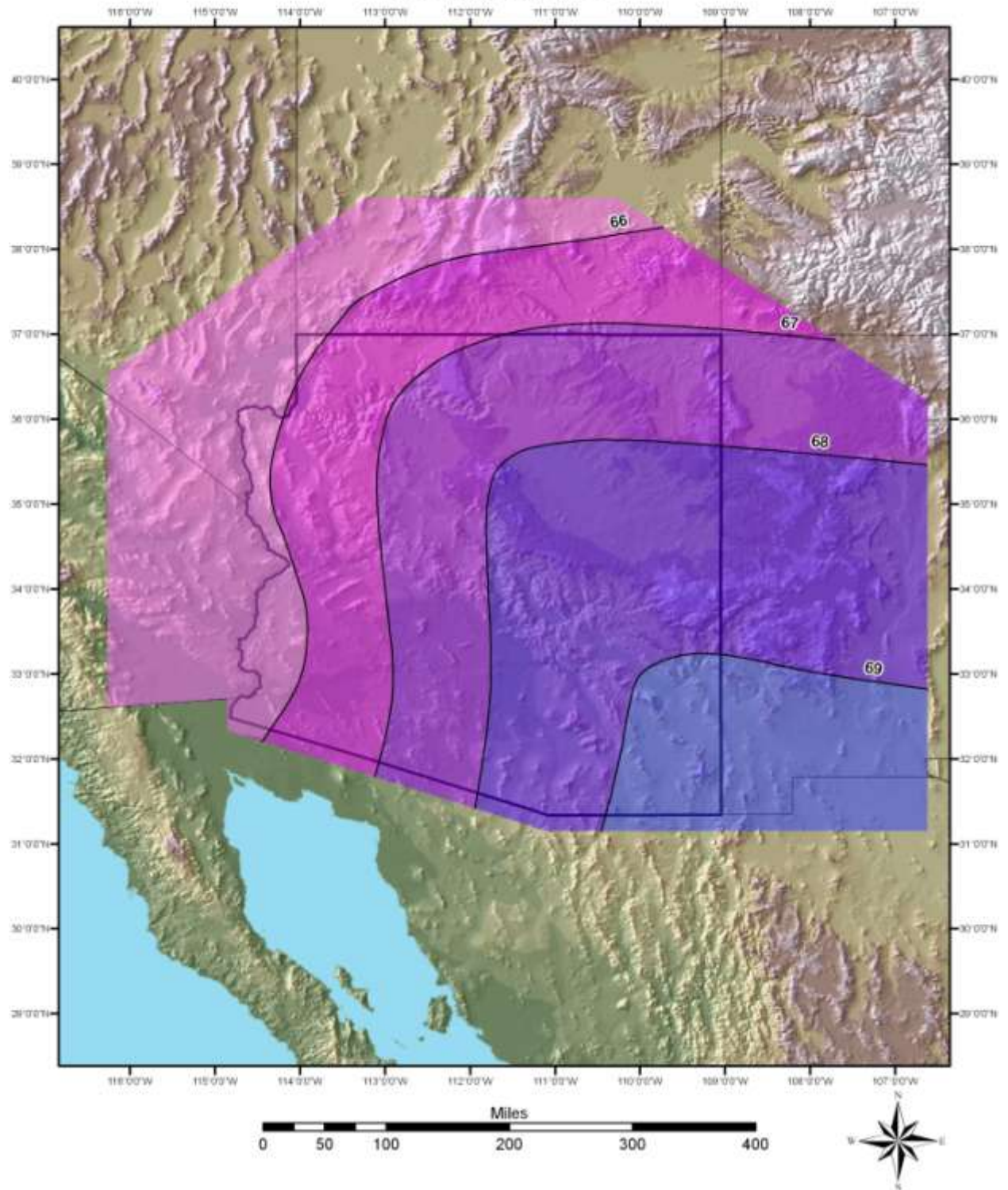
June 12-Hour 100-Year
Dew Point °F
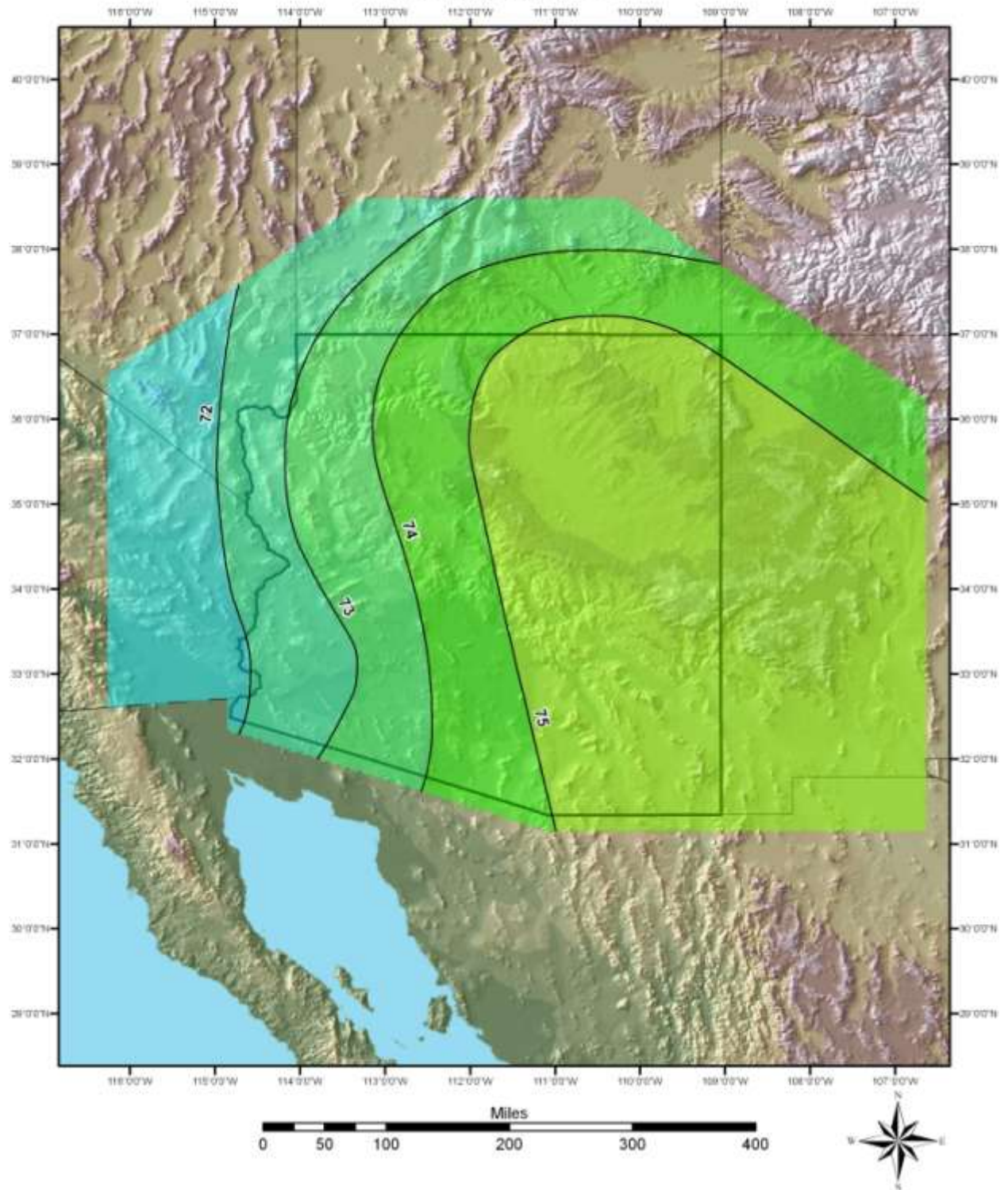
July 12-Hour 100-Year
Dew Point °F

A-20
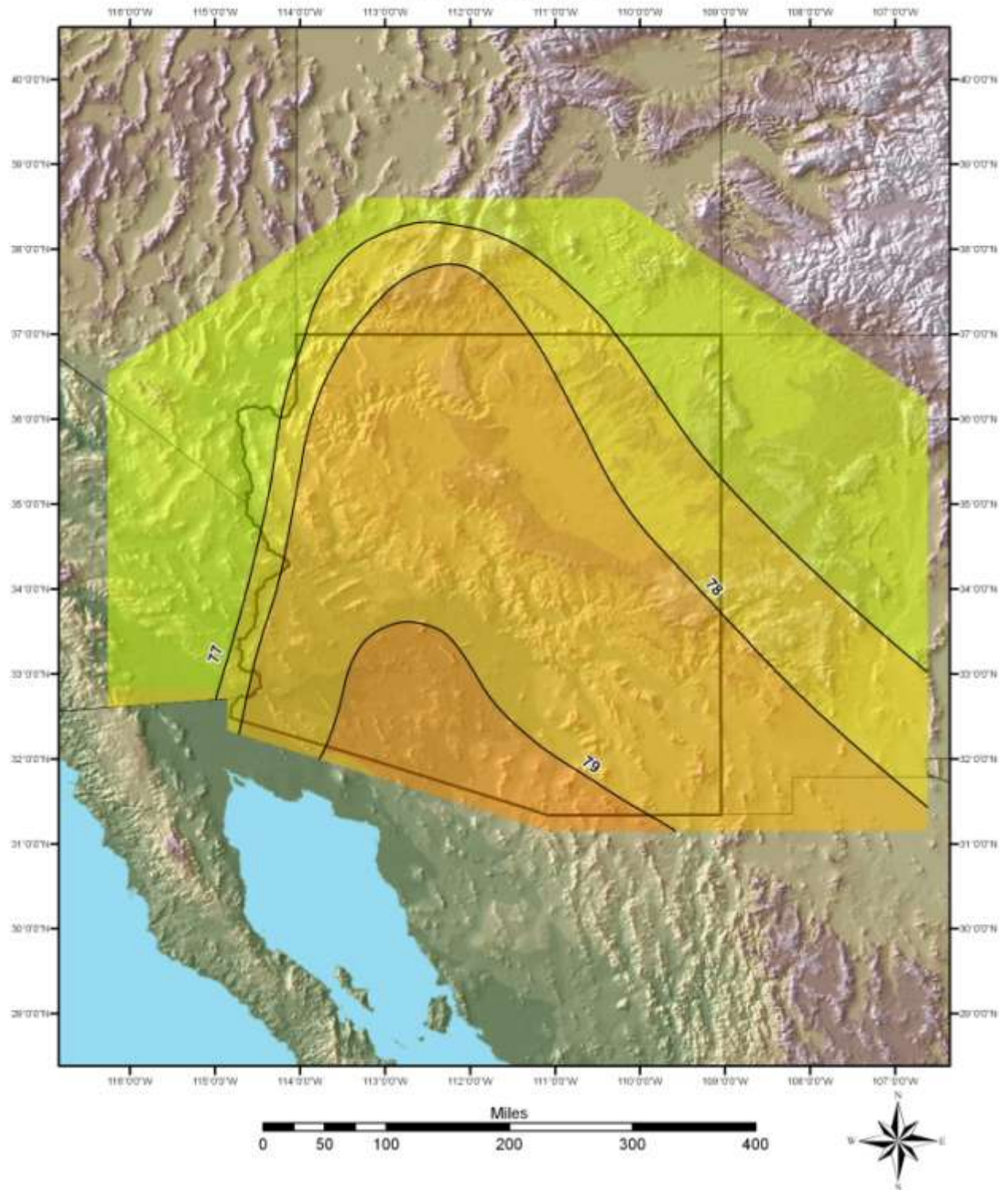
August 12-Hour 100-Year
Dew Point °F
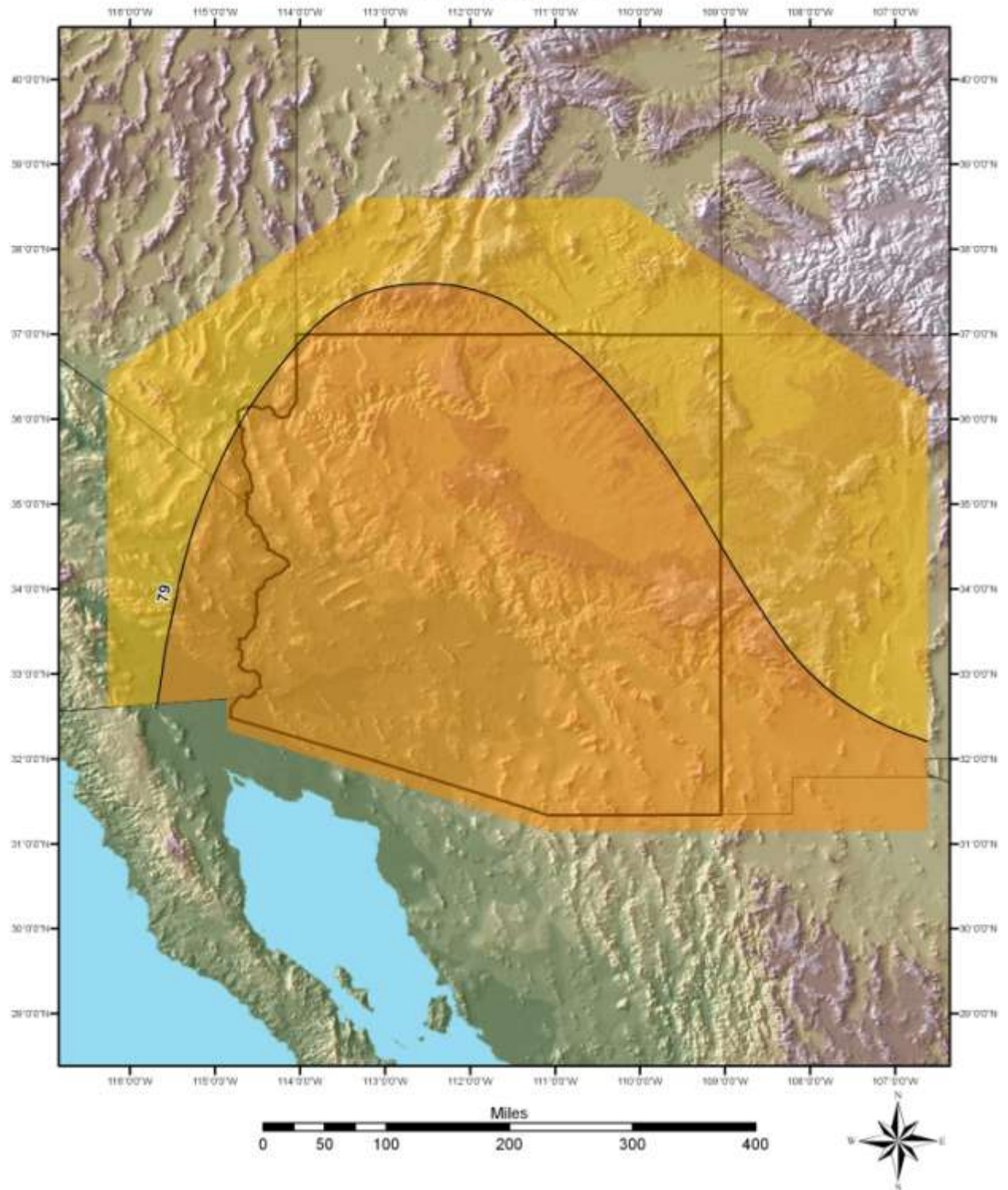
September 12-Hour 100-Year
Dew Point °F
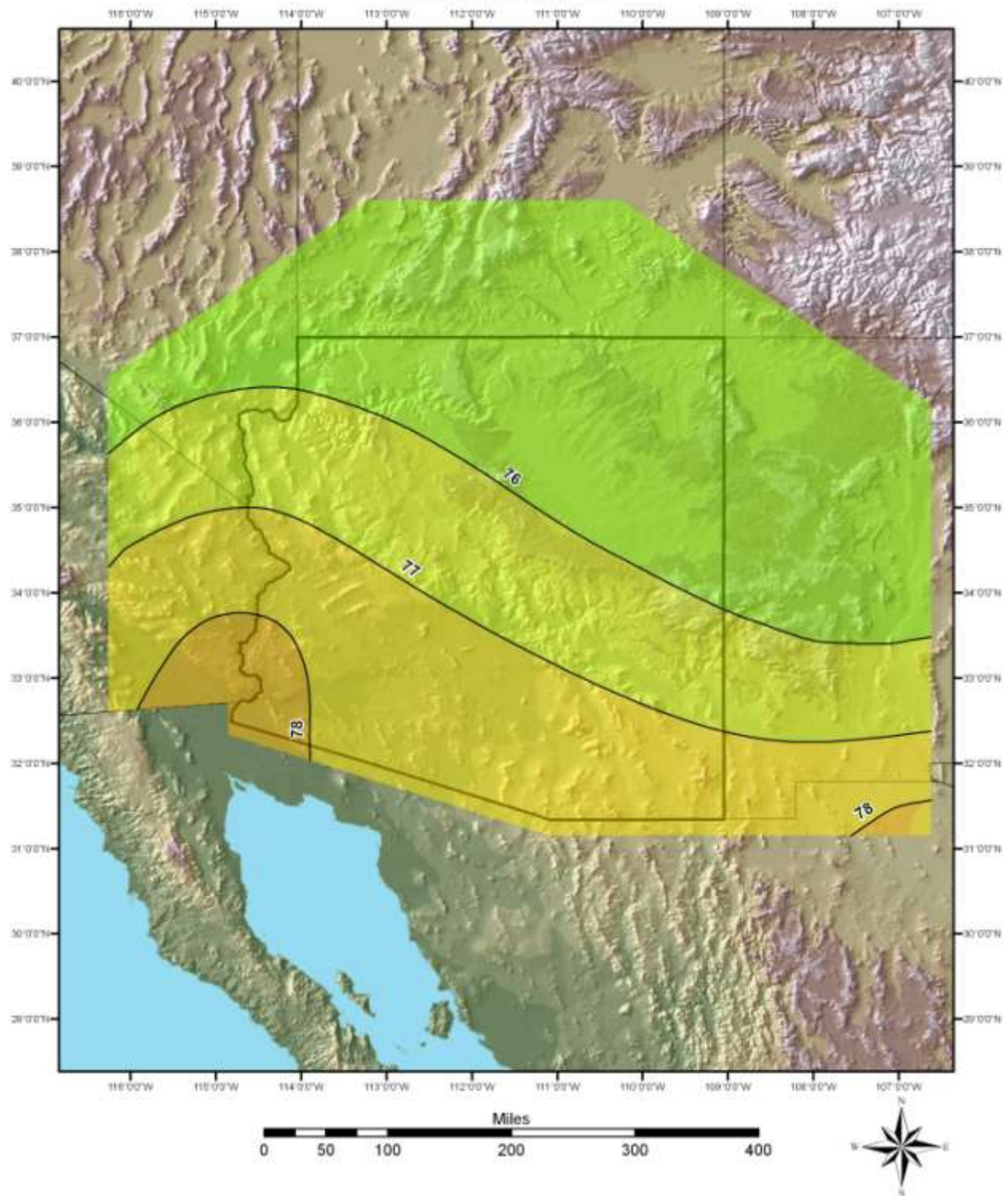
October 12-Hour 100-Year
Dew Point °F

A-23
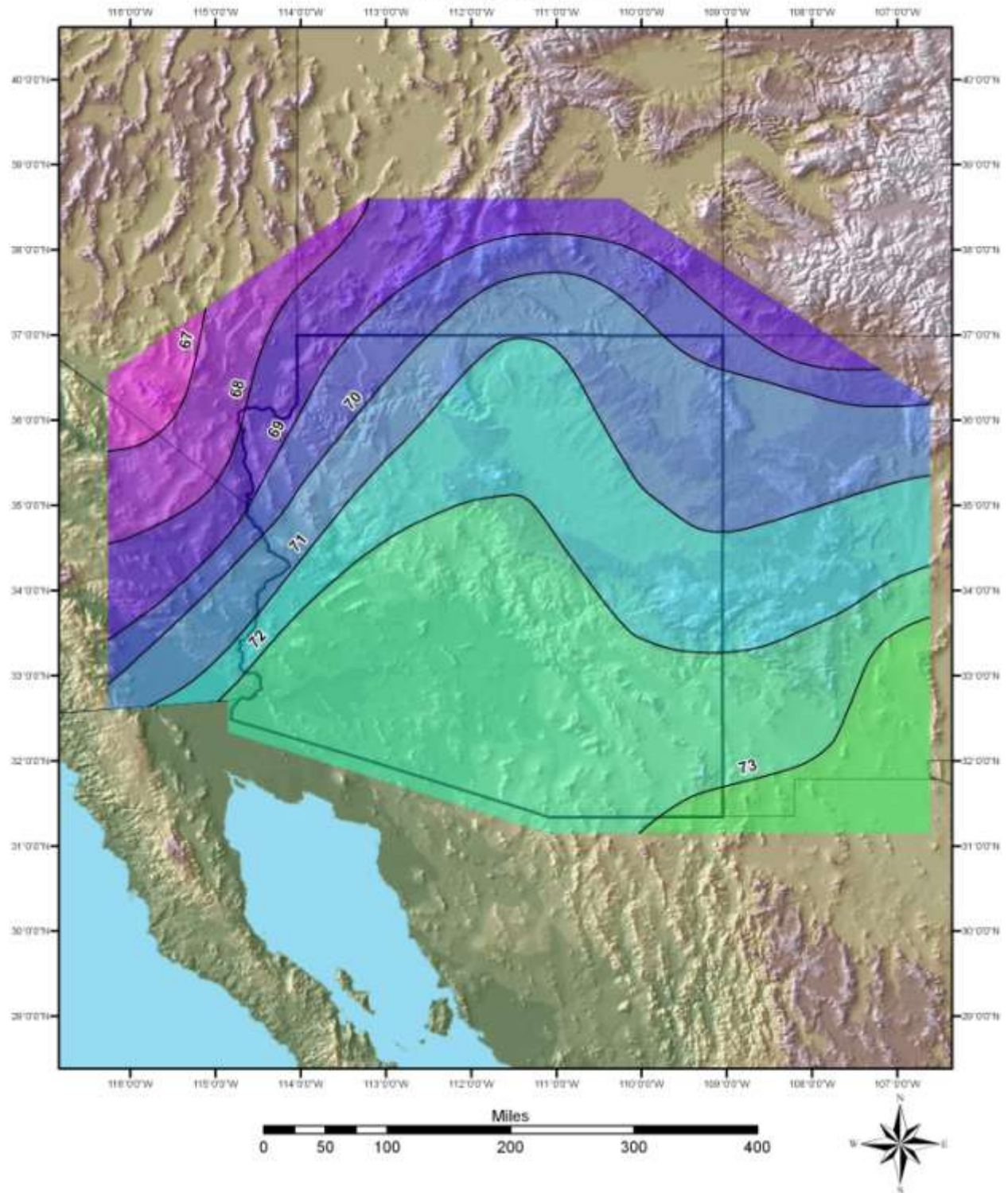
November 12-Hour 100-Year
Dew Point °F
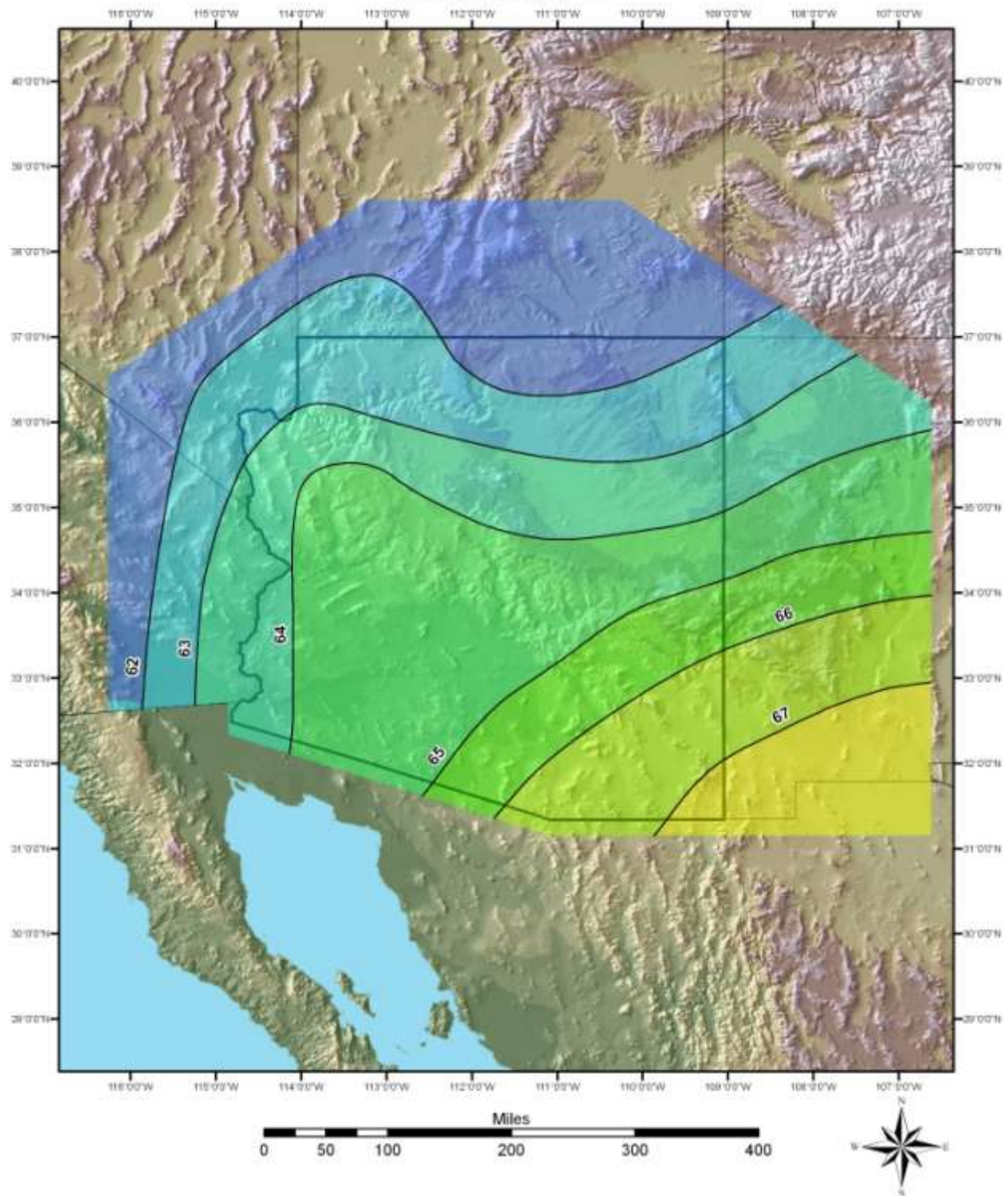
December 12-Hour 100-Year Dew Point °F
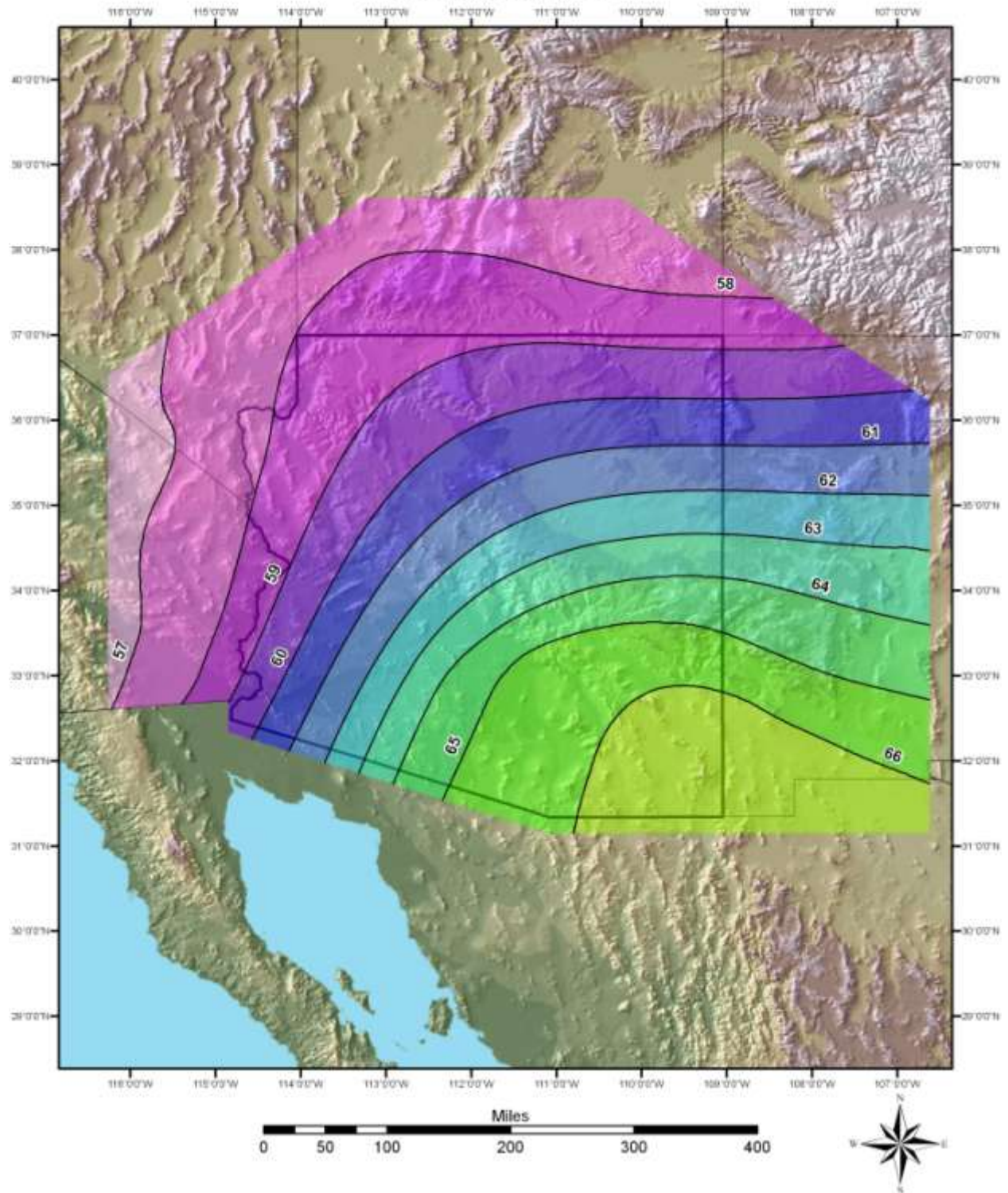
January 24-Hour 100-Year
Dew Point °F
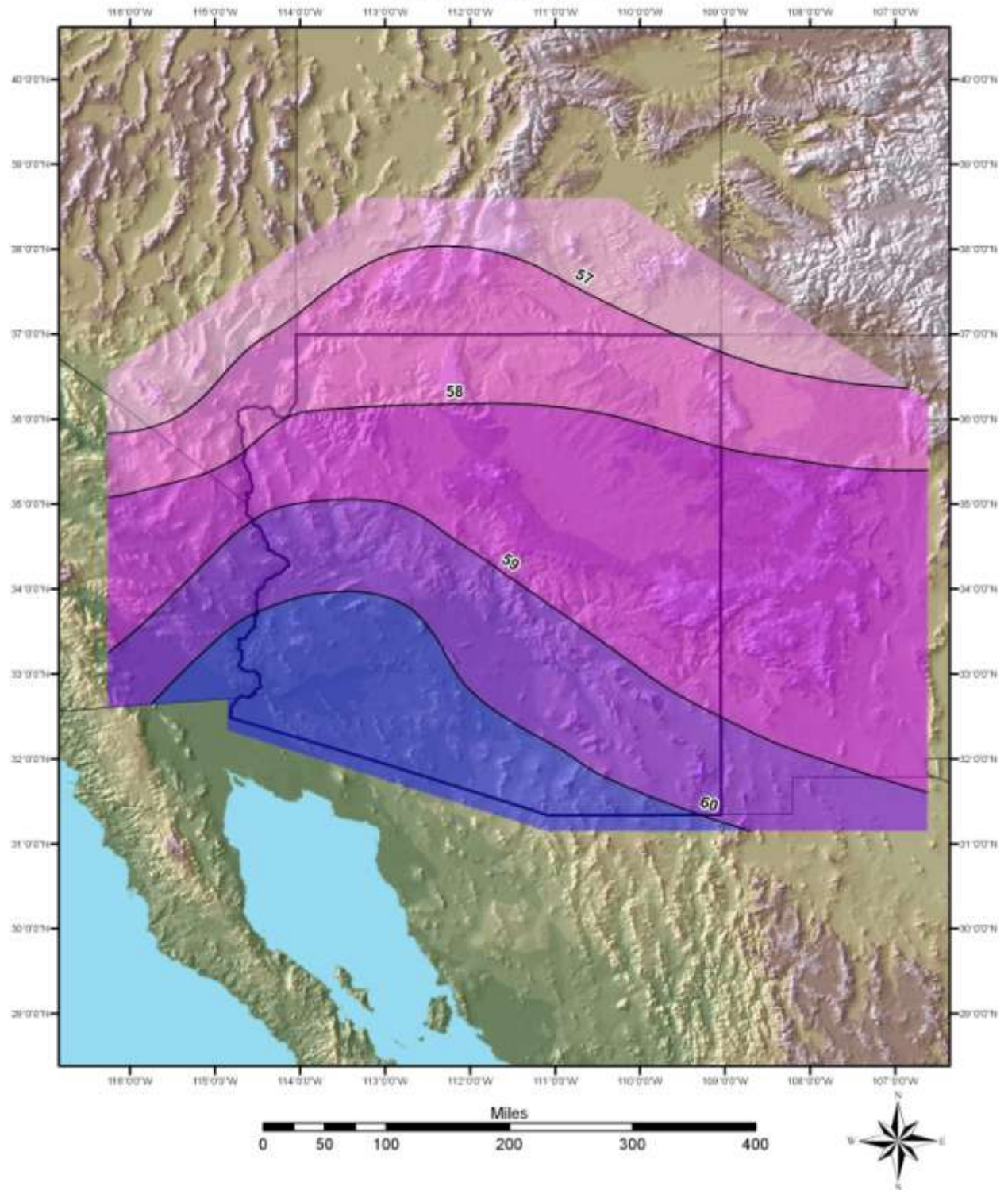
February 24-Hour 100-Year
Dew Point °F

A-27
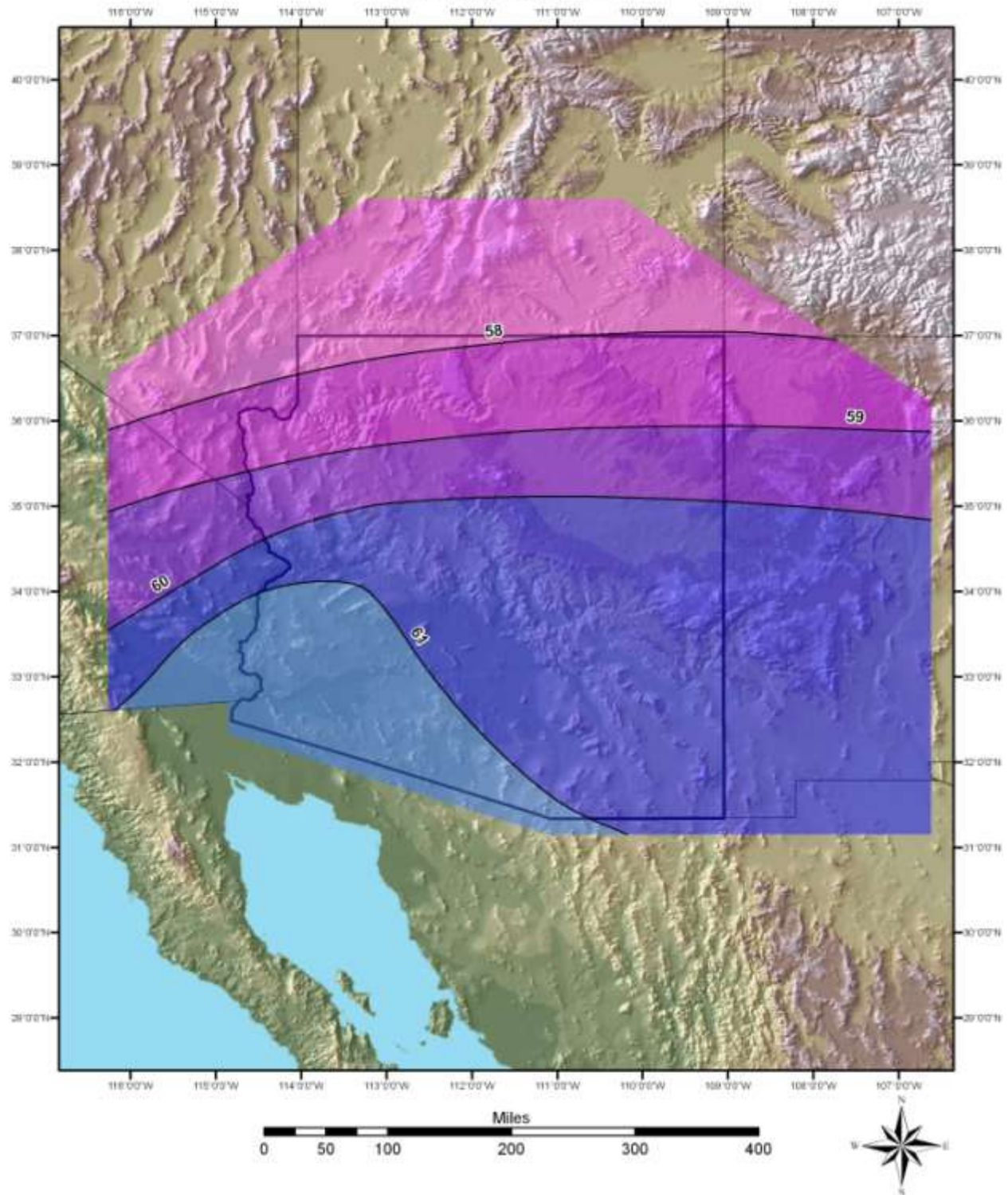
March 24-Hour 100-Year
Dew Point °F

A-28
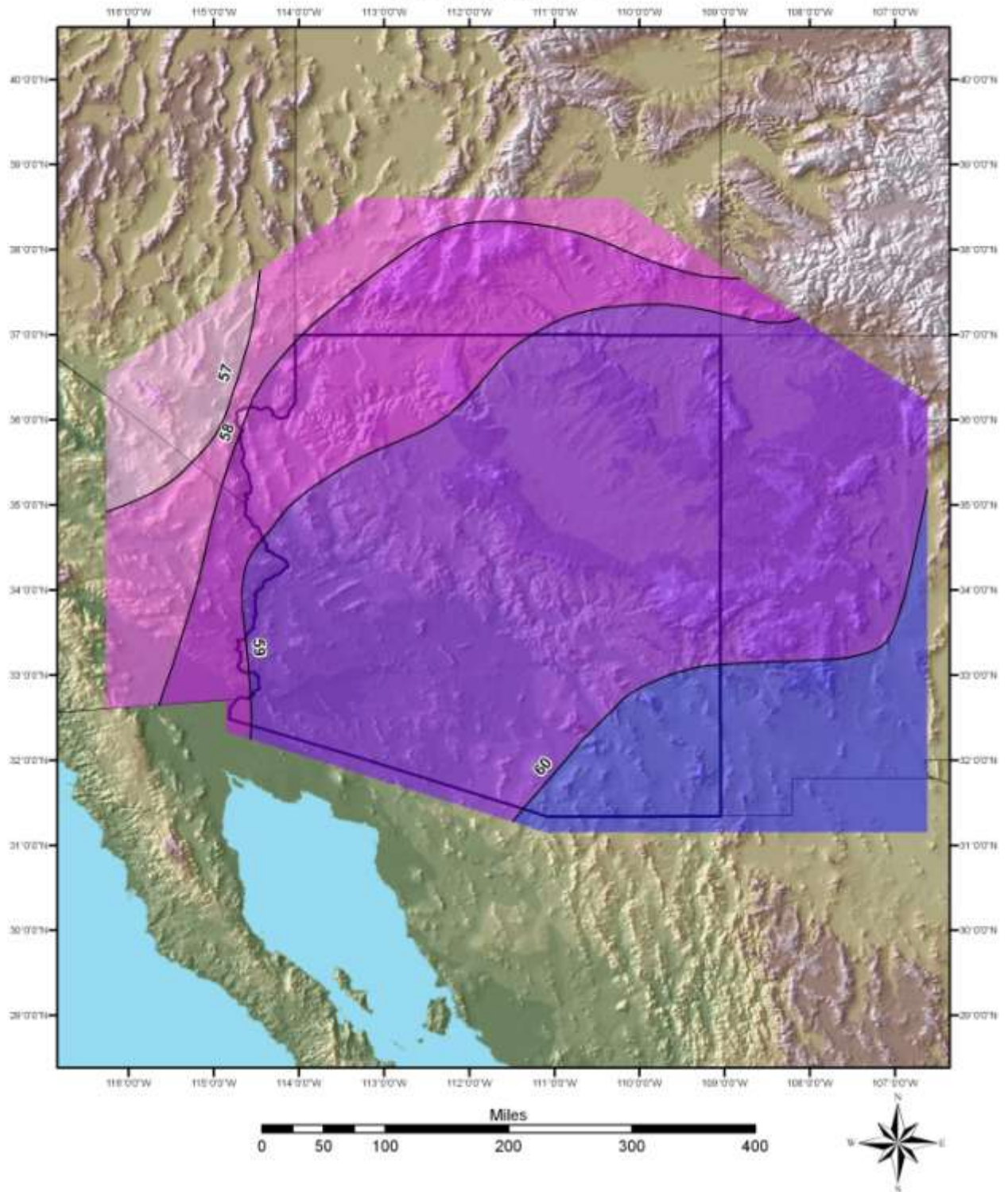
April 24-Hour 100-Year
Dew Point °F
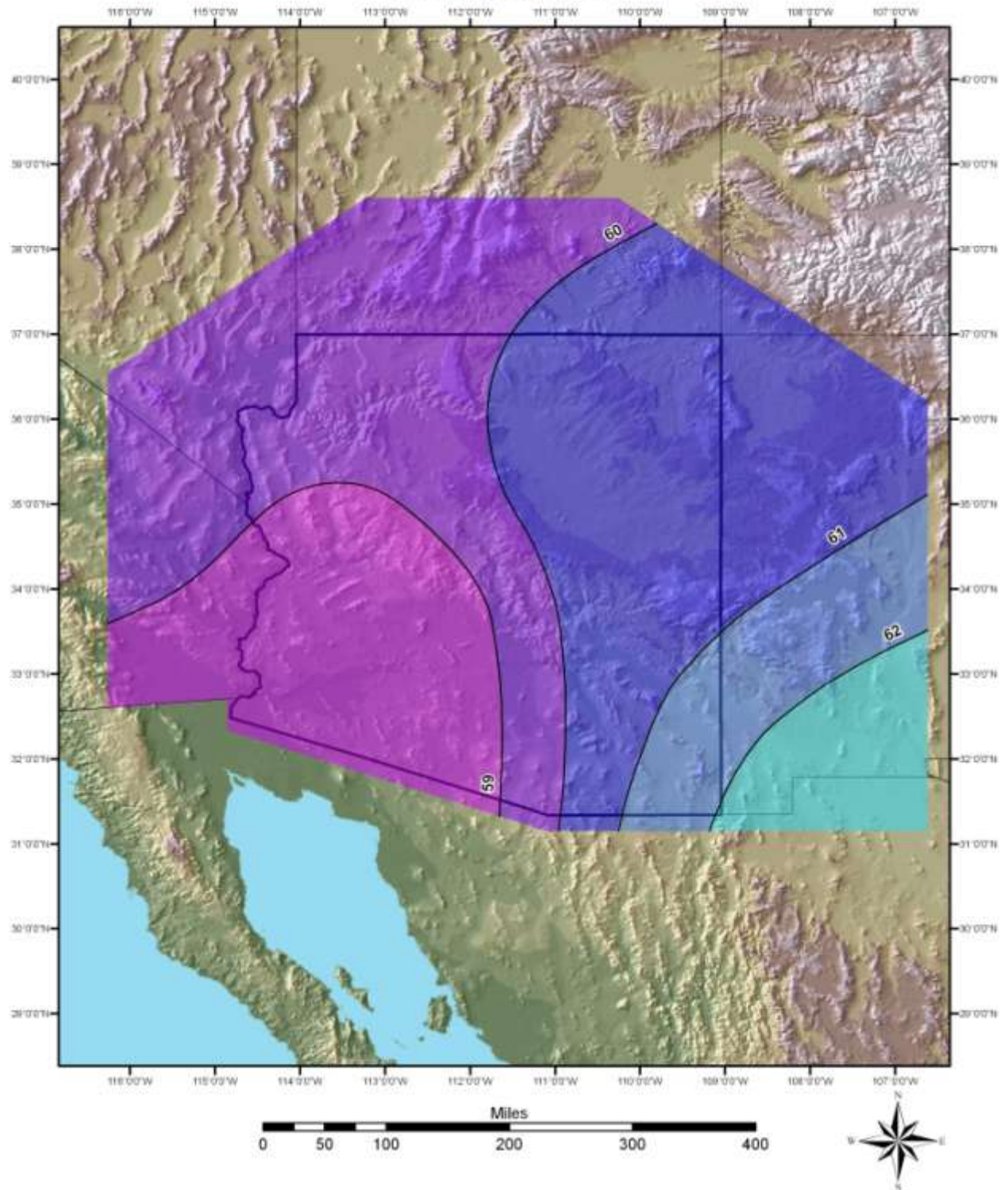
May 24-Hour 100-Year
Dew Point °F

A-30
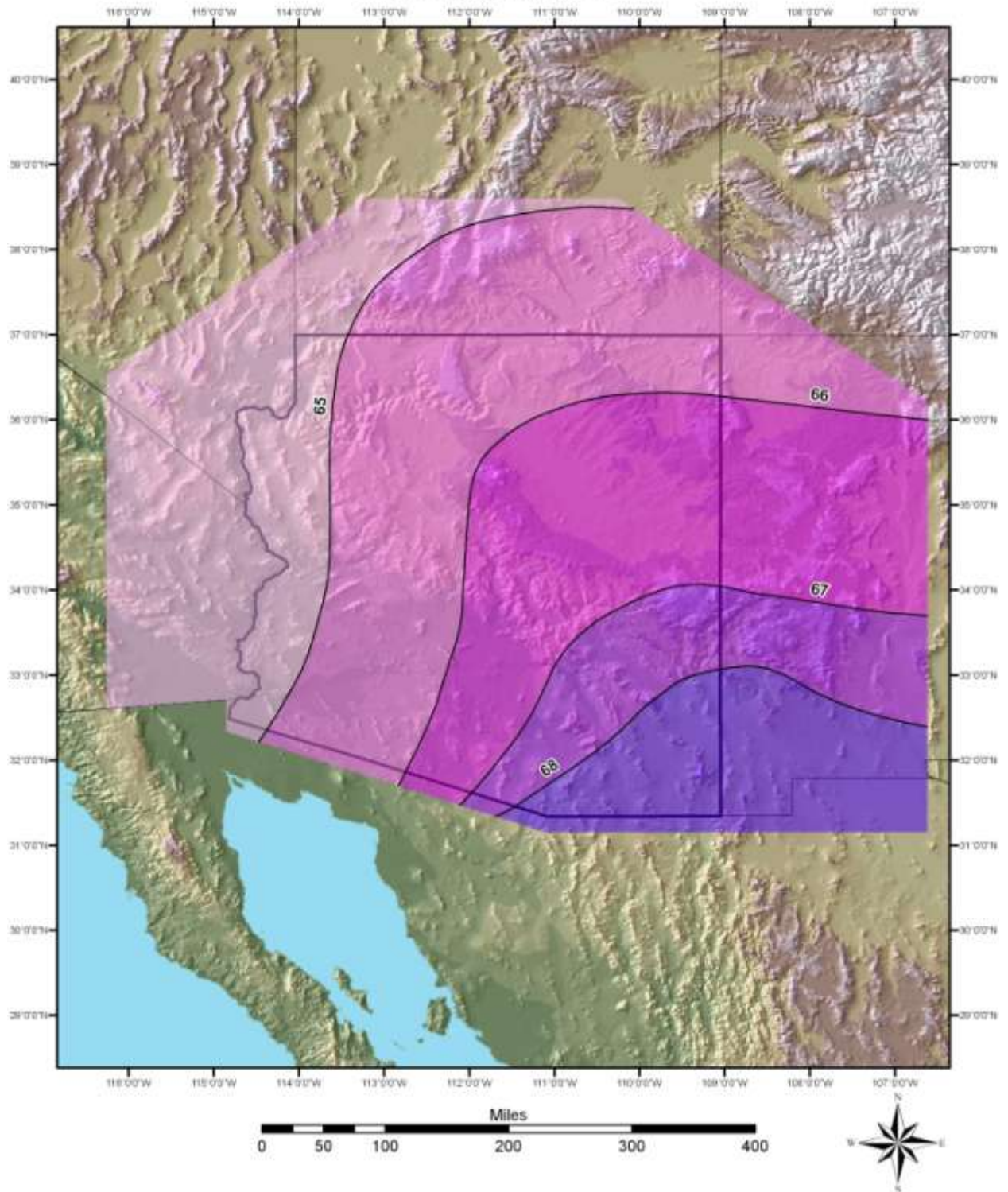
June 24-Hour 100-Year
Dew Point °F

A-31
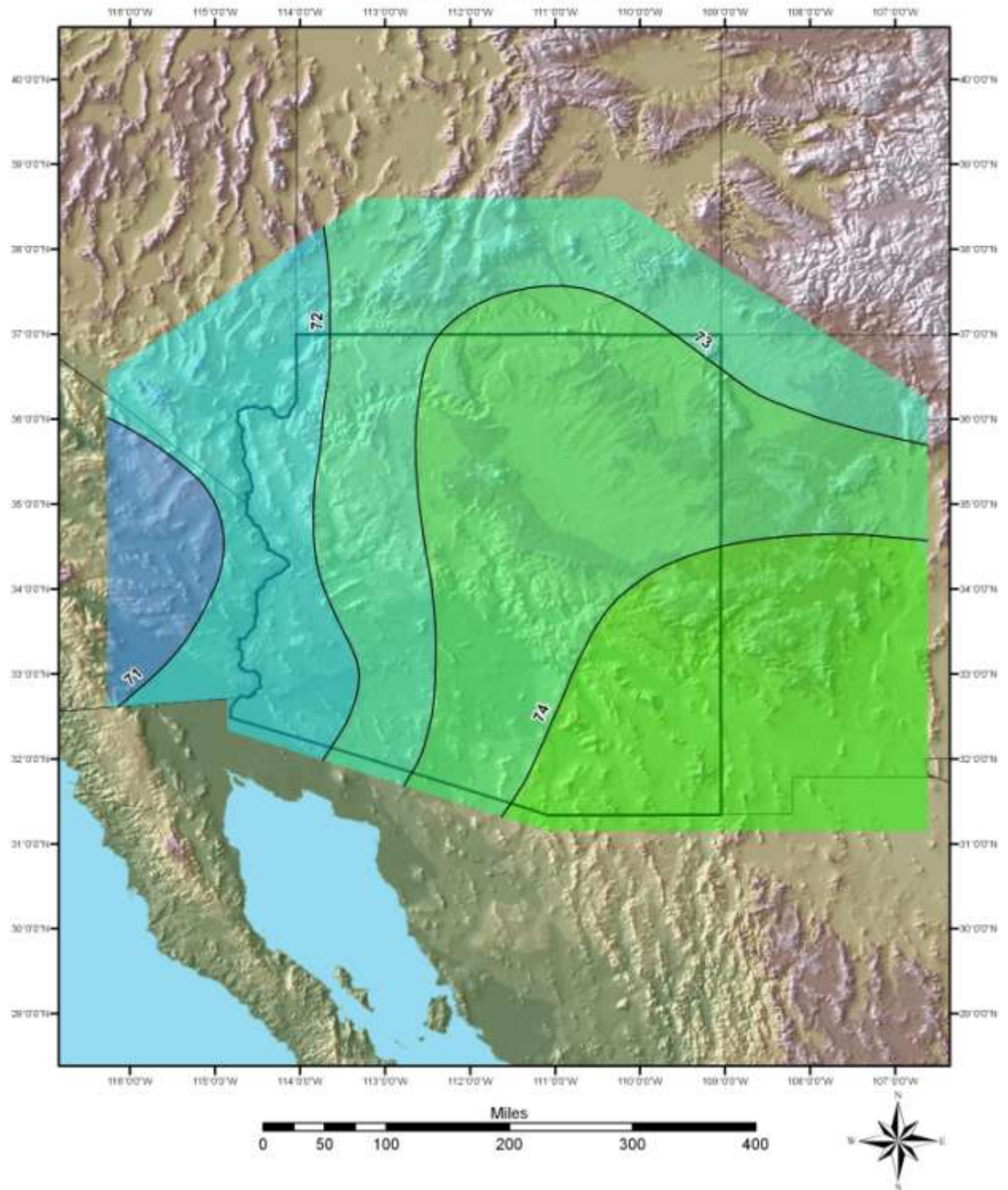
July 24-Hour 100-Year
Dew Point °F

A-32
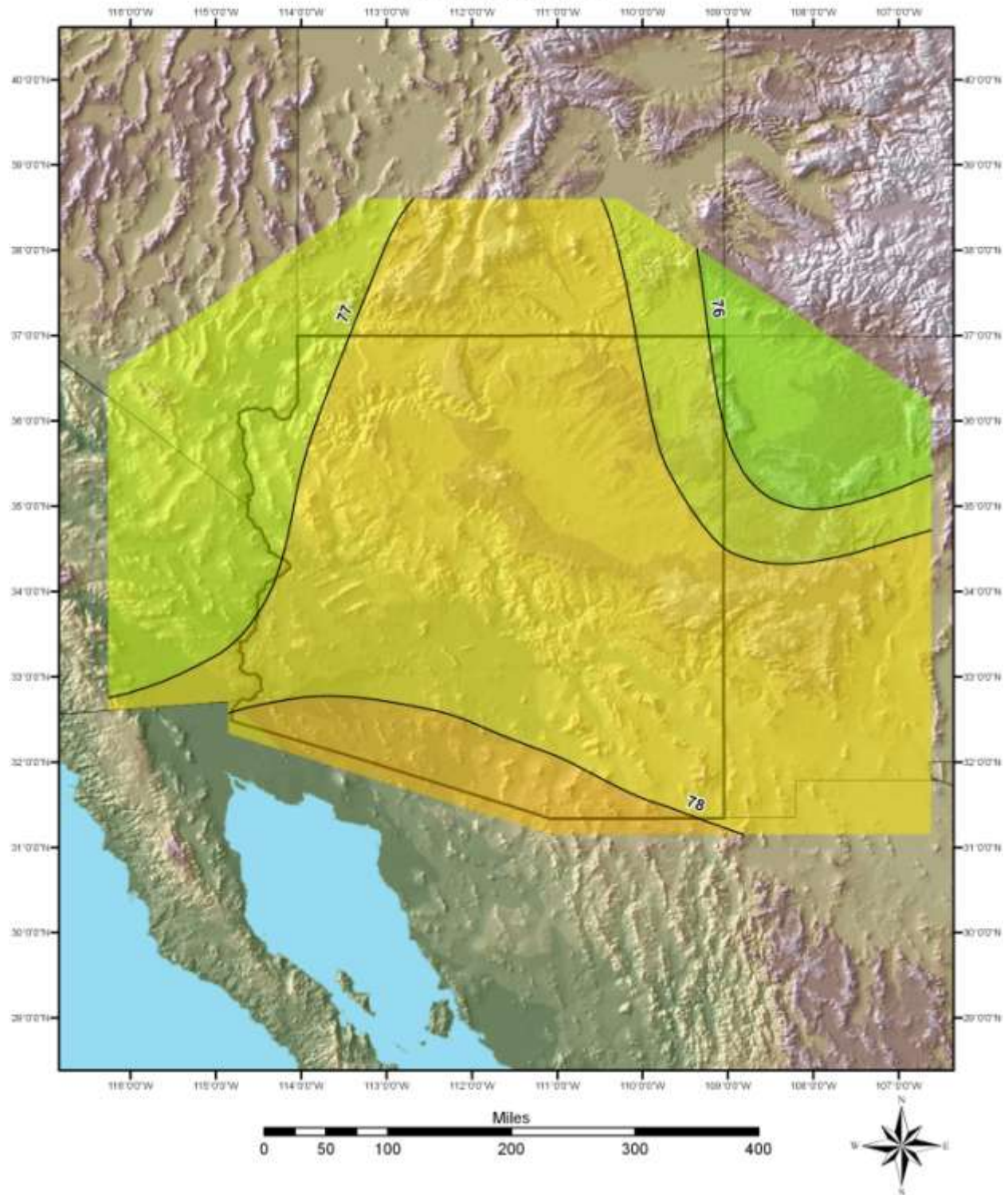
August 24-Hour 100-Year
Dew Point °F

Miles

0   50   100   200   300   400
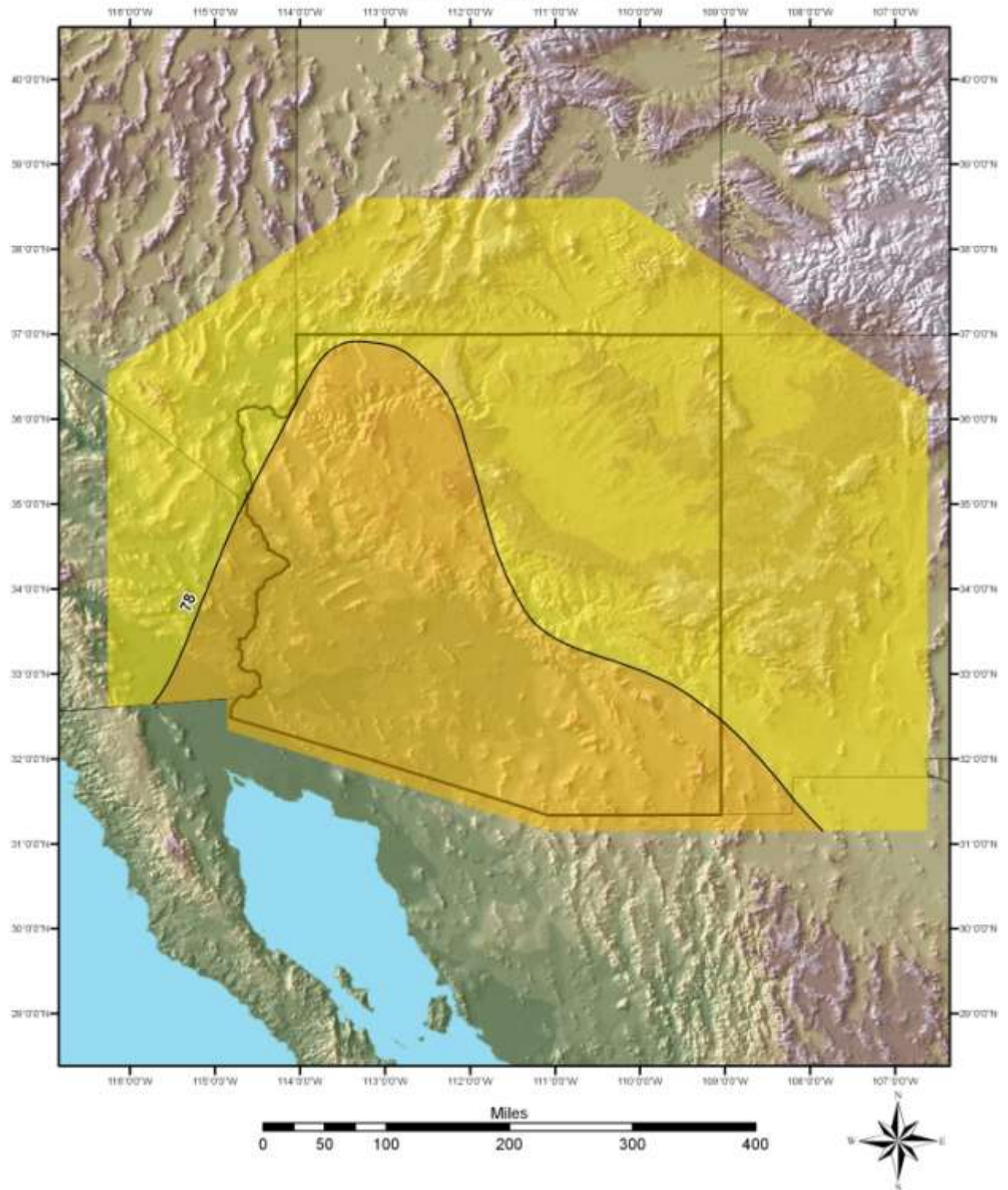
September 24-Hour 100-Year
Dew Point °F
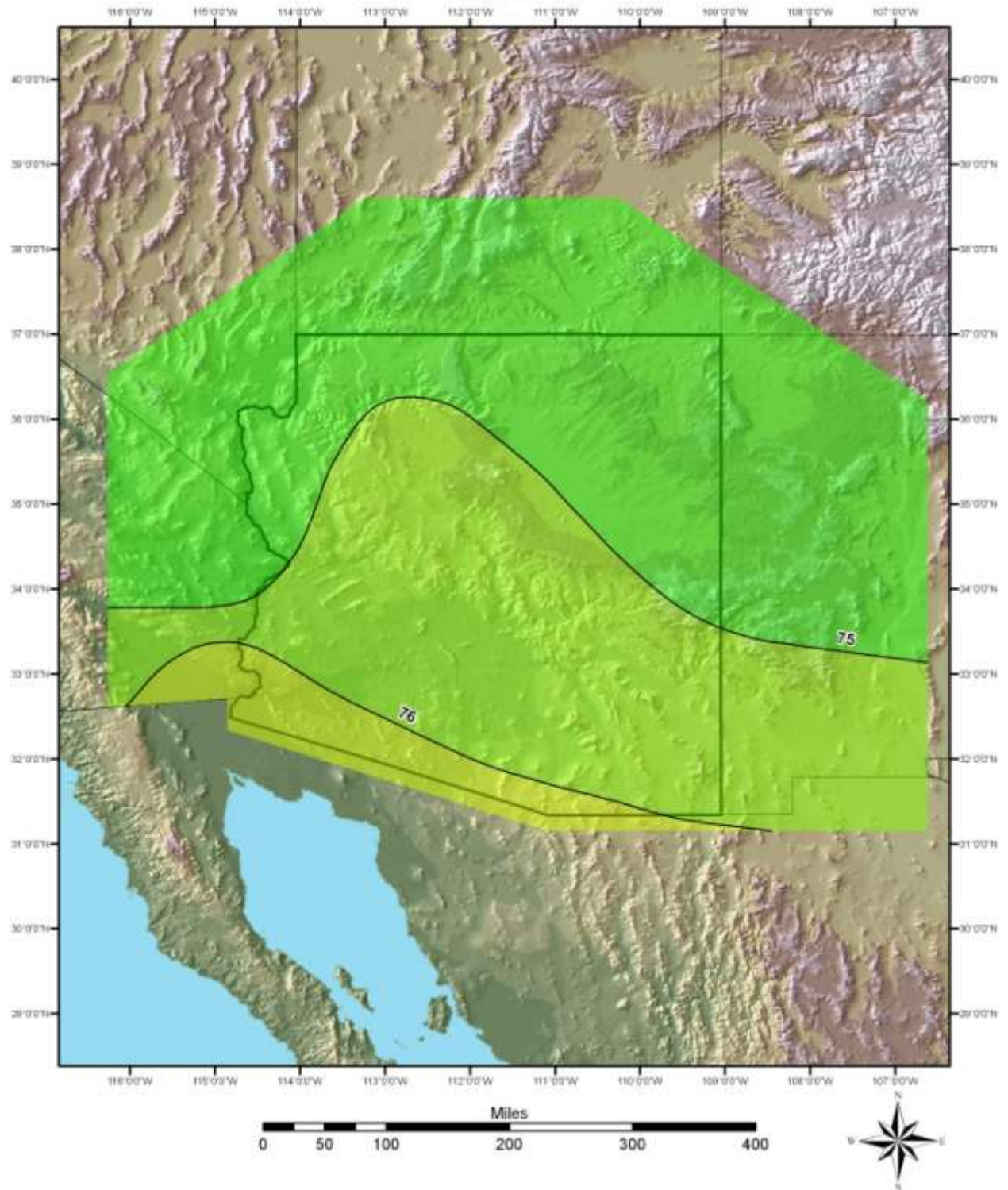
October 24-Hour 100-Year
Dew Point °F
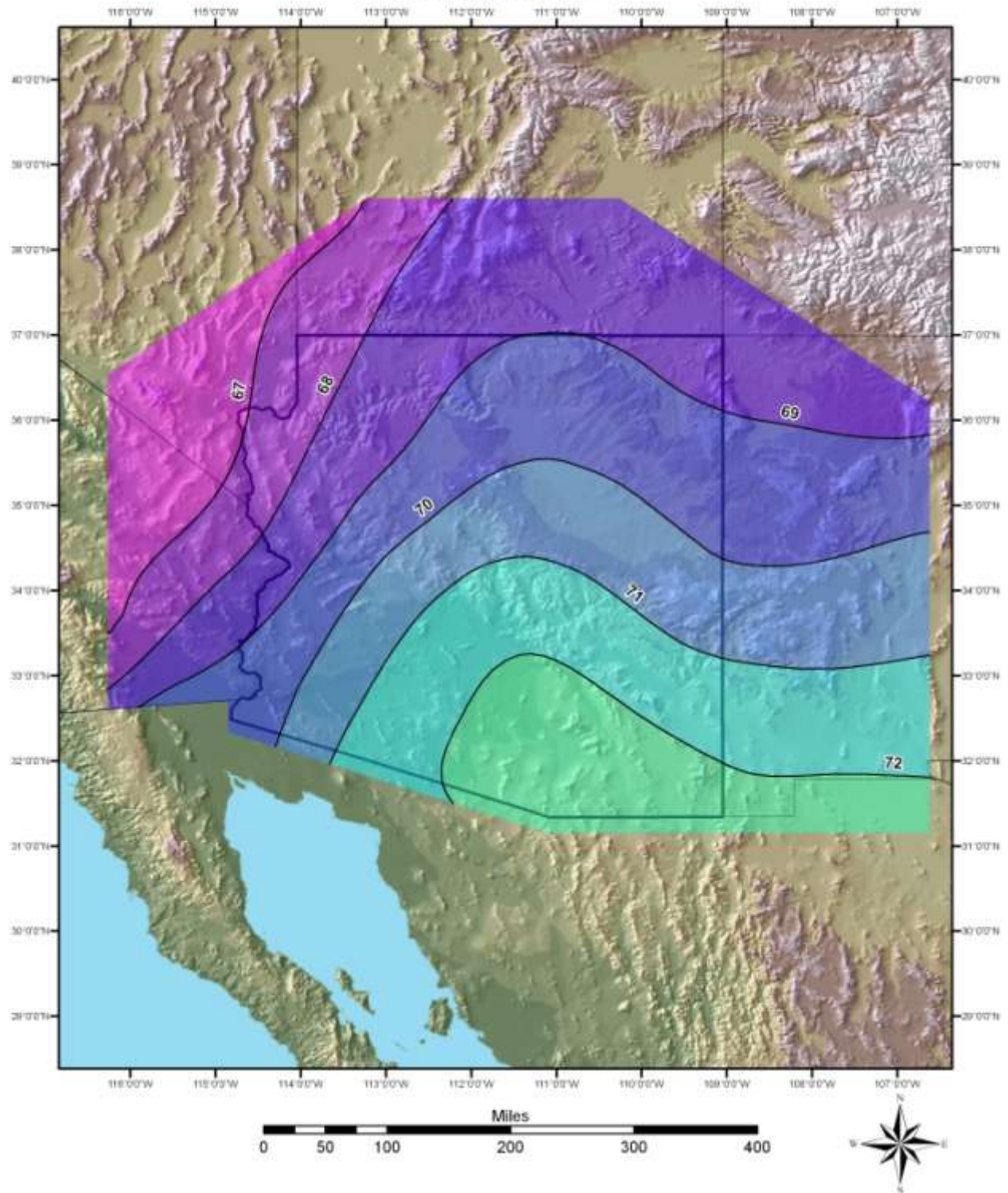
November 24-Hour 100-Year
Dew Point °F
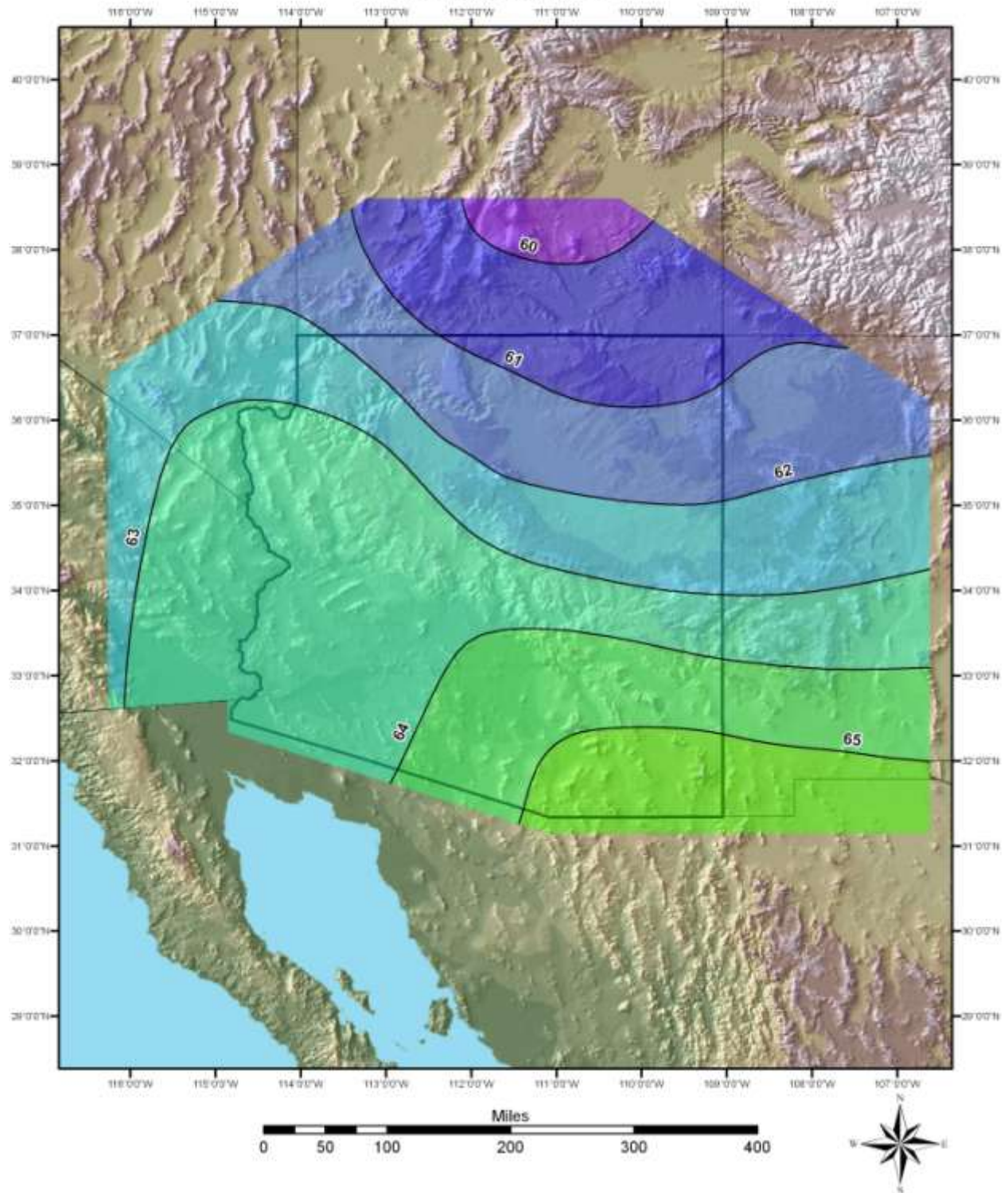
December 24-Hour 100-Year
Dew Point °F

January 2 Sigma SST °F
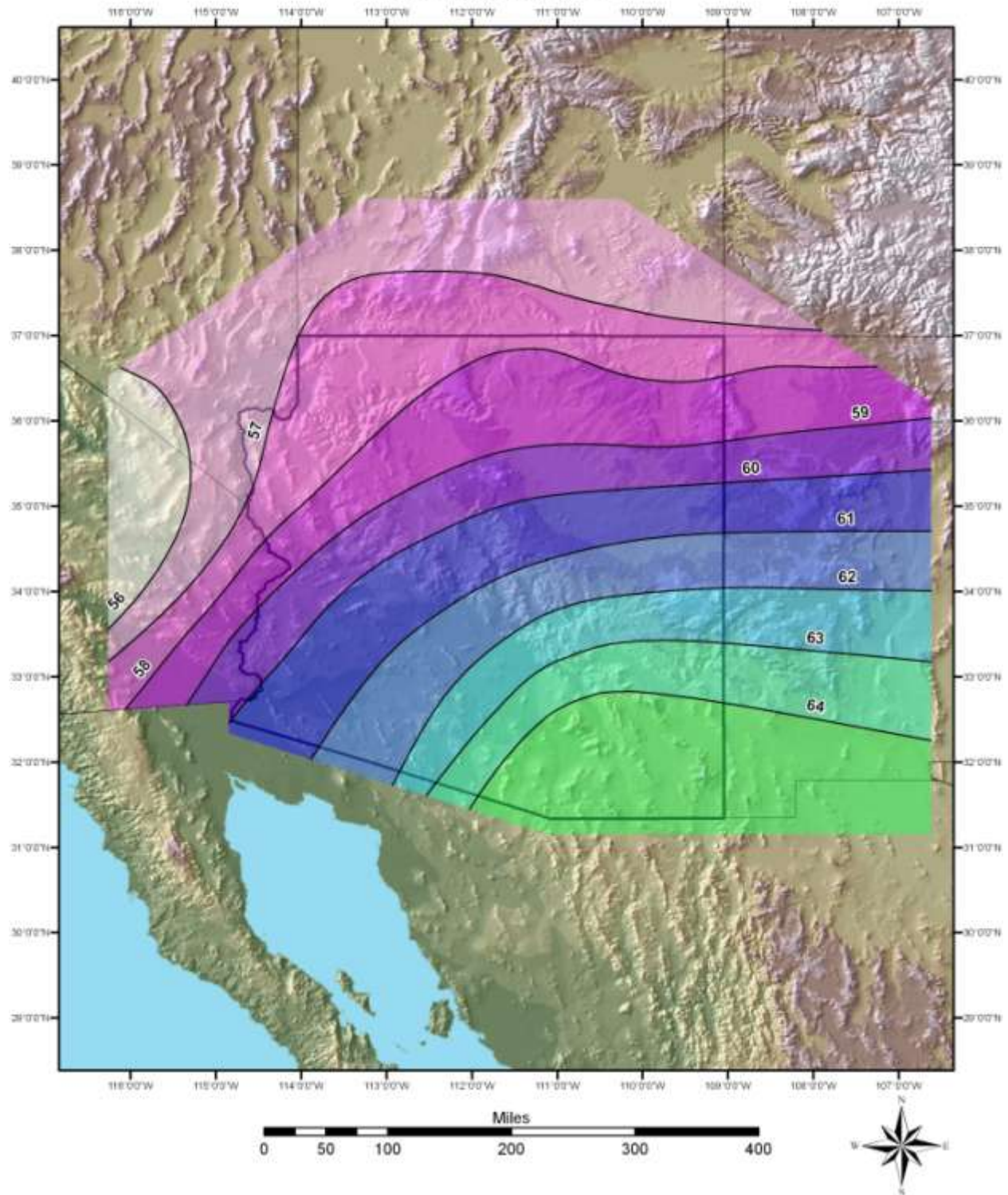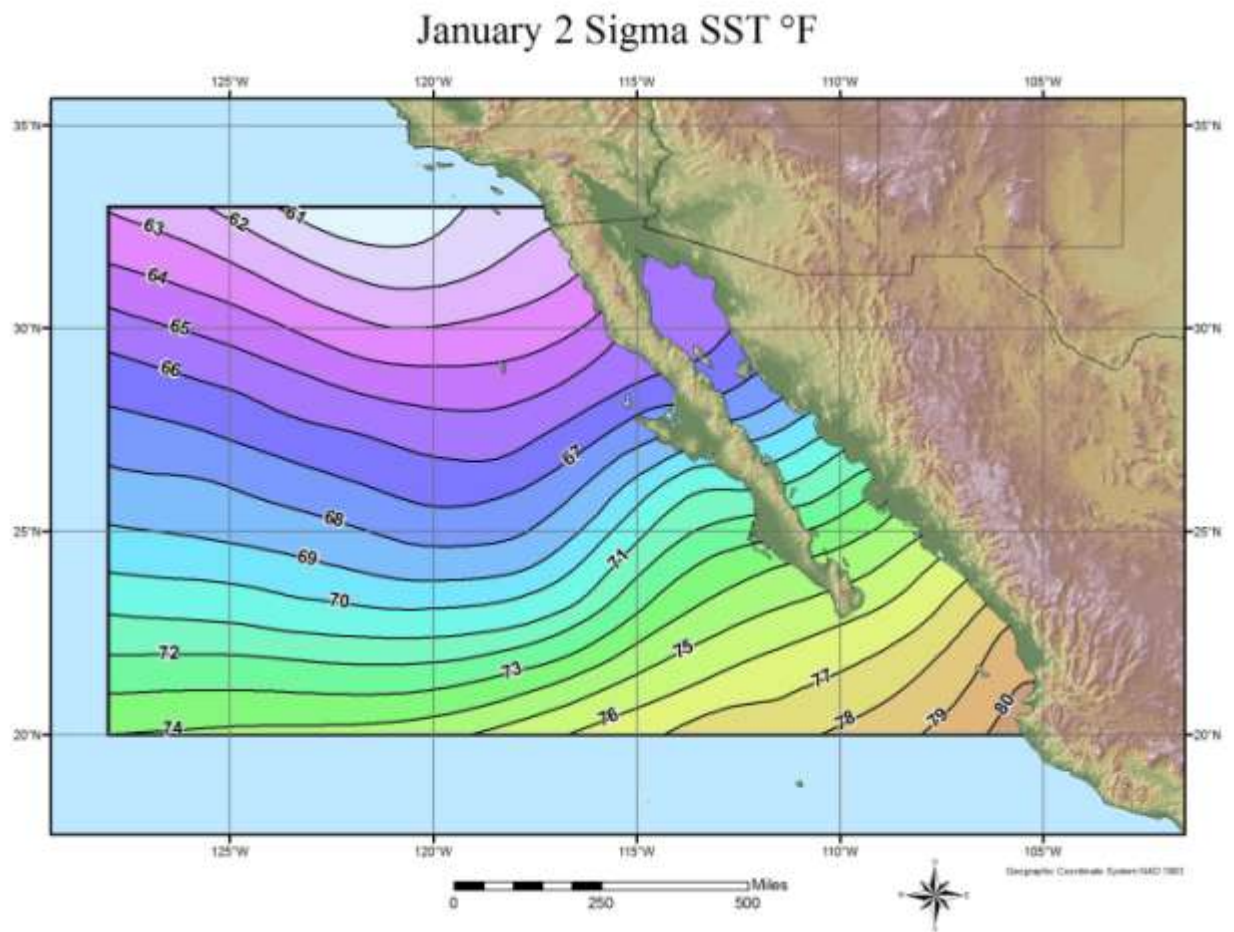
February 2 Sigma SST °F

A-39
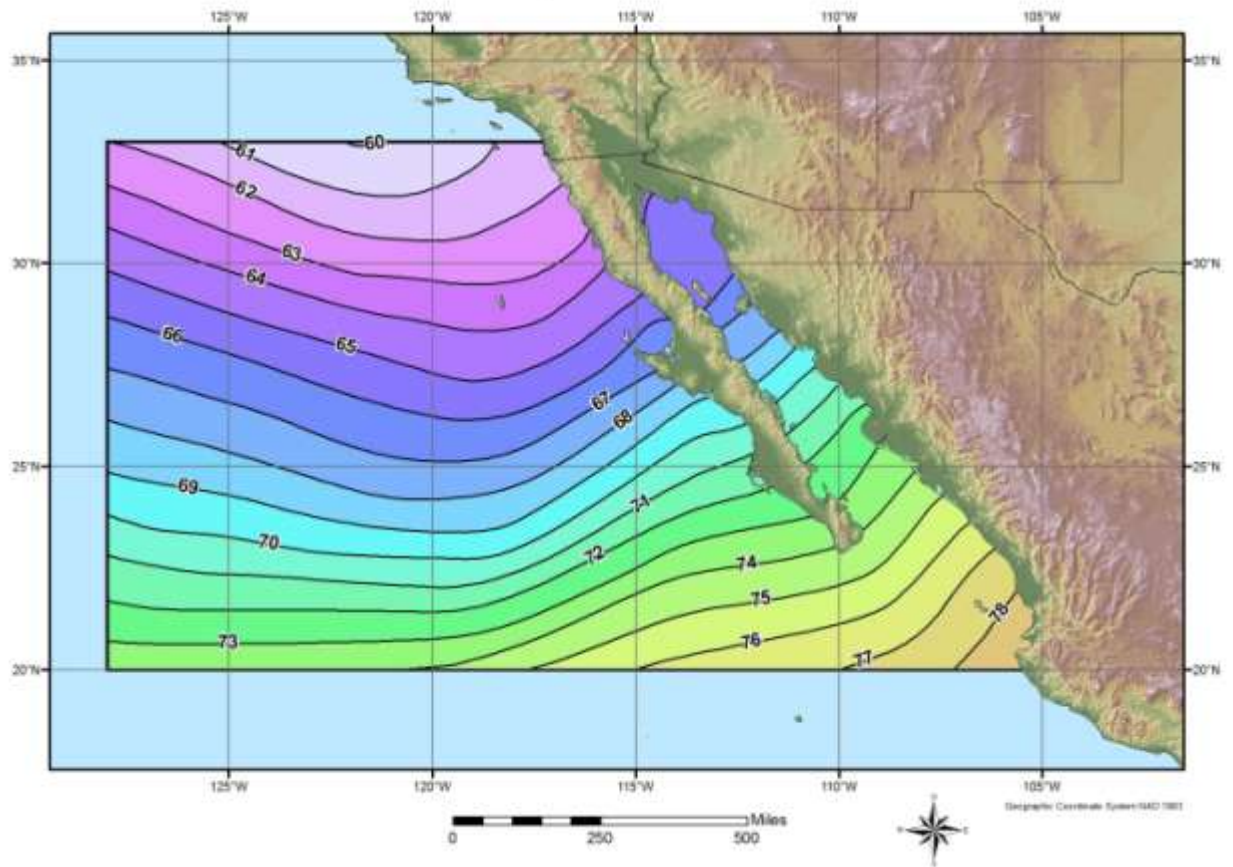
March 2 Sigma SST °F
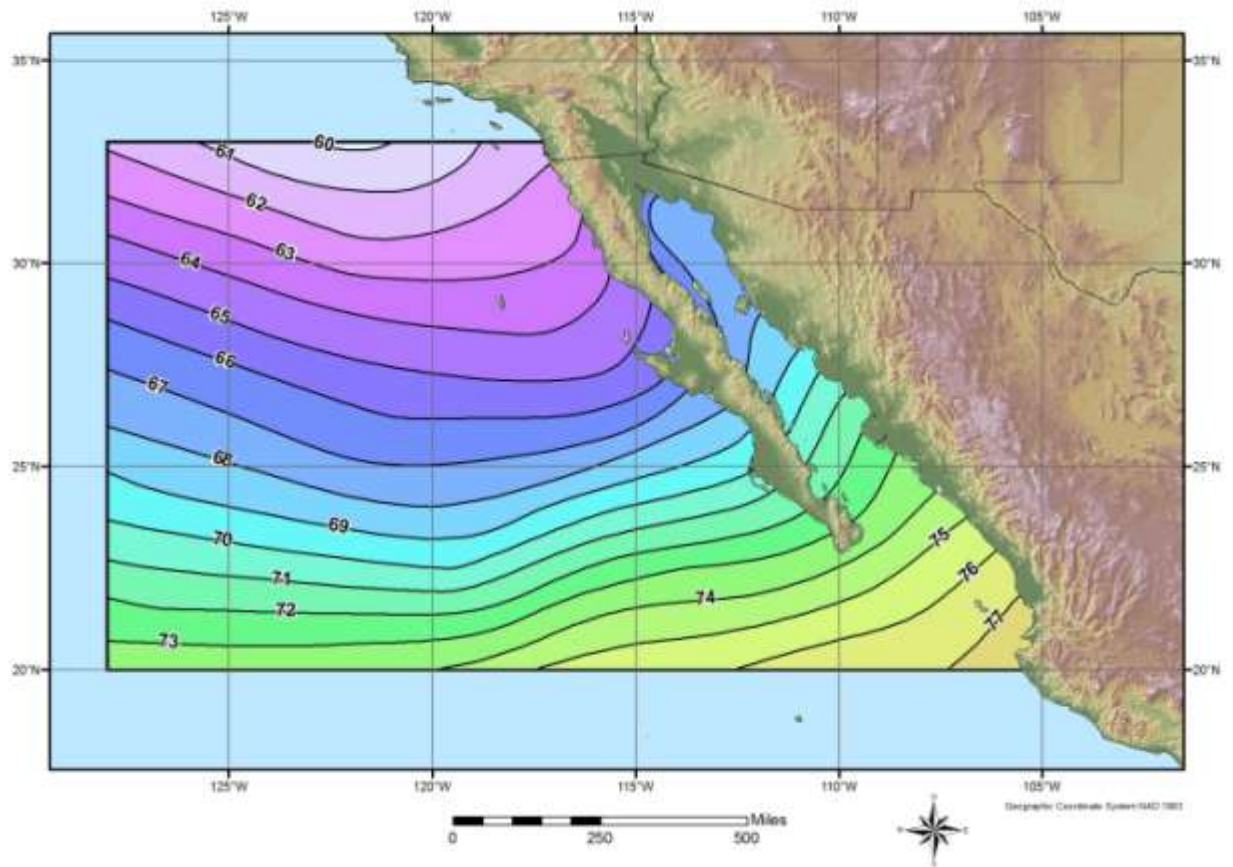
April 2 Sigma SST °F
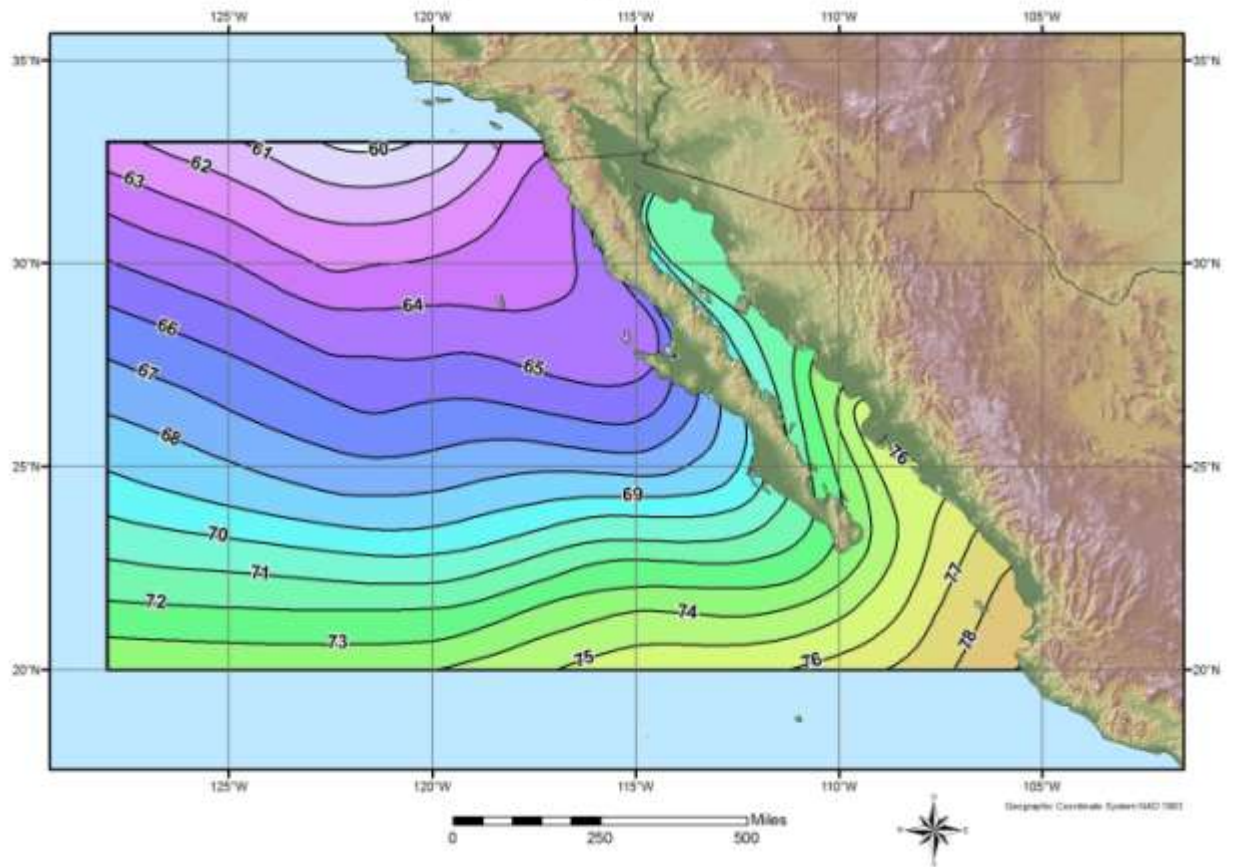
May 2 Sigma SST °F
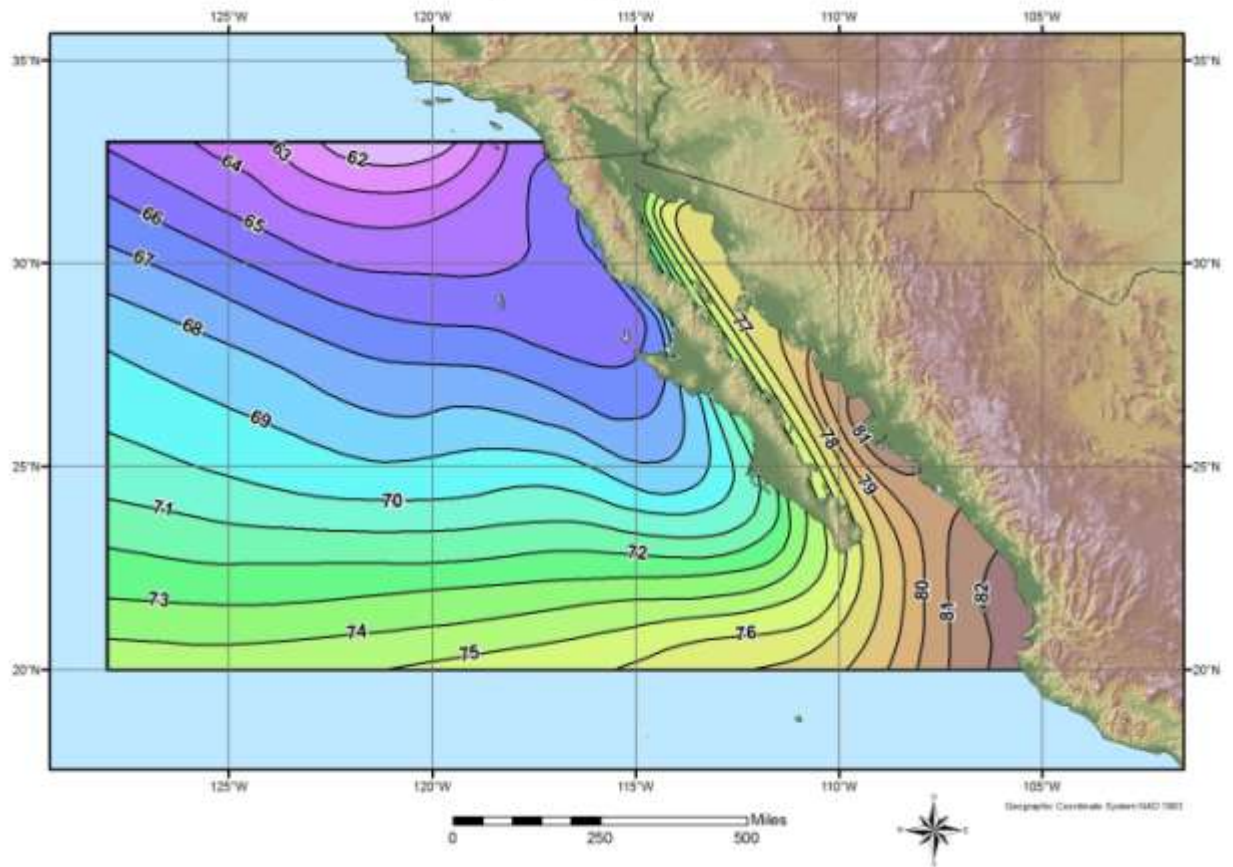
June 2 Sigma SST °F
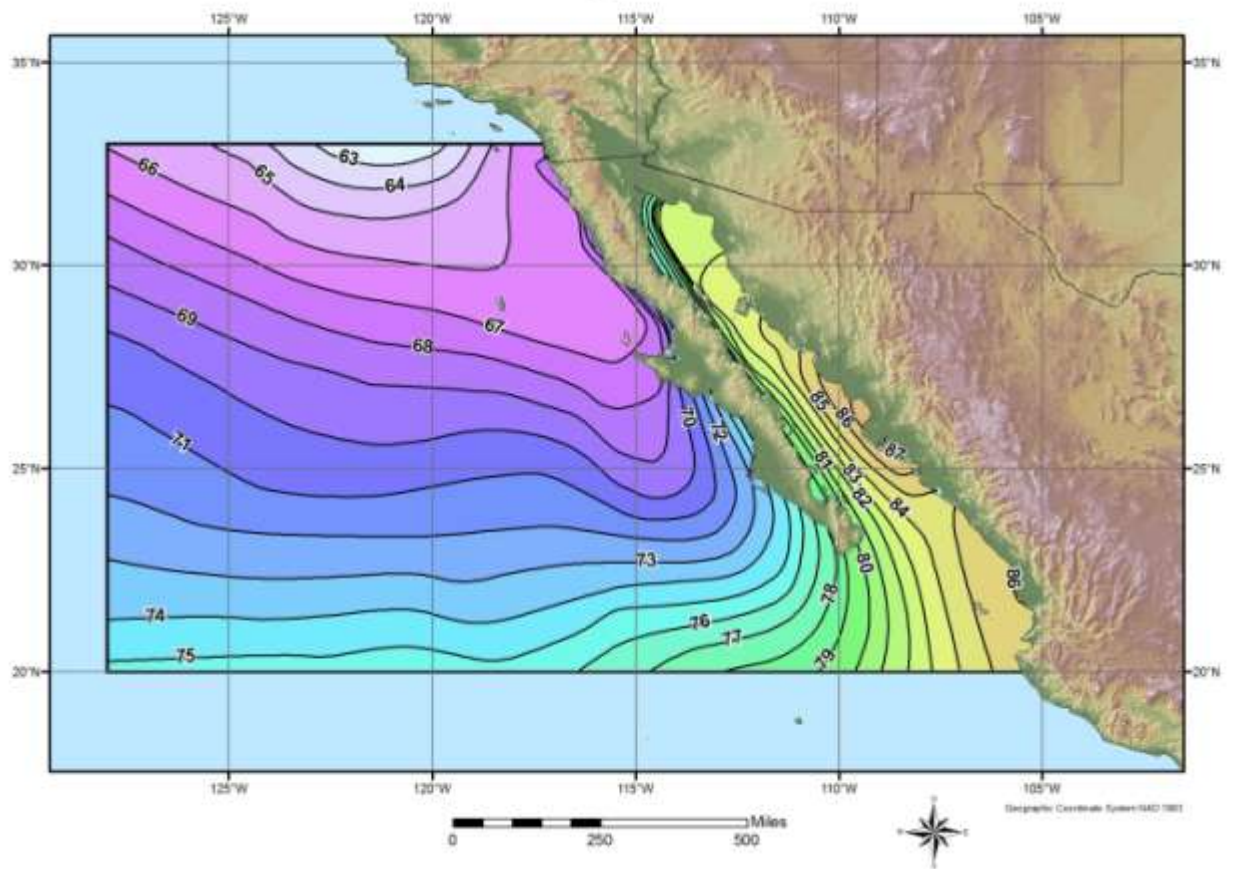
July 2 Sigma SST °F
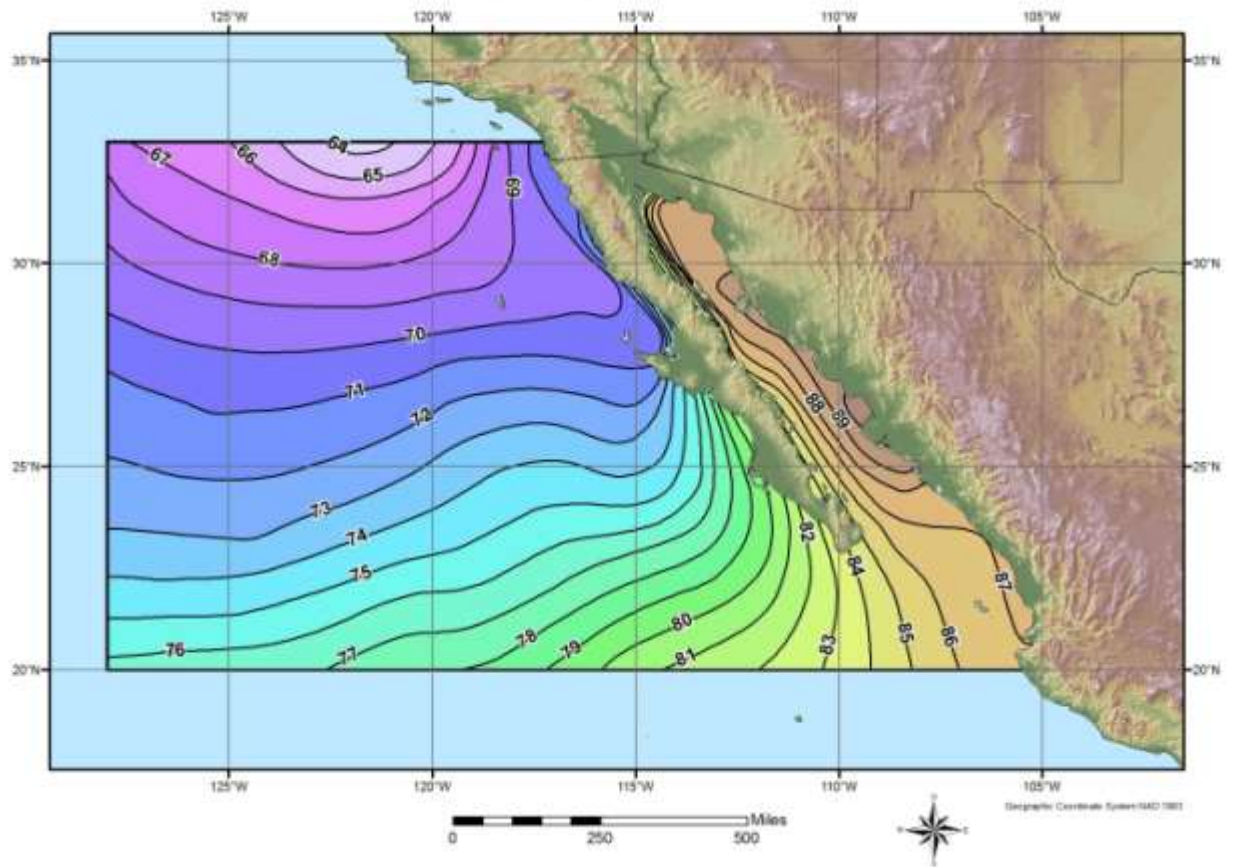
August 2 Sigma SST °F
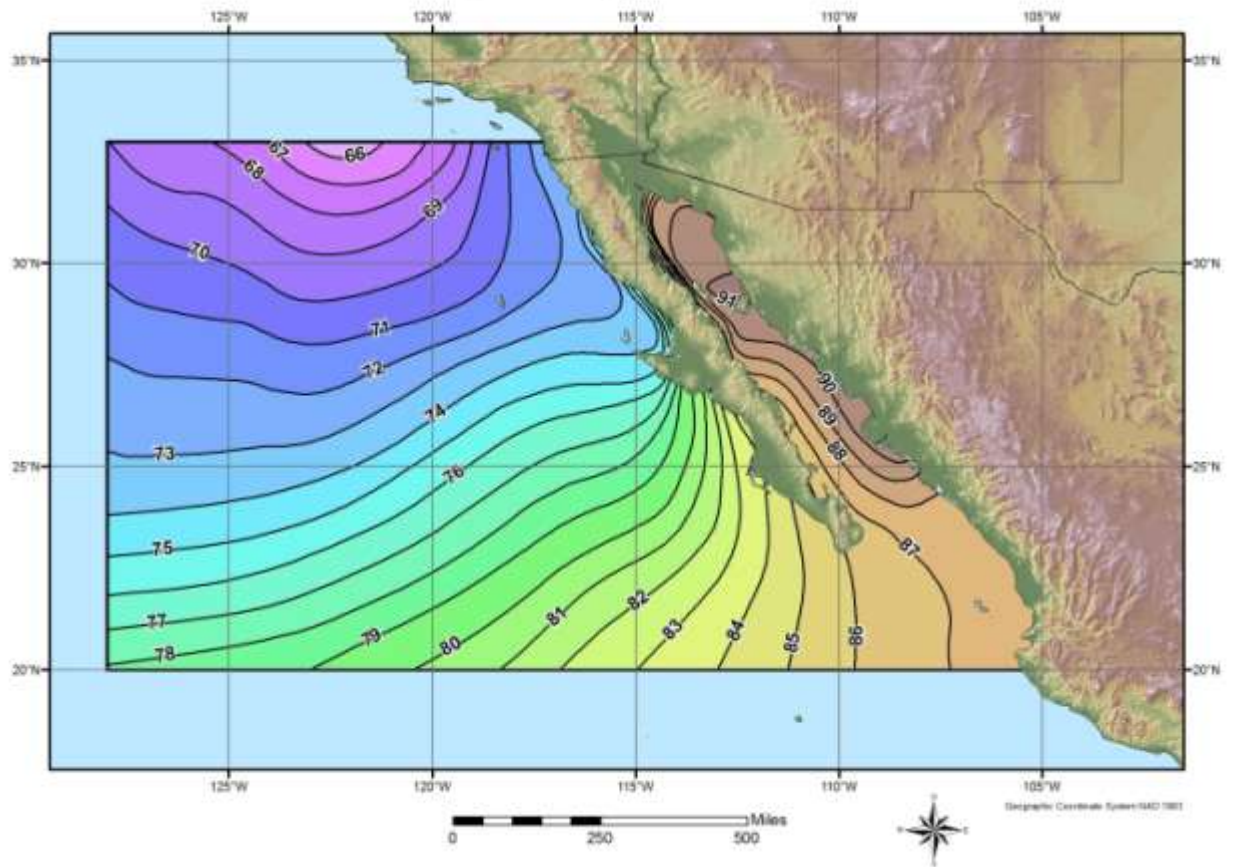
September 2 Sigma SST °F
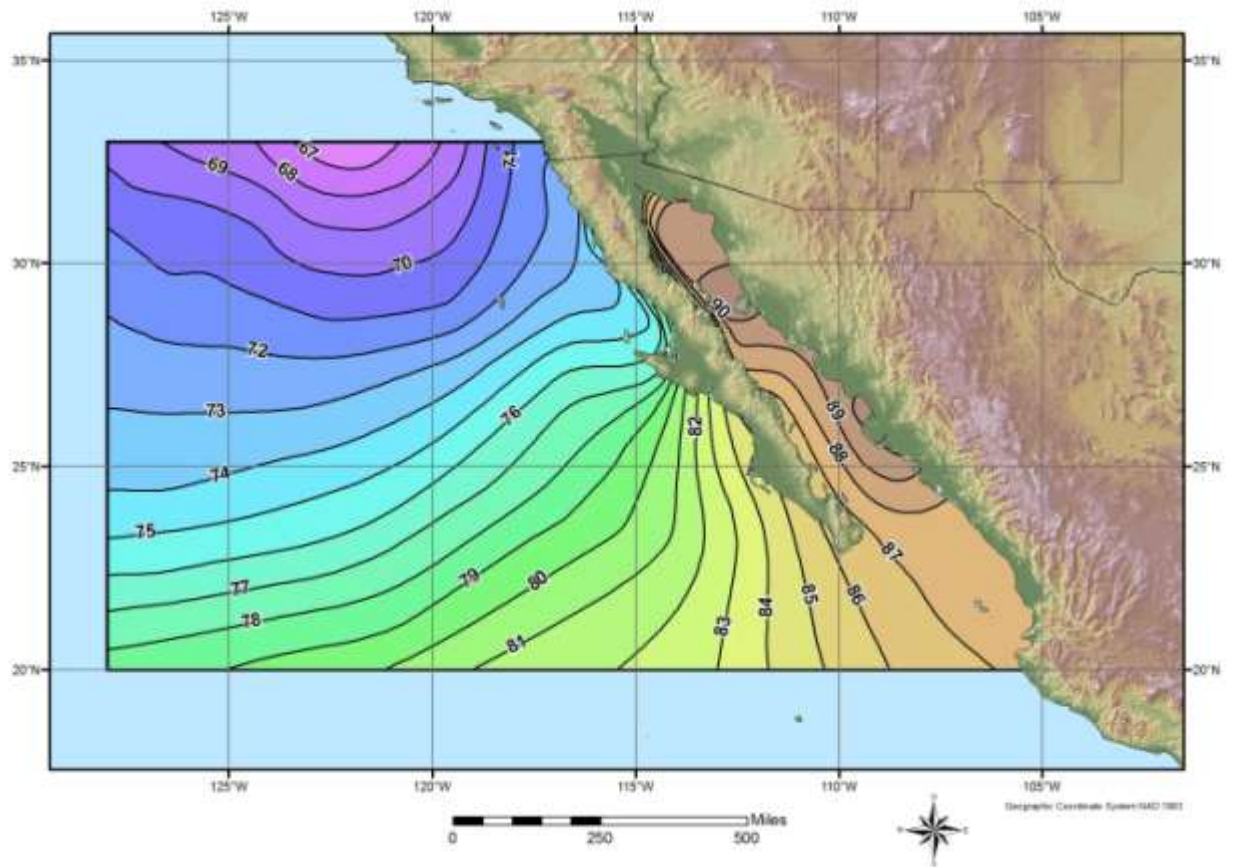
October 2 Sigma SST °F
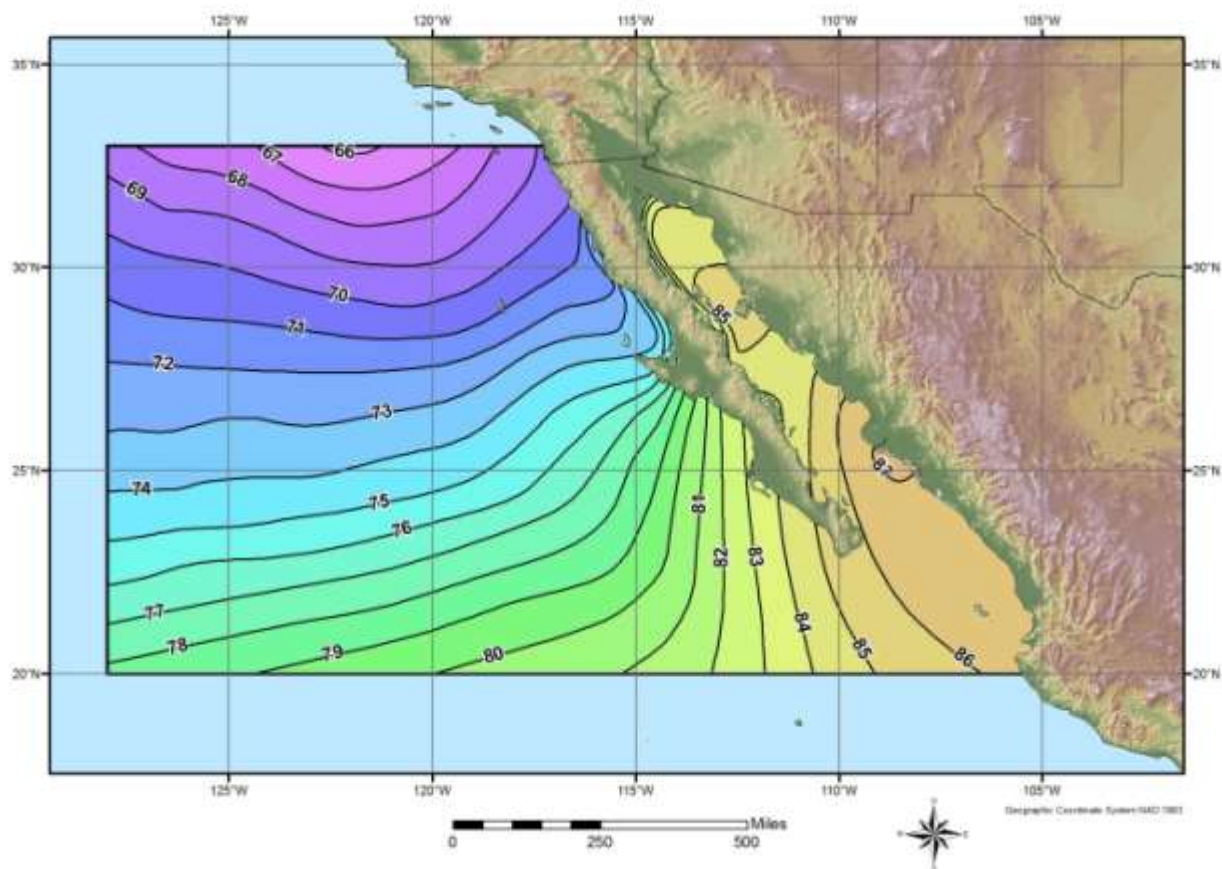
November 2 Sigma SST °F
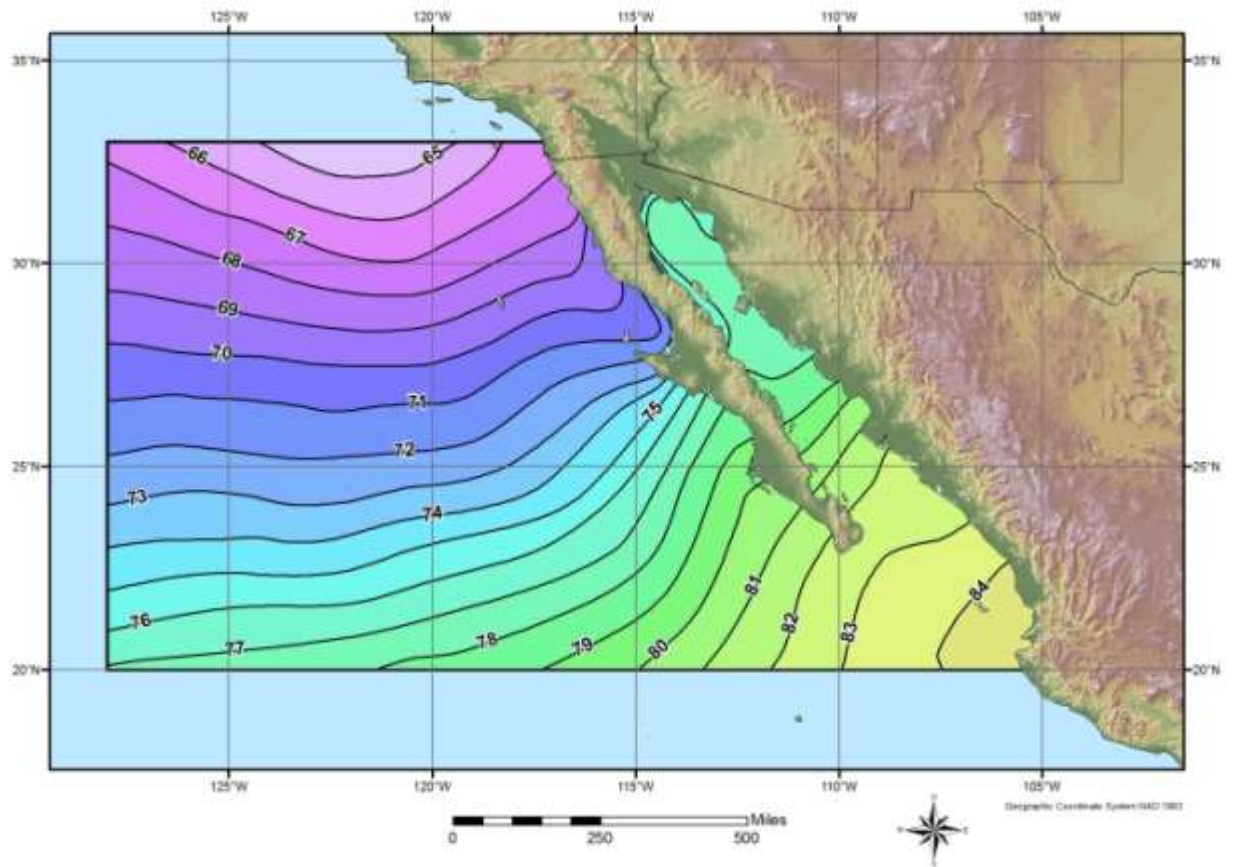
December 2 Sigma SST °F
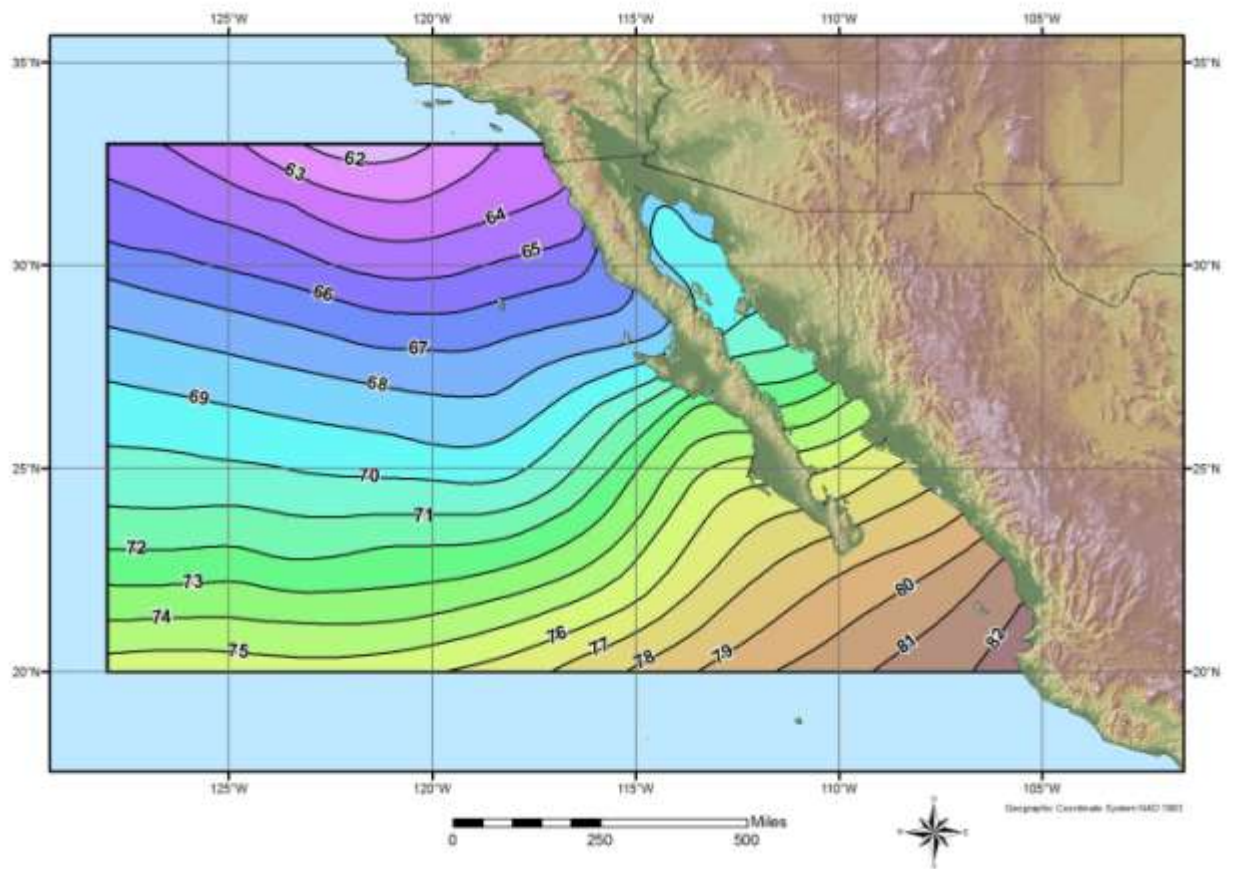
Appendix B

Discussion on Average vs Persisting Dew Point and Errors with HMR 49/50 Dew Point Climatologies

A major issue associated with the determination of dew point values are the use by the NWS of persisting dew points. Historically, 12-hour persisting dew point values have been used in the development and storm maximization in the HMRs. A 12-hour persisting dew point is defined as the highest dew point value that persists for a 12 hour period. In reality, it is the lowest of 12 hours of observed dew point values. It should be remembered that the dew point values are supposed to be representative of the moisture in the air mass associated with the rainfall. Using the lowest observed dew point vs. the average dew point may not be appropriate. Further, using a 12-hour duration vs. 3-hour or 24-hour duration more representative of the actual storm event may not be appropriate. NWS has in HMRs 57 and 59 used 3-hour and 12-hour durations but continues to use persisting dew point values. Other site-specific and regional PMP studies have adopted the use of 6-, 12-, and 24-hour dew point values that use average vs. persisting dew point values to better quantify the atmospheric moisture associated with the rainfall production (Tomlinson 1993, Tomlinson et al 2007, Tomlinson et al 2008).

HMR 50 (a companion document to HMR 49) provides maximum dew point maps. There are two sets of maps, one for use with local storms and one for use with general storms. Both use 12-hour persisting dew points. An explicit discussion on how these maps were derived as well as the data sets used is not provided nor are discussions related to the differences in the values between local and general storm dew point values. There is a statement made that "considerations of local and general storm situations suggested a difference of 2° to 3°". The authors of HMR 50 did give a high level overview of the processes and stations used to develop their dew point climatology (HMR 50 Section 4.3), but it is greatly lacking in detail and therefore cannot be verified or replicated.

Table 4.1 of HMR 50 Section 4.2.2.1.1 lists the four highest warm season 12-hour 1000-mb dew point situations at Phoenix. AWA attempted to verify these values and then compare the 3-hour, 12-hour and 24-hour average dew point values for the same periods with the 12-hour persisting values using the historic dew point observations at Phoenix. This analysis revealed several issues with the HMR 50 dew point data as presented. The most significant being that we could not replicate the values as presented in the table, either using the actual station data or adjusting the observations to 1000-mb (Table 4.0).

For this comparison, AWA used the hourly observations from the Phoenix Weather Bureau station location for the dates presented in HMR 50 Table 4.1 for a 72-hour period starting the day previous to the date listed and ending the following day. This ensured all the data that could have potentially been used to determine their 12-hour 1000-mb dew point value were evaluated. Unfortunately, the author's of HMR 50 did not explicitly identify the 12-hour period used to determine the listed dew point value. AWA used the 12-hour period within the 72-hour window that

produced the highest 12-hour persisting value since the values listed in HMR 50 Table 4.1 were identified as the highest warm season values at Phoenix. Observational data for Phoenix from AWA's in-house data server (data acquired from the National Weather Service National Climatic Data Center) were used since the Phoenix observational data were not include in HMR 50 for the dates listed in Table 4.1.

The analysis shows that the values listed in Table 4.1 of HMR 50 are not reproducible based on the hourly dew point observations from Phoenix. The values are listed as the highest 12-hour 1000-mb persisting dew points for the dates provided. The HMR 50 Table 4.1 values and results of the AWA analysis are shown in Table B.1 below.

Table B.1 Comparison of HMR 50 Table 4.1 persisting 12-hour 1000-mb dew point values and the AWA analyzed persisting 12-hour 1000-mb dew point values for Phoenix[5]

HMR 50 Dew Point Date	HMR 50 Dew Point Adjusted to 1000-mb	AWA Dew Point Adjusted to 1000-mb
August 3, 1951	73°	75.5°
August 4, 1954	72°	73.5°
August 13, 1955	73°	74.5°
August 1, 1964	73°	73.5°
August 1, 1980	73°	*65.5°*

No consistent bias is observed. From this analysis, it is unknown how the HMR 50 values were determined but using the Phoenix observations for the dates provided, the HMR 50 Table 4.1 values could not be reproduced.

Using the HMR 50 dew point values listed in Table B.1 above, comparisons were made with the HMR 50 maximum dew point maps for July and August for both local and general storms, Figures 4.22 – 4.25. The map values for the Phoenix location are approximately 5° F higher than the HMR 50 Table 4.1 values for the local storm and 2.5° F higher for the general storm. The seasonal plot shown in HMR 50 Figures 4.9 does not seem to have all four values from Table 4.1 plotted. Additionally, there are some return frequency values plotted for the 50% and 1% probability levels. These are determined applying the normal distribution to a series of monthly maxima using 21 years of data. There are a couple of issues with this statistical analysis. The first is that maximum dew point observations are not well represented by the normal distribution, GEV currently is considered the best distribution to use. The second is the use of 21 years of data to determine a 1% probability value (one in a hundred years). The curves developed in HMR 50 for other individual stations were developed similar to the plot in Figure 4.9 for Phoenix using both maximum observed and return frequency values. However, HMR 50 states that "An iterative process was carried out until realistic and compatible single station curves and regional analyses were completed." Therefore it is not surprising that the adopted curves do not consistently represent the maximum dew point data used in the analyses. Given that adopted curves for the seasonal local storm maximum dew point were developed subjectively (see previous quote from HMR 50), a comparison of the August maximum local storm value from Figure 4.9 was compared to the value from the August local storm map,

---

[5] The date of 8/1/1980 listed in HMR 50 Table 4.1 appears to be in error. In the text describing the table, the author's of HMR 50 mention August 1, 1964 as the appropriate date and after analyzing the dew point observations for the two dates, it seems reasonable that 1964 is the appropriate date to use.

Figure 4.24, for the Phoenix location. The map value is 78° F whereas the curve value is 76° F. Somewhere between the adopted local storm curve in Figure 4.9 and the construction of the maximum dew point local storm map, the maximum dew point value for Phoenix increased 2° F. It is important to note that a change of 1° F in the dew point value equates to approximate a 5% change in the maximization factor for individual storms. Since the maximization factor is a linear multiplier in the PMP determination process, the resulting change in rainfall amounts is 5%. Any errors in the development of the maximum dew point maps reflect directly on the reliability of the resulting PMP values.

A comparison was completed using this same data set used to evaluate the maximum dew point values in HMR 50 Table 4.1 to determine the 3-hour, 12-hour, and 24-hour *average* dew point values (these values have been used in the most recent site-specific PMP reports). This analysis compared variable duration average dew point values to the HMR 50 12-hour 1000-mb persisting and AWA 12-hour 1000-mb persisting dew points. Tables B.2A-B.2C show the difference between the HMR 50 12-hr 1000-mb persisting dew point values versus the 3-hour, 12-hour, and 24-hour average dew points.

Table B.2A Comparison of HMR 50 12-hour 1000-mb *persisting* dew point versus AWA analyzed 3-hour *average* 1000-mb dew points

HMR 50 Dew Point Date	HMR 50 Dew Point Adjusted to 1000-mb	AWA 3-hour Average Dew Point Adjusted to 1000-mb
August 3, 1951	73°	77.5°
August 4, 1954	72°	76.5°
August 13, 1955	73°	77.5°
August 1, 1964	73°	76.5°

Table B.2B Comparison of HMR 50 12-hour 1000-mb *persisting* dew point versus AWA analyzed 12-hour *average* 1000-mb dew points

HMR 50 Dew Point Date	HMR 50 Dew Point Adjusted to 1000-mb	AWA 12-hour Average Dew Point Adjusted to 1000-mb
August 3, 1951	73°	76.5°
August 4, 1954	72°	75°
August 13, 1955	73°	76.5°
August 1, 1964	73°	75.5°

Table B.2C Comparison of HMR 50 12-hour 1000-mb *persisting* dew point versus AWA analyzed 24-hour *average* 1000-mb dew points

HMR 50 Dew Point Date	HMR 50 Dew Point Adjusted to 1000-mb	AWA 24-hour Average Dew Point Adjusted to 1000-mb
August 3, 1951	73°	75.5°
August 4, 1954	72°	74°
August 13, 1955	73°	75°
August 1, 1964	73°	75.5°

Tables B.3A-B.3C show the difference between the AWA analyzed 12-hour 1000-mb persisting dew point values versus the 3-hour, 12-hour, and 24-hour average dew points.

Table B.3A Comparison of AWA 12-hour 1000-mb *persisting* dew point versus AWA analyzed
3-hour *average* 1000-mb dew points

HMR 50 Dew Point Date	AWA Dew Point Adjusted to 1000-mb	AWA 3-hour Average Dew Point Adjusted to 1000-mb
August 3, 1951	75.5°	77.5°
August 4, 1954	74°	76.5°
August 13, 1955	74.5°	77.5°
August 1, 1964	74°	76.5°

Table B.3B Comparison of AWA 12-hour 1000-mb *persisting* dew point versus AWA
analyzed 12-hour *average* 1000-mb dew points

HMR 50 Dew Point Date	AWA Dew Point Adjusted to 1000-mb	AWA 12-hour Average Dew Point Adjusted to 1000-mb
August 3, 1951	75.5°	76.5°
August 4, 1954	74°	75°
August 13, 1955	74.5°	76.5°
August 1, 1964	74°	75.5°

Table B.3C Comparison of AWA 12-hour 1000-mb *persisting* dew point versus AWA
analyzed 24-hour *average* 1000-mb dew points

HMR 50 Dew Point Date	AWA Dew Point Adjusted to 1000-mb	AWA 24-hour Average Dew Point Adjusted to 1000-mb
August 3, 1951	75.5°	75.5°
August 4, 1954	74°	74°
August 13, 1955	74.5°	75°
August 1, 1964	74°	75.5°

In all cases, the average dew point values are higher than the 12-hour persisting values given by the author's of HMR 50 and in all but two of the 24-hour values analyzed by AWA. These differences are most pronounced at the 3-hour duration and become smaller from 12-hours to 24-hours. This same occurrence was found and adjusted for in previous site-specific PMP studies (Tomlinson 1993, Tomlinson et al 2007, Tomlinson et al 2008) and referenced but not implemented in HMR 57. The authors of the most recent HMRs (HMR 57 and HMR 59) recognized that using a 12-hour persisting dew point value may not accurately represent the moisture that fed the storm event being analyzed. This is especially true for local storms where the moisture tongue which fed the storm was of short duration and/or occurred within a limited spatial extent. Therefore, using the average dew point values for periods of time consistent with the rainfall duration better represents the storm environment and as such, should be the preferred way to analyze the moisture associated with a storm event and develop storm maximization values.

It is very important to have confidence that the climatological maximum dew point maps be reliable in providing appropriate dew point values for use in both the maximization and transpositioning process. For some recent PMP studies, e.g. the statewide PMP study for Nebraska

(Tomlinson et al 2008), return frequency analyses of maximum average dew point values for various durations have been completed. These return frequency maps for durations appropriate for various storm types provide reliable climatological maps for use in PMP studies.

Appendix C

Procedure for using Dew Point Temperatures and Sea Surface Temperatures (SSTs) for Storm Maximization and Transposition

Maximum dew point temperatures (hereafter referred to as dew points) have historically been used for two primary purposes in the PMP computation process:

1. To increase the observed rainfall amounts to a maximum value based on a potential increase in atmospheric moisture available to the storm.
2. To adjust the available atmospheric moisture to account for any increases or decreases associated with the maximized storm potentially occurring at another location within the transposition limits for that storm.

HMR and WMO procedures for storm maximization use a representative storm dew point as the parameter to represent available moisture to a storm. Prior to the mid-1980s, maps of maximum dew point values from the *Climatic Atlas of the United States*, Environmental Data Services, Department of Commerce (1968), were the source for maximum dew point values. HMR 55 published in 1984 updated maximum dew point values for a portion of the United States from the Continental Divide eastward into the central plains. A regional PMP study for Michigan and Wisconsin produced return frequency maps using the L-moments method (Tomlinson 1993). The Review Committee for that study included representatives from NWS, FERC, Bureau of Reclamation, and others. They agreed that the 50-year return frequency values were appropriate for use in PMP calculations. HMR 57 was published in 1994 and HMR 59 in 1999. These latest NWS publications also update the maximum dew point climatology but use maximum observed dew points instead of return frequency values. This study used an updated maximum dew point and sea surface temperature (SST) climatology for use in storm maximization and transpositioning.

The procedure for determining a storm representative dew point begins with the determination of the inflow wind vector (direction and magnitude) for the air mass that contains the atmospheric moisture available to the storm. Beginning and ending times of the rainfall event at locations of the most extreme rainfall amounts are determined using rainfall mass curves from those locations.

The storm inflow wind vector is determined using available wind data and the HYSPLIT trajectory model. The HYSPLIT trajectory model data are available back to 1948. Use of these reanalysis fields provides much improved reliability in the determination of the storm inflow wind vectors. The program is available through an online interface through the Air Resources Laboratory section of NOAA and is called HYSPLIT. Users are able to enter in specific

parameters that then output a wind inflow from a starting point going backwards (or forwards) for a specified amount of time. Users can define variables such as the starting point (using latitude and longitude or a map interface), the date and time to start the trajectory, the length of time to run the trajectory, and the pressure level at which to delineate the inflow vector. Figures C.1 to C.3 show example inflow vectors generated by HYSPLIT at three levels; 700mb, 850mb, surface for the Harquahala Mountain-Hurricane Nora September 1997 extreme rainfall event. Each of these three levels were evaluated for each storm that occurred from 1948 through present. The data generated from the HYSPLIT runs is then used in conjunction with standard methods to help delineate the source region of the air mass responsible for the storm precipitation.
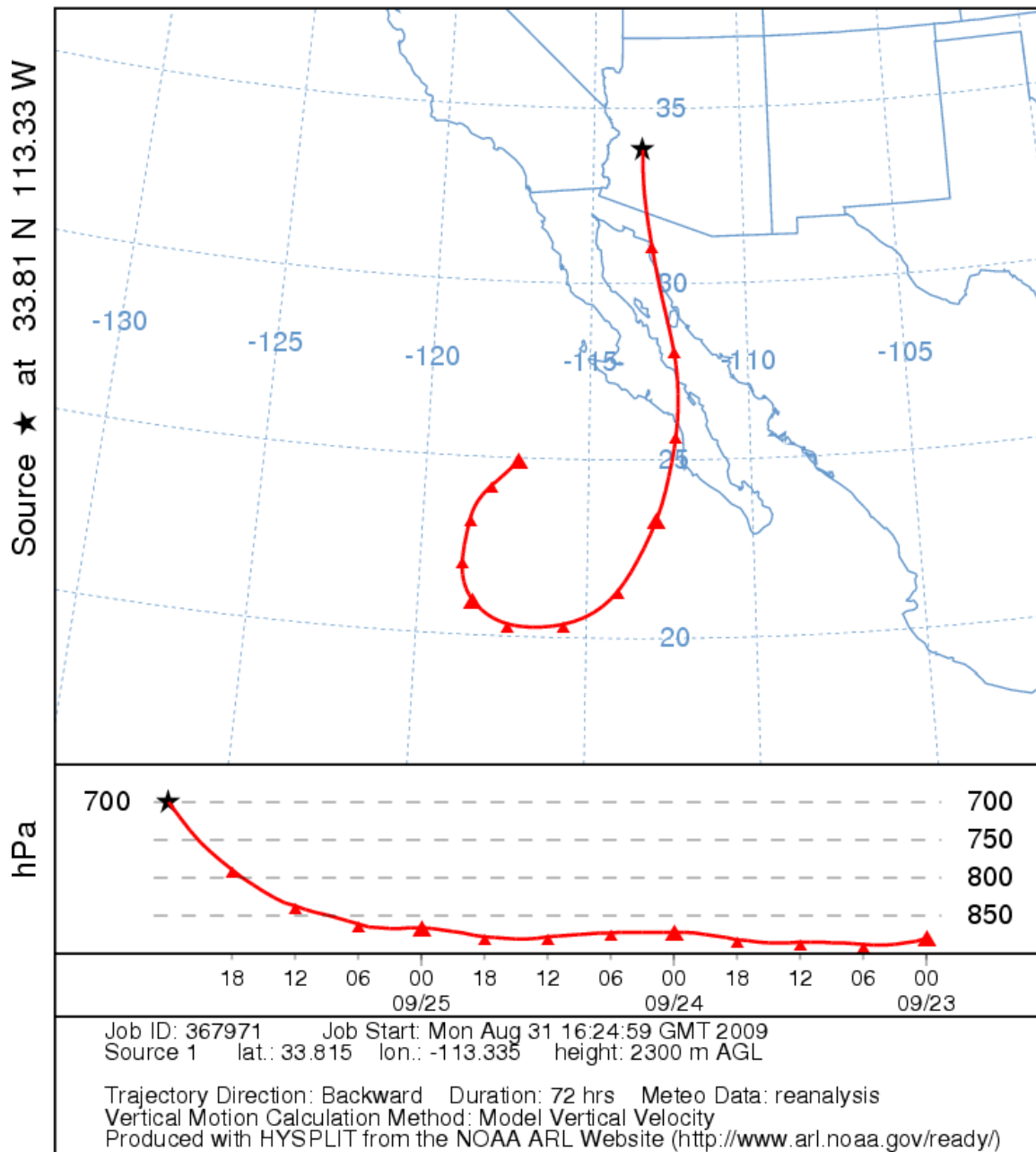
Figure C.1 HYSPLIT model results for 700mb Hurricane Nora September 1997
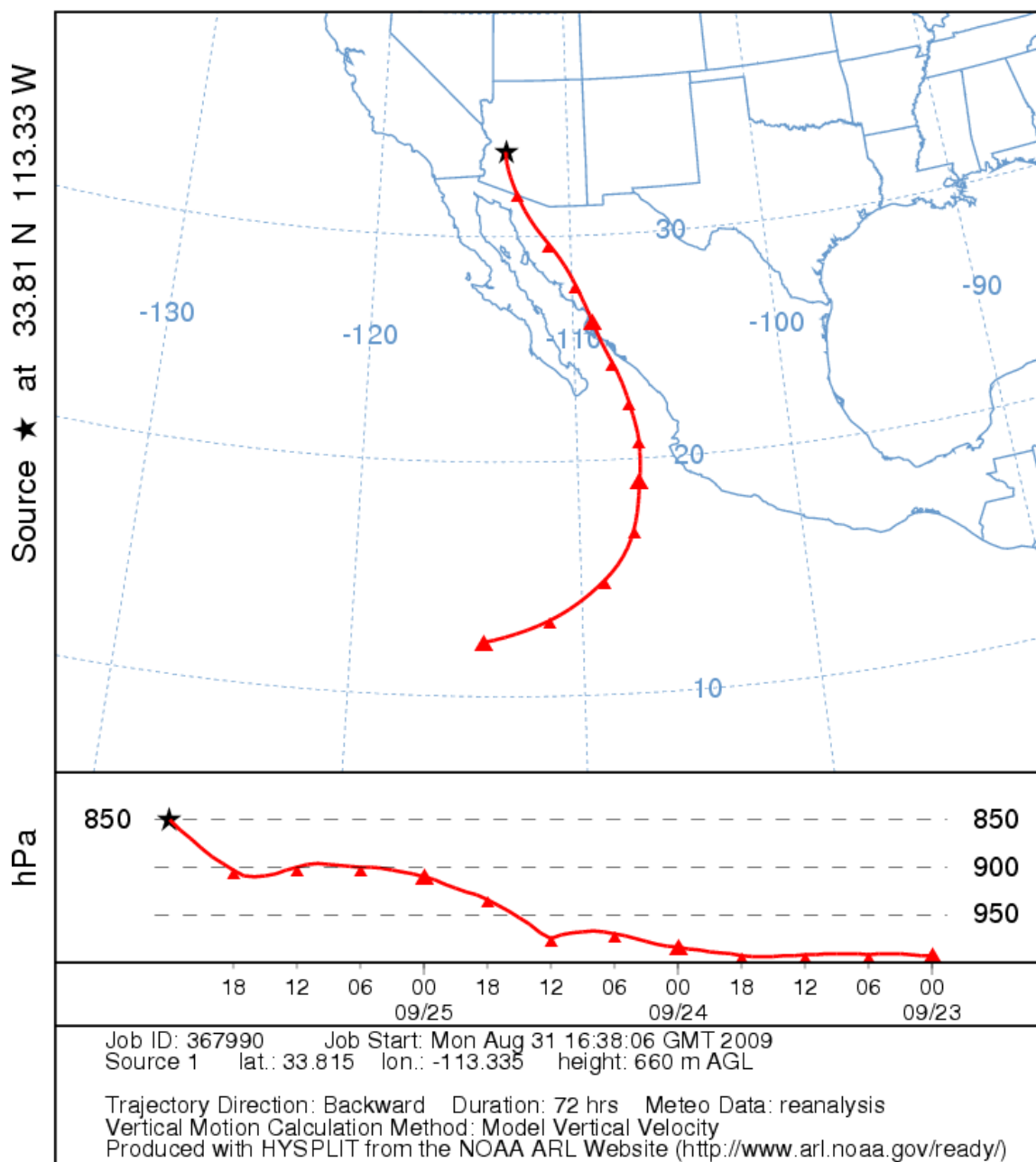
Figure C.2 HYSPLIT model results for 850mb Hurricane Nora September 1997
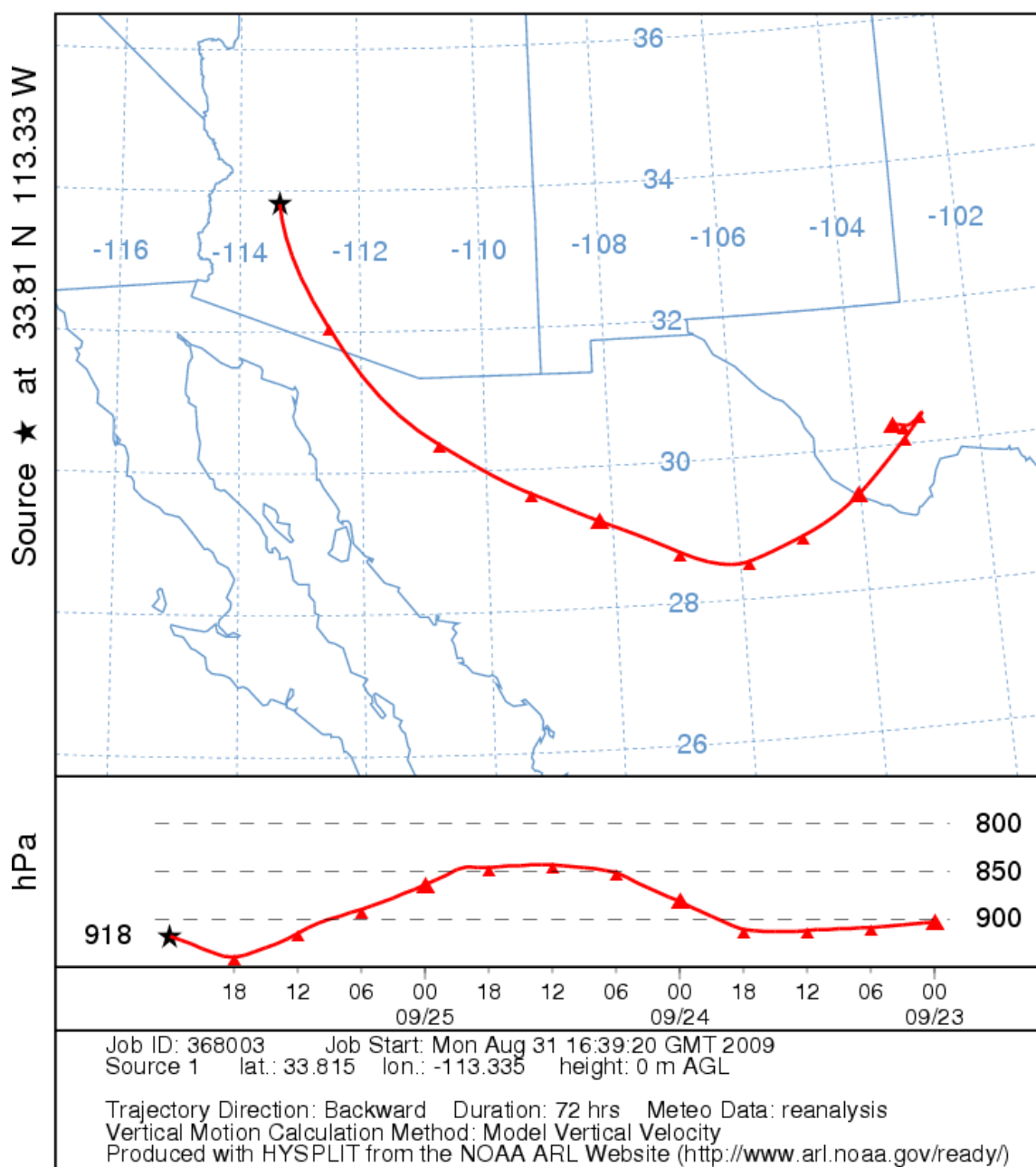
Figure C.3 HYSPLIT model results for surface Hurricane Nora September 1997

For moisture source regions over the oceans, dew point observations are not generally available with the exception of occasional ship reports. NWS has adopted a procedure for using sea surface temperatures (SSTs) as substitutes for dew points over the ocean. The best available observations are used to determine the storm representative dew point. This could be a dew

point values from a ship report, SST observation or daily SST analysis. The value used as the maximum SST value in PMP calculations is determined using the SST which is two standard deviations warmer than the mean SST. This provides a value for the maximum SST that has a probability of occurrence of about 0.025, i.e., about the 40-year return frequency value.

Using SSTs for in-place maximization and storm transpositioning follows a similar procedure to that used with dew points. The HYSPLIT trajectory model provides a significant improvement in determining the inflow wind vector as compared to older methods.   This is particularly significant when extrapolating coastal wind observations over long distances to reach warmer ocean regions.

The inflow wind vector is followed upwind until a location is reached that is at the sea surface. A point which represents a blend of the 850mb and 700mb trajectories that have been in contact with the sea surface and/or boundary is chosen as representative to contributing the moisture to the storm. Once this general location is determine, the location of the storm representative SST was determined when the SSTs are changing less than 1° F in a half-degree latitude and/or longitude following the inflow upwind. This procedure was developed to identify the homogeneous (or near homogeneous) region of SSTs associated with the atmospheric moisture source for the storms. The value from the SST daily analysis for that location was used for the storm representative SST, which was used in-place of the storm representative dew point in the maximization procedure.

Timing is not as critical for inflow wind vectors extending over the oceans since SSTs change very slowly with time compared to dew point values over land. What is important is the changing wind direction, especially for situations where there was curvature in the wind fields as the inflow wind vector was followed upwind. Any changes in wind curvature and variations in timing are inherently captured in the HYSPLIT model reanalysis fields, thereby eliminated another subjective and often unknown parameter.

The value for the maximum SST was determined using the mean plus two sigma (two standard deviations warmer than the mean) SST for that location (see discussion on 2-sigma SST in Section 4.1.3). The storm representative SST and the mean plus 2-sigma SST were used in the same manner as the storm representative dew point and the maximum dew point in the maximization and transpositioning procedure

The storm representative dew point determined from the SST observations is inherently corrected to the 1000mb level.

The procedure that computes the in-place maximized rainfall for a storm provides an estimate of the maximum amount of rainfall that could have been produced by the same storm at the same location if the maximum amount of atmospheric moisture had been available. This procedure requires that a maximum value for the storm representative dew point be determined. The maximum dew point value is selected at the same location where the storm dew point was determined using a maximum dew point climatology. The precipitable water in the atmosphere is determined using the storm representative and maximum dew point values. Precipitable water is defined in this study as the total amount of moisture in a column of the atmosphere from sea

level to 30,000 feet, assuming a vertically saturated atmosphere. Values of atmospheric precipitable water are determined using the moist pseudo-adiabatic assumption, i.e. assume that for the given 1000-mb dew point value, the atmosphere holds the maximum amount of moisture possible. The ratio of the precipitable water associated with the maximum 1000mb dew point to the precipitable water associated with the 1000-mb storm representative dew point is the maximization factor.

For example, consider the following case:

1000mb storm representative dew point:	72°F
1000mb maximum dew point:	76°F
Precipitable water associated with a 1000mb dew point of 72°F:	2.47 inches
Precipitable water associated with a 1000mb dew point of 76°F:	2.99 inches
Maximization factor: PW(76°F)/PW(72°F) = 2.99"/2.47" = 1.21	

For transpositioning, the storm inflow vector (determined by connecting the storm representative dew point location with the location of maximum rainfall) is moved to the basin location being studied. The new location of the upwind end of the vector is determined. The maximum dew point associated with that location is then selected using the same maximum dew point climatology map used for in-place maximization. The transpositioning factor is the ratio of the precipitable water associated with the maximum 1000mb dew point value at the transpositioned location to the precipitable water associated with the maximum 1000mb dew point for the storm representative dew point location.

An example is provided.

1000mb maximum dew point at the storm representative dew point location:	76°F
1000mb maximum dew point at the transpositioned location:	74°F
Precipitable water associated with a 1000mb dew point of 76°F:	2.99 in
Precipitable water associated with a 1000mb dew point of 74°F:	2.73 in
Transposition factor: PW(74°F)/PW(76°F) = 2.73"/2.99" = 0.91	

Appendix D

Procedure for Deriving PMP Values from Storm Depth-Area-Duration (DAD) Analyses

Although PMP rainfall amounts are theoretical values, there currently is no theoretical method for determining the values. The accepted procedure for determining PMP values begins with the largest identified historic observed rainfall amounts and applies the following procedures:

1. Increase the rainfall amounts to some maximized value (in-place maximization),
2. Adjust the "maximized" rainfall amounts to the potential situation where the historic storm occurs over the basin being studied (transposition),
3. Adjust the "maximized transpositioned" rainfall amounts for elevation changes or orographic differences.

The procedure begins with the Depth-Area-Duration (DAD) analysis from the largest of the identified storms that have occurred over regions that are climatologically and topographically similar to the basin being studied. Identification of the largest rainfall events is relatively straightforward and is accomplished by identifying the largest station rainfall amounts and correlating the dates among adjacent stations to identify the areal extent of the heavy rainfall and the storm period. The DAD for each storm is computed using isohyetal analyses for each hour during the storm and determining the largest rainfall totals for each duration of interest over each area size of interest.

The US Army Corps of Engineers, the Bureau of Reclamation and the National Weather Service have performed storm studies and produced DADs for many storms. However, for Arizona and HMR 49 in particular, no DADs were produced for any of the storms used. Therefore, all storms used in this study are being analyzed with DADs for the first time[6]. This is because HMR 49 was the last HMR to not use a storm based DAD approach to derive PMP values. These DADs quantify the rainfall associated with each storm event, providing the largest rainfall amounts for each of the durations and area sizes used in this study.

Identification of storms that can be transpositioned to any point within the state of Arizona is largely based on subjective judgment. For a storm to be transpositionable, it should have occurred over a region that is climatologically and topographically similar to the area being

---

[6] A Bureau of Reclamation report "Determination of an Upper Limit Design rainstorm for the Colorado River Basin Above Hoover Dam (1990) did produce DADs for thirteen storm events considered in the statewide study. Further, HMR 59 includes DAD values for two storm used in the statewide study.

studied. Storms generally should not be transpositioned across significant topographic features or into different climate regions (WMO, 1986).

Maximization of the storm DADs involves use of dew point temperatures and /or SSTs associated with the air mass that provided the moisture for the production of rainfall by the storm dynamics. To determine the storm representative dew point, winds coming into the storm are evaluated using the HYSPLIT trajectory model and hourly surface observations. The direction of the wind provides the direction to the region from which the air mass came and the speed provides the rate at which the air mass was transported into the storm. The procedure is to go upwind along the inflow wind direction until a position is found which best represents the moisture source location. This location is chosen to ensure that the data represents the available moisture which can be converted into precipitation as part of the storm environment based on the dew point/SST values. Using this location, an inflow vector (direction and distance) is determined. The dew point/SST data are used to determine the storm representative dew point/SST temperature for the storm. This value is used together with the maximum dew point or SST climatology value to determine a maximization factor for the storm.

The maximum dew point/SST represents the greatest amount of atmospheric moisture that potentially could have been available to the storm. Using a maximum dew point climatology (2-sigma SST temperatures at the same location), the maximum dew point/SST is determined for the same location as was selected for the storm representative dew point/SST. Precipitable water associated with each of these values is used to determine the in-place maximization factor. This procedure assumes that the storm dynamics of the largest historic storms are very close to being as efficient as is physically possible and are representative of a PMP storm. The assumption is also made that if additional atmospheric moisture had been available to the storm, the storm rainfall would have increased by a ratio directly proportional to the increase in atmospheric moisture. Hence, once a dew point or SST associated with the storm air mass is determined, the moisture in the actual storm air mass, referred to as the "in-place" storm precipitable water (storm PW), can be quantified.   The moisture in an air mass with the maximum dew point/SST for the same location, referred to as maximum precipitable water (maximum PW) can also be quantified. The ratio of maximum PW to storm PW is the in-place maximization factor.

The equation for this computation is as follows:

   In-place maximization factor = (in-place maximum PW)/(in-place storm PW)

Unless the actual storm occurred within the boundaries of the basin under investigation, a transpositioning procedure is followed to adjust the maximized storm DAD for "moving" the storm to the study basin. i.e. determine the maximum potential rainfall if the same storm were to occur over the study basin. The transpositioning procedure is separated into two distinct processes: the moisture transpositioning and the orographic transpositioning. The moisture transpositioning procedure attempts to account for change in rainfall due to available atmospheric moisture. The orographic transpositioning procedure attempts to account for change in rainfall due to the effects of topography and terrain such as changes in elevation, rain shadow, aspect, and slope effects.

The moisture transpositioning process occurs when the storm inflow vector is moved to the study basin location and the location at the upwind end of the vector (the end away from the basin) is determined. Using that location and the maximum dew point (SST) climatology, a transpositioned maximum dew point value is selected. The precipitable water values associated with the in-place maximum dew point/SST and the transpositioned maximum dew point/SST are used to compute the transposition factor.

The equation for this computation is as follows:

Moisture transposition factor = (transpositioned maximum PW)/(in-place maximum PW)

The orographic transposition process quantifies the topographic effect by spatially evaluating the NOAA Atlas 14 precipitation frequency estimates (PFE's) for change between the storm center location and the target basin location. The NOAA Atlas 14 dataset inherently accounts for the orographic effect within the datasets spatial distribution. Therefore, determining the proportionality (m) of precipitation depth at the target location to the precipitation depth at the source location provides a reasonable factor describing the orographic influence on that particular spatial transposition. The 10-year through 1,000-year return frequency estimates are all evaluated in an effort to encompass the typical recurrence intervals exhibited by the storms analyzed within this study. Linear regression is used to estimate the precipitation in the target location Po due to the relationship between the PFE's at the target and source locations. The linear trend line can be expressed in the slope intercept form:

$$P_o = mP_i + b$$

where,

Po	=	orographically adjusted rainfall (target)
Pi	=	in-place rainfall
m	=	proportionality coefficient (slope)
b	=	error term (y-intercept)

Once the orographically adjusted rainfall, or transpositioned rainfall, is predicted for the target location, a ratio of the transpositioned rainfall depth to the in-place rainfall provides the orographic transposition factor.

Orographic transposition factor = (transpositioned rainfall)/(in-place rainfall)

:

The entire analysis domain for this study contains terrain that could potentially affect rainfall. For this reason, the orographic transposition factor is always considered along with the

moisture transposition factor and in-place maximization factor. The total adjustment factor is the product of each of the adjustment factors.

Total adjustment factor =

In-place maximization factor
x
Moisture transposition factor
x
Orographic transposition factor

When a target grid cell shares the same location of the storm center there is no translocation and the moisture and orographic transposition factors will always be 1. These adjustment factors are applied as a linear multiplier for each storm for all rainfall amounts in the storm DAD.

For this study, all computations associated with historic storms are computed at the 1000mb level (approximately sea level). The elevation of the maximum rainfall location is used as the storm elevation. An adjustment is applied to the storm moisture to account for the elevation of the storm above sea level. For example, if the greatest rainfall occurred at an average elevation of 500 feet, the total atmospheric moisture (500 to 30,000 feet) is increased by the amount of moisture between sea level and 500 feet.

As an example, the DAD from the Harquahala Mountain-Nora-1997 SPAS 1084 storm center is maximized and transpositioned to grid point #1. The following are values for the parameters used in computing the adjustments:

Storm representative dew point:	73.5° F
In-place maximum dew point:	76.0° F
Transpositioned maximum dew point:	77.0° F
Storm center elevation:	4900'

Total atmospheric precipitable water for 73.5° F:	2.67"
Total atmospheric precipitable water for 76.0° F:	2.99"
Total atmospheric precipitable water for 77.0° F:	3.14"
Adjustment for storm elevation, 1000mb to 4900' at 73.5°F:	1.02"
Adjustment for storm elevation, 1000mb to 4900' at 76.0°F:1.11"	
Adjustment for storm elevation, 1000mb to 4900' at 77.0°F:	1.15"
24-hour SPAS in-place rainfall:	12.09"
Orographically adjusted 24-hour rainfall:	9.42"

Total adjustment factor = (In-place max factor) (moisture transposition factor) (orographic transposition factor)

$$= [(2.99-1.11) / (2.67-1.02)]$$
$$* [(3.14-1.15) / (2.99-1.11)]$$
$$* (9.42/12.09)$$

$$= (1.14) * (1.06) * (0.78)$$

$$= 0.94$$

To explicitly show how each adjustment factor (in-place maximization, moisture, and orographic transposition) affects the total adjustment, separate computations are provided.

<u>In-place maximization factor</u>

Storm representative dew point:	73.5°F
In-place maximum dew point:	76.0°F
Storm atmospheric precipitable water for 73.5° F:	2.67"
Maximum atmospheric precipitable water for 76.0° F:	2.99"
Adjustment for storm elevation, 1000mb to 4900' at 73.5°F:	1.02"
Adjustment for storm elevation, 1000mb to 4900' at 76.5°F:	1.11"

In-place maximization factor = (in-place maximum PW at storm elevation)/(in-place storm PW at storm elevation)
$$= (2.99\text{-}1.11 / (2.67\text{-}1.02)$$
$$= 1.14$$

<u>Moisture transposition factor</u>

In-place maximum dew point:	76.0°F
Transpositioned maximum dew point:	77.0°F
Maximum atmospheric precipitable water for 76.0° F:	2.99"
Maximum atmospheric precipitable water for 77.0° F:	3.14"
Adjustment for storm elevation, 1000mb to 4900' at 76.0°F:	1.11"
Adjustment for basin elevation, 1000mb to 3650' at 77.0°F:	1.15"

Moisture Transposition factor = (transpositioned maximum PW at storm elevation)/(in-place maximum PW at storm elevation)
$$= (3.14 – 1.15 / 2.99 – 1.11)$$
$$= 1.06$$

<u>Orographic transposition factor</u>

24-hour SPAS in-place rainfall:	12.09"
NOAA Atlas 14 proportionality coefficient (slope):	0.72
NOAA Atlas 14 error term (y-intercept):	0.72"

Orographically adjusted rainfall = (in-place rainfall)(proportionality coefficient) + error term
$$= (12.09") * (0.72) + 0.72"$$
$$= 9.42"$$

Orographic transposition factor $\quad$ = $\quad$ (transpositioned rainfall)/(in-place rainfall)

$\qquad\qquad\qquad\qquad\qquad\qquad$ = $\quad$ 9.42" / 12.09"

$\qquad\qquad\qquad\qquad\qquad\qquad$ = $\quad$ 0.78

This is the same total adjustment computed earlier (within round-off error) using the single equation to compute the total adjustment factor.

Since these procedures involve linear multiplication, Excel spread sheets are used to incorporate the storm DAD and apply the factors to compute the transpositioned, maximized, barrier and orographic adjusted DAD. In this study, this procedure is applied to each of the 51 storms within Microsoft Excel and each of the computational storm spreadsheets are listed in Appendix F.

Appendix E

Storm Precipitation Analysis System (SPAS) Description

INTRODUCTION

The Storm Precipitation Analysis System (SPAS) is grounded on years of scientific research with a demonstrated reliability in hundreds of post-storm precipitation analyses. It has evolved into a trusted hydrometeorological tool that provides accurate precipitation data at a high spatial and temporal resolution for use in a variety of sensitive hydrologic applications (Faulkner et al. 2004, Tomlinson et al. 2003-2012). Applied Weather Associates, LLC and METSTAT, Inc. initially developed SPAS in 2002 for use in producing Depth-Area-Duration values for Probable Maximum Precipitator (PMP) analyses. SPAS utilizes precipitation gauge data, "basemaps" and radar data (when available) to produce gridded precipitation at time intervals as short as 5-minutes, at spatial scales as fine as 1 km^2 and in a variety of customizable formats. To date (April 2012) SPAS has been used to analyze over 230 storm centers across all types of terrain, among highly varied meteorological settings and some occurring over 100-years ago.

SPAS output has many applications including, but not limited to: hydrologic model calibration/validation, flood event reconstruction, storm water runoff analysis, forensic cases and PMP studies. Detailed SPAS-computed precipitation data allow hydrologists to accurately model runoff from basins, particularly when the precipitation is unevenly distributed over the drainage basin or when rain gauge data is limited or not available. The increased spatial and temporal accuracy of precipitation estimates has eliminated the need for commonly made assumptions about precipitation characteristics (such as uniform precipitation over a watershed), thereby greatly improving the precision and reliability of hydrologic analyses.

In order to instill consistency in SPAS analyses, many of the core methods have remained consistent from beginning. However, SPAS is constantly evolving and improving through new scientific advancements and as new data and improvements are incorporated. This write-up describes the current inter-workings of SPAS, but the reader should realize SPAS can be customized on a case-by-case basis to account for special circumstances; these adaptations are documented and included in the deliverables. The over arching goal of SPAS is to combine the strengths of rain gauge data and radar data (when available) to provide sound, reliable and accurate spatial precipitation data.

Hourly precipitation observations are generally limited to a small number of locations, with many basins lacking observational precipitation data entirely. Meanwhile Next Generation Radar (NEXRAD) data provides valuable spatial and temporal information over data-sparse basins; it has historically lacked reliability for determining precipitation rates and reliable quantitative precipitation estimates (QPE). The improved reliability in SPAS is made possible

by hourly calibration of the NEXRAD radar-precipitation relationship using data from locations with hourly rainfall observations within the overall SPAS analysis domain, combined with local hourly bias adjustments to force consistency between the final result and "ground truth" precipitation measurements. If NEXRAD radar data is available (generally for storm events since the mid-1990's), precipitation at temporal scales as frequent as 5-minutes is available, otherwise the precipitation data is available hourly. A summary of the general SPAS processes are shown in flow chart in Figure E.1.
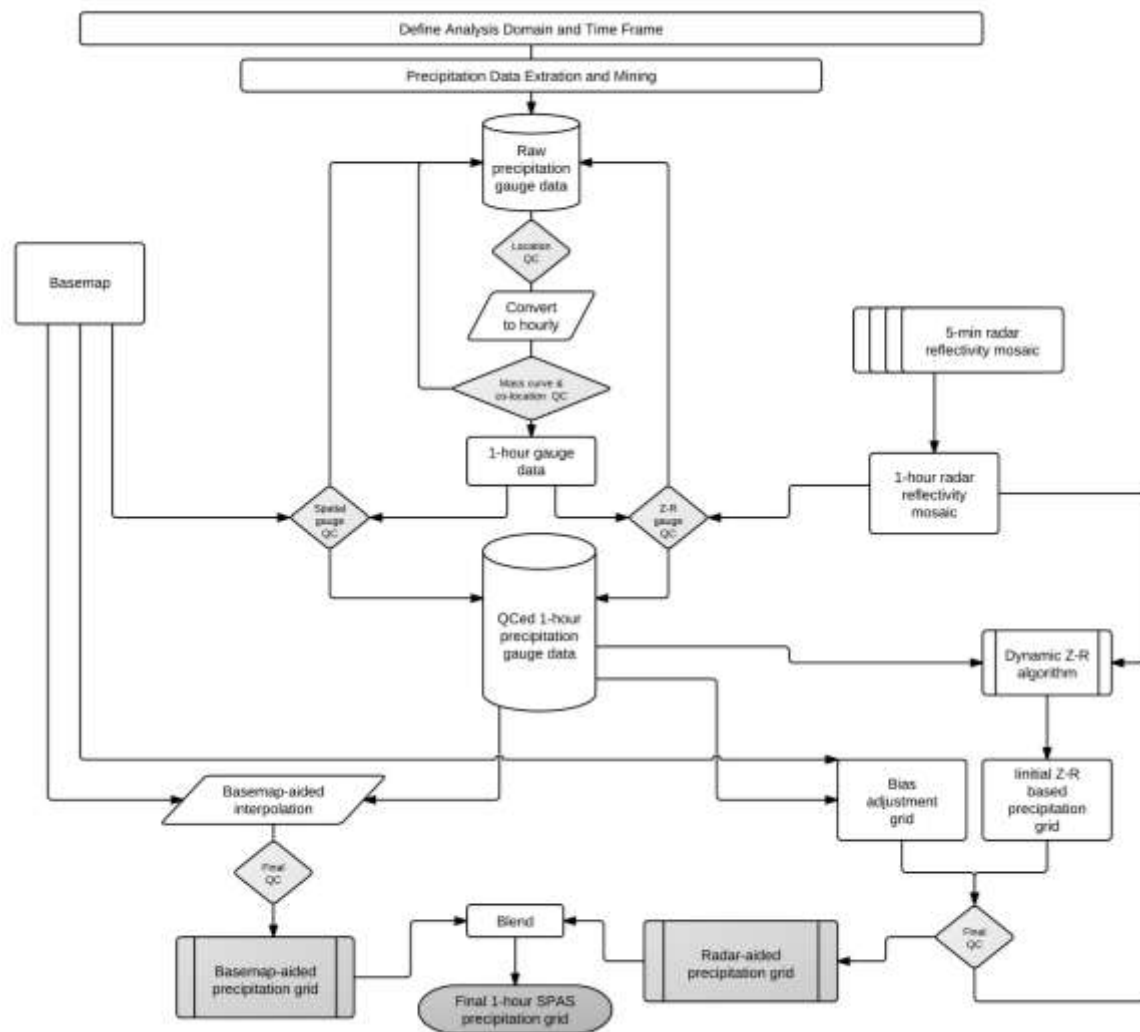
Figure E.1 SPAS flow chart

SETUP

Prior to a SPAS analysis careful definition of the storm analysis domain and time frame to be analyzed is established. Several considerations are made to ensure the domain (longitude-latitude box) and time frame are sufficient for the given application.

SPAS Analysis Domain

For PMP applications it is important to establish an analysis domain that completely encompasses a storm center, meanwhile hydrologic modeling applications are more concerned about a specific basin, watershed or catchment. If radar data is available, then it is also important to establish an area large enough to encompass enough stations (minimum of ~30) to adequately derive reliable radar-precipitation intensity relationships (discussed later). The domain is defined by evaluating existing documentation on the storm as well as plotting and evaluating initial precipitation gauge data on a map. The analysis domain is defined to include as many hourly recording gauges as possible given their importance in timing. The domain must include enough of a buffer to accurately model the nested domain of interest. The domain is defined as a longitude-latitude (upper left and lower right corner) rectangular region.

SPAS Analysis Time Frame

Ideally, the analysis time frame, also referred to as the Storm Precipitation Period (SPP), will extend from a dry period through the target wet period then back into another dry period. This is to ensure that total storm precipitation amounts can be confidently associated with the storm in question and not contaminated by adjacent wet periods. If this is not possible, a reasonable time period is selected that is bounded by relatively lighter precipitation. The time frame of the hourly data must be sufficient to capture the full range of daily gauge observational periods in order for the daily observations to be disaggregated into estimated incremental hourly values (discussed later). For example, if a daily gauge takes observations at 8:00 AM, then the hourly data must be available from 8:00 AM the day prior. Given the configuration of SPAS, the minimum SPP is 72 hours and aligns midnight to midnight.

The core precipitation period (CPP) is a sub-set of the SPP and represents the time period with the most precipitation and the greatest number of reporting gauges. The CPP represents the time period of interest and where our confidence in the results is highest.

DATA

The foundation of a SPAS analysis is the "ground truth" precipitation measurements. In fact, the level of effort involved in "data mining" and quality control represent over half of the total level of effort needed to conduct a complete storm analysis. SPAS operates with three primary data sets: precipitation gauge data, a "basemap" and, if available, radar data. Table G.1 conveys the variety of precipitation gauges usable by SPAS. For each gauge, the following elements are gathered, entered and archived into to SPAS database:

- Station ID
- Station name
- Station type (H=hourly, D=Daily, S=Supplemental, etc.)
- Longitude in decimal degrees
- Latitude in decimal degrees
- Elevation in feet above MSL
- Observed precipitation

- Observation times
- Source
- If unofficial, the measurement equipment and/or method is also noted.

Based on the SPP and analysis domain, hourly and daily precipitation gauge data are extracted from our in-house database as well as the Meteorological Assimilation Data Ingest System (MADIS). Our in-house database contains data dating back to the late 1800s, while the MADIS system (described below) contains archived data back to 2002.

Hourly Precipitation Data

Our hourly precipitation database is largely comprised of data from NCDC TD-3240, but also precipitation data from other mesonets and meteorological networks (e.g., ALERT, Flood Control Districts, etc.) that we have collected and archived as part of previous studies. Meanwhile, MADIS provides data from a large number of networks across the U.S., including NOAA's HADS (Hydrometeorological Automated Data System), numerous mesonets, the Citizen Weather Observers Program (CWOP), departments of transportation, etc. (see http://madis.noaa.gov/mesonet_providers.html for a list of providers). Although our automatic data extraction is fast, cost-effective and efficient, it never captures all of the available precipitation data for a storm event. For this reason, a thorough "data mining" effort is undertaken to acquire all available data from sources such as U.S. Geological Survey (USGS), Remote Automated Weather Stations (RAWS), Community Collaborative Rain, Hail & Snow Network (CoCoRaHS), National Atmospheric Deposition Program (NADP), Clean Air Status and Trends Network (CASTNET), local observer networks, Climate Reference Network (CRN), Global Summary of the Day (GSD) and Soil Climate Analysis Network (SCAN). Unofficial hourly precipitation observations are gathered to give guidance on either timing or magnitude in areas otherwise void of precipitation data. The WeatherUnderground and MesoWest, two of the largest weather databases on the Internet, contain a good deal of official data, but also unofficial gauges.

Table E.1 Different precipitation gauge types used by SPAS

Precipitation Gauge Type	Description
Hourly	Hourly gauges with complete, or nearly complete, incremental hourly precipitation data.
Hourly estimated	Hourly gauges with some estimated hourly values, but otherwise reliable.
Hourly pseudo	Hourly gauges with reliable temporal precipitation data, but the magnitude is questionable in relation to co-located daily or supplemental gauge.
Daily	Daily gauge with complete data and known observation times.
Daily estimated	Daily gauges with some or all estimated data.
Supplemental	Gauges with unknown or irregular observation times, but reliable total storm precipitation data. (e.g., public reports, storms reports, "Bucket surveys", etc.)
Supplemental estimated	Gauges with estimated total storm precipitation values based on other information (e.g., newspaper articles, stream flow discharge, inferences from nearby gauges, pre-existing total storm isohyetal maps, etc.)

Daily Precipitation Data

Our daily database is largely based on NCDC's TD-3206 (pre-1948) and TD-3200 (1948 through present) as well as SNOTEL data from NRCS. Since the late 1990s, the CoCoRaHS network of more than 15,000 observes in the U.S. has become a very important daily precipitation source. Other daily data is gathered from similar, but smaller gauge networks, for instance the High Spatial Density Precipitation Network in Minnesota.

As part of the daily data extraction process, the time of observation, as indicted in database (if available), accompanies each measured precipitation value. Accurate observation times are necessary for SPAS to disaggregate the daily precipitation into estimated incremental values (discussed later). Knowing the observation time also allows SPAS to maintain precipitation amounts within given time bounds, thereby retaining known precipitation intensities. Given the importance of observation times, efforts are taken to insure the observation times are accurate. Hardcopy reports of "Climatological Data," scanned observational forms (available on-line) and/or gauge metadata forms have proven to be valuable and accurate resources for validating observation times. Furthermore, erroneous observation times are

identified in the mass-curve quality-control procedure (discussed later) and can be corrected at that point in the process.

Supplemental Precipitation Gauge Data

For gauges with unknown or irregular observation times, the gauge is considered a "supplemental" gauge. A supplemental gauge can either be added to the storm database with a storm total and the associated SPP as the temporal bounds or as a gauge with the known, but irregular observation times and associated precipitation amounts. For instance, if all that is known is 3" fell between 0800-0900, then that information can be entered. Gauges or reports with nothing more than a storm total are often abundant, but in order to use them, it is important the precipitation is only from the storm period in question. Therefore, it is ideal to have the analysis time frame bounded by dry periods.

Perhaps the most important source of data, if available, is from "bucket surveys," which provide comprehensive lists of precipitation measurements collected during a post-storm field exercise. Although some bucket survey amounts are not from conventional precipitation gauges, they provide important information, especially in areas lacking data. Particularly for PMP-storm analysis applications, it is customary to accept extreme, but valid non-measured precipitation values in order to capture the highest precipitation values.

Basemap

"Basemaps" are independent grids of spatially distributed weather or climate variables that are used to govern the spatial patterns of the hourly precipitation. The basemap also governs the spatial resolution of the final SPAS grids, unless radar data is available/used to govern the spatial resolution. Note that a base map is not required as the hourly precipitation patterns can be based on a station characteristics and an inverse distance weighting technique (discussed later). Basemaps in complex terrain are often based on the PRISM mean monthly precipitation (Figure E.2a) or Hydrometeorological Design Studies Center precipitation frequency grids (Figure E.2b) given they resolve orographic enhancement areas and micro-climates at a spatial resolution of 30-seconds (about 800 m). Basemaps of this nature in flat terrain are not as effective given the small terrain forced precipitation gradients. Therefore, basemaps for SPAS analyses in flat terrain are often developed from pre-existing (hand-drawn) isohyetal patterns (Figure E.2c), composite radar imagery or a blend of both.
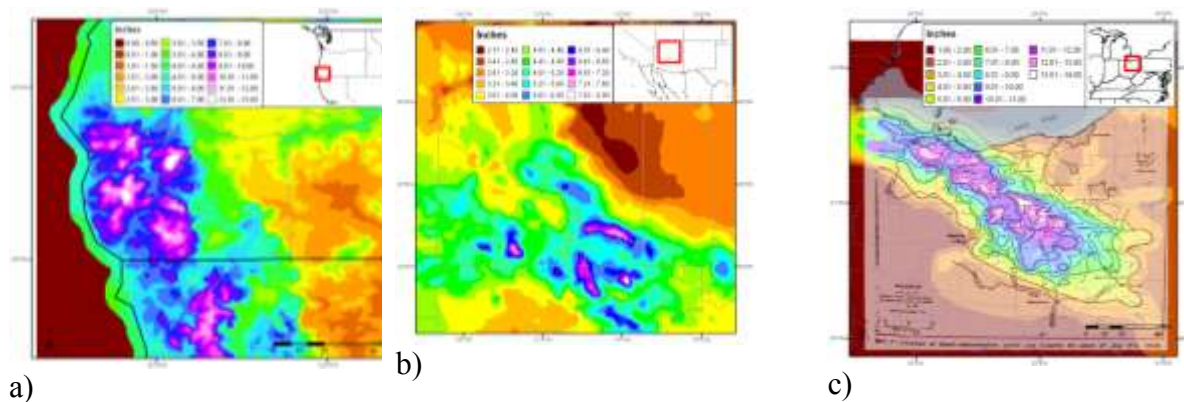
Figure E.2 Sample SPAS "basemaps" (a) A pre-existing (USGS) isohyetal pattern across flat terrain (SPAS 1209), (b) PRISM mean monthly (October) precipitation (SPAS 1192) and (c) A 100-year 24-hour precipitation grid from NOAA Atlas 14 (SPAS 1138)

Radar Data

For storms occurring since approximately the mid-1990's, weather radar data is available to supplement the SPAS analysis. A fundamental requirement for high quality radar-estimated precipitation is a high quality radar mosaic, which is a seamless collection of concurrent weather radar data from individual radar sites, however in some cases a single radar is sufficient (i.e. for a small area size storm event such as a thunderstorm). Weather radar data has been in use by meteorologists since the 1960's to estimate precipitation depths, but it was not until the early 1990's that new, more accurate NEXRAD Doppler radar (WSR88D) was placed into service across the United States. Currently efforts are underway to convert the WSR88D radars to dual polarization (DualPol) radar. Today, NEXRAD radar coverage of the contiguous United States is comprised of 159 operational sites and 30 in Canada. Each U.S. radar covers an approximate 285 mile (460 km) radial extent while Canadian radars have approximately 256 km (138 nautical miles) radial extent over which the radar can detect precipitation. (see Figure E.3) The primary vendor of NEXRAD weather radar data for SPAS is Weather Decision Technologies, Inc. (WDT), who accesses, mosaics, archives and quality-controls NEXRAD radar data from NOAA and Environment Canada. SPAS utilizes Level II NEXRAD radar reflectivity data in units of dBZ, available every 5-minutes in the U.S. and 10-minutes in Canada.

NEXRAD Coverage Below 10,000 Feet AGL
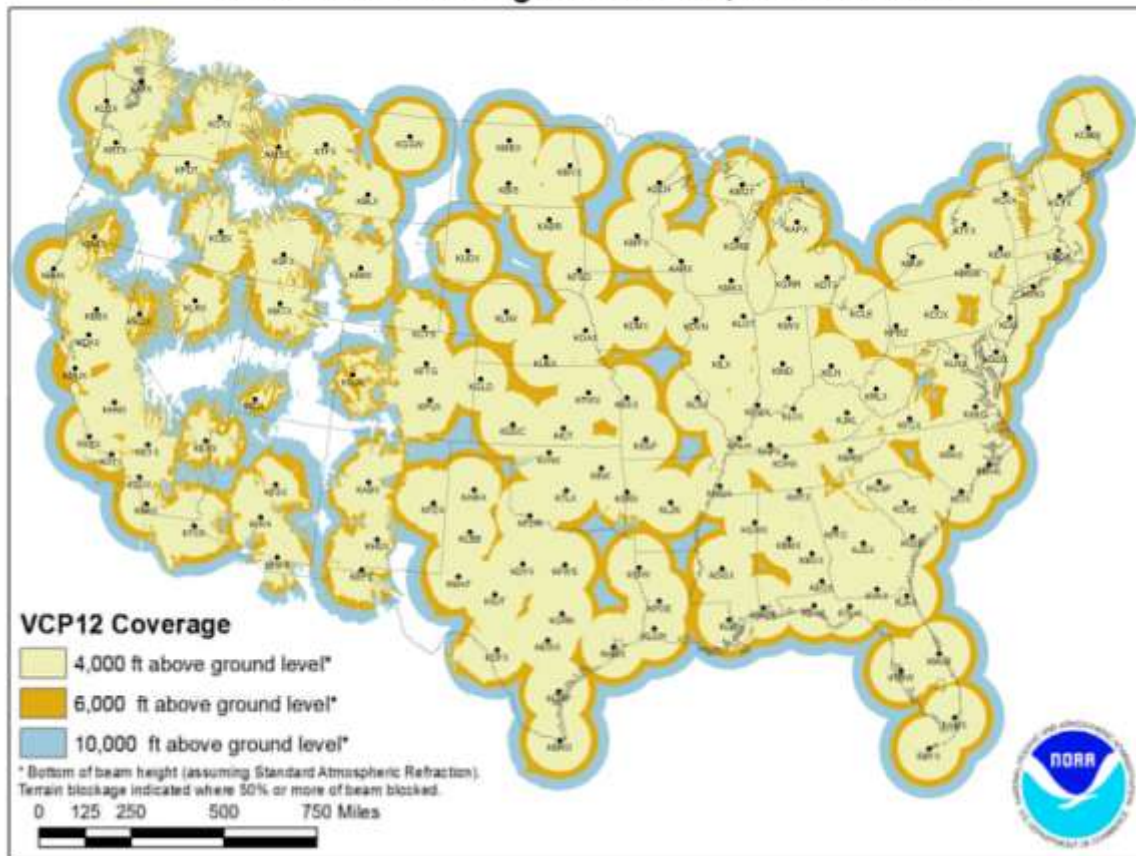
Figure E.3 U.S. radar locations and their radial extents of coverage below 10,000 feet above ground level (AGL). Each U.S. radar covers an approximate 285 mile radial extent over which the radar can detect precipitation.

     The WDT and National Severe Storms Lab (NSSL) Radar Data Quality Control Algorithm (RDQC) removes non-precipitation artifacts from base Level–II radar data and remaps the data from polar coordinates to a Cartesian (latitude/longitude) grid. Non-precipitation artifacts include ground clutter, bright banding, sea clutter, anomalous propagation, sun strobes, clear air returns, chaff, biological targets, electronic interference and hardware test patterns. The RDQC algorithm uses sophisticated data processing and a Quality Control Neural Network (QCNN) to delineate the precipitation echoes caused by radar artifacts (Lakshmanan and Valente 2004). Beam blockages due to terrain are mitigated by using 30 meter DEM data to compute and then discard data from a radar beam that clears the ground by less than 50 meters and incurs more than 50% power blockage. A clear-air echo removal scheme is applied to radars in clear-air mode when there is no precipitation reported from observation gauges within the vicinity of the radar. In areas of radar coverage overlap, a distance weighting scheme is applied to assign reflectivity to each grid cell, for multiple vertical levels. This scheme is applied to data from the nearest radar that is unblocked by terrain.

Once the data from individual radars have passed through the RDQC, they are merged to create a seamless mosaic for the United States and southern Canada as shown in Figure E.4. A multi-sensor quality control can be applied by post-processing the mosaic to remove any remaining "false echoes". This technique uses observations of infra-red cloud top temperatures by GOES satellite and surface temperature to create a precipitation/no-precipitation mask. Figure 4 shows the impact of WDT's quality control measures. Upon completing all QC, WDT converts the radar data from its native polar coordinate projection (1 degree x 1.0 km) into a longitude-latitude Cartesian grid (based on the WGS84 datum), at a spatial resolution of ~1/3rd-square mile for processing in SPAS.

a)   b)
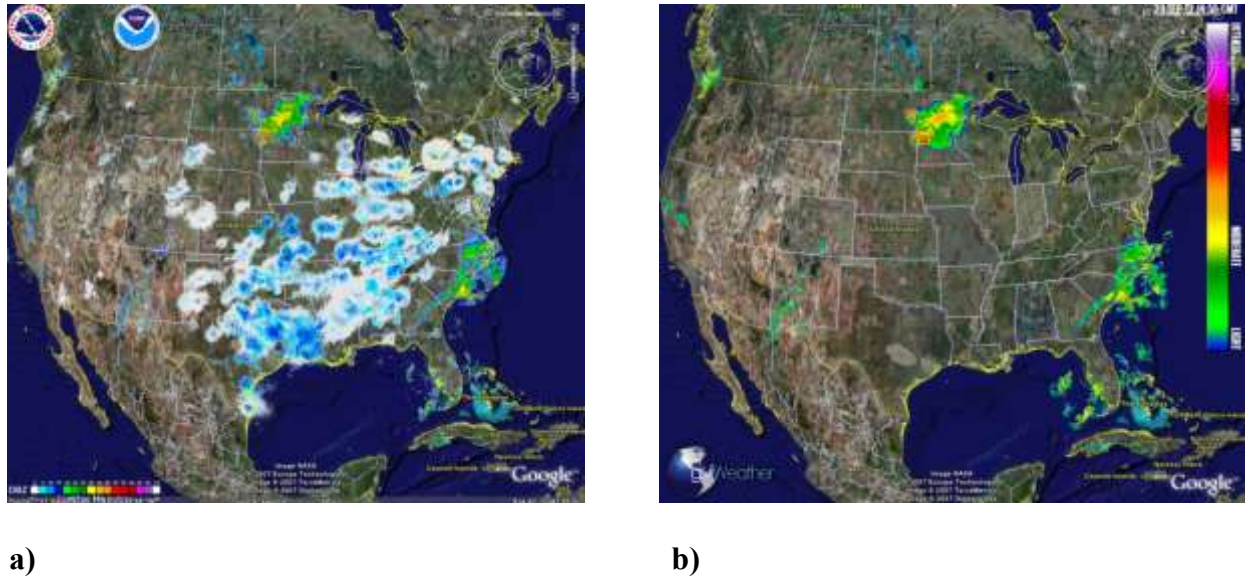
Figure E.4 (a) Level-II radar mosaic of CONUS radar with no quality control, (b) WDT quality controlled Level-II radar mosaic

SPAS conducts further QC on the radar mosaic by infilling areas contaminated by beam blockages. Beam blocked areas are objectively determined by evaluating total storm reflectivity grid which naturally amplifies areas of the SPAS analysis domain suffering from beam blockage as shown in Figure E.5.
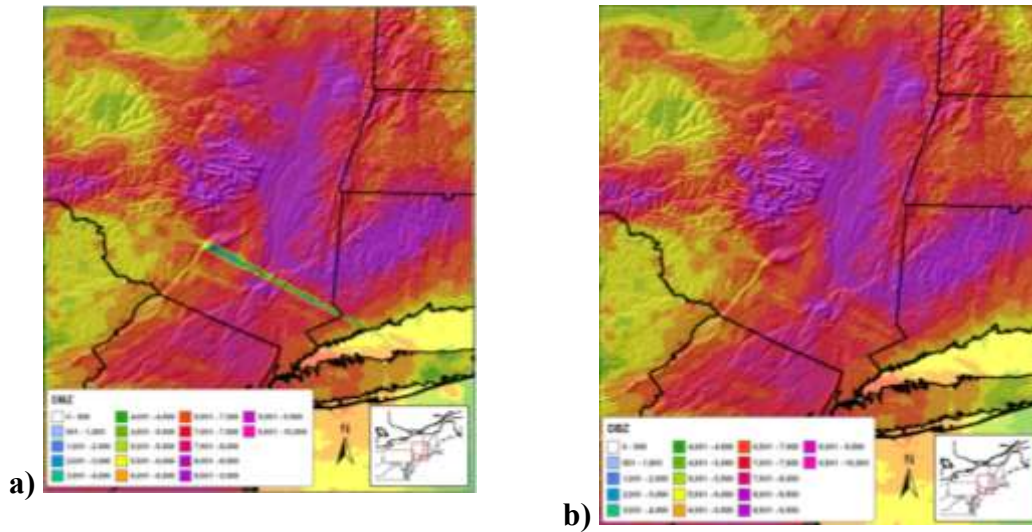
Figure E.5 Illustration of SPAS-beam blockage infilling where (a) is raw, blocked radar and (b) is filled for a 42-hour storm event

METHODOLOGY

Daily and Supplemental Precipitation to Hourly

To obtain one hour temporal resolutions and utilize all gauge data, it is necessary to disaggregate the daily and supplemental precipitation observations into estimated hourly amounts. This process has traditionally been accomplished by distributing (temporally) the precipitation at each daily/supplemental gauge in accordance to a single nearby hourly gauge (Thiessen polygon approach). However, this may introduce biases and not correctly represent hourly precipitation at daily/supplemental gauges situated in-between hourly gauges. Instead, SPAS uses a spatial approach by which the estimated hourly precipitation at each daily and supplemental gauge is governed by a distance weighted algorithm of all nearby true hourly gauges.

In order to disaggregate (i.e. distribute) daily/supplemental gauge data into estimate hourly values, the true hourly gauge data is first evaluated and quality controlled using synoptic maps, nearby gauges, orographic effects, gauge history and other documentation on the storm. Any problems with the hourly data are resolved, and when possible/necessary accumulated hourly values are distributed. If an hourly value is missing, the analyst can choose to either estimate it or leave it missing for SPAS to estimate later based on nearby hourly gauges. At this point in the process, pseudo (hourly) gauges can be added to represent precipitation timing in topographically complex locations, areas with limited/no hourly data or to capture localized convention. In order to adequately capture the temporal variations of the precipitation a pseudo hourly gauge is sometimes necessary. A pseudo gauge is created by distributing the precipitation at a co-located daily gauge or by creating a completely new pseudo gauge from other information such as inferences from COOP observation forms, METAR visibility data (if hourly precipitation isn't already available), lightning data, satellite data, or radar data. Often radar data

is the best/only choice for creating pseudo hourly gauges, but this is done cautiously given the potential differences (over-shooting of the radar beam equating to erroneous precipitation) between radar data and precipitation. In any case, the pseudo hourly gauge is flagged so SPAS only uses it for timing and not magnitude. Care is taken to ensure hourly pseudo gauges represent justifiably important physical and meteorological characteristics before being incorporated into the SPAS database. Although pseudo gauges provide a very important role, their use is kept to a minimum. The importance of insuring the reliability of every hourly gauge cannot be over emphasized. All of the final hourly gauge data, including pseudos, are included in the hourly SPAS precipitation database.

Using the hourly SPAS precipitation database, each hourly precipitation value is converted into a percentage that represents the incremental hourly precipitation divided by the total SPP precipitation. The GIS-ready x-y-z file is constructed for each hour that contains the latitude (x), longitude(y) and percent of precipitation (z) for a particular hour. Using the GRASS GIS, an inverse-distance-weighting squared (IDW) interpolation technique is applied to each of the hourly files. The result is a continuous grid with percentage values for the entire analysis domain, keeping the grid cells on which the hourly gauge resides faithful to the observed/actual percentage. Since the percentages typically have a high degree of spatial autocorrelation, the spatial interpolation has skill in determining the percentages between gauges, especially since the percentages are somewhat independent of the precipitation magnitude. The end result is a GIS grid for each hour that represents the percentage of the SPP precipitation that fell during that hour.

After the hourly percentage grids are generated and QC'ed for the entire SPP, a program is executed that converts the daily/supplemental gauge data into incremental hourly data. The timing at each of the daily/supplemental gauges is based on (1) the daily/supplemental gauge observation time, (2) daily/supplemental precipitation amount and (3) the series of interpolated hourly percentages extracted from grids (described above).

This procedure is detailed in Figure E.6 below. In this example, a supplemental gauge reported 1.40" of precipitation during the storm event and is located equal distance from the three surrounding hourly recording gauges. The procedure steps are:

Step 1.   For each hour, extract the percent of SPP from the hourly gauge-based percentage at the location of the daily/supplemental gauge. In this example, assume these values are the average of all the hourly gauges.

Step 2.   Multiply the individual hourly percentages by the total storm precipitation at the daily/supplemental gauge to arrive at estimated hourly precipitation at the daily/supplemental gauge. To make the daily/supplemental accumulated precipitation data faithful to the daily/supplemental observations, it is sometimes necessary to adjust the hourly percentages so they add up to 100% and account for 100% of the daily observed precipitation.

	Hour						
Precipitation	**1**	**2**	**3**	**4**	**5**	**6**	**Total**
Hourly station 1	0.02	0.12	0.42	0.50	0.10	0.00	1.16
Hourly station 2	0.01	0.15	0.48	0.62	0.05	0.01	1.32
Hourly station 3	0.00	0.18	0.38	0.55	0.20	0.05	1.36
	Hour						
Percent of total storm precip.	**1**	**2**	**3**	**4**	**5**	**6**	**Total**
Hourly station 1	2%	10%	36%	43%	9%	0%	100%
Hourly station 2	1%	11%	36%	47%	4%	1%	100%
Hourly station 3	0%	13%	28%	40%	15%	4%	100%
Average	*1%*	*12%*	*34%*	*44%*	*9%*	*1%*	*100%*
Storm total precipitation at daily gauge				1.40			
	Hour						
Precipitation (estimated)	**1**	**2**	**3**	**4**	**5**	**6**	**Total**
Daily station	0.01	0.16	0.47	0.61	0.13	0.02	1.40

Figure E.6 Example of disaggregation of daily precipitation into estimated hourly precipitation based on three (3) surrounding hourly recording gauges

In cases where the hourly grids do not indicate any precipitation falling during the daily/supplemental gauge observational period, yet the daily/supplemental gauge reported precipitation, the daily/supplemental total precipitation is evenly distributed throughout the hours that make up the observational period; although this does not happen very often, this solution is consistent with NWS procedures. However, the SPAS analyst is notified of these cases in a comprehensive log file, and in most cases they are resolvable, sometimes with a pseudo hourly gauge.

GAUGE QUALITY CONTROL

Exhaustive quality control measures are taken throughout the SPAS analysis. Below are a few of the most significant QC measures taken.

Mass Curve Check

A mass curve-based QC-methodology is used to ensure the timing of precipitation at all gauges is consistent with nearby gauges. SPAS groups each gauge with the nearest four gauges (regardless of type) into a single file. These files are subsequently used in software for graphing and evaluation. Unusual characteristics in the mass curve are investigated and the gauge data corrected, if possible and warranted. See Figure E.7 for an example.
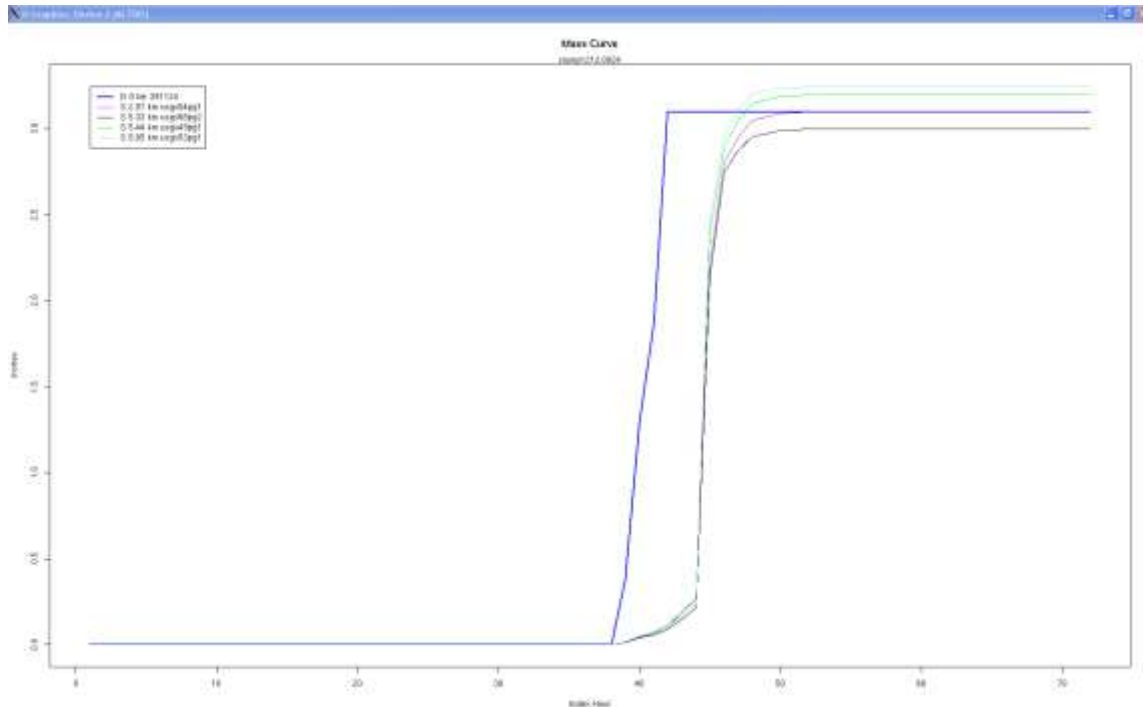
Figure E.7 Sample mass curve plot depicting a precipitation gauge with an erroneous
observation time (blue line). X-axis is the SPAS index hour and the y-axis is inches.
The statistics in the upper left denote gauge type, distance from target gauge (in km),
and gauge ID. In this example, the center gauge (blue line) was found to have an
observation error/shift of 1 day.

Gauge Mis-location Check

Although the gauge elevation is not explicitly used in SPAS, it is however used as a
means of QC'ing gauge location. Gauge elevations are compared to a high-resolution 15-second
DEM to identify gauges with large differences, which may indicate erroneous longitude and/or
latitude values.

Co-located Gauge QC

Care is also taken to establish the most accurate precipitation depths at all co-located
gauges. In general, where a co-located gauge pair exists, the highest precipitation is accepted (if
accurate). If the hourly gauge reports higher precipitation, then the co-located daily (or
supplemental) is removed from the analysis since it would not add anything to the analysis.
Often daily (or supplemental) gauges report greater precipitation than a co-located hourly station
since hourly tipping bucket gauges tend to suffer from gauge under-catch, particularly during
extreme events, due to loss of precipitation during tips. In these cases the daily/supplemental is
retained for the magnitude and the hourly used as a pseudo hourly gauge for timing. Large
discrepancies between any co-located gauges are investigated and resolved since SPAS can only
utilize a single gauge magnitude at each co-located site.

E-   13

SPATIAL INTERPOLATION

At this point the QC'ed observed hourly and disaggregated daily/supplemental hourly precipitation data are spatially interpolated into hourly precipitation grids. SPAS has three options for conducting the hourly precipitation interpolation, depending on the terrain and availability of radar data, thereby allowing SPAS to be optimized for any particular storm type or location. Figure E.8 depicts the results of each spatial interpolation methodology based on the same precipitation gauge data.
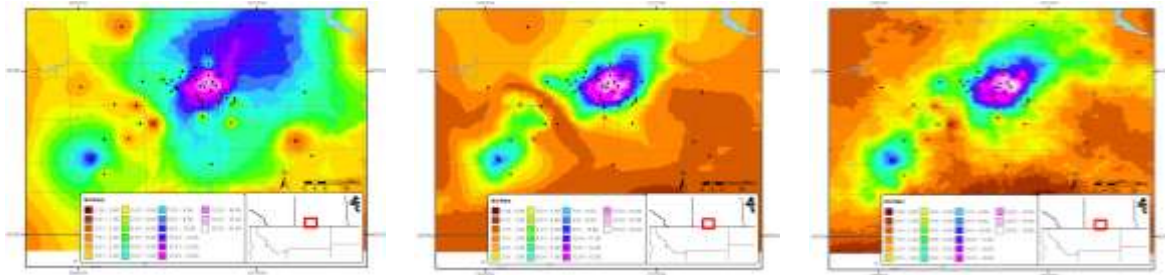
Figure E.8 Depictions of total storm precipitation based on the three SPAS interpolation methodologies for a storm (SPAS #1177, Vanguard, Canada) across flat terrain: (a) no basemap, (b) basemap-aided and (3) radar

Basic Approach

The basic approach interpolates the hourly precipitation point values to a grid using an inverse distance weighting squared GIS algorithm. This is sometimes the best choice for convective storms over flat terrain when radar data is not available, yet high gauge density instills reliable precipitation patterns. This approach is rarely used.

Basemap Approach

Another option includes the use of a "basemap", also known as a climatologically-aided interpolation (Hunter 2005). As noted before, the spatial patterns of the basemap govern the interpolation between points of hourly precipitation estimates, while the actual hourly precipitation values govern the magnitude. This approach to interpolating point data across complex terrain is widely used. In fact, it was used extensively by the NWS during their storm analysis era from the 1940s through the 1970s.

In application, the hourly precipitation gauge values are first normalized by the corresponding grid cell value of the basemap before being interpolated. The normalization allows information and knowledge from the basemap to be transferred to the spatial distribution of the hourly precipitation. Using an IDW squared algorithm, the normalized hourly precipitation values are interpolated to a grid. The resulting grid is then multiplied by the basemap grid to produce the hourly precipitation grid. This is repeated each hour of the storm.

Radar Approach

The coupling of SPAS with NEXRAD provides the most accurate method of spatially and temporally distributing precipitation. To increase the accuracy of the results however, quality-controlled precipitation observations are used for calibrating the radar reflectivity to rain rate relationship (Z-R relationship) each hour instead of assuming a default Z-R relationship. Also, spatial variability in the Z-R relationship is accounted for through local bias corrections (described later). The radar approach involves several steps, each briefly described below. The radar approach cannot operate alone – either the basic or basemap approach must be completed before radar data can be incorporated.

Z-R Relationship

SPAS derives high quality precipitation estimates by relating quality controlled level–II NEXRAD radar reflectivity radar data with quality-controlled precipitation gauge data in order to calibrate the Z-R (radar reflectivity, Z, and precipitation, R) relationship. Optimizing the Z-R relationship is essential for capturing temporal changes in the Z-R. Most current radar-derived precipitation techniques rely on a constant relationship between radar reflectivity and precipitation rate for a given storm type (e.g., tropical, convective), vertical structure of reflectivity and/or reflectivity magnitudes. This non-linear relationship is described by the Z-R equation below:

$$Z = A\,R^b \qquad (1)$$

Where Z is the radar reflectivity (measured in units of dBZ), R is the precipitation (precipitation) rate (millimeters per hour), A is the "multiplicative coefficient" and b is the "power coefficient". Both A and b are directly related to the rain drop size distribution (DSD) and rain drop number distribution (DND) within a cloud (Martner and Dubovskiy 2005). The variability in the results of Z versus R is a direct result of differing DSD, DND and air mass characteristics (Dickens 2003). The DSD and DND are determined by complex interactions of

Figure E.9 Example SPAS (denoted as "Exponential") vs. default Z-R relationship (SPAS #1218, Georgia September 2009)

microphysical processes that fluctuate regionally, seasonally, daily, hourly, and even within the same cloud. For these reasons, SPAS calculates an optimized Z-R relationship across the analysis domain each hour based on observed precipitation rates and

radar reflectivity (see Figure E.9).

The National Weather Service (NWS) utilizes different default Z-R algorithms, depending on the precipitation-causing event, to estimate precipitation through the use of NEXRAD radar reflectivity data across the United States (see Figure E.10) (Baeck and Smith 1998 and Hunter 1999). A default Z-R relationship of $Z = 300R^{1.4}$ is the primary algorithm used throughout the continental U.S. However, it is widely known that this, compared to unadjusted radar-aided estimates of precipitation, suffers from deficiencies that may lead to significant over or under-estimation of precipitation.

RELATIONSHIP	Optimum for:	Also recommended for:
Marshall-Palmer $(z=200R^{1.6})$	General stratiform precipitation	
East-Cool Stratiform $(z=130R^{2.0})$	Winter stratiform precipitation - east of continental divide	Orographic rain - East
West-Cool Stratiform $(z=75R^{2.0})$	Winter stratiform precipitation - west of continental divide	Orographic rain - West
WSR-88D Convective $(z=300R^{1.4})$	Summer deep convection	Other non-tropical convection
Rosenfeld Tropical $(z=250R^{1.2})$	Tropical convective systems	

Figure E.10 Commonly used Z-R algorithms used by the NWS

Instead of adopting a standard Z-R, SPAS utilizes a least squares fit procedure for optimizing the Z-R relationship each hour of the SPP. The process begins by determining if sufficient (minimum 12) observed hourly precipitation and radar data pairs are available to compute a reliable Z-R. If insufficient (<12) gauge pairs are available, then SPAS adopts the previous hour Z-R relationship, if available, or applies a user-defined default Z-R algorithm from Figure 9. If sufficient data are available, the one hour sum of NEXRAD reflectivity (Z) is related to the 1-hour precipitation at each gauge. A least-squares-fit exponential function using the data points is computed. The resulting best-fit, one hour-based Z-R is subjected to several tests to determine if the Z-R relationship and its resulting precipitation rates are within a certain tolerance based on the R-squared fit measure and difference between the derived and default Z-R precipitation results. Experience has shown the actual Z-R versus the default Z-R can be significantly different (Figure E.11).
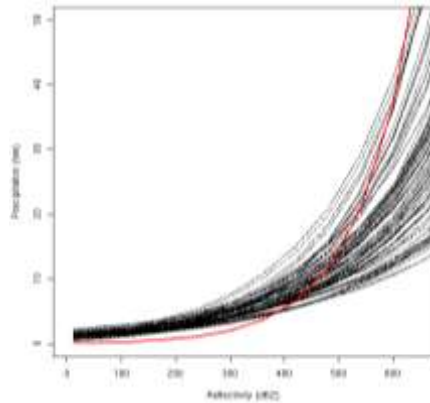
Figure E.11 Comparison of the SPAS optimized hourly Z-R relationships (black lines) versus a default Z=75R2.0 Z-R relationship (red line) for a period of 99 hours for a storm over southern California

Radar-aided Hourly Precipitation Grids

Once a mathematically optimized hourly Z-R relationship is determined, it is applied to the total hourly Z grid to compute an initial precipitation rate (inches/hour) at each grid cell. To account for spatial differences in the Z-R relationship, SPAS computes residuals, the difference between the initial precipitation analysis (via the Z-R equation) and the actual "ground truth" precipitation (observed – initial analysis), at each gauge. The point residuals, also referred to as local biases, are normalized and interpolated to a residual grid using an inverse distance squared weighting algorithm. A radar-based hourly precipitation grid is created by adding the residual grid to the initial grid; this allows the precipitation at the grid cells for which gauges are "on" to be true and faithful to the gauge measurement. The pre-final radar-aided precipitation grid is subject to some final, visual QC checks to ensure the precipitation patterns are consistent with the terrain; these checks are particularly important in areas of complex terrain where even QC'ed radar data can be unreliable. The next incremental improvement with SPAS program will come as the NEXRAD radar sites are upgraded to dual-polarimetric capability.

Radar- and Basemap-Aided Hourly Precipitation Grids

At this stage of the radar approach, a radar- and basemap-aided hourly precipitation grid exists for each hour. At locations with precipitation gauges, the grids are equal, however elsewhere the grids can vary for a number of reasons. For instance, the basemap-aided hourly precipitation grid may depict heavy precipitation in an area of complex terrain, blocked by the radar, whereas the radar-aided hourly precipitation grid may suggest little, if any, precipitation fell in the same area. Similarly, the radar-aided hourly precipitation grid may depict an area of heavy precipitation in flat terrain that the basemap-approach missed since the area of heavy precipitation occurred in an area without gauges. SPAS uses an algorithm to compute the hourly precipitation at each pixel given the two results. Areas that are completely blocked from a radar

signal are accounted for with the basemap-aided results (discussed earlier). The precipitation in areas with orographically effective terrain and reliable radar data are governed by a blend of the basemap- and radar-aided precipitation. Elsewhere, the radar-aided precipitation is used exclusively. This blended approach has proven effective for resolving precipitation in complex terrain, yet retaining accurate radar-aided precipitation across areas where radar data is reliable. Figure E.12 illustrates the evolution of final precipitation from radar reflectivity in an area of complex terrain in southern California.

a)   b)

c)   d)
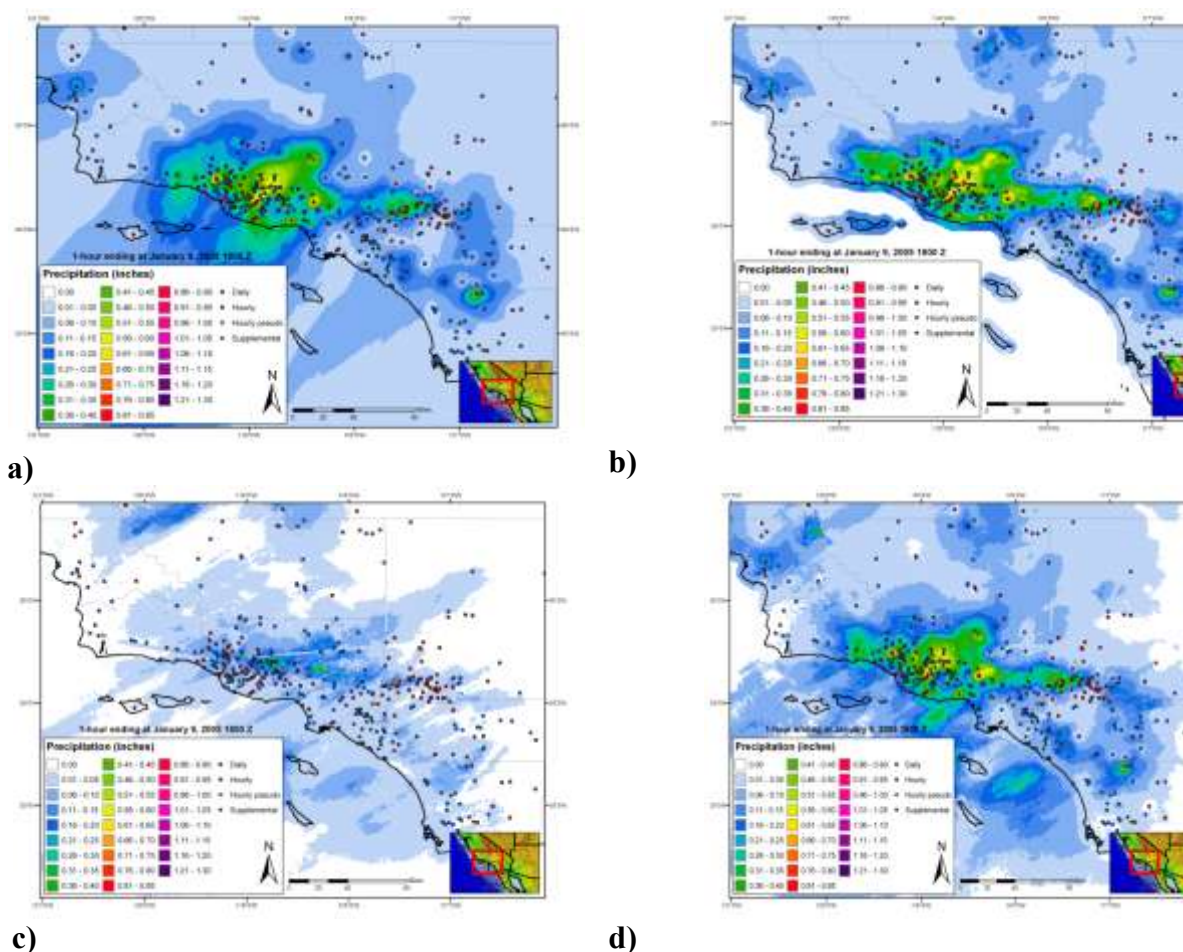
Figure E.12 A series of maps depicting 1-hour of precipitation utilizing (a) inverse distance weighting of gauge precipitation, (b) gauge data together with a climatologically-aided interpolation scheme, (c) default Z-R radar-estimated interpolation (no gauge correction) and (d) SPAS precipitation for a January 2005 storm in southern California

SPAS versus Gauge Precipitation

Performance measures are computed and evaluated each hour to detect errors and inconsistencies in the analysis. The measures include: hourly Z-R coefficients, observed hourly

maximum precipitation, maximum gridded precipitation, hourly bias, hourly mean absolute error (MAE), root mean square error (RMSE), and hourly coefficient of determination (r^2).
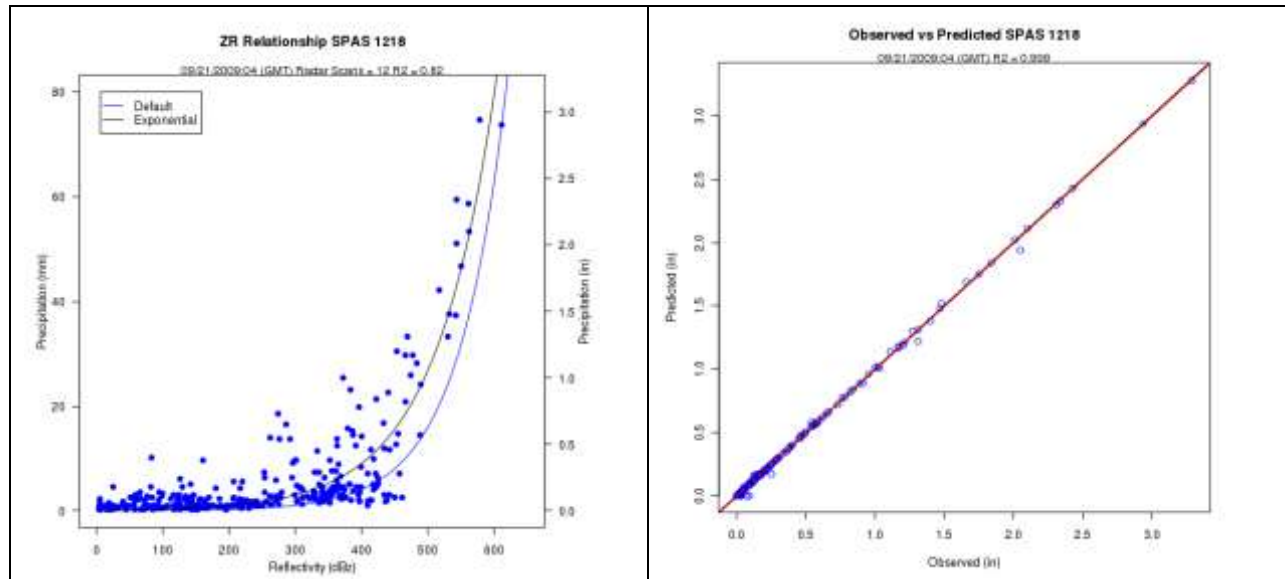
Figure E.13 Z-R plot (a), where the blue line is the SPAS derived Z-R and the black line is the default Z-R, and the (b) associated observed versus SPAS scatter plot at gauge locations

Comparing SPAS-calculated precipitation (R_{spas}) to observed point precipitation depths at the gauge locations provides an objective measure of the consistency, accuracy and bias. Generally speaking SPAS is usually within 5% of the observed precipitation (see Figure E.13). Less-than-perfect correlations between SPAS precipitation depths and observed precipitation at gauged locations could be the result of any number of issues, including:

- **Point versus area:** A rain gauge observation represents a much smaller area than the area sampled by the radar. The area that the radar is sampling is approximately 1 km^2, whereas a rain gauge only samples approximately 8.0×10^{-9} km^2. Furthermore, the radar data represents an average reflectivity (Z) over the grid cell, when in fact the reflectivity can vary across the 1 km^2 grid cell. Therefore, comparing a grid cell radar derived precipitation value to a gauge (point) precipitation depth measured may vary.

- **Precipitation gauge under-catch:** Although we consider gauge data "ground truth," we recognize gauges themselves suffer from inaccuracies. Precipitation gauges, shielded and unshielded, inherently underestimate total precipitation due to local airflow, wind under-catch, wetting, and evaporation. The wind under-catch errors are usually around 5% but can be as large as 40% in high winds (Guo et al. 2001, Duchon and Essenberg 2001, Ciach 2003, Tokay et al. 2010). Tipping buckets miss a small amount of precipitation during each tip of the bucket due to the bucket travel and tip time. As precipitation intensities increase, the volumetric loss of precipitation due to tipping tends to increase.

Smaller tipping buckets can have higher volumetric losses due to higher tip frequencies, but on the other hand capture higher precision timing.

- **Radar Calibration:** NEXRAD radars calibrate reflectivity every volume scan, using an internally generated test. The test determines changes in internal variables such as beam power and path loss of the receiver signal processor since the last off-line calibration. If this value becomes large, it is likely that there is a radar calibration error that will translate into less reliable precipitation estimates. The calibration test is supposed to maintain a reflectivity precision of 1 dBZ. A 1 dBZ error can result in an error of up to 17% in R_{spas} using the default Z-R relationship $Z=300R^{1.4}$. Higher calibration errors will result in higher R_{spas} errors. However, by performing correlations each hour, the calibration issue is minimized in SPAS.

- **Attenuation:** Attenuation is the reduction in power of the radar beams' energy as it travels from the antenna to the target and back. It is caused by the absorption and the scattering of power from the beam by precipitation. Attenuation can result in errors in Z as large as 1 dBZ especially when the radar beam is sampling a large area of heavy precipitation. In some cases, storm precipitation is so intense (>12 inches/hour) that individual storm cells become "opaque" and the radar beam is totally attenuated. Armed with sufficient gauge data however, SPAS will overcome attenuation issues.

- **Range effects:** The curvature of the Earth and radar beam refraction result in the radar beam becoming more elevated above the surface with increasing range. With the increased elevation of the radar beam comes a decrease in Z values due to the radar beam not sampling the main precipitation portion of the cloud (i.e. "over topping" the precipitation and/or cloud altogether). Additionally, as the radar beam gets further from the radar, it naturally samples a larger and larger area, therefore amplifying point versus area differences (described above).

- **Radar Beam Occultation/Ground Clutter:** Radar occultation (beam blockage) results when the radar beam's energy intersects terrain features as depicted in Figure E.14. The result is an increase in radar reflectivity values that can result in higher than normal precipitation estimates. The WDT processing algorithms account for these issues, but SPAS uses GIS spatial interpolation functions to infill areas suffering from poor or no radar coverage.

- **Anomalous Propagation (AP)** - AP is false reflectivity echoes produced by unusual rates of refraction in the atmosphere. WDT algorithms remove most of the AP and false echoes, however in extreme cases the air near the ground may be so cold and dense that a radar beam that starts out moving upward is bent all the way down to the ground. This produces erroneously strong echoes at large distances from the radar. Again, equipped with sufficient gauge data, the SPAS bias corrections will overcome AP issues.
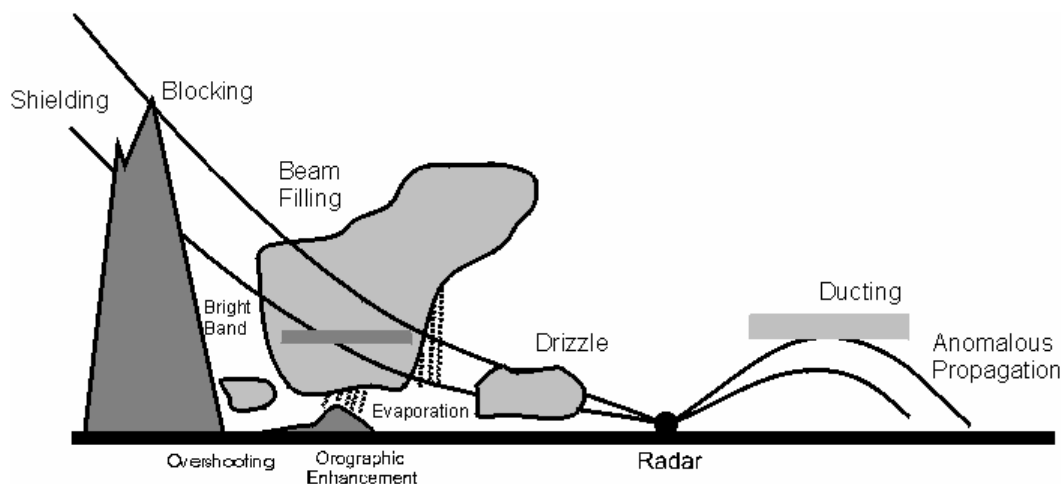
Figure E.14 Depiction of radar artifacts (Source: Wikipedia)

SPAS is designed to overcome many of these short-comings by carefully using radar data for defining the spatial patterns and relative magnitudes of precipitation, but allowing measured precipitation values ("ground truth") at gauges to govern the magnitude. When absolutely necessary, the observed precipitation values at gauges are nudged up (or down) to force the SPAS results to be consistent with observed gauge values. Nudging gauge precipitation values helps to promote better consistency between the gauge value and the gridcell value, even though these two values sometimes should not be the same since they are sampling different area sizes. For reasons discussed in the "SPAS versus Gauge Precipitation" section, the gauge value and gridcell value can vary. Plus, SPAS is designed to toss observed individual hourly values that are grossly inconsistent with the radar data, hence driving a difference between the gauge and gridcell. In general, when the gauge and gridcell value differ by more than 15% and/or 0.50 inches, and the gauge data has been validated, then it is justified to nudge (artificially increase or decrease) the observed gauge value to "force" SPAS to derive a gridcell value equal to the observed value. Sometimes simply shifting the gauge location to an adjacent gridcell resolves the problems. Regardless, a large gauge versus gridcell difference is a "red flag" and sometimes the result of an erroneous gauge value or a mis-located gauge, but in some cases the difference can only be resolved by nudging the precipitation value.

Before final results are declared, a precipitation intensity check is conducted to ensure the spatial patterns and magnitudes of the maximum storm intensities at 1-, 6-, 12-, etc. hours are consistent with surrounding gauges and published reports. Any erroneous data are corrected and SPAS re-run. Considering all of the QA/QC checks in SPAS, it typically requires 5-15 basemap SPAS runs and, if radar data is available, another 5-15 radar-aided runs, to arrive at the final output.

Test Cases

To check the accuracy of the DAD software, three test cases were evaluated.
"Pyramidville" Storm

E-   21

The first test was that of a theoretical storm with a pyramid shaped isohyetal pattern. This case was called the Pyramidville storm. It contained 361 hourly stations, each occupying a single grid cell. The configuration of the Pyramidville storm (see Figure E.15) allowed for uncomplicated and accurate calculation of the analytical DA truth independent of the DAD software. The main motivation of this case was to verify that the DAD software was properly computing the area sizes and average depths.

1.   Storm center: 39°N 104°W
2.   Duration: 10-hours
3.   Maximum grid cell precipitation: 1.00"
4.   Grid cell resolution: 0.06 sq.-miles (361 total cells)
5.   Total storm size: 23.11 sq-miles
6.   Distribution of precipitation:
    Hour 1:   Storm drops 0.10" at center (area 0.06 sq-miles)
    Hour 2:   Storm drops 0.10" over center grid cell AND over one cell width around hour 1
                  center
     Hours 3-10:
          1.   Storm drops 0.10" per hour at previously wet area, plus one cell width around previously
               wet area
          2.   Area analyzed at every 0.10"
          3.   Analysis resolution: 15-sec (~.25 square miles)
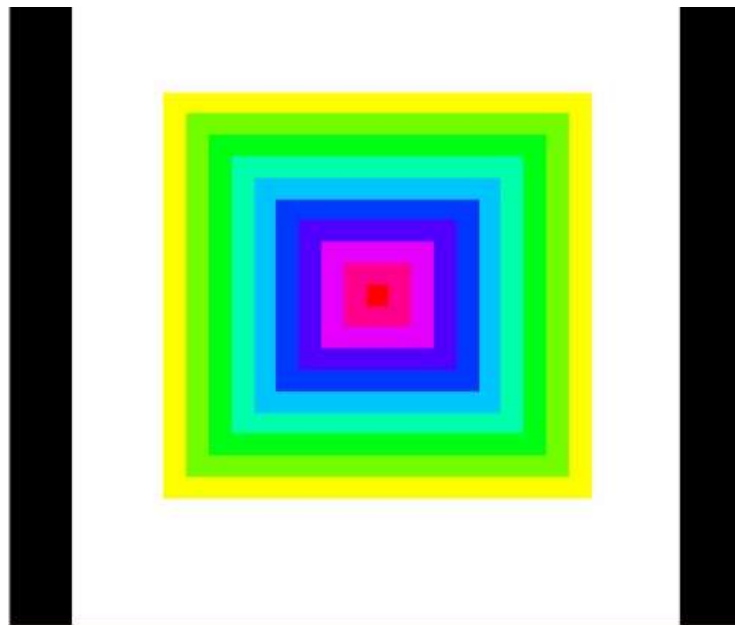
Figure E.15 "Pyramidville" Total precipitation. Center = 1.00", Outside edge = 0.10"

The analytical truth was calculated independent of the DAD software, and then compared to the DAD output. The DAD software results were equal to the truth, thus demonstrating that the DA estimates were properly calculated (Figure E.16).
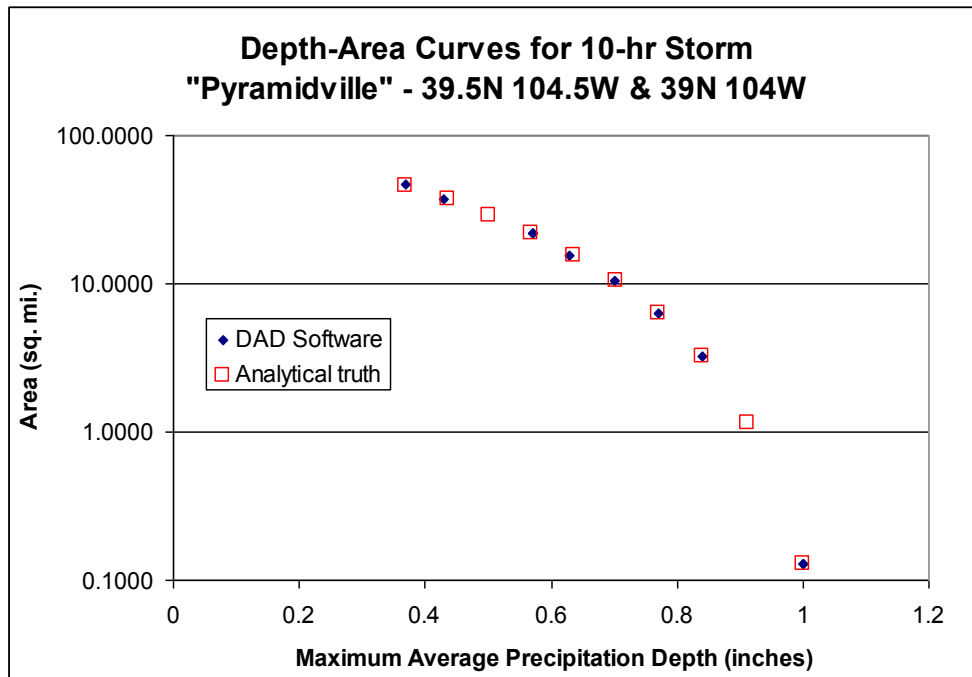
Figure E.16 10-hour DA results for "Pyramidville"; truth vs. output from DAD software

The Pyramidville storm was then changed such that the mass curve and spatial interpolation methods would be stressed. Test cases included:

- Two-centers, each center with 361 hourly stations
- A single center with 36 hourly stations, 0 daily stations
- A single center with 3 hourly stations and 33 daily stations

As expected, results began shifting from the 'truth,' but minimally and within the expected uncertainty.

Ritter, Iowa Storm, June 7, 1953

Ritter, Iowa was chosen as a test case for a number of reasons. The NWS had completed a storm analysis, with available DAD values for comparison. The storm occurred over relatively flat terrain, so orographics was not an issue. An extensive "bucket survey" provided a great number of additional observations from this event. Of the hundreds of additional reports, about 30 of the most accurate reports were included in the DAD analysis.

The DAD software results are very similar to the NWS DAD values (Table E.2).

Table E.2 The percent difference [(AWA-NWS)/NWS] between the AWA DA results and those
published by the NWS for the 1953 Ritter, Iowa storm

%
Difference

Area (sq.mi.)	Duration (hours)			
	6	12	24	total
10	-15%	-7%	2%	2%
100	-7%	-6%	1%	1%
200	2%	0%	9%	9%
1000	-6%	-7%	4%	4%
5000	-13%	-8%	2%	2%
10000	-14%	-6%	0%	0%

Westfield, Massachusetts Storm, August 8, 1955

Westfield, Massachusetts was also chosen as a test case for a number of reasons. It is a
probable maximum precipitation (PMP) driver for the northeastern United States. Also, the
Westfield storm was analyzed by the NWS and the DAD values are available for comparison.
Although this case proved to be more challenging than any of the others, the final results are very
similar to those published by the NWS (Table E.3).

Table E.3 The percent difference [(AWA-NWS)/NWS] between the AWA DA results and those
published by the NWS for the 1955 Westfield, Massachusetts storm

%
Difference

Area (sq. mi.)	Duration (hours)						
	6	12	24	36	48	60	total
10	2%	3%	0%	1%	-1%	0%	2%
100	-5%	2%	4%	-2%	-6%	-4%	-3%
200	-6%	1%	1%	-4%	-7%	-5%	-5%
1000	-4%	-2%	1%	-6%	-7%	-6%	-3%
5000	3%	2%	-3%	-3%	-5%	-5%	0%
10000	4%	9%	-5%	-4%	-7%	-5%	1%
20000	7%	12%	-6%	-3%	-4%	-3%	3%

The principal components of SPAS are: storm search, data extraction, quality control
(QC), conversion of daily precipitation data into estimated hourly data, hourly and total storm
precipitation grids/maps and a complete storm-centered DAD analysis.

OUTPUT

Armed with accurate, high-resolution precipitation grids, a variety of customized output can be created (see Figures G.17a-d). Among the most useful outputs are sub-hourly precipitation grids for input into hydrologic models. Sub-hourly (i.e. 5-minute) precipitation grids are created by applying the appropriate optimized hourly Z-R (scaled down to be applicable for instantaneous Z) to each of the individual 5-minute radar scans; 5-minutes is often the native scan rate of the radar in the US. Once the scaled Z-R is applied to each radar scan, the resulting precipitation is summed up. The proportion of each 5-minute precipitation to the total 1-hour radar-aided precipitation is calculated. Each 5-minute proportion (%) is then applied to the quality controlled, bias corrected 1-hour total precipitation (created above) to arrive at the final 5-minute precipitation for each scan. This technique ensures the sum of 5-minute precipitation equals that of the quality controlled, bias corrected 1-hour total precipitation derived initially.

Depth-area-duration (DAD) tables/plots, shown in Figure E.17d, are computed using a highly-computational extension to SPAS. DADs provide an objective three dimensional (magnitude, area size, and duration) perspective of a storms' precipitation. SPAS DADs are computed using the procedures outlined by the NWS Technical Paper 1 (1946).

Figure E.17 Various examples of SPAS output, including (a) total storm map and its associated (b) basin average precipitation time series, (c) total storm precipitation map, (d) depth-area-duration (DAD) table and plot, and (e) precipitation gauge catalog with total storm statistics.

SUMMARY

Grounded on years of scientific research with a demonstrated reliability in post-storm analyses, SPAS is a hydro-meteorological tool that provides accurate precipitation analyses for a

variety of applications. SPAS has the ability to compute precise and accurate results by using sophisticated timing algorithms, "basemaps", a variety of precipitation data and most importantly NEXRAD weather radar data (if available). The approach taken by SPAS relies on hourly, daily and supplemental precipitation gauge observations to provide quantification of the precipitation amounts while relying on basemaps and NEXRAD data (if available) to provide the spatial distribution of precipitation between precipitation gauge sites. By determining the most appropriate coefficients for the Z-R equation on an hourly basis, the approach anchors the precipitation amounts to accepted precipitation gauge data while using the NEXRAD data to distribute precipitation between precipitation gauges for each hour of the storm. Hourly Z-R coefficient computations address changes in the cloud microphysics and storm characteristics as the storm evolves. Areas suffering from limited or no radar coverage, are estimated using the spatial patterns and magnitudes of the independently created basemap precipitation grids. Although largely automated, SPAS is flexible enough to allow hydro-meteorologists to make important adjustments and adapt to any storm situation.

REFERENCES

Baeck M.L., Smith J.A., 1998: "Precipitation Estimation by the WSR-88D for Heavy Precipitation Events", Weather and Forecasting: Vol. 13, No. 2, pp. 416–436.

Ciach, G.J., 2003: Local Random Errors in Tipping-Bucket Rain Gauge Measurements. *J. Atmos. Oceanic Technol.*, **20**, 752–759.

Dickens, J., 2003: "On the Retrieval of Drop Size Distribution by Vertically Pointing Radar", American Meteorological Society 32nd Radar Meteorology Conference, Albuquerque, NM, October 2005.

Duchon, C.E., and G.R. Essenberg, 2001: Comparative Precipitation Observations from Pit and Above Ground Rain Gauges with and without Wind Shields, *Water Resources Research,* Vol. 37, N. 12, 3253-3263.

Faulkner, E., T. Hampton, R.M. Rudolph, and Tomlinson, E.M., 2004: Technological Updates for PMP and PMF – Can They Provide Value for Dam Safety Improvements? Association of State Dam Safety Officials Annual Conference, Phoenix, Arizona, September 26- 30, 2004

Guo, J. C. Y., Urbonas, B., and Stewart, K., 2001: Rain Catch under Wind and Vegetal Effects. ASCE, *Journal of Hydrologic Engineering*, Vol. 6, No. 1.

Hunter, R.D. and R.K. Meentemeyer, 2005: Climatologically Aided Mapping of Daily Precipitation and Temperature, Journal of Applied Meteorology, October 2005, Vol. 44, pp. 1501-1510.

Hunter, S.M., 1999: Determining WSR-88D Precipitation Algorithm Performance Using The Stage III Precipitation Processing System, Next Generation Weather Radar Program, WSR-88D Operational Support Facility, Norman, OK.

Lakshmanan, V. and M. Valente, 2004: Quality control of radar reflectivity data using satellite data and surface observations, 20th Int'l Conf. on Inter. Inf. Proc. Sys. (IIPS) for Meteor., Ocean., and Hydr., Amer. Meteor. Soc., Seattle, CD-ROM, 12.2.

Martner, B.E, and V. Dubovskiy, 2005: Z-R Relations from Raindrop Disdrometers: Sensitivity To Regression Methods And DSD Data Refinements, 32nd Radar Meteorology Conference, Albuquerque, NM, October, 2005

Tokay, A., P.G. Bashor, and V.L. McDowell, 2010: Comparison of Rain Gauge Measurements in the Mid-Atlantic Region. *J. Hydrometeor.*, **11**, 553-565.

Tomlinson, E.M., W.D. Kappel, T.W. Parzybok, B. Rappolt, 2006: Use of NEXRAD Weather Radar Data with the Storm Precipitation Analysis System (SPAS) to Provide High Spatial

Resolution Hourly Precipitation Analyses for Runoff Model Calibration and Validation, ASDSO Annual Conference, Boston, MA.

Tomlinson, E.M. and T.W. Parzybok, 2004: Storm Precipitation Analysis System (SPAS), proceedings of Association of Dam Safety Officials Annual Conference, Technical Session II, Phoenix, Arizona.

_____, R.A. Williams, and T.W. Parzybok, September 2003: Site-Specific Probable Maximum Precipitation (PMP) Study for the Great Sacandaga Lake / Stewarts Bridge Drainage Basin, Prepared for Reliant Energy Corporation, Liverpool, New York.

_____, R.A. Williams, and T.W. Parzybok, September 2003: Site-Specific Probable Maximum Precipitation (PMP) Study for the Cherry Creek Drainage Basin, Prepared for the Colorado Water Conservation Board, Denver, CO.

_____, Kappel W.D., Parzybok, T.W., Hultstrand, D., Muhlestein, G., and B. Rappolt, May 2008: Site-Specific Probable Maximum Precipitation (PMP) Study for the Wanahoo Drainage Basin, Prepared for Olsson Associates, Omaha, Nebraska.

_____, Kappel W.D., Parzybok, T.W., Hultstrand, D., Muhlestein, G., and B. Rappolt, June 2008: Site-Specific Probable Maximum Precipitation (PMP) Study for the Blenheim Gilboa Drainage Basin, Prepared for New York Power Authority, White Plains, NY.

_____, Kappel W.D., and T.W. Parzybok, February 2008: Site-Specific Probable Maximum Precipitation (PMP) Study for the Magma FRS Drainage Basin, Prepared for AMEC, Tucson, Arizona.

_____, Kappel W.D., Parzybok, T.W., Hultstrand, D., Muhlestein, G., and P. Sutter, December 2008: Statewide Probable Maximum Precipitation (PMP) Study for the state of Nebraska, Prepared for Nebraska Dam Safety, Omaha, Nebraska.

_____, Kappel, W.D., and Tye W. Parzybok, July 2009: Site-Specific Probable Maximum Precipitation (PMP) Study for the Scoggins Dam Drainage Basin, Oregon.

_____, Kappel, W.D., and Tye W. Parzybok, February 2009: Site-Specific Probable Maximum Precipitation (PMP) Study for the Tuxedo Lake Drainage Basin, New York.

_____, Kappel, W.D., and Tye W. Parzybok, February 2010: Site-Specific Probable Maximum Precipitation (PMP) Study for the Magma FRS Drainage Basin, Arizona.

_____, Kappel W.D., Parzybok, T.W., Hultstrand, D.M., Muhlestein, G.A., March 2011: Site-Specific Probable Maximum Precipitation Study for the Tarrant Regional Water District, Prepared for Tarrant Regional Water District, Fort Worth, Texas.

_____, Kappel, W.D., Hultstrand, D.M., Muhlestein, G.A., and T. W. Parzybok, November 2011: Site-Specific Probable Maximum Precipitation (PMP) Study for the Lewis River basin, Washington State.

_____, Kappel, W.D., Hultstrand, D.M., Muhlestein, G.A., and T. W. Parzybok, December 2011: Site-Specific Probable Maximum Precipitation (PMP) Study for the Brassua Dam basin, Maine.

U.S. Weather Bureau, 1946: Manual for Depth-Area-Duration analysis of storm precipitation. *Cooperative Studies Technical Paper No. 1*, U.S. Department of Commerce, Weather Bureau, Washington, D.C., 73pp.

Appendix F

Short Storm List Storm Analysis

See Separate Binding

Appendix G

PMP Values Compared to SPAS Rainfall Values at Storm Center Locations

Comparisons were made between the PMP values derived in this study and the actual rainfall amounts analyzed by SPAS at each SPAS storm center location. The comparisons provided a sense of the amount of envelopment at the locations with the highest analyzed rainfall amounts compared to PMP at those locations and therefore how much larger PMP values are than the highest analyzed rainfall amounts to occur in Arizona. Tables G.1 through G.3 provide the results of these comparisons, while Figure G.1 through G.3 display the locations and the resulting comparisons.

Table G.1 Comparison of Local Storm PMP values against SPAS analyzed rainfall values at each storm center for the 1- and 6-hour durations

Storm ID	Storm Place Name	Date	Latitude	Longitude	1-hr Storm Rainfall	6-hr Storm Rainfall	1-hr Local PMP	6-hr Local PMP	Storm Percent of 1-hour PMP	Storm Percent of 6-hour PMP
1042_1	Yuma Valley, AZ	Aug. 1977	32.611	-114.631	2.18	5.10	12.51	14.98	17%	34%
1043_1	Sols Wash, AZ	Aug. 2000	34.130	-113.080	1.39	4.59	12.79	16.80	11%	27%
1051_1	Magma, AZ	Jul. 2008	33.194	-111.347	1.64	4.30	9.88	10.46	17%	41%
1059_1	Sahaurita, AZ	Sep. 1964	32.006	-110.904	1.60	3.20	6.61	13.19	24%	24%
1060_1	North Tucson, AZ	Sep. 1964	32.304	-111.004	3.33	5.05	6.44	12.85	52%	39%
1061_1	Thatcher, AZ	Sep. 1939	32.763	-109.829	2.88	4.00	5.73	11.44	50%	35%
1062_1	Phoenix, AZ	June. 1972	33.517	-112.023	3.59	5.08	9.66	10.23	37%	50%
1063_1	Prescott, AZ	Sep. 1983	34.621	-112.554	3.70	12.08	9.80	16.16	38%	75%
1064_1	Wellton, AZ	Aug. 1955	32.579	-114.338	4.38	6.34	12.79	15.27	34%	42%
1073_1	Sedona, AZ	Jul. 1975	34.882	-111.765	N/A	3.78	11.95	13.53	N/A	28%
1085_1	Wenden Bouse, AZ	Aug. 2008	33.823	-113.542	3.69	4.30	12.79	16.42	29%	26%
1086_1	Tucson, AZ	Sep. 1996	32.390	-110.800	3.21	5.47	7.87	15.69	41%	35%
1087_1	Sabino Canyon, AZ	Jul. 1999	32.385	-110.705	2.72	6.59	7.66	15.28	36%	43%
1091_1	Camp Creek, AZ	Sep. 2005	34.040	-111.810	2.99	4.41	12.51	15.21	24%	29%
1091_2	Camp Creek, AZ	Sep. 2005	34.380	-111.180	3.16	4.61	10.01	16.79	32%	27%
1094_1	Circle City, AZ	Aug. 2003	33.950	-112.340	4.07	8.80	11.78	13.95	35%	63%
1096_1	Queen Creek, AZ	Aug. 1954	33.203	-111.145	2.39	7.51	11.87	13.38	20%	56%
1109_1	Roosevelt Lakes, AZ	Sep. 2003	33.596	-110.996	5.47	10.91	11.42	12.86	48%	85%
1113_1	Petrified Forest, AZ	Jul. 2007	34.725	-109.645	5.83	6.29	7.30	7.86	80%	80%
1115_1	Joseph City, AZ	Jul. 1998	34.956	-110.335	3.66	4.16	7.19	7.74	51%	54%
1118_1	Seligman, AZ	Jul. 1970	35.317	-112.883	4.79	5.76	9.60	10.35	50%	56%
1122_1	Harquahala Valley, AZ	Sep. 1984	33.488	-113.254	2.96	7.70	12.79	13.54	23%	57%
1128_1	Havasupai, AZ	Aug. 2008	35.885	-112.475	1.67	3.36	9.11	9.81	18%	34%
1128_2	Havasupai, AZ	Aug. 2008	35.155	-112.575	2.27	4.18	8.62	14.29	26%	29%
1128_3	Havasupai, AZ	Aug. 2008	35.695	-112.375	1.86	2.05	9.20	9.91	20%	21%
1130_1	Page, AZ	Aug. 1963	36.917	-111.450	1.72	1.97	8.33	8.98	21%	22%
1131_1	Bluff, UT	Aug. 2001	37.283	-109.550	5.68	6.12	6.44	6.94	88%	88%
1166_1	Wagon Bow, AZ	Jul. 2009	34.865	-113.455	3.71	7.59	10.59	18.02	35%	42%
1249_1	Blanding, UT	Aug. 1968	37.826	-109.543	1.00	3.49	8.12	8.75	12%	40%
1262_1	Anthem, AZ	Jul. 2012	33.859	-112.141	3.33	5.34	11.15	11.81	30%	45%

Note, the 1-hour PMP was not calculated for SPAS 1073_1, Sedona, AZ July 1975. Therefore, an N/A is inserted for the storm percent of 1-hour PMP cell.
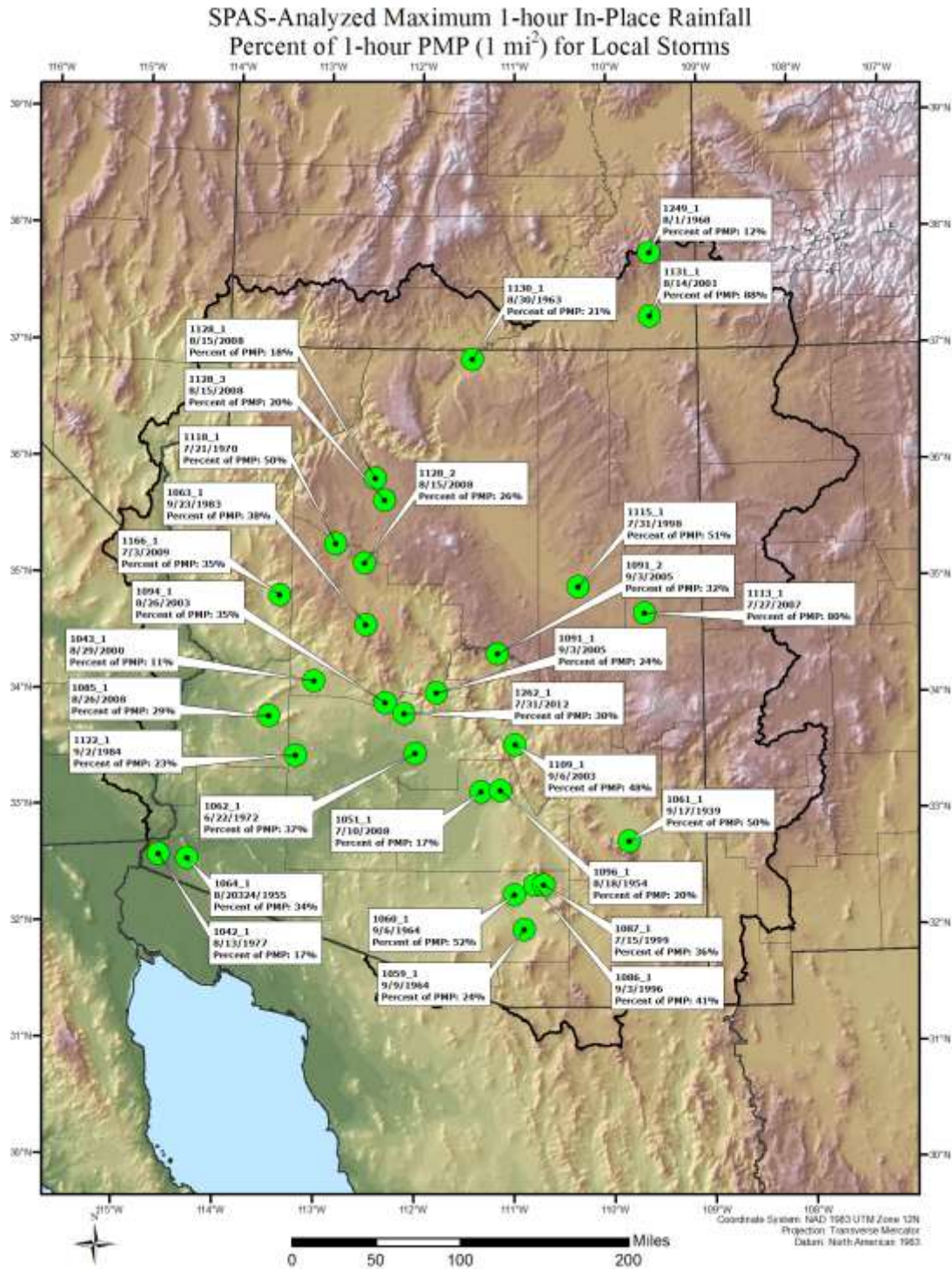
Figure G.1 Comparison of Local Storm PMP values against SPAS analyzed rainfall values at each storm center at the 1-hour duration. No comparison is available for the SPAS 1073_1, Sedona, AZ July 1975 event because there was no 1-hour PMP calculated for that storm.
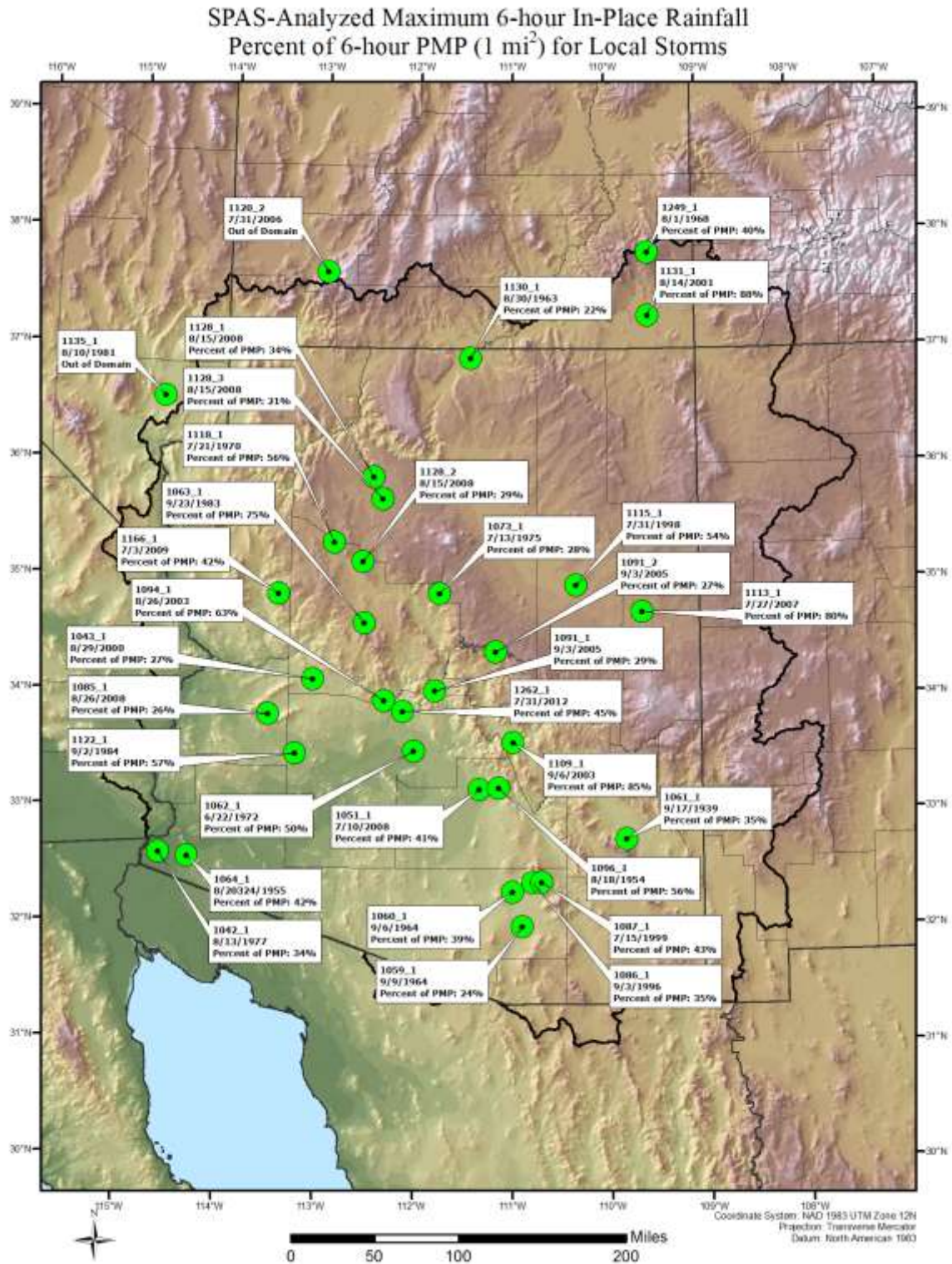
Figure G.2 Comparison of Local Storm PMP values against SPAS analyzed rainfall values at each storm center at the 6-hour duration

Table G.2 Comparison of Remnant Tropical Storm PMP values against SPAS analyzed rainfall values at each storm center for the 24- and 72-hour durations

Storm ID	Storm Place Name	Date	Latitude	Longitude	24-hr Storm Rainfall	72-hr Storm Rainfall	24-hr General PMP	72-hr General PMP	Storm Percent of 24-hour PMP	Storm Percent of 72-hour PMP
1074_2	Mt. Graham, AZ	Sep. 1983	33.288	-109.104	6.45	12.45	12.35	14.19	52%	88%
1075_1	Workman Creek, AZ	Sep. 1970	31.961	-111.613	6.05	7.56	20.39	25.18	30%	30%
1075_2	Workman Creek, AZ	Sep. 1970	33.820	-110.904	11.09	11.80	26.31	29.35	42%	40%
1075_3	Workman Creek, AZ	Sep. 1970	35.495	-110.421	6.25	6.75	7.38	7.97	85%	85%
1076_1	Crown King, AZ	Aug. 1951	34.013	-112.263	6.93	10.01	16.85	19.28	41%	52%
1077_1	Crossman Peak, AZ	Sep. 1939	34.546	-114.196	5.04	9.31	12.64	17.35	40%	54%
1077_2	Crossman Peak, AZ	Sep. 1939	34.771	-113.779	5.07	9.21	13.41	18.48	38%	50%
1077_3	Crossman Peak, AZ	Sep. 1939	36.338	-112.071	4.35	6.78	15.30	16.52	28%	41%
1083_1	Senora Desert Museum, AZ	Sep. 1962	32.179	-111.388	7.07	7.07	15.10	18.03	47%	39%
1083_2	Senora Desert Museum, AZ	Sep. 1962	32.696	-109.854	3.72	3.72	17.18	20.41	22%	18%
1084_1	Harquahala Mountain, AZ	Sep. 1997	33.815	-113.335	12.05	12.09	14.49	19.40	83%	62%
1084_2	Harquahala Mountain, AZ	Sep. 1997	35.005	-113.895	7.05	7.26	16.64	18.53	42%	39%
1084_3	Harquahala Mountain, AZ	Sep. 1997	33.835	-113.650	7.78	7.83	11.14	16.34	70%	48%
1088_1	Queen Valley, AZ	Sep. 2004	34.520	-113.860	6.80	6.80	10.70	15.24	64%	45%
1088_2	Queen Valley, AZ	Sep. 2004	34.730	-113.020	9.79	9.79	17.42	21.99	56%	45%
1097_1	Nogales, AZ	Oct. 1977	31.339	-110.935	7.09	15.50	15.24	18.50	47%	84%
1102_2	Joanne, AZ	Oct. 1972	33.821	-110.921	6.08	9.91	29.49	32.86	21%	30%
1102_3	Joanne, AZ	Oct. 1972	37.838	-109.471	2.43	3.88	13.75	14.85	18%	26%

Figure G.3 Comparison of Remnant Tropical Storm PMP values against SPAS analyzed rainfall values at each storm center at the 24-hour duration

Figure G.4 Comparison of Remnant Tropical Storm PMP values against SPAS analyzed rainfall
values at each storm center at the 72-hour duration

Table G.3 Comparison of General Frontal Storm PMP values against SPAS analyzed rainfall values at each storm center for the 24- and 72-hour durations

Storm ID	Storm Place Name	Date	Latitude	Longitude	24-hr Storm Rainfall	72-hr Storm Rainfall	24-hr General PMP	72-hr General PMP	Storm Percent of 24-hour PMP	Storm Percent of 72-hour PMP
1133_1	Jakes Corner, AZ	Dec. 1967	31.679	-110.863	3.09	3.99	9.94	16.56	31%	24%
1133_2	Jakes Corner, AZ	Dec. 1967	34.021	-111.379	7.05	8.70	12.30	17.61	57%	49%
1134_1	Big Pine Flat, AZ	Dec. 1978	33.425	-111.445	3.21	5.25	7.09	13.29	45%	40%
1134_2	Big Pine Flat, AZ	Dec. 1978	33.675	-111.335	6.36	10.15	13.82	19.80	46%	51%
1134_3	Big Pine Flat, AZ	Dec. 1978	32.445	-110.775	7.05	9.17	9.64	15.53	73%	59%
1137_1	Young, AZ	Nov. 1965	33.988	-112.354	2.51	4.09	8.65	12.39	29%	33%
1137_2	Young, AZ	Nov. 1965	33.821	-110.921	7.13	10.88	14.68	21.02	49%	52%
1137_4	Young, AZ	Nov. 1965	36.813	-109.179	2.44	2.72	6.19	8.86	39%	31%
1137_6	Young, AZ	Nov. 1965	32.438	-110.763	3.35	5.41	9.51	15.31	35%	35%
1138_1	Crown King, AZ	Feb. 1980	34.013	-112.263	5.67	7.84	8.64	12.38	66%	63%
1138_2	Crown King, AZ	Feb. 1980	34.221	-112.346	4.52	8.37	13.44	19.25	34%	43%
1138_3	Crown King, AZ	Feb. 1980	36.313	-112.079	3.58	5.04	9.74	13.95	37%	36%
1139_1	Knoles Hole Spring, AZ	Jan. 1993	33.038	-111.004	3.55	5.62	7.82	12.61	45%	45%
1139_2	Crown King, AZ	Jan. 1993	33.829	-110.913	7.34	11.81	14.68	21.02	50%	56%
1139_3	Crown King, AZ	Jan. 1993	32.413	-110.746	7.03	9.55	8.96	14.43	78%	66%
1141_1	Junipine, AZ	Dec. 1966	34.979	-111.771	5.17	9.49	10.45	14.97	49%	63%
1141_2	Junipine, AZ	Dec. 1966	36.229	-112.063	7.89	11.30	8.97	12.84	88%	88%
1141_3	Junipine, AZ	Dec. 1966	36.821	-109.188	1.84	2.63	5.95	8.52	31%	31%
1144_1	Mt. Ord, AZ	Jan. 1916	33.754	-111.563	5.78	7.21	10.88	15.58	53%	46%
1144_2	Mt. Ord, AZ	Jan. 1916	33.904	-111.413	5.85	10.09	14.05	20.12	42%	50%
1144_3	Mt. Ord, AZ	Jan. 1916	35.113	-108.196	2.50	5.67	5.94	8.51	42%	67%
1144_4	Mt. Ord, AZ	Jan. 1916	32.429	-110.813	5.99	9.01	9.01	14.90	66%	60%
1147_1	Big Pine Flat, AZ	Feb. 2005	33.355	-111.325	5.18	5.83	9.04	12.94	57%	45%
1147_2	Big Pine Flat, AZ	Feb. 2005	33.685	-111.325	6.06	8.42	13.82	19.80	44%	43%
1149_1	Cooks Mesa, AZ	Nov. 2007	35.410	-114.160	5.11	5.31	6.41	12.59	80%	42%
1149_2	Cooks Mesa, AZ	Nov. 2007	34.460	-111.230	6.94	8.33	12.19	17.45	57%	48%
1149_3	Cooks Mesa, AZ	Nov. 2007	32.440	-110.780	5.23	6.31	9.64	15.53	54%	41%
1150_1	Bear Spring, AZ	Feb. 1978	33.704	-111.596	5.87	11.71	9.38	13.44	63%	87%
1150_2	Bear Spring, AZ	Feb. 1978	34.038	-111.488	7.12	14.00	13.95	19.98	51%	70%
1154_1	Horseshoe Dam, AZ	Oct. 1959	33.038	-110.996	5.63	6.43	7.82	12.61	72%	51%
1154_2	Horseshoe Dam, AZ	Oct. 1959	33.938	-111.738	8.04	10.43	12.06	17.27	67%	60%
1200_1	Peterson Ranch, AZ	Jan. 2010	34.080	-112.160	5.63	7.40	8.43	12.08	67%	61%
1200_2	Peterson Ranch, AZ	Jan. 2010	33.810	-110.910	9.72	13.43	13.31	19.07	73%	70%
1200_3	Peterson Ranch, AZ	Jan. 2010	35.990	-113.840	3.22	4.99	4.74	9.23	68%	54%
1200_4	Peterson Ranch, AZ	Jan. 2010	31.760	-110.840	3.67	5.52	8.98	14.97	41%	37%

Figure G.5 Comparison of General Frontal Storm PMP values against SPAS analyzed rainfall values at each storm center at the 24-hour duration
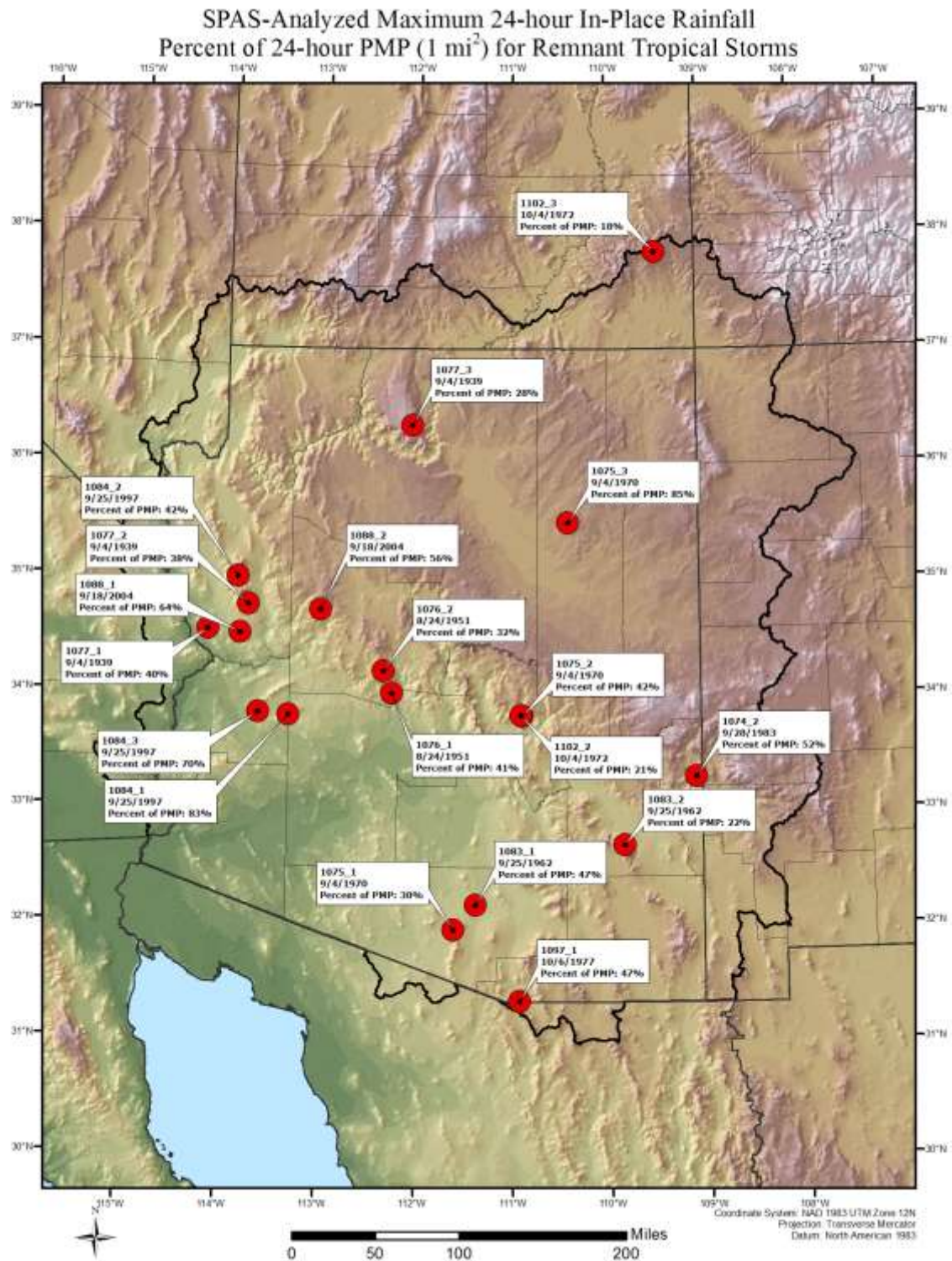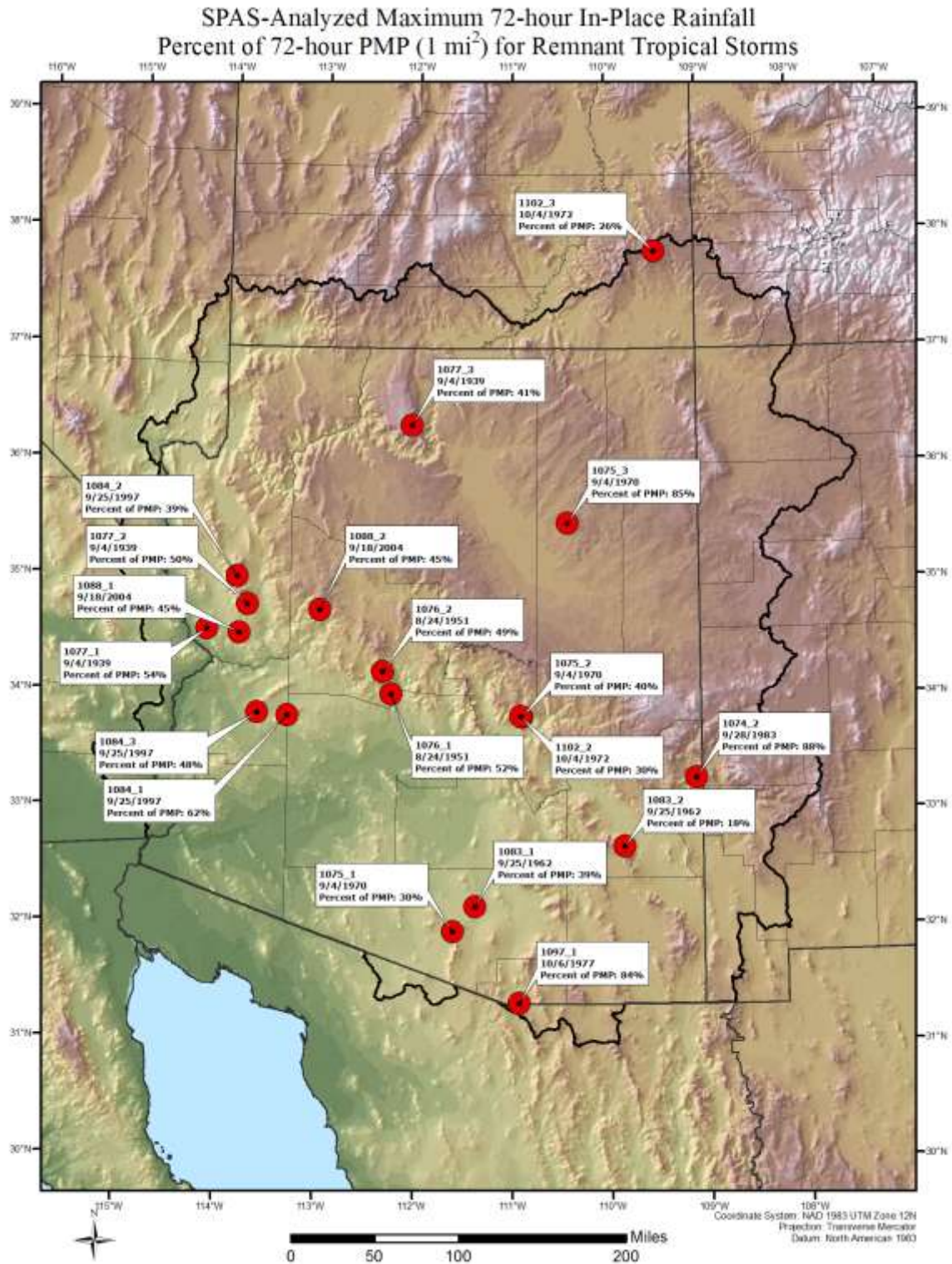
Figure G.6 Comparison of General Frontal Storm PMP values against SPAS analyzed rainfall values at each storm center at the 72-hour duration

Appendix H

PYTHON Code Used in the PMP Evaluation Tool

```
''' -------------------------------------------------------------------------
Name: PMP_Calc.py

Version: 1.00

ArcGIS Version: ArcGIS Desktop 10.1 SP1 (2013)

Author: Applied Weather Associates, LLC for Arizona Department of Water Resources

Usage:  The tool is designed to be executed within an the ArcMap or ArcCatalog desktop environment.

Required Arguments:
- A basin outline polygon shapefile or feature class

Description:
    This tool calculates PMP depths for a given drainage basin for the
specified durations (1-,2-,3-,4-,5-, and 6-hour for local storms; 6-, 12-, 18-,
24-, 48-, and 72-hour for general winter and tropical storms.  PMP values are
calculated (in inches) for each grid point (spaced at 90 arc-second intervals)
within (or adjacent to) the drainage basin. A GRID raster layer is created over
the basin from the grid point PMP values. The PMP values are then temporally
distributed to the specified time steps for the duration of the storm analysis
(36 ten-minute blocks for local storms and 12 six-hour blocks for tropical and
general winter storms).
-------------------------------------------------------------------------'''

#############################################################################
## import Python modules

import sys
import arcpy
from arcpy import env
import arcpy.management as dm
import arcpy.conversion as con

arcpy.env.overwriteOutput = True                       # Set overwrite option

#############################################################################
## get input parameters

basin = arcpy.GetParameter(0)                          # get AOI Basin Shapefile
home = arcpy.GetParameterAsText(1)                         # get location of 'PMP' Project Folder

dadGDB = home + "\\Input\\DAD_Tables.gdb"                   # location of DAD tables
adjFactGDB = home + "\\Input\\Storm_Adj_Factors.gdb"            # location of feature datasets containing total adjustment factors

def pmpAnalysis(aoiBasin, stormType):

  #############################################################################
  ## Create PMP Point Feature Class from points within AOI basin and add fields
  def createPMPfc():
    global outPath
    env.workspace = outPath + "PMP.gdb"                          # set environment workspace

    arcpy.AddMessage("\nCreating feature class: PMP_Points...")
    dm.MakeFeatureLayer(home + "\\Input\Non_Storm_Data.gdb\\Vector_Grid\\Vector_Grid_AZ", "vgLayer")   # make a feature layer
of vector grid cells
```

```
    dm.SelectLayerByLocation("vgLayer", "INTERSECT", aoiBasin)                    # select the vector grid cells that intersect the
aoiBasin polygon
    dm.MakeFeatureLayer(home + "\\Input\Non_Storm_Data.gdb\\Vector_Grid\\Grid_Points_AZ", "gpLayer")   # make a feature layer
of grid points
    dm.SelectLayerByLocation("gpLayer", "HAVE_THEIR_CENTER_IN", "vgLayer")                # select the grid points within the
vector grid selection
    con.FeatureClassToFeatureClass("gpLayer", env.workspace, "PMP_Points")                # save feature layer as "PMP_Points"
feature class
    arcpy.AddMessage("(" + str(dm.GetCount("gpLayer")) + " grid points will be analyzed)")

    # Add PMP Fields
    for dur in durList:
        arcpy.AddMessage("\n\t...adding field: PMP_" + str(dur))
        dm.AddField("PMP_Points", "PMP_" + dur, "DOUBLE")

    # Add STORM Fields (this string values identifies the driving storm by SPAS ID number)
    for dur in durList:
        arcpy.AddMessage("\n\t...adding field: STORM_" + str(dur))
        dm.AddField("PMP_Points", "STORM_" + dur, "TEXT", "", "", 16)

    # Add DIST Fields (DIST = "temporally distributed PMP")
    if stormType == "General":
        timeSteps = 12
        distList = ["06", "12", "18", "24", "30", "36", "42", "48", "54", "60", "66", "72"]     # 6-hour durational blocks for temporal distibution.
(eg. 'DIST_06' = 0 to 6-hour block.)
    elif stormType == "Tropical":
        timeSteps = 12
        distList = ["06", "12", "18", "24", "30", "36", "42", "48", "54", "60", "66", "72"]
    elif stormType == "Local":
        timeSteps = 36
        distList = ["010", "020", "030", "040", "050", "060", "070", "080", "090", "100", "110", "120", "130", "140", "150", "160", "170",
"180", "190", "200", "210", "220", "230", "240", "250", "260", "270", "280", "290", "300", "310", "320", "330", "340", "350", "360"] # 10-
minute time steps for temporal distibution.  (eg. 'DIST_010' = 0 to 10-min time step, 'DIST_020' = 10-min to 20-min time step.) 6-hours
total.
    i = 0
    while i < timeSteps:
        arcpy.AddMessage("\n\t...adding field: DIST_" + str(distList[i]))
        dm.AddField("PMP_Points", "DIST_" + distList[i], "DOUBLE")
        i += 1
    del timeSteps, distList

    ###########################################################################
    ## Define getAOIarea() function:
    ## getAOIarea() calculates the area of AOI (basin outline) input shapefile/
    ## featureclass.  The basin outline shapefile must be projected.  The area
    ## is sqaure miles, converted from the basin layers projected units (feet
    ## or meters).  The aoiBasin feature class should only have a single feature
    ## (the basin outline).  If there are multiple features, the area will be stored
    ## for the final feature only.

    def getAOIarea():
        sr = arcpy.Describe(aoiBasin).SpatialReference          # Determine aoiBasin spatial reference system
        srname = sr.name
        srtype = sr.type
        srunitname = sr.linearUnitName                # Units
        arcpy.AddMessage("\nAOI Basin Spatial Reference:  " + srname + "\nUnit Name: " + srunitname + "\nSpatial Ref. type: " + srtype)

        aoiArea = 0.0
        rows = arcpy.SearchCursor(aoiBasin)
        for row in rows:
            feat = row.getValue("Shape")
            aoiArea += feat.area
        if srtype == 'Geographic':                      # Must have a surface projection
            arcpy.AddMessage("\nThe basin shapefile's spatial reference '" + srtype + "' is not supported.  Please use a 'Projected' shapefile or
feature class.\n")
            raise SystemExit
        elif srtype == 'Projected':
```

```python
        if srunitname == "Meter":
            aoiArea = aoiArea * 0.000000386102            # Converts square meters to square miles
        elif srunitname == "Foot":
            aoiArea = aoiArea * 0.00000003587             # Converts square feet to square miles
        else:
            arcpy.AddMessage("\nThe basin shapefile's unit type '" + srunitname + "' is not supported.")
            sys.exit("Invalid linear units")              # Units must be meters or feet

    aoiArea = round(aoiArea, 3)
    arcpy.AddMessage("\nArea of interest: " + str(aoiArea) + " square miles.")

    # aoiArea = 100    ## Enable a constant area size
    arcpy.AddMessage("\n***Area used for PMP analysis: " + str(aoiArea) + " sqmi***")
    return aoiArea

##############################################################################
## Define dadLookup() function:
## The dadLookup() function determines the DAD value for the current storm
## and duration according to the basin area size.  The DAD depth is interpolated
## linearly between the two nearest areal values within the DAD table.
def dadLookup(stormLayer, duration, area):             # dadLookup() accepts the current storm layer name (string), the current
duration (string), and AOI area size (float)
    #arcpy.AddMessage("\t\tfunction dadLookup() called.")
    durField = "H_" + duration                 # defines the name of the duration field (eg., "H_06" for 6-hour)
    dadTable = dadGDB + "\\" + stormLayer
    rows = arcpy.SearchCursor(dadTable)
    for row in rows:                           # Iterates through each row in DAD table.  The last DAD area and depth less than the basin area
are record as x1 and y1.
        if row.AREASQMI < area:                # The next DAD depth and area greater than the basin area are recorded as x2 awnd y2.
            try:
                x1 = row.AREASQMI
                y1 = row.getValue(durField)
            except RuntimeError:               # return if duration does not exist in DAD table
                return
        else:
                x2 = row.AREASQMI
                y2 = row.getValue(durField)
                break
    del row

    try:                                       # If the basin area is greater than the largest area in the DAD table, x2 will bot be defined.
        x2                                     # In this case, y (the DAD depth) is estimated by extrapolating the DAD area to the basin area size.
    except:
        arcpy.AddMessage("\nThe basin area size '" + area + " sqmi' is greater than the largest DAD area '" + str(x1) + " sqmi'.  DAD value is
estimated by extrapolation.")
        x2 = area
        y = x1 / x2 * y1
        return y                               # The extrapolated DAD depth (in inches) is returned.


    x = area                                   # If the basin area size is within the DAD table area range, the DAD depth is interpolated
    deltax = x2 - x1                           # to determine the DAD value (y) at area (x) based on next lower (x1) and next higher (x2) areas.
    deltay = y2 - y1
    diffx = x - x1

    y = y1 + diffx * deltay / deltax
    return y                                   # The interpolated DAD depth (in inches) is returned.



##############################################################################
## Define updatePMP() function:
## This function updates the 'PMP_XX_' and 'STORM_XX' fields of the PMP_Points
## feature class with the largest value from all analyzed storms stored in the
## pmpValues list.
def updatePMP(pmpValues, stormID, duration):                     # Accepts four arguments: pmpValues - largest adjusted
rainfall for current duration (float list); stormID - driver storm ID for each PMP value (text list); and duration (string)
```

H-   3

```python
        pmpfield = "PMP_" + duration
        stormfield = "STORM_" + duration
        gridRows = arcpy.UpdateCursor(outPath + "PMP.gdb\\PMP_Points")           # iterates through PMP_Points rows
        i = 0
        for row in gridRows:
            row.setValue(pmpfield, pmpValues[i])                           # Sets the PMP field value equal to the Max Adj. Rainfall value (if
larger than existing value).
            row.setValue(stormfield, stormID[i])                          # Sets the storm ID field to indicate the driving storm event
            gridRows.updateRow(row)
            i += 1
        del row, gridRows, pmpfield, stormfield
        arcpy.AddMessage("\n\t" + duration + "-hour PMP values update complete. \n")
        return


    ############################################################################
    ## The temporalDistSixHour() function distributes the 72-hour PMP depths over 3 days broken into 12 6-hour block increments.
    ## The first day consists of the second largest 24-hour PMP period uniformly distributed.  The second day consists
    ## of the largest 24-hour PMP period, sequenced as follows: 24-30 hour is the 3rd largest 6-hr period, 30-36 hour is
    ## the 2nd largest 6-hour period, 36-42 hour is the 1st largest 6-hour period, and 42-48-hour is the 4th largest 6-hour
    ## period.  The third day consits of the smallest 24-hour period uniformly sequenced.
    ## The temporally distributed PMP values are recorded in the 'DIST_*' fields for gridpoint within the basin AOI.
    def temporalDistSixHour():

        pmpRows = arcpy.UpdateCursor(outPath + "PMP.gdb\\PMP_Points")
        arcpy.AddMessage("\nRunning temporalDistSixHour() function...")
        arcpy.AddMessage("\n\titerating through PMP_Points rows...")

        for row in pmpRows:
            day1 = row.PMP_24
            day2 = row.PMP_48 - row.PMP_24
            day3 = row.PMP_72 - row.PMP_48
            dayList = [day1, day2, day3]         # Determine the total PMP for each 24-hour period

            if day1 == max(dayList):
                firstLargest24 = row.PMP_24
            else:
                arcpy.AddMessage("\n***Error - Day 1 is not the largest 24-hour period")
                break
            if day3 > day2:
                secondLargest24 = day3
                thirdLargest24 = day2
            else:
                secondLargest24 = day2
                thirdLargest24 = day3

            sixhrList = [row.PMP_06, row.PMP_12 - row.PMP_06, row.PMP_18 - row.PMP_12, row.PMP_24 - row.PMP_18]
            sortSixList = sorted(sixhrList)

            row.DIST_06 = secondLargest24 / 4
            row.DIST_12 = secondLargest24 / 4
            row.DIST_18 = secondLargest24 / 4
            row.DIST_24 = secondLargest24 / 4
            row.DIST_30 = sortSixList[1]     #  Third largest 6-hour period depth
            row.DIST_36 = sortSixList[2]     #  Second largest 6-hour period depth
            row.DIST_42 = sortSixList[3]     #  Largest 6-hour period depth
            row.DIST_48 = sortSixList[0]     #  Fourth largest 6-hour period depth
            row.DIST_54 = thirdLargest24 / 4
            row.DIST_60 = thirdLargest24 / 4
            row.DIST_66 = thirdLargest24 / 4
            row.DIST_72 = thirdLargest24 / 4
            pmpRows.updateRow(row)
        del row, pmpRows
        arcpy.AddMessage("\nSix hour temporal distribution complete.")

    ####################################################################################
    ## The temporalDistTenMin() function distributes the 6-hour local storm PMP depths over
    ## 36 ten-minute time steps.  The LS-6 hypothetical distribution percentages are applied
```

```
## to the 6-hour PMP to calculate the time-distributed PMP depths at each 10-minute interval
## and are recorded under the appropriate "DIST_XXX" field in the PMP_Points feature class.
## The distribution percentages used are listed below in the variable 'distPct'.
def temporalDistTenMin():
    pmpRows = arcpy.UpdateCursor(outPath + "PMP.gdb\\PMP_Points")
    arcpy.AddMessage("\nRunning temporalDistTenMin() function...")
    distPct =
[0.001,0.001,0.0029,0.0041,0.0041,0.0041,0.0041,0.0041,0.0041,0.0041,0.0041,0.0041,0.0086,0.0104,0.0197,0.1065,0.1343,0.2088,0.16
67,0.1158,0.1065,0.0197,0.0104,0.0086,0.0041,0.0041,0.0041,0.0041,0.0041,0.0041,0.0041,0.0041,0.0029,0.001,0.001]
#Distribution percentages for each time step.
    arcpy.AddMessage("\n\t10-min distribution percentages: " + str(distPct))
    arcpy.AddMessage("\n\tIterating through PMP_Points rows...")
    arcpy.AddMessage("\n\tApplying percentages to 6-hour PMP...")
    fields = arcpy.ListFields(outPath + "PMP.gdb\\PMP_Points", "DIST*")
    for row in pmpRows:                              # iterate through each row updating each DIST field with the temp. disrtibuted
PMP
        i = 0
        for field in fields:
            row.setValue(field.name, row.PMP_06 * distPct[i])          # sets the DIST PMP to the product of the 3-hour PMP and the
distribution percentage for the i time step
            i +=1
        pmpRows.updateRow(row)
    del row, pmpRows, i, field, fields
    arcpy.AddMessage("\nTemporal distribution complete.")


    ###############################################################################
    ## The outputPMP() function produces raster GRID files for each of the PMP durations.
    ## Aslo, a space-delimited PMP_Distribition.txt file is created in the 'Text_Output' folder.
    def outputPMP():

        global outPath
        pmpPoints = outPath + "PMP.gdb\\PMP_Points"                 # Location of 'PMP_Points' feature class which will provide data for
output

        arcpy.AddMessage("\nBeginning PMP Raster Creation...")

        for dur in durList:                                    # This code creates a raster GRID from the current PMP point layer
            durField = "PMP_" + dur
            outLoc = outPath + "GRIDs.gdb\\pmp_" + dur
            arcpy.AddMessage("\n\tInput Path: " + pmpPoints)
            arcpy.AddMessage("\tOutput raster path: " + outPath)
            arcpy.AddMessage("\tField name: " + durField)
            con.FeatureToRaster(pmpPoints, durField, outLoc, "0.025")
            arcpy.AddMessage("\tOutput raster created...")
        del durField

        outFile = open(outPath + "Text_Output\\PMP_Distribution.txt", 'w')

        arcpy.AddMessage("\nPMP Raster Creation complete.")

        arcpy.AddMessage("\nCreating PMP_Distribution.txt file output...")

        arcpy.AddMessage("\n\tAdding Column Headers...")
        if stormType == "General" or stormType == "Tropical":
            fileText = "ID" + " LON" + " LAT" + " PMP(6-hour)" + " PMP(12-hour)" + " PMP(18-hour)" + " PMP(24-hour)" + " PMP(48-hour)" + "
PMP(72-hour)" + " T_PMP(0to6-hour)" + " T_PMP(6to12-hour)" + " T_PMP(12to18-hour)" + " T_PMP(18to24-hour)" + " T_PMP(24to30-
hour)" + " T_PMP(30to36-hour)" + " T_PMP(36to42-hour)" + " T_PMP(42to48-hour)" + " T_PMP(48to54-hour)" + " T_PMP(54to60-
hour)" + " T_PMP(60to66-hour)" + " T_PMP(66to72-hour)"
            arcpy.AddMessage("\tAdding rows...")
            gridRows = arcpy.SearchCursor(pmpPoints)
            for row in gridRows:
                fileText += "\n" + str(row.ID) + " " + str(row.LON) + " " + str(row.LAT) + " " + str(row.PMP_06) + " " + str(row.PMP_12) + " " +
str(row.PMP_18) + " " + str(row.PMP_24) + " " + str(row.PMP_48) + " " + str(row.PMP_72) + " " + str(row.DIST_06) + " " +
str(row.DIST_12) + " " + str(row.DIST_18) + " " + str(row.DIST_24) + " " + str(row.DIST_30) + " " + str(row.DIST_36) + " " +
str(row.DIST_42) + " " + str(row.DIST_48) + " " + str(row.DIST_54) + " " + str(row.DIST_60) + " " + str(row.DIST_66) + " " +
str(row.DIST_72)
            del row, gridRows
```

```
            outFile.write(fileText)                                          # Write string text to .txt file
            outFile.close()
        elif stormType == "Local":
            fileText = "ID" + " LON" + " LAT" + " PMP(1-hour)" + " PMP(2-hour)" + " PMP(3-hour)" + " PMP(4-hour)" + " PMP(5-hour)" + "
PMP(6-hour)" + " T_PMP(10-min)" + " T_PMP(20-min)" + " T_PMP(30-min)" + " T_PMP(40-min)" + " T_PMP(50-min)" + " T_PMP(60-
min)" + " T_PMP(70-min)" + " T_PMP(80-min)" + " T_PMP(90-min)" + " T_PMP(100-min)" + " T_PMP(110-min)" + " T_PMP(120-min)" + "
T_PMP(130-min)" + " T_PMP(140-min)" + " T_PMP(150-min)" + " T_PMP(160-min)" + " T_PMP(170-min)" + " T_PMP(180-min)" + "
T_PMP(190-min)" + " T_PMP(200-min)" + " T_PMP(210-min)" + " T_PMP(220-min)" + " T_PMP(230-min)" + " T_PMP(240-min)" + "
T_PMP(250-min)" + " T_PMP(260-min)" + " T_PMP(270-min)" + " T_PMP(280-min)" + " T_PMP(290-min)" + " T_PMP(300-min)" + "
T_PMP(310-min)" + " T_PMP(320-min)" + " T_PMP(330-min)" + " T_PMP(340-min)" + " T_PMP(350-min)" + " T_PMP(360-min)"
            arcpy.AddMessage("\tAdding rows...")
            gridRows = arcpy.SearchCursor(pmpPoints)
            for row in gridRows:
                fileText += "\n" + str(row.ID) + " " + str(row.LON) + " " + str(row.LAT) + " " + str(row.PMP_01) + " " + str(row.PMP_02) + " " +
str(row.PMP_03) + " " + str(row.PMP_04) + " " + str(row.PMP_05) + " " + str(row.PMP_06) + " " + str(row.DIST_010) + " " +
str(row.DIST_020) + " " + str(row.DIST_030) + " " + str(row.DIST_040) + " " + str(row.DIST_050) + " " + str(row.DIST_060) + " " +
str(row.DIST_070) + " " + str(row.DIST_080) + " " + str(row.DIST_090) + " " + str(row.DIST_100) + " " + str(row.DIST_110) + " " +
str(row.DIST_120) + " " + str(row.DIST_130) + " " + str(row.DIST_140) + " " + str(row.DIST_150) + " " + str(row.DIST_160) + " " +
str(row.DIST_170) + " " + str(row.DIST_180) + " " + str(row.DIST_190) + " " + str(row.DIST_200) + " " + str(row.DIST_210) + " " +
str(row.DIST_220) + " " + str(row.DIST_230) + " " + str(row.DIST_240) + " " + str(row.DIST_250) + " " + str(row.DIST_260) + " " +
str(row.DIST_270) + " " + str(row.DIST_280) + " " + str(row.DIST_290) + " " + str(row.DIST_300) + " " + str(row.DIST_310) + " " +
str(row.DIST_320) + " " + str(row.DIST_330) + " " + str(row.DIST_340) + " " + str(row.DIST_350) + " " + str(row.DIST_360)
            del row, gridRows
            outFile.write(fileText)                                          # Write string text to .txt file
            outFile.close()
        else:
            arcpy.AddMessage("\nError Storm Type")
            outFile.close()
        arcpy.AddMessage("\nPMP_Distribution.txt file output complete.")

        ######  This section of code outputs a file geodatabase table in the PMP.gdb tabulating the mean PMP values from the PMP_Points
feature class ######
        meanPath = outPath + "PMP.gdb\\PMP_Points_Mean"
        arcpy.AddMessage("\nCreating '" + meanPath + "' table to store average PMP values...")
        if stormType == "General" or stormType == "Tropical":
            arcpy.Statistics_analysis(pmpPoints, meanPath,"PMP_06 MEAN;PMP_12 MEAN;PMP_18 MEAN;PMP_24 MEAN;PMP_48
MEAN;PMP_72 MEAN;DIST_06 MEAN;DIST_12 MEAN;DIST_18 MEAN;DIST_24 MEAN;DIST_30 MEAN;DIST_36 MEAN;DIST_42
MEAN;DIST_48 MEAN;DIST_54 MEAN;DIST_60 MEAN;DIST_66 MEAN;DIST_72 MEAN","#")
        elif stormType == "Local":
            arcpy.Statistics_analysis(pmpPoints, meanPath,"PMP_01 MEAN;PMP_02 MEAN;PMP_03 MEAN;PMP_04 MEAN;PMP_05
MEAN;PMP_06 MEAN;DIST_010 MEAN;DIST_020 MEAN;DIST_030 MEAN;DIST_040 MEAN;DIST_050 MEAN;DIST_060 MEAN;DIST_070
MEAN;DIST_080 MEAN;DIST_090 MEAN;DIST_100 MEAN;DIST_110 MEAN;DIST_120 MEAN;DIST_130 MEAN;DIST_140 MEAN;DIST_150
MEAN;DIST_160 MEAN;DIST_170 MEAN;DIST_180 MEAN;DIST_190 MEAN;DIST_200 MEAN;DIST_210 MEAN;DIST_220 MEAN;DIST_230
MEAN;DIST_240 MEAN;DIST_250 MEAN;DIST_260 MEAN;DIST_270 MEAN;DIST_280 MEAN;DIST_290 MEAN;DIST_300 MEAN;DIST_310
MEAN;DIST_320 MEAN;DIST_330 MEAN;DIST_340 MEAN;DIST_350 MEAN;DIST_360 MEAN","#")
        else:
            arcpy.AddMessage("\nError Storm Type")
        arcpy.AddMessage("\nMean PMP table output complete.")

        ######  This section applies the metadata templates to the output GIS files ######
        pointMetaLoc = outPath + "Metadata_Templates\\PMP_Points_Metadata_" + stormType + "_FGDC.xml"               # Location of
'PMP_Points' feature class metadata template
        rasMetaLoc = outPath + "Metadata_Templates\\PMP_Raster_Metadata_FGDC.xml"                        # Location of 'PMP_XX'
raster file metadata template

        arcpy.AddMessage("\nAdding metadata to output files...")
        arcpy.AddMessage("\n\tPMP_Points feature class")
        con.MetadataImporter(pointMetaLoc, pmpPoints)                                          # Applies metadata to 'PMP_Points' feature
class
        for dur in durList:                                          # Applies metadata to 'PMP_XX' GRIDs
            targetPath = outPath + "GRIDs.gdb\\pmp_" + dur
            arcpy.AddMessage("\tPMP_" + str(dur) + " feature class")
            con.MetadataImporter(rasMetaLoc, targetPath)
        arcpy.AddMessage("\nOutput metadata import complete.")

 ################################################################################
 ## This portion of the code iterates through each storm feature class in the
```

```
    ## 'Storm_Adj_Factors' geodatabase (evaluating the feature class only within
    ## the Local, Tropical, or general feature dataset).  For each duration,
    ## at each grid point within the aoi basin, the transpositionality is
    ## confirmed.  Then the DAD precip depth is retrieved and applied to the
    ## total adjustement factor to yield the total adjusted rainfall.  This
    ## value is then sent to the updatePMP() function to update the 'PMP_Points'
    ## feature class.

##~~~~~~~~~~~~~~~~~~~~~~~~~~~~~~~~~~~~~~~~~~~~~~~~~~~~~~~~~~~~~~~~~~~~~~~~~~~~~~~~~~~~~~~~~~~~~~~
~~~~~~~~~~~~~~~~~~~~~~~~~~~~~~~~~~~~~~~~~~~~~~~~~~~~~~~~~~~~~~~~~~~~~~~~~~~~~~~~~~~~~~~~~##

    desc = arcpy.Describe(basin)                              # Check to ensure AOI input shape is a Polygon. If not - exit.
    basinShape = desc.shapeType
    if desc.shapeType == "Polygon":
        arcpy.AddMessage("\nBasin shape type: " + desc.shapeType)
    else:
        arcpy.AddMessage("\nBasin shape type: " + desc.shapeType)
        arcpy.AddMessage("\nError: Input shapefile must be a polygon!\n")
        sys.exit()

    createPMPfc()                                             # Call the createPMPfc() function to create the PMP_Points feature class.

    env.workspace = adjFactGDB                               # the workspace environment is set to the 'Storm_Adj_Factors' file
geodatabase

    aoiSQMI = round(getAOIarea(),2)                          # Calls the getAOIarea() function to assign area of AOI shapefile to
'aoiSQMI'

    for dur in durList:
        stormList = arcpy.ListFeatureClasses("", "Point", stormType)           # List all the total adjustment factor feature classes within the
storm type feature dataset.

        arcpy.AddMessage("\n*************************************************************\nEvaluating " + dur + "-hour duration...")

        pmpList = []
        driverList = []
        gridRows = arcpy.SearchCursor(outPath + "PMP.gdb\\PMP_Points")
        try:
            for row in gridRows:
                pmpList.append(0.0)                          # creates pmpList of empty float values for each grid point to store final PMP
values
                driverList.append("STORM")                   # creates driverList of empty text values for each grid point to store final
Driver Storm IDs
            del row, gridRows
        except UnboundLocalError:
            arcpy.AddMessage("\n***Error: No data present within basin/AOI area.***\n")
            sys.exit()

        for storm in stormList:
            arcpy.AddMessage("\n\tEvaluating storm: " + storm + "...")
            dm.MakeFeatureLayer(storm, "stormLayer")                     # creates a feature layer for the current storm
            dm.SelectLayerByLocation("stormLayer", "HAVE_THEIR_CENTER_IN", "vgLayer")   # examines only the grid points that lie within
the AOI
            gridRows = arcpy.SearchCursor("stormLayer")
            pmpField = "PMP_" + dur
            i = 0
            try:
                dadPrecip = round(dadLookup(storm, dur, aoiSQMI),3)
                arcpy.AddMessage("\t\t" + dur + "-hour DAD value:  " + str(dadPrecip) + chr(34))
            except TypeError:                                # In no duration exists in the DAD table - move to the next storm
                arcpy.AddMessage("\t***Duration '" + str(dur) + "-hour' is not present for " + str(storm) + ".***\n")
                continue
            arcpy.AddMessage("\t\tComparing " + storm + " adjusted rainfall values against current driver values...\n")
            for row in gridRows:
                if row.TRANS == 1:                           # Only continue if grid point is transpositionable ('1' is transpostionable, '0' is not).
                    try:                                     # get total adj. factor if duration exists
                        maxAdjRain = round(dadPrecip * row.TAF,2)
```

```
            if maxAdjRain > pmpList[i]:
                pmpList[i] = maxAdjRain
                driverList[i] = storm
        except RuntimeError:
            arcpy.AddMessage("\t\t  *Warning* PMP value falied to set for row " + str(row.CNT))
            break
        i += 1
      del row
    del storm, stormList, gridRows, dadPrecip
    updatePMP(pmpList, driverList, dur)         # calls function to update "PMP Points" feature class
  del dur, pmpList

  arcpy.AddMessage("\n'PMP_Points' Feature Class 'PMP_XX' fields update complete for all '" + stormType + "' storms.")

  if stormType == "General" or stormType == "Tropical":
    temporalDistSixHour()         # calls temporalDistSixHour() function for Tropical and General Storms
  elif stormType == "Local":
    temporalDistTenMin()          # calls temporalDistTenMin() function for Local storms.
  else:
    arcpy.AddMessage("\nError: Storm Type")
  outputPMP()                     # calls outputPMP() function


##~~~~~~~~~~~~~~~~~~~~~~~~~~~~~~~~~~~~~~~~~~~~~~~~~~~~~~~~~~~~~~~~~~~~~~~~~~~~~~~~~~~~~~~~~
~~~~~~~~~~~~~~~~~~~~~~~~~~~~~~~~~~~~~~~~~~~~~~~~~~~~~~~~~~~~~~~~~~~~~~~~~~~~~~~~~~~~~~~##

type = "General"
durList = ["06", "12", "18", "24", "48", "72"]
outPath = home + "\\Output\\General_Winter\\"
arcpy.AddMessage("\nRunning PMP analysis for storm type: " + type)
pmpAnalysis(basin, type)        # Calls the pmpAnalysis() function to calculate the General Winter storm PMP
arcpy.AddMessage("\nGeneral Winter storm analysis
complete...\n*****************************************************************************************")

type = "Tropical"
durList = ["06", "12", "18", "24", "48", "72"]
outPath = home + "\\Output\\Tropical\\"
arcpy.AddMessage("\nRunning PMP analysis for storm type: " + type)
pmpAnalysis(basin, type)        # Calls the pmpAnalysis() function to calculate the Tropical storm PMP
arcpy.AddMessage("\nTropical storm analysis
complete...\n*****************************************************************************************")

type = "Local"
durList = ["01", "02", "03", "04", "05", "06"]
outPath = home + "\\Output\\Local\\"
arcpy.AddMessage("\nRunning PMP analysis for storm type: " + type)
pmpAnalysis(basin, type)        # Calls the pmpAnalysis() function to calculate the Local storm PMP
arcpy.AddMessage("\nLocal storm analysis
complete...\n*****************************************************************************************")
```

Appendix I

Supplemental Digital Data DVD

1   Storm Spreadsheets

This folder contains the digital format of the Excel storm spreadsheet .xlsx files (Appendix F). These spreadsheets provide a summary of the storm's metatdata, DAD, in-place maximization calculations, and transposition calculations to the analysis domain grid point #1.

2   Storm Adjustment Factor Spreadsheets

This folder contains the adjustment factor Excel spreadsheets for each analyzed storm center. The spreadsheets hold the calculations for the storm in-place maximization and transposition (moisture and orographic) to each of the 64,103 analysis grid points. The values in the 'Adjustment Factor' sheet are exported to the Storm_Adj_Factors.gdb for use as input with the GIS PMP Evaluation Tool.

3   Monthly Dew Point Climatology GIS Files

The GIS files for the 100-year 3-hour, 12-hour, and 24-hour monthly dew point climatologies used within the storm maximization and moisture transposition analysis are contained within this folder. The 'Raster' folder contains the dew point raster layers in ESRI GRID format. The 'Shapefiles' folder contains the isotherm vector lines in ESRI Shapefile format.

4   Monthly Sea Surface Temperature (+2 sigma) GIS Files

The GIS files for the monthly $+2\sigma$ sea surface temperature (SST) climatologies used within the storm maximization and moisture transposition analysis are contained within this folder. The 'Raster' folder contains the SST raster layers in ESRI GRID format. The 'Shapefiles' folder contains the isotherm vector lines in ESRI Shapefile format. The 'Images' folder contains the plots of the SST datasets.

5   DAD Tables

The DAD tables for each analyzed storm center are stored within subfolder by storm type. The DAD tables are in comma-delimited text format.

6   NOAA Atlas 14 Precipitation Frequency Estimates

This folder contains the gridded precipitation frequency estimates (PFE's) used for the orographic transposition analysis. The PFE's are generalized from the nearest neighbor NOAA Atlas 14 Semiarid Southwest (vol. 1) depths; with the exception of the Colorado grid cells, which use NOAA Atlas 14 Midwest (vol.8); and the Mexico grid cells, which use estimated PFE's extrapolated using the depth-elevation relationship between existing neighboring NOAA Atlas 14 values.

7   PMP Evaluation GIS Tool (version 1.0)

This folder contains the ArcGIS 10.x Arizona PMP Evaluation Tool v. 1.0. The tool contains the input folder geodatabases (DAD tables, storm adjustment factors), output folders for each storm type, and the Python script and enclosing Toolbox.

8   Map Images – ANSI D Format

8.1   Full Domain PMP

This folder contains the JPEG and PDF format map images for remnant tropical, general frontal, and local storm PMP for the entire project domain in 22" x 34" ANSI D layout. The 72-hour tropical and general PMP is calculated at the 75 square mile area size. The 6-hour local PMP is calculated at the 10 square mile area size. There are also maps of the control storms driving PMP over the domain for each storm type.

- JPEG
    - General PMP – 72hr 75sqmi – ANSI D.jpg
    - General PMP – Control Storms - 72hr 75sqmi – ANSI D.jpg
    - Local PMP – 6hr 10sqmi – ANSI D.jpg
    - Local PMP – Control Storms - 6hr 10sqmi – ANSI D.jpg
    - Tropical PMP – 72hr 75sqmi – ANSI D.jpg
    - Tropical PMP – Control Storms - 72hr 75sqmi – ANSI D.jpg
- PDF
    - General PMP – 72hr 75sqmi – ANSI D.pdf
    - General PMP – Control Storms - 72hr 75sqmi – ANSI D.pdf
    - Local PMP – 6hr 10sqmi – ANSI D.pdf
    - Local PMP – Control Storms - 6hr 10sqmi – ANSI D.pdf
    - Tropical PMP – 72hr 75sqmi – ANSI D.pdf
    - Tropical PMP – Control Storms - 72hr 75sqmi – ANSI D.pdf

8.2   Storm Rainfall Percent of PMP

This folder contains the JPEG and PDF format map images for remnant tropical, general frontal, and local storm SPAS analyzed maximum rainfall values at each storm center, as a percent of 1 square mile PMP, in 22" x 34" ANSI D layout. The tropical and general storm

rainfall is compared to the 24-hour and 72-hour PMP. The local storm rainfall is compared to the 1-hour and 6-hour PMP.

- JPEG
    - General Storms - Percent 24-hr PMP - ANSI D.jpg
    - General Storms - Percent 72-hr PMP - ANSI D.jpg
    - Local Storms - Percent 1-hr PMP - ANSI D.jpg
    - Local Storms - Percent 6-hr PMP - ANSI D.jpg
    - Tropical Storms - Percent 24-hr PMP - ANSI D.jpg
    - Tropical Storms - Percent 72-hr PMP - ANSI D.jpg
- PDF
    - General Storms - Percent 24-hr PMP - ANSI D.jpg
    - General Storms - Percent 72-hr PMP - ANSI D.jpg
    - Local Storms - Percent 1-hr PMP - ANSI D.jpg
    - Local Storms - Percent 6-hr PMP - ANSI D.jpg
    - Tropical Storms - Percent 24-hr PMP - ANSI D.jpg
    - Tropical Storms - Percent 72-hr PMP - ANSI D.jpg

8.3   Orographic Transposition Zones

This folder contains the JPEG and PDF format map images the five orographic transposition zones in 22" x 34" ANSI D layout.

- JPEG
    - Orographic Transposition Zones - ANSI D.jpg
- PDF
    - Orographic Transposition Zones - ANSI D.jpg

9   Individual Storm Transposition Limits

This folder contains the Excel file for each storm on the short storm list and the individual transposition limits for each SPAS analyzed DAD zone.